UNIVERSITY OF DERBY

Characterisation and validation of novel, stable apelin-13 analogues on neurodegeneration in AD.

Priya Sharma

B.Sc., M.Res.

A submission is partial fulfilment of the requirements of the University of Derby for the award of the degree of Doctor of Philosophy.

College of Science and Engineering

Doctor of Philosophy 2025

Dedication

To my family and friends

Acknowledgements

I am profoundly grateful to GOD Almighty for strength, knowledge, ability and opportunity to undertake this research and complete it. This journey of PhD has been challenging but most rewarding in my life. I would like to say big thank you to University of Derby for an incredible journey as a student and the whole academic team, my peers and technical staff.

My deepest gratitude to my supervisors Dr Vadivel Parthsarathy, and Dr Shiva Sivasubramaniam who somehow had the patience to tolerate my endless emails, emotion breakdowns, and crisis. Your guidance, encouragement and feedback has been invaluable, and I wouldn't be able to come this far if it wasn't you.

Special thanks to my parents (Simar and Baljeet), my sibling (Ashu, Geetu and Hem) and Jony for unconditional support and love. I am grateful of you for being there for me, feeding me and reminding me that I am not too far with this journey. To my extended family and friends, especially (Jumman, Tunni and Nishad), who endured my endless rants about failed experiments, coffee breaks, motivation and for keeping me on track.

Finally, my PhD itself: you have been challenging, and exhausting at times, but at end we made it.

Abstract

Introduction: Alzheimer's disease is characterised by the cognitive decline, neuronal loss linked to oxidative stress, neuroinflammation, autophagy and endoplasmic reticulum (ER) stress. There are number of factors involved like lifestyle, genetics, age, and environment. After decades of research there is still no cure for Alzheimer's. This thesis investigates the neuroprotective role of novel stable peptide apelin-13 analogues on cell survival and cell growth against various stressors induced in SH-SY5Y cells *in-vitro*.

Methods and results: SH-SY5Y neuronal cells were cultured and treated with the apelin-13 analogues in presence or absence of stressors under controlled condition to evaluate the effects on cell stress response and cell survival pathways. The cells were differentiated with retinoic acid to look at the cell proliferation and neurite extension. The treatments with apelin-13 analogues enhanced the cell viability , proliferation, modulated the oxidative stress and ER markers and promoted neurite outgrowth and differentiation. Furthermore, apelin-13 analogues reduced the pro-apoptotic and ER stress markers and led to increase in autophagy related proteins. The mechanistic study by AMPK knockdown showed that apelin-13 is AMPK dependant.

Conclusion: The result demonstrated that apelin-13 analogues protect against the neurotoxicity and oxidative stress by improving cell viability, proliferation and reducing cell toxicity. The apelin-13 analogues restored the autophagy and moderated the UPR activation via AMPK and PI3K/Akt pathway activation. Although further in-vivo studies are required to validate the results. This study provides new insight to the role of apelin-13 analogues as a therapeutic agent and pave a way for novel intervention targeting neurodegeneration.

Publication and Conferences

Manuscript under review

Sharma, P. et al. (2025) ‘Stable Apelin-13 analogues promote cell proliferation, differentiation and protect inflammation induced cell death’, Molecular Neuroscience.

Conference

Priya Sharma, Sivasubramaniam, S., and Parthsarathy, V. (2024) ‘Effects of stable apelin-13 improving neuronal cell protection and proliferation ’, Alzheimer’s research UK (ARUK) 2024 international conference in Liverpool.

Research Presentation

Priya Sharma, Sivasubramaniam, S., and Parthsarathy, V. (2024) ‘Apelin as a novel drug in treatment of alzheimer-related neurodegeneration’, Theme research Showcase, University of Derby.

Public Engagement

Priya Sharma, Vadivel Parthsarathy (2023) ‘Novel drugs in treatment of Alzheimer-related neurodegeneration’, Dementia and Deaf community Event.

Declaration

I hereby declare that with effect from the date on which the thesis is deposited in the Research Office of the University of Derby, I permit the Librarian of the University to allow the thesis to be copied in whole or in part without reference to me on the understanding that such authority applies to the provision of single copies made for study purposes or for inclusion within the stock of another library and that the thesis to be made available through the University of Derby Repository. “IT IS A CONDITION OF USE OF THIS THESIS THAT ANYONE WHO CONSULTS IT MUST RECOGNISE THAT THE COPYRIGHT RESTS WITH THE AUTHOR AND THAT NO QUOTATION FROM THE THESIS AND NO INFORMATION DERIVED FROM IT MAY BE PUBLISHED UNLESS THE SOURCE IS PROPERLY ACKNOWLEDGED".

Table of Contents

List of Tables

List of Figures

Abbreviations

AD	Alzheimer's disease
ADRDA	AD and Related Disorders Association
AICD	APP intracellular cytoplasmic domain
AMPK	AMP-activated protein kinase
APOE	Apo-lipoprotein E
APP	Amyloid precursor protein
ATP	Adenosine triphosphate
BACE1	β-site APP-cleaving enzyme 1
BBB	Blood brain barrier
BDNF	Brain-derived neurotrophic factors
BSA	Bovine serum albumin
C83	83 amino acid Carboxy-terminal fragment
C99	C terminal
CDK	Cyclin-dependent kinase
CNS	Central nervous system
COSHH	Control of substances hazardous to health

cpYFP	Circularly permuted yellow-fluorescent protein
CSF	Cerebrospinal fluid
CTF	C terminal fragment
CTFα	Carboxy-terminus fragment
CTFβ	Carboxy-terminus fragment β
DAB	3,3'-diaminobenzidine
DAPI	4',6-Diamidino-2-phenylindole
DNA	Deoxyribonucleic acid
DSM-III	Diagnostic and Statistical Manual of Mental Disorders
EDTA	Ethylenediaminetetraacetic acid
EGTA	Thylene glycol-bis(β-aminoethyl ether)-N,N,N',N'-tetraacetic acid
eNO	Endothelial nitric oxide
EOFAD	Early-onset familial Alzheimer's disease
ER	Endoplasmic reticulum
ERK	Extracellular Signal-Regulated Kinase
FBS	Fetal bovine serum
FFAs	Free fatty acids
GAPDH	Glyceraldehyde-3-Phosphate Dehydrogenase
GSH	Glutathione
GSK	Glycogen synthase kinase
GSK3β)	Glycogen synthesis kinase 3 beta

GSSG Glutathione disulphide

GWAS Genome-wide association studies

H_2O_2. Hydrogen peroxide

HD Huntington's disease

ICC immunocytochemistry

ICD International Classification of Diseases

IDE Insulin degrading Enzyme

IHC Immunohistochemistry

JNK c-Jun N-terminal kinase

LDH lactate dehydrogenase

LOAD late-onset sporadic Alzheimer's disease

LPS Lipopolysaccharide

LRP1 Lipoprotein receptor-related protein 1

LTP Long term potentiation

MABs Anti-amyloid monoclonal antibodies

MAP2 Microtubule Associated Protein-2

MAPKs Mitogen-activated protein kinases

MDA Malondialdehyde

MMSE Mini-Mental State Examination

MRI Magnetic resonance imaging

mTOR Mammalian target of rapamycin

MTT 3-(4,5-Dimethylthiazol-2-yl)-2,5-Diphenyltetrazolium Bromide

NEP Neprilysin

NFT Neurofibril tangles

NHS National Health Service

NINCDS National Institute of Neurological and Communicative Disorders and Stroke

NRF2 Nuclear factor erythroid 2-related factor 2

OD Optical density

PA Palmitic acid

PBS Phosphate buffer saline

PD Parkinson disease

PDI Protein Disulfide Isomerase

PET Positron emission tomography

PHF Paired helical filament

PP Precursor protein

RA Retinoic acid

RAGE Receptor for advanced glycation end products

RFU Relative fluorescence units

ROIs Regions of interest

ROS Reactive oxygen species

sAPPα Soluble APP fragment α

sAPPβ Soluble APP fragment β

SD	Standard deviation
SERCA	Sarco/endoplasmic reticulum Ca2+-ATPase
SOD	Superoxide Dismutase
TBA	Thiobarbituric acid
TLR4	Toll-like- receptor 4
TLRs	Toll-like receptors
TrkB	Tyrosine receptor kinase B
TTP	Tocopherol transfer protein
UPR	Unfolded protein response
WAT	White adipose tissues
ΔΨm	Mitochondrial membrane potential

Chapter 1

General Introduction

1.1. Introduction

Dementia is a wide umbrella term that refers to the decline in cognitive ability, memory loss, which can impact on daily life activities. These progressive neurological disorders are characterised by the deaths of the nerve of the central nervous system (Kovacs, 2018). There are number of types of dementia like Alzheimer's disease (AD), Parkinson disease (PD), Lewy's body dementia, Vascular dementia and frontal lobar degeneration (NIH, 2023).

The most common types of neurodegenerative diseases are AD and PD. AD is the most progressive neurodegenerative disease with the highest outbreaks (Hippius, 2003; World Health Organisation, 2023). AD is marked by a gradual deterioration of cognitive abilities, including memory loss and a decline in neuronal activity (Sun et al., 2014).

AD was first described by physician Alois Alzheimer in 1906 in the 37th Conference of South-West German Psychiatrists, following the death of his 51-year-old patient named Auguste Deter (Maurer *et al.,* 1997). Auguste Deter had key feature of AD as she suffered from memory loss, paranoia, confusion, aggression and erratic sleeping patterns (Hippius and Neundörfer, 2003; Maurer et al., 1997). The women died 5 years after the clinical symptoms and the post-mortem autopsy revealed moderate hydrocephalus, arteriosclerotic changes in cerebral vessels and cerebral atrophy (Bondi et al., 2017). Histopathological examinations showed numerous tiny miliary foci in the superior layers and abnormally thick and impermeable neurofibrils in cells, which were linked to the deposition of an odd material known as neuritic plaques (Maurer et al., 1997). Alzheimer later worked on four other case and found similarity in disease progression and the disease was named after his name (Bondi et al., 2017).

1.2. Epidemiology and Incidence

AD accounts for approximately 60-80% of the dementia cases and it is the most common form of dementia. There are nearly 55 million people living with dementia worldwide and every year there is rise of around 10 million cases (Dementia, 2023). Presently, the UK has over 982,000 people with existing dementia, and it will grow twofold by 2025, and AD constitutes the large percentage of these cases (Alzheimer's Society & Carnell Farrar, 2024). Dementia cases are predicted to rise by 1.4 million in 2040 and one in three people born in the UK today will develop dementia in their lifetime. In the UK, 25,000 cases of dementia are from ethnic minority groups (Alzheimer's Society & Carnell Farrar, 2024). More than 6.9 million Americans are living with AD, one in nine people aged 65 and over has AD and the percentage of the cases increases with age, people aged 65 to 74 by 5%, age 75 to 84 by 13.2% and 33.4% in people ages 85 and older (Alzheimer's disease Facts and Figures, 2024). The prevalence of the AD increasing significantly with age and in women due to their longer life expectance, its disproportionally afflicted making up about two-third of cases (Zhang et al., 2021).

Increasing cases of AD worldwide poses a huge burden on the healthcare system and economy of the country. The latest report by Alzheimer's society reveals that the cost of dementia in the UK has reached a staggering £42 billion per year and is set to rise to £90 billion by 2040 (ARUK, 2024). As dementia worsens, the costs increase dramatically, due to the increasing demand for more complicated social and unpaid care. The annual cost per person for moderate dementia is £28,700, while the cost for severe dementia is £80,500 (Alzheimer's Society, 2024). Approximately more than £26.3 billion yearly is spent by the National Health Service (NHS) and other charities on dementia (Georgiev et al., 2024). The expense of dementia is predicted to double by £55 billion in 2040 in the UK and to $2 trillion by 2030 globally. The direct healthcare cost of Alzheimer's disease in US was estimated to $321 billion in 2022 and projected to increase by $1 trillion in 2025 as population ages (Wong, 2020).

Well-being and societal cost of dementia are beyond than cancer and persistent cardiovascular diseases combined (The Lancet, 2018). AD not only affect the patient but

also their families and communities. Unpaid carers assisting somebody with dementia save the UK economy £21 billion yearly and will increase by £40 billion in 2040 (Facts for the media about dementia, 2024). More than 11 million Americans offer unpaid care for the family with dementia and contribute to the nation valued at $359 billion (Alzheimer's disease Facts and Figures, 2024). Most of the caregiving duties fall on families, often at the price of their own mental and physical health. Unpaid caregivers often endure high levels of stress, depression and anxiety because of the emotional toll of the witnessing the cognitive decline of their family members (Schulz & Sherwood, 2008).

According to statistics, AD and other dementias have a significant financial and care-related impact on public health care systems worldwide. Therefore, improvements in diagnostic, care, and treatment methods are required to save costs and enhance quality of life.

1.3. Clinical manifestation

AD is one of the utmost destructive and complicated progressive neurogenerative disorders, symbolised by cognitive destruction, spatial uncertainty, aphasia, reduced social behaviour counting, nervousness, and apathy (Evans, 1989). Memory loss is earliest and most common symptom of AD mainly affecting short term memory (episodic), as long-term memory (semantic) remains relatively in early stage. Over time AD progresses and lead to neuronal loss in the hippocampus and medial temporal lobe. The common symptom at the early stage is difficulty to recall the daily activities like: date of important events, location of objects and names (Kumar et al., 2025). Later patients suffer from language difficulties, disorientation, impaired judgement and confusion (Banovic et al., 2018). In addition to the symptoms listed above, advance stages of AD cause mutism, dependency, seizures, incontinence and myoclonus. The disease often lasts 8 to 10 years, and mild respiratory complications such pneumonia or aspiration, as well as malnourishment, are the main causes of death (Barnes et al., 2018).

1.4. Diagnosis

AD and Related Disorders Association (ADRDA) and the National Institute of Neurological and Communicative Disorders and Stroke (NINCDS) developed the diagnostic criteria, now known as the NINCDS-ADRDA criteria, in 1984. For past 28 years until 2011, these criteria have been effective in diagnosing of AD. The NINCDS-ADRDA criteria have a sensitivity of 81% and a specificity of 70% (McKhann et al., 2011). Furthermore, these criteria associate with the International Classification of Diseases (ICD) and Diagnostic and Statistical Manual of Mental Disorders (DSM-III) (McKhann et al., 1984). These guidelines state that the Mini-Mental State Examination (MMSE), clinical examination, neuropsychological testing, laboratory tests like computed tomography (CT) scans, cerebrospinal fluid (CSF) examination and medical history should be used to diagnose probable AD (Folstein et al., 1975; McKhann et al., 1984). The possibility should be based on the lack of neurological, mental and systemic disorders and advanced AD should be diagnosed based on the histological evidence from post-mortem examination and all criteria from probable AD.

However, due to the advancement in scientific understanding of the disease the National Institute of Ageing and Alzheimer's Association established revisions to these standards in 2011 (McKhann et al., 2011). The diagnosis includes a combined approach of biomarker evaluation, clinical assessment, cognitive testing, and imaging techniques (McGleenon et al., 1999). While functional imaging, such as amyloid and tau positron emission tomography (PET) scans, detects amyloid plaques, tau tangles, and decreased brain metabolism, imaging techniques, such as MRI or CT scans, identify structural alterations such as hippocampus atrophy (Kulasiri et al., 2023; McKhann et al., 1984). To distinguish between different forms of dementia, such as frontotemporal and Lewy body dementia, or other causes of cognitive impairment, such as tumours, differential diagnosis depends on assessment tools like the ADAS Cog (Alzheimer’s Disease Assessment Scale Cognitive Subscale) and imaging technologies like CT and magnetic resonance imaging (MRI) scans (McGleenon et al., 1999).

By detecting intracellular NFT aggregation and extracellular Aβ tangles in comparison to age-matched individuals free of dementia, neuropathological investigations offer post-mortem confirmation (Bird, 2008). AD is indicated by biomarkers in cerebrospinal fluid, such as higher tau proteins and decreased amyloid-beta 42 and new blood-based diagnostics, such as plasma p-tau, offer (Gonzalez-Ortiz et al., 2023; Tapiola et al., 2009). For those with a strong family history or early-onset instances, genetic testing may be considered, with an emphasis on APOE ε4 or mutations in APP, Presenilin 2 (PSEN1), and (Presenilin 1) PSEN2.

1.5. Aetiology of AD

AD is a complicated disease with multifactorial aetiology, including factors like lifestyle, genetics, environment, age and lack of understanding of the biological mechanism (Zhang et al., 2024). Studies have showed that high educational activities, and intellectual leisure activities like reading, gaming, social engagements reduced the risk of AD (Scarmeas & Stern, 2003).

1.6. Genetic Risk Factors

Early-onset familial Alzheimer's disease (EOFAD) and late-onset sporadic Alzheimer's disease (LOAD) are the two groups into which genetic risk factors for Alzheimer's are classified (Bird, 2018). The EOFAD is rare, which occurs before the age of 65, is caused on by mutations in specific genes, Amyloid precursor protein (APP) on chromosome 21, Presenilin 1 (PSEN1) on chromosome 14, and PSEN2 on chromosome 1, and is inherited as autosomal dominant disease (Bird, 2018; Van Cauwenberghe et al., 2016). Familial AD is genetically found to be linked with the missense mutation of either APP or Presenilin (Thinakaran, 1999). The APP gene is type I membrane protein involved in synaptic formation, neuronal growth and repair (TCW & Goate, 2016). The mutation of APP results in the substitution of the amino acid Valine (Val) by Isoleucine (Ile) close to the carboxy

terminus of beta amyloid peptide (Brouwers et al., 2008). Various mutations have been classified including, Swedish ($APP_{670/671}$), Dutch (APP_{693}), Flemish (APP_{692}), London (APP_{717}), and Florida (APP_{716}) mutations (Bi et al., 2019; Hardy, 1997). There are three distinct secretase cleavage locations where these mutations might occur, before the β-secretase site, around the α-secretase site, or close to the γ-secretase site (MacLeod et al., 2015). These missense mutations lie in the vicinity of proteolytic processing of APP and change how APP is normally processed. Down syndrome is another cause of APP overexpression and presence of an extra chromosome 21 leads to the overproduction of Aβ (Head et al., 2015; TCW & Goate, 2016). The most common cause of familial AD is missense mutation in PSEN gene, and these mutations results $Aβ_{42}/Aβ_{40}$ ratio increase either by rising $Aβ_{42}$ levels or by decreasing $Aβ_{40}$ levels (Zou et al., 2022).

On the other hand, genetic variants like as the Apo-lipoprotein E (APOE) and other risk-associated genes identified through genome-wide association studies (GWAS) influence LOAD, which is more common and happens after the age of 65 (Armstrong, 2019). The APOE gene is involved in making a protein, apolipoprotein E (apoE) that helps carry cholesterol and other fats in the bloodstream (Armstrong, 2019). The human APOE is a 299 amino acid glycoprotein and abundantly expressed in the astrocytes, vascular mural cells, and microglial cells. It is located on chromosome 19 with three polymorphic alleles (ε2, ε3 and ε4) (Chen et al., 2017). The least prevalent allele, APOE-ε2, is the least prevalent allele, linked to a lower risk of AD and provides neuroprotection through improving lipid transport and synaptic plasticity. The most common allele, APOE-ε3, is believed to be neutral and has no evident effect on AD risk (Liu et al., 2013). APOE-ε4 is the major genetic risk factor for late-onset AD, which increases the probability of developing the disease and accelerates cognitive loss by boosting amyloid-beta deposition, neuroinflammation, and vascular dysfunction (Liu et al., 2013).

Neuropathological and clinical studies have shown that Aβ homeostasis and metabolism are significantly associated with APOE genotype (Hampel et al., 2021). APOE is crucial in the mechanism of Aβ clearance and interact with Lipoprotein receptor-related protein 1 (LRP1) to facilitate the transport of Aβ across the blood-brain barrier into blood circulation and RAGE (Receptor for advanced glycation end products) aid in Aβ transport

out of the blood-brain barrier toward the peripheral movement into the brain (Ries and Sastre, 2016). Disruption of Aβ clearance is triggered by the gene alteration of the proteins, therefore, Aβ growth signs toward the development of AD (Selkoe & Hardy, 2016). The risk of Alzheimer's disease is also further modulated by epigenetic changes caused about by environmental and lifestyle factors. Early detection of high-risk patients and the development of targeted treatments depend on an understanding of these genetic and epigenetic variables (Bufill et al., 2020).

1.7. Lifestyle

Several modifiable lifestyle factors like smoking, poor diet, low level of education, and lack of exercise have been identified as risk factors for AD, (DeTure and Dickson, 2019). Physical activity is shown to slow down the progression of AD and enhances neurogenesis, reduce inflammation and oxidative stress. It also helps regulating other disease which are the risk factors for AD like diabetes, obesity and cardiovascular health (Pahlavani, 2023; Wang et al., 2014). Diets high in saturated fats, trans fats, and refined sugars are linked to increase inflammation and oxidative stress, which play key role in the development of AD (Tan & Norhaizan, 2019). The studies have shown that Mediterranean diet and Vitamin D intake are associated with the reduction of risk of AD (Bhuiyan et al., 2023). Cigarette smoking has been known as a risk factor for several diseases and has been proven as a risk factor for AD, as the study suggested that smoke induced oxidative stress and pre-AD like pathological changes in the rat brain (Ho et al., 2012; Durazzo et al., 2014). Several studies showed the impact of cigarette smoking on AD and other diseases like cardiovascular and diabetes (Śliwińska-Mossoń & Milnerowicz, 2017; Roy et al., 2017).

Antecedent	Direction	Possible mechanisms
Cardiovascular disease	Increased	Parenchymal destruction, strategic location, Aβ deposition
Smoking	Increased	Cerebrovascular effects, oxidative stress
Hypertension	Increased risk of AD in midlife hypertension and may decreased risk of AD in later life	Microvascular disease
Type II diabetes	Increased	Cerebrovascular effect, Insulin and Aβ compete for clearance
Obesity	Increased	Increased risk of type II diabetes, inflammatory
Traumatic head injury	Increased	Increased Aβ and amyloid precursor protein deposition
Education	Decreased	Provides cognitive reserve
Leisure activity	Decreased	Improves lipid metabolism, mental stimulation
Mediterranean diet	Decreased	Antioxidant, anti-inflammatory
Physical activity	Decreased	Activates brain plasticity, promotes brain vascularization

Table 1: Lifestyle factors and diseases that alter risk for AD (Adapted from Mayeux and Stern, 2012).

Number of studies showed that age is the most important factor associated with AD and cognitive decline and mostly people develop AD when they are 65 or older. The prevenance of AD increased with the age and only 10% of people below the age of 65 are affected with AD (Armstrong, 2019). The relationship among age-dependent disorder and inflammation, oxidative stress, inflammation from cytokines and chemokines, is known to play a key role in maintaining the chronic inflammation and are other important factors involved in the pathogenesis of AD (Tangestani Fard and Stough, 2019).

1.8. Pathogenesis

There are number of other factors involved in progression of AD. The enzymes used for the breakdown of Aβ involves, Neprilysin (NEP) and Insulin degrading Enzyme (IDE) (Yamamoto et al., 2021). These enzymes instigate catabolism and reduce the levels of Aβ in the brain NEP is a type II membrane-anchored peptidase and mainly expressed in pre-synaptic terminal of neurons. However, IDE is most prevalent in cystol and can be exported to the extracellular space by neurons and glial cells (Folch et al., 2016). Levels of NEP and IDE declines in normal brain due to aging and have been shown to correlates with Aβ-related pathology (de Dios et al., 2019).

Studies have shown that neuroinflammation plays a crucial role in neurodegenerative disorders. Neuroinflammation promotes Aβ plaque deposition and tau hyperphosphorylation. It is described by increased activated glial cells and proinflammatory cytokine, chemokines and complement proteins (Ribarič, 2018). Proinflammatory factors lead to excessive activation of astrocytes to produce a multitude of inflammatory factors, cytotoxic substances and decline the secretion of neurotrophies, for instance, brain-derived neurotrophic factors (BDNF) (Min et al., 2015). BDNF is highly involved in the synthesis of neurotransmitters, neurogenesis and protects neurons from damage, which can lead to cognitive performance. By activating tyrosine receptor kinase B (TrkB) receptor, BDNF exerts the above biological effect. Studies have found that compared to healthy controls, patients with AD exhibited significantly lower serum of

BDNF (Luo et al., 2019). From these observations, it is assumed that treatments of BDNF upregulation or anti-inflammatory may be useful for Alzheimer's disease.

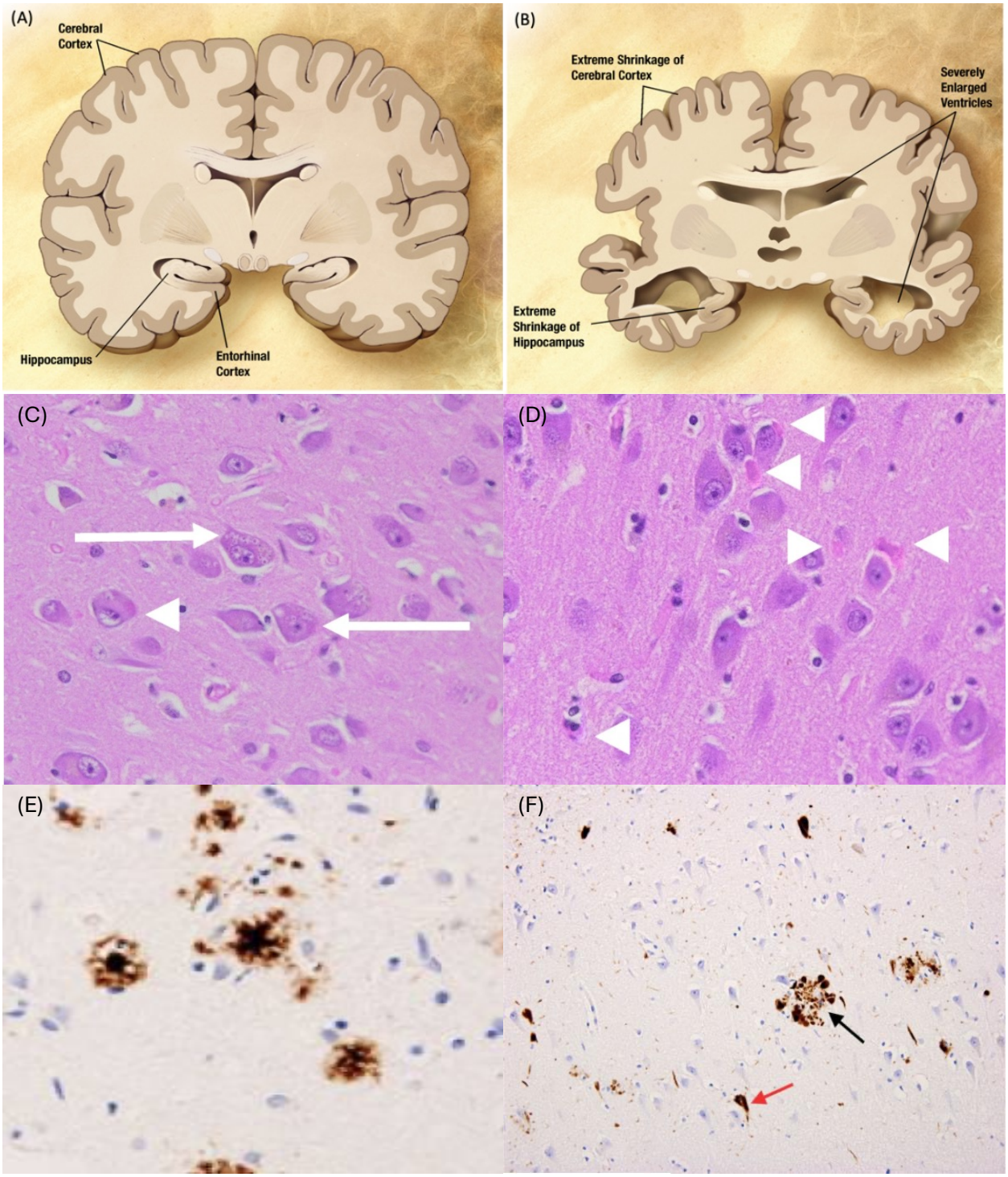

Figure 1: Morphological and histological changes in brains of AD patients (Perl, 2010; *DeTure & Dickson, 2019)*).

Figure 1 shows that (A) under normal conditions the brain mass and volume remail unaltered and wee- structured but (B) under pathological condition of AD, hippocampal and cortex region shrink, loss of cerebral mass and enlarged ventricles. (C) Representative hematoxylin and eosin (H&E) stained section displaying neurons with numerous vacuoles housing a dense granule indicated by arrows, (D) Hirano bodies are often observed as eosinophilic pink rods within the neurons. (E) Temporal cortex of a patient with Alzheimer's disease (immunohistochemical stain; original magnification, 100×) illustrates several senile plaques present in this case of advanced AD and shows the extent of amyloid accumulation and (F) Temporal cortex of a patient with Alzheimer's disease (immunohistochemical stain; original magnification, 100×) shows neurofibrillary tangles (red arrow) and swollen dystrophic neurites that form the outer edge of the senile plaques (black arrow).

The major cause for the progression of AD pathogenesis was known to be the imbalance of intracellular reactive oxygen species and the defense mechanism of antioxidants (Aliev et al., 2008). Therefore, this leads to an increase of several oxidants and lower antioxidants levels in the brain (Forman, Zhang and Rinna, 2009). The most abundant endogenous antioxidant in brain cells is known as glutathione (GSH) which assists in the removal of reactive oxidative species. The GSH reacts with ROS and produces glutathione disulphide (GSSG) by oxidising its products. The main cause of the production of ROS in AD patients is mitochondrial dysfunction (Fang, Yang and Wu, 2002). During normal metabolism pro-oxidants produce ROS including hydrogen peroxide and superoxide anion (Zhu et al., 2004). Excessive production of these two ROS can lead to damage to tissues, proteins, amino acids and nucleic acids (Zhu et al., 2004). The anti-oxidative defence system is responsible for the removal of ROS and intracellular Tau Tangles and extracellular amyloid-beta plaques are considered to have major roles in the process of age-related neurodegeneration and cognitive decline.

The glycogen synthase kinase 3 beta (GSK3) is an active serine/threonine kinase that involves in glycogen metabolism to gene transcription process (Hooper, Killick and Lovestone, 2007). This protein-coding gene is associated with the development of amyloid-beta plaques and tau tangles. Studies have demonstrated that GSK3 becomes

activated during early AD and shows an elevated production of tyrosine phosphorylation in the brain (Kremer, 2011). The findings predicted that GSK3 is contributing to the pathogenesis of AD.

The mammalian target of rapamycin (mTOR) plays an essential role in balancing protein synthesis and degeneration. In contrast, the mTOR pathway in the nervous system controls synaptic restoration and long-term potentiation (Yates et al., 2013). Yates et al. highlighted that there is a link between activated mTOR and the accumulation of extracellular amyloid-beta plaques and intracellular tau tangles (2013). The downstream of mTORC1 gene expression has demonstrated lower expression of beta-amyloid therefore, further research is required to identify the signalling pathway of mTORC1 associated with the decline in AD (Yates et al., 2013).

1.9. Pathophysiology

There are diverse theories about pathophysiological mechanisms of AD leading to neurodegeneration. The main mechanisms of AD are amyloid cascade hypothesis, tau hypothesis, mitochondrial cascade hypothesis, oxidative stress hypothesis and insulin resistant hypothesis (Zhang et al., 2024).

1.9.1. The amyloid hypothesis

1.9.1.1. Amyloid Precursor Protein (APP)

AD is classified as a leading cause of dementia and cognitive deficit, accounting for 60-80% cases worldwide. A key hallmark of AD is the accumulation of Aβ in hippocampus and it is closely associated with memory impairment. Elevated levels of Aβ disrupt the

neuronal function and lead to cognitive deficit (Aminyavari et al., 2019). Amyloid cascade hypothesis is a combination of failures in amyloid production, degradation, and clearance. Amyloid precursor protein (APP) is a transmembrane glycoprotein, undergoes proteolytic cleavage via two pathways non-amyloidogenic and amyloidogenic (Lansdall, 2014). In regular circumstances, the non-amyloidogenic pathway occurs, and it involves a cleavage of APP by α-secretase at amino acid position 16 and 17 and generate C83 (83 amino acid Carboxy-terminal fragment) and sAPPα (extra-cellular N-terminus ectodomain) (Kametani and Hasegawa, 2018). Then the C83 fragment residual in the membrane is cleaved by γ-secretase and products P3 fragment and CTF (C terminal fragment). sAPPα has neurotrophic and neuroprotective characteristics that promote neuronal survival and plasticity by shielding neurons from oxidative stress and excitotoxic shocks (Habib et al., 2016).

In the neurotoxic condition, the amyloidogenic pathway take place and β-secretase cleaved the APP to produce sAPPβ and a membrane 99 C-terminal (C99) (Lansdall, 2014). The γ-secretase cleaved the persisting C99 in the membrane to form Aβ protein 1-40 residues and more prone to accumulate to cause neurotoxicity leading to AD development (Kametani and Hasegawa, 2018). $A\beta_{40}$ including 40 amino acids and $A\beta_{42}$, including 42 amino acid remains, are key factors for the accumulation of Aβ. The Aβ amyloid fibril formation is produced by the growth in the proportion of $A\beta_{42}$, and the collected Aβ fibrils grow into senile plaque, which initiate aggravation of tau pathology and neurotoxicity. The neurotoxicity and aggravation in tau pathology lead to deaths of neurons and neurodegeneration (Kametani and Hasegawa, 2018).

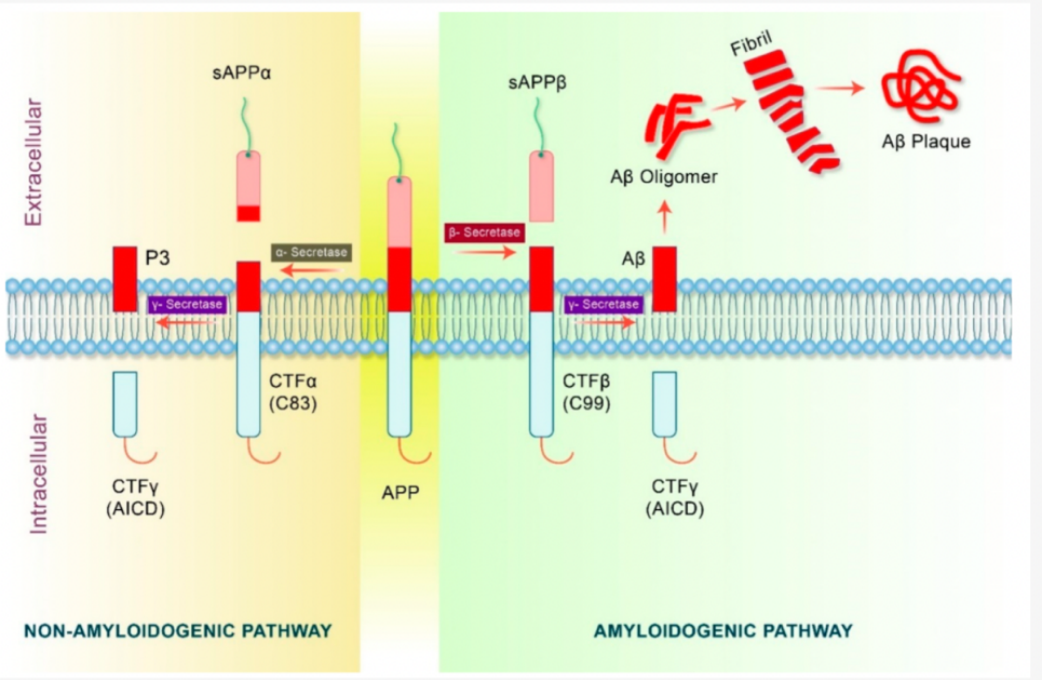

Figure 2: Amyloidogenic, and non-amyloidogenic pathway (Rahman et al., 2020).

Two pathways are included in the of precursor protein (PP) cleavage, non- amyloidogenic, and amyloidogenic. This figure shows that the PP processing and cleavage products. In amyloidogenic pathway APP is cleaved by β-secretases and generate C terminal fragments including carboxy-terminus fragment β (CTFβ) (C99). The β-secretase and APP are initially internalised into an endosome. For cleavage of APP by β-secretase which results in carboxy-terminus fragment β (CTFβ) and soluble APP fragment β (sAPPβ) requires an acidic environment which is ideal inside the endosome. CTFβ is then cleaved by γ-secretases, developing in APP intracellular cytoplasmic domain (AICD) and the Aβ segment. Through exocytosis, Aβ and sAPPβ are discharged into the extracellular space. Aβ fragments oligomers and fibrillates leading to the pathology of AD.

In the non-amyloidogenic pathway, APP is cleaved via α-secretase, which then results into the carboxy-terminus fragment (CTFα) and soluble APP fragment a (sAPPα). Next the l-secretases cleaved CTF83, resultant in APP intracellular cytoplasmic domain (AICD) and soluble peptide p3. The absence of endothelial nitric oxide (eNO) in the brain upsurges the amount of APP and β-site APP-cleaving enzyme 1(BACE1) expression, which leads to the growth in the production of Aβ. Whereas, these procedures are

repressed and the amount of Aβ reduces in the occurrence of eNOS and NO production (Austin et al., 2010).

1.9.1.2. Aβ clearance and degradation

Aβ clearance plays a key role in the pathological features of AD and in healthy brains (Yamamoto et al., 2021). Aβ is removed through blood brain barrier (BBB), enzymatic degradation and microglial phagocytosis (Lee & Landreth, 2010). NEP and IDE are the key enzymes involved in the degradation of Aβ (Yamamoto et al., 2021). BBB regulates the Aβ clearance via low density lipoprotein receptor-related protein 1 (LRP1). Aβ is transported by LRP1 across BBB, and it bonds to the number of ligands like APP, apoE, and α2-macroglobulin. LRP1 promotes Aβ efflux from the brain into circulation, whereas Receptor for Advanced Glycation End Products (RAGE) mediates Aβ influx, contributing to the accumulation in AD (Lee & Landreth, 2010).

The impaired BBB function leads to the disruption in Aβ degradation and induce neurotoxicity (Che et al., 2024). The endopeptidase IDE and NEP plays key role in the degradation of the Aβ (Holscher, 2005; Yamamoto et al., 2021). These enzymes break down the Aβ monomer into non-toxic fragments. Furthermore, Aβ interacts with microglia's LRP1 and Toll-like receptors (TLRs), initiating intracellular signalling cascades that aid in phagocytosis (Lee et al., 2010). As this process is slow the toxic Aβ fibrils may accumulate starts the degenerative processes in AD (Lee et al., 2010).

1.9.1.3. Aβ Toxicity

Under normal condition, Aβ is produced and cleared efficiently, and involved in the synaptic plasticity, antimicrobial defence and neuronal repair in normal brain (Sadigh-Eteghad et al., 2014). The excessive deposition of Aβ in the extracellular space is the key

hallmark of the AD. There are number of forms of Aβ but $A\beta_{42}$ is known to be the most toxic form and aggregates more quickly than $A\beta_{40}$ (Azargoonjahromi, 2024). Studies have demonstrated that $A\beta_{42}$ can also accumulate and aggregate in neurons which lead to the synaptic loss, axonopathy and death of neurons (Lansdall, 2014). Aβ lead to chronic inflammation and memory deficit by impairing long term potentiation (LTP) (Srivareerat et al., 2011). Aβ also triggers activation of microglial and astrocytes and disrupts the mitochondrial function. Aβ toxicity promotes tau phosphorylation that leads to the formation of neurofibrillary tangles, another hallmark of AD (Sadigh-Eteghad et al., 2014).

1.9.2. Tau hypothesis

The hyperphosphorylation of tau to generate the neurofibril tangles (NFT) is the key hallmark of the AD. Tau is an extremely soluble microtubule-associated protein (MAP) that plays a function in the elevation and maintenance of tubulin association into microtubules-site specific phosphorylation (Mietelska-Porowska et al., 2014). It is abundantly present in central nervous system (CNS), predominantly associated with axonal microtubules and present at lower end in dendrites (Mietelska-Porowska et al., 2014).

Under normal conditions, tau undergoes controlled phosphorylation to ensure smooth function. However, in AD patient's tau undergo hyperphosphorylation through an initiation of cyclin-dependent kinase (CDK), and glycogen synthase kinase (GSK) (Mohandas et al., 2009). The detached tau from microtubules changed into the NFT and paired helical filament (PHF) tau. It activates deterioration of microtubules leading to damaged axonal transport, disrupts microtubule stability and leads ultimately to neuronal cell death (Mohandas et al., 2009). The microglial and astrocytes are activated when the tau filaments are released into the extracellular space leading to neuronal cell death in AD (Vogels et al., 2019). The misfolding of the tau protein and the principal origin of AD appears later to Aβ plaque development (Lansdall, 2014).

1.9.3. The mitochondrial cascade hypothesis

Mitochondrial dysfunction in Alzheimer's is the primary factor, progressing and worsening hallmarks of AD like Tau hyperphosphorylation and amyloid-beta accumulation (Wang et al., 2020). The dysfunction of mitochondria promotes tau phosphorylation that disrupts the microtubule and neuronal transport and increases the amyloidogenic processing of APP (Rajmohan & Reddy, 2017). As the age increases, the mitochondrial potential decreases, leading to the impaired ATP proception and rise in ROS. The excessive production of ROS leads to oxidative stress and inflammation (Maldonado et al., 2023). Accumulation of Aβ is triggered by mitochondrial dysfunction, which in turn disrupts mitochondrial function and causes neuronal toxicity (Swerdlow and Khan, 2004; Swerdlow, 2018). Number of studies have focused on the mitochondrial dysfunction and progression of AD either as a primary driver or as a Aβ toxicity (Wang et al., 2020).

1.9.4. Oxidative stress hypothesis

In the progression of AD oxidative stress is also recognised to trigger neurodegeneration and neuronal loss is a hallmark of the progression of AD (Vogels et al., 2019). Increased ROS is observed in the brain affected by neurodegenerative disease. The brain is more susceptible to the oxidative stress induced damage due to lower levels of the antioxidant enzymes present in the brain compared to other tissues (Wang et al., 2014). Several factors are involved in the oxidative stress like tissue injury, Aβ aggregation, cytokines and mitochondrial dysfunction (Wang et al., 2014). In case of AD, oxidative stress plays key role in neuronal loss or neuronal dysfunction due to the Aβ aggregation and accumulation of tau NFTs in the brain (Luo et al., 2019).

1.9.5. Calcium hypothesis

Calcium ions (Ca^{2+}) are essential for neuronal functions, synaptic plasticity and cellular homeostasis (Brini et al., 2014). Calcium levels in healthy brain are regulated tightly by intracellular stores such as calcium binding proteins, ER, and mitochondria (Zündorf & Reiser, 2011). However, in AD this regulation is disrupted and lead to abnormal increase in intracellular calcium levels (Ge et al., 2022). Studies have shown that number of factors can be involved in the dysregulation of calcium levels like Aβ oligomers, tau and uncontrolled calcium reflux (Ge et al., 2022). Increased calcium levels disrupt the function of mitochondria, activate apoptotic pathways and increase the production of ROS that leads to the neuronal death and damage (Moon, 2023).

1.9.6. Insulin resistance hypothesis

Insulin receptors are abundantly expressed in brain and neuronal growth and survival, metabolism, protein synthesis, differentiation, synapses plasticity a formation is significantly influenced by insulin and Insulin like Growth factor1 (IGF-1) (de la Monte, 2012). Energy homeostasis and memory formation are regulated by insulin and its receptors in healthy brain, however in the brain of AD the neurons become resistant to insulin (Sędzikowska & Szablewski, 2021). Insulin resistance leads to the reduced activation of the key insulin signalling pathways which then leads to mitochondrial dysfunction, oxidative stress, and inflammation.

Studies showed that insulin resistance is not only a key risk factor for diabetes but also contributes to the pathogenesis of AD (Nguyen et al., 2020). A study represented by Jason et al, illustrated that 85% of the AD patients also have type II diabetes. The deficiency of insulin signalling in the brain damages the neurons and leave them more exposed to the toxic influences, it is suggested that insulin can also be the key to develop

neurodegenerative diseases (Hölscher and Li, 2010). Previous studies illustrated that insulin impairments and IGF1 pathways increase the risk of cognitive decline and different forms of dementia. There is several studies performed but the exact mechanism is not known by which it can improve the cognitive function of the brain (Morris and Burns, 2012).

1.10. Therapeutic strategies in AD

After decades of research, Alzheimer's remains incurable, and current available treatments only control symptoms or delay the disease's progression. However, due to the recent developments in therapeutic techniques, there is a hope for a more effective management and disease-modifying interventions. Alzheimer's disease treatment strategy has traditionally focussed on symptom management, addressing behavioural abnormalities, disorientation, and memory impairments.

1.10.1. Current strategies

Cholinesterase inhibitors, such as donepezil, rivastigmine, and galantamine, are approved pharmaceutical treatments that increase cholinergic signalling by preventing the breakdown of acetylcholine, thereby enhancing neurotransmission in the brain, mainly in areas affected by Alzheimer's disease (Birks, 2006). Memantine in the NMDA receptor antagonist, control glutamate activity to avoid excitotoxicity, which can impair neurones. Combination of treatments like donepezil and memantine, are frequently used for moderate to severe stages of the diseases. Although many patients find that these

medications enhance their quality of life and ability to operate daily, they do not stop or reverse the progression of Alzheimer's disease (Kutzing et al., 2011).

Lipoic acid is a disulphide compound which is found naturally, and it is known to have diverse actions in different mechanism. It is recognised to be cofactor for mitochondrial bio generic enzymes. Studies conducted by smith et. al., suggested that lipoic acid is a micronutrient with diverse pharmacological and antioxidant properties (Holmquist et al., 2007). Studies proved that it also works as an anti-inflammatory antioxidant. In the process of AD, chronic inflammation is the main factor which cause the death of the neurons and increase the levels of the pro-inflammatory cytokines and levels of free radicals. Lipoic acid might delay the onset of disease and slow down the progression of the Alzheimer’s disease. it downregulates the release for free radicals and the cytotoxic cytokines (Farr et al., 2012).

Moreover, there is another essential endogenous antioxidant is tocopherol (Vitamin E) which was utilised to treat AD. The vitamin E is an essential micro-nutrient for a human being derived from the diet. A recent research study has found that the levels of tocopherol were low in mild AD patients (Aliev et al., 2008). Therefore, to provide antioxidant protection to the brain, the high tocopherol transfer protein (TTP) gene expression controls the level and secretion of tocopherol (Gugliandolo, Bramanti and Mazzon, 2017).

In recent years disease-modifying treatments have gained significant attention, and two anti-amyloid monoclonal antibodies (MABs), lecanemab and aducanumab have been approved in USA (Cummings, 2023). By reducing the amyloid-beta buildup in the brain, these antibodies are designed to treat main pathophysiological causes of the disease. The studies have shown that these antibody therapies have been effective in the early stage of Alzheimer’s but are controversial due to the high cost and potential side effects (Cummings, 2023).

1.10.2. Apelin-13 a stable novel peptide

Apelin is produced as a 77-amino acid precursor known as preproapelin and it is an adipokine that has been identified as an endogenous ligand for the G-protein-coupled receptor APJ . This precursor undergoes proteolytic processing to generate several active isoforms, including apelin-13, apelin-17, apelin-19, and apelin-36, though apelin-13 is most potent (Falcão-Pires et al., 2010). Apelin and APJ are majorly expressed in several tissues for instance lung, brain, and kidney. Apelin function depends on the interaction of G-protein-coupled to APJ receptor (Reaux et al., 2001).

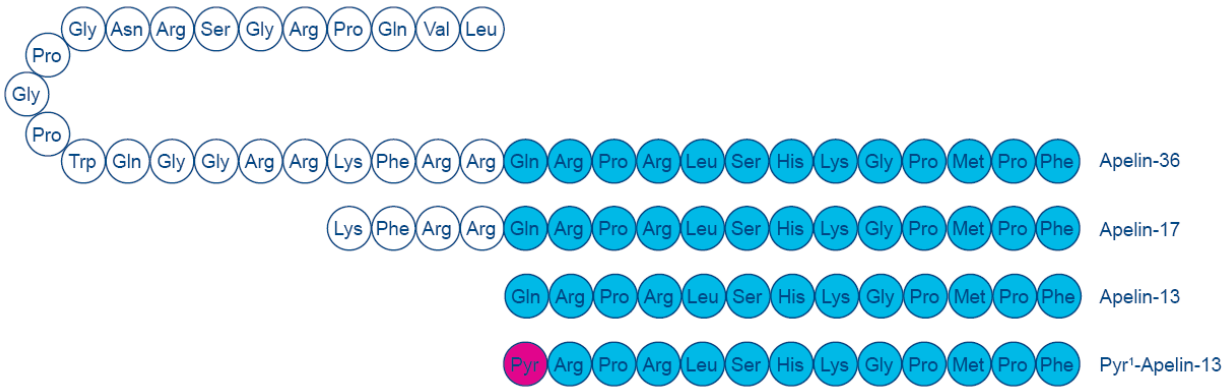

Figure 3: Amino acid sequence of Apelin peptide (Read et al., 2019).

Apelin-13 is a bioactive peptide derived from apelin precursor. It is involved in the regulation of many physiological functions including food intake, glucose utilisation and blood pressure (Reaux et al., 2001). Studies showed that apelin-13 treatments significantly improved the pancreatic insulin release (Habata et al., 1999).

To enhance the stability, bioavailability and therapeutic potential modified forms, Apelin-13 amide and (Lys^{8}GluPal)apelin-13 amide have been developed (Parthsarathy et al., 2017). Apelin-13 is composed of 13 amino acid chain with hydrophilic residue at N-terminus and hydrophobic residue at C-terminus important for APJ binding (O'Harte et al., 2017). The amidation at C-terminus improved biological activity of apelin-13 by reduced enzymatic degradation and improved binding affinity to APJ (O'Harte et al., 2017; Parthsarathy et al., 2017). By adding a palmitoylated glutamic acid at position 8, an

advanced synthetic analogue known as (Lys^{8}GluPal)apelin-13 amide enhances the peptide's lipophilicity and improve its ability to cross the blood-brain barrier, making it a viable treatment option for neurodegenerative diseases like Alzheimer's (O'Harte et al., 2018; Lu et al., 2024).

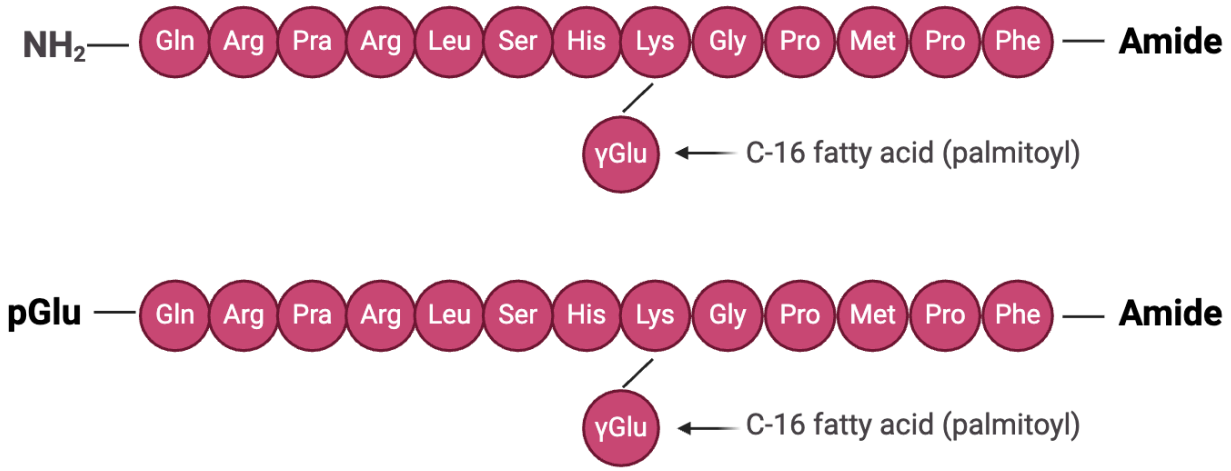

Figure 4: Amino acid sequence of apelin-13 amide and (Lys^{8}GluPal)apelin-13 amide (O'Harte et al., 2017).

Apelin-13 and its analogues have shown the neuroprotective and anti-inflammatory properties. Apelin plays an essential function in energy metabolism by improving insulin sensitivity and glucose intake (O'Harte et al., 2017). Recent research study has denoted that there is an elevated plasma apelin-12 concentration in a diabetic patient which led to increased predisposition (Wysocka et al., 2018). The risk factors of these two overlaps, for instance, the mechanism of diabetes and AD are inflammation, oxidative stress, and mitochondrial dysfunction. Between the mentioned mechanism, brain insulin resistance and amyloidogenic are central for hyperglycaemia-induced impairment of cognitive function (Lee et al., 2018). Oxidative stress, inflammation, and mitochondrial dysfunction are known to exaggerate brain insulin resistance and amyloid beta accumulation in brain injury (Lu et al., 2024). Worsening of neuronal structure and function can lead by the long exposure of hyperglycaemia and hyperinsulinemia as well as high levels of amyloid-beta in the brain, which results in deprived cognitive performance (Lee et al., 2018).

The serum level of apelin-13 drops significantly in AD patients, however, apelin administration plays a neuroprotective role by inhibiting inflammation response, including the activation of microglia and astrocytes and the secretion of inflammatory mediators like TNF-a and IL-1b. APJ combined with apelin can regulate several signaling pathways that are related to BDNF transcription (Luo et al., 2019).

1.11. Cellular stress models

In this study we have used five cellular stress models including palmitate, H2O2, LPS, thapsigargin and $A\beta_{42}$. These cellular stress models play key role to study AD and other neurodegenerative diseases as they mimic key pathological mechanisms observed in disease progression. These models are important for research on AD and neuroscience as they offer a controlled setting for studying disease pathology, evaluating treatments, and increasing the development of new drugs for neurodegenerative diseases.

1.11.1. Palmitic acid

Palmitic acid (PA) is a most common saturated long-chain fatty acid found in the human body as serve as energy storage. It is also known as palmitate and naturally found in both animals and plant fats. PA is produced by the human body from acetyl-CoA and is crucial for lipid metabolism and energy storage. However, studies have demonstrated that higher intake of PA for longer periods generated metabolic impairment and lipotoxicity which cause increase in the inflammatory response of different cells (Unger et al., 2010). PA contributed to the disease progression by neuroinflammation, insulin-resistance, amyloid-beta aggregation and lipotoxicity.

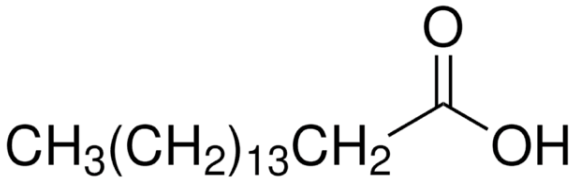

Figure 5: Chemical structure of palmitic acid (Sigma-Aldrich, 2024).

Previous studies indicated that PA induces a pro-inflammatory microenvironment, which is critical to damaging the blood brain barrier (BBB) and after BBB breakdown PA concentration is increased in the brain which leads to the harmful effect to the glial cells. PA induces neuroinflammation by activating toll-like- receptor 4(TLR4) on microglial cells in the brain and the activation of TLR4 leads to the release of pro-inflammatory cytokines like TNF-a and IL-6. These pro-inflammatory cytokines lead to the continued inflammation and neuronal damage.

Studies have stated that excessive palmitate can cause lipotoxicity, defined as a toxic accumulation of fatty acids in the brain cells. By inducing oxidative stress, and mitochondrial dysfunction, lipotoxicity disrupts the cellular mechanism. Palmitate accumulation is known to cause the memory and cognitive impairments by impairing the synaptic functions and altering the lipid metabolism. Palmitate is also involved on the APP palmitoylation, which increases the protein's amyloidogenic processing and leads to the increased production and aggregation of amyloid beta. Additionally, palmitate is involved in the insulin resistance in neurons by impairing the insulin signalling pathways. The triggering cause of PA induced damage in the brain is unknown and its relationship to the neurodegenerative disease is still not fully understood (Vesga-Jiménez et al., 2022). In this study in chapter 3 we have used palmitate as a disease model to induce stress in SH-SY5Y cells.

1.11.2. Hydrogen Peroxide (H_2O_2)

The progression of neuronal damage is derived by one key factor, oxidative stress in AD. Hydrogen peroxide (H_2O_2) is one of the commonly used *in-vitro* approaches to model oxidative stress (Lennicke et al., 2015; Yang et al., 2016). Studies have shown that H_2O_2, mimics the same oxidative stress environment observed in AD (Halliwell et al., 2000). H_2O_2 is the key member of the class of reactive oxygen species (ROS) and is next to the superoxide anion and hydroxyl radical (Milton, 2004). The leak of electrons from the electron transport chain during mitochondrial oxidative phosphorylation, generates superoxide anion and these anions are converted into H_2O_2 by superoxide dismutase (SOD) (Lennicke et al., 2015).

ROS are mostly generated by the respiratory chain cascade but can also be a byproduct of the cellular metabolism, like protein folding (Lennicke et al., 2015). H_2O_2 is a small, unstable molecule that quickly diffuse across cellular membranes and biological systems (Milton, 2004). H_2O_2 is composed of two hydrogen atoms and two oxygen atoms connected by a weak single covalent bond which makes it highly reactive (Andrés et al., 2022).

The effects of the H_2O_2 are dual it plays role as a signalling molecule and mediated of oxidative stress (Milton, 2004). The effects of H_2O_2 are depending on the concentration and its exposure time, as it is known to be involved in many physiological processes like cell differentiation and proliferation (Andrés et al., 2022). The excessive exposure to H_2O_2 overwhelms the defence systems and leads to the oxidative stress, mitochondrial dysfunction, impaired antioxidant systems, overactivation of microglial (Halliwell et al., 2000). Previous research illustrated that H_2O_2 exposure showed to cause loss of mitochondrial membrane potential, impaired the mitochondrial function and activated the apoptosis pathways (Saputra et al., 2024). H_2O_2 also activates the UPR pathway and induce Endoplasmic stress when exposed in excess (Pallepati & Averill-Bates, 2011).

In chapter 4 we have used H_2O_2 to induce stress in SH-SY5Y cells, a neuroblastoma cell line that is widely used to study neurodegenerative diseases. This model is instrumental

to understand the cellular mechanism that underlie oxidative stress caused by H_2O_2 and the role of novel peptide on the rescue of the cells.

1.11.3. Lipopolysaccharide

Lipopolysaccharide (LPS) act as powerful endotoxin and is found in the outer membrane of Gram-negative bacteria (Brown, 2019). Studies shows that it has been the potential contributor to neuroinflammation and neurodegeneration (Azzam et al., 2023). LPS as a stress induced in SH-SY5Y cells is used in chapter 5 to model neuroinflammation. LPS is used commonly in the neurodegenerative research because of its ability to activate immune responses and the production of the pro-inflammatory cytokines (Kar et al., 2022). It is a large molecule composed of three regions, Lipid A (toxic component of LPS), core oligosaccharide (Provide structural stability) and O-antigen (provide antigen diversity) (Brown, 2019).

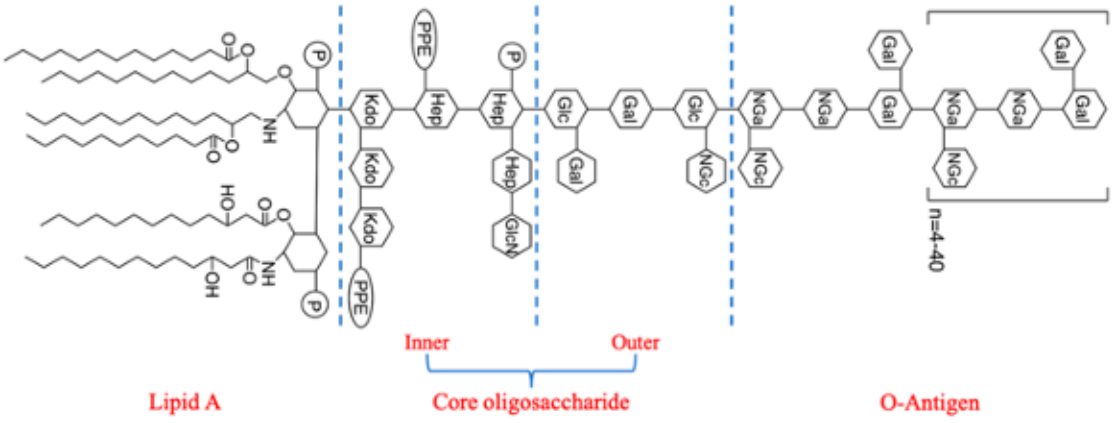

Figure 6: Chemical structure of LPS (Huang et al., 2024).

LPS binds to the TLR4, a pattern recognition receptor and interacts with the immune system like microglial in the brain (Soares et al., 2010). During bacterial infections when

the LPS enters in the brain in normal action it binds to the TLR4 on the surface of microglial cells with the help of co-receptor myeloid differentiation factor 2(MS-2) and CD14 and activates immune response in a controlled manner (Ciesielska et al., 2020; Na et al., 2023). The binding of the LPS with the TLR4 activates the TLR4/MyD88-dependant pathway and TLR4/MyD88-independant pathway (Kuzmich et al., 2017; Soares et al., 2010). The MyD88-dependant pathway activation leads to the activation of nuclear factor kappa B (NF-κB) and mitogen-activated protein kinases (MAPKs), such as ERK, JNK, and p38 and MyD88-independant pathway promotes the production of type I interferons and late-phase inflammatory responses (Kuzmich et al., 2017; Soares et al., 2010; Ciesielska et al., 2020).

To combat the pathogens the pro-inflammatory cytokines like TNF- α, IL-1β, and IL-6 are produced by these pathways. And after the neutralisation the signalling is resolved (Soares et al., 2010). In the normal brain the APP is not significantly affected by LPS but in AD brain the APP possessing and amyloid-beta production is enhanced by LPS (Zhou et al., 2019).

In AD models the LPS causes excessive microglial activation and can trigger a persistent inflammatory response in the brain (Batista et al., 2019). This activation leads to the release of pro-inflammatory molecules, including cytokines and reactive oxygen species, which can cause damage to neurons and contribute to the progression of AD pathology (Ying Wang & Shan Tan, 2015). Studies have shown that excessive LPS leads to the prolonged neuroinflammation and damages the synapses (Kim et al., 2021). LPS leads to the excessive production of the ROS, overwhelms the immune response and leads to oxidative stress and neuronal death (Erridge et al., 2002).

1.11.4. Thapsigargin

Thapsigargin is extracted from plant Thapsia garganica and it is not naturally present in the human body. Thapsigargin is known as a cytotoxin for of its ability to disrupts the

intracellular homeostasis (Askari et al., 2022). It is potent inhibitor of the sarco/endoplasmic reticulum Ca2+-ATPase (SERCA) pump and decreases the amount of calcium stored in the endoplasmic reticulum (ER) (Jaskulska et al., 2020). It is widely used in research to study the ER stress and its effect on the cell death (Ullrich & Humpel, 2009). In chapter 6 we have used thapsigargin to induce the stress in SH-SY5Y cells due to its ability to cause the ER stress and disruption of calcium homeostasis (Ullrich & Humpel, 2009). Thapsigargin has a complex structure, it has a 15-carbon sesquiterpene backbone with multiple oxygen containing functional groups, including lactone rings and hydroxyl groups (Andersen et al., 2015). Because of the hydrophobic side chain, it can easily interact with the lipid bilayer of ER membrane and inhibit SERCA pump (Sehgal et al., 2017).

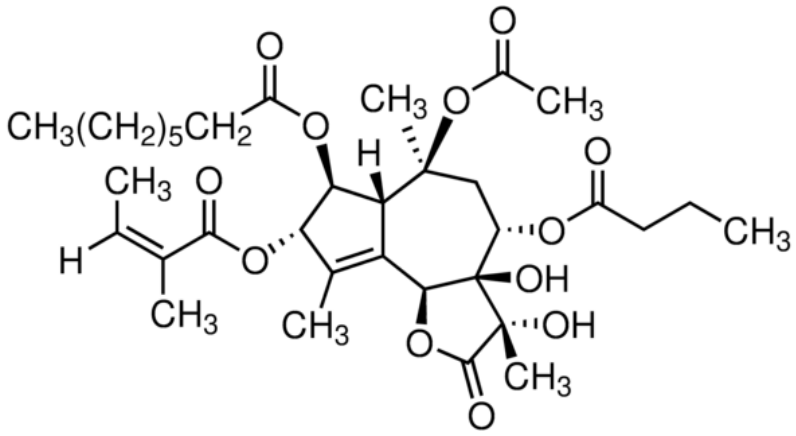

Figure 7: Chemical structure of Thapsigargin (Sigma Aldrich, 2024).

In normal Brain, the SERCA pump maintains the critical calcium gradient by transporting calcium ions from the cytosol into the ER, which is essential for protein folding, cellular signalling and post-translational modifications (Sehgal et al., 2017; Aguayo-Ortiz & Espinoza-Fonseca, 2020). Thapsigargin cause depletion of the calcium stores in ER by binding irreversibly to the SERCA pump and leads to an increase in cytosolic calcium levels and calcium deficit in the ER (Manjarrés et al., 2010; Lindner et al., 2020). The increased cytosolic calcium disrupts the protein folding and triggers the UPR (Lindner et al., 2020). The activation of UPR then upregulates the chaperone protein to refold the misfolded proteins. As a survival mechanism in response to ER stress, Thapsigargin

induces autophagy, However the prolonged exposure to thapsigargin triggers apoptosis and leads to programmed cell death (Takadera et al., 2006).

In AD, the cells undergo ER Stress by increased expression of UPR markers like CHOP (C/EBP homologous protein) to promote apoptosis and ATF-6 **(**Activating Transcription Factor 6) to mitigate cellular stress (Malhotra & Kaufman, 2007). Caspase-12 an ER specific caspase is also activated by thapsigargin to enhance the apoptotic pathways (Morishima et al., 2002). Calcium dysregulation also impacts largely on the mitochondrial function and disruption in ATP production and generation of ROS (Malhotra & Kaufman, 2007).

1.11.5. Amyloid beta-42

Amyloid deposits in the AD brain were the most important early discoveries to understand the aetiology of AD (Findeis, 2007). Amyloid-beta 42 ($A\beta_{42}$) is peptide derived and cleaved from the amyloid precursor protein (APP) (Azargoonjahromi, 2024). $A\beta_{42}$ plays a critical role in the pathology of AD as its tendency to aggregate into oligomers, fibrils and plaques (Azargoonjahromi, 2024). The $A\beta_{42}$ plaques are the key hallmark of the AD and studies have showed that how $A\beta_{42}$ *in-vitro* can be used as a disease model (Lansdall, 2014). To mimic the disease-relevant pathway in SH-SY5Y cells we have used $A\beta_{42}$ in chapter 6. $A\beta_{42}$ is known to be more toxic and more prone to aggregation than the $A\beta_{40}$ a shorter counterpart (Sgourakis et al., 2007). $A\beta_{42}$ is composed of 42 amino acids and the sequence includes the hydrophilic residues at the N-terminus and highly hydrophobic residues at the C-terminus (Sgourakis et al., 2007).

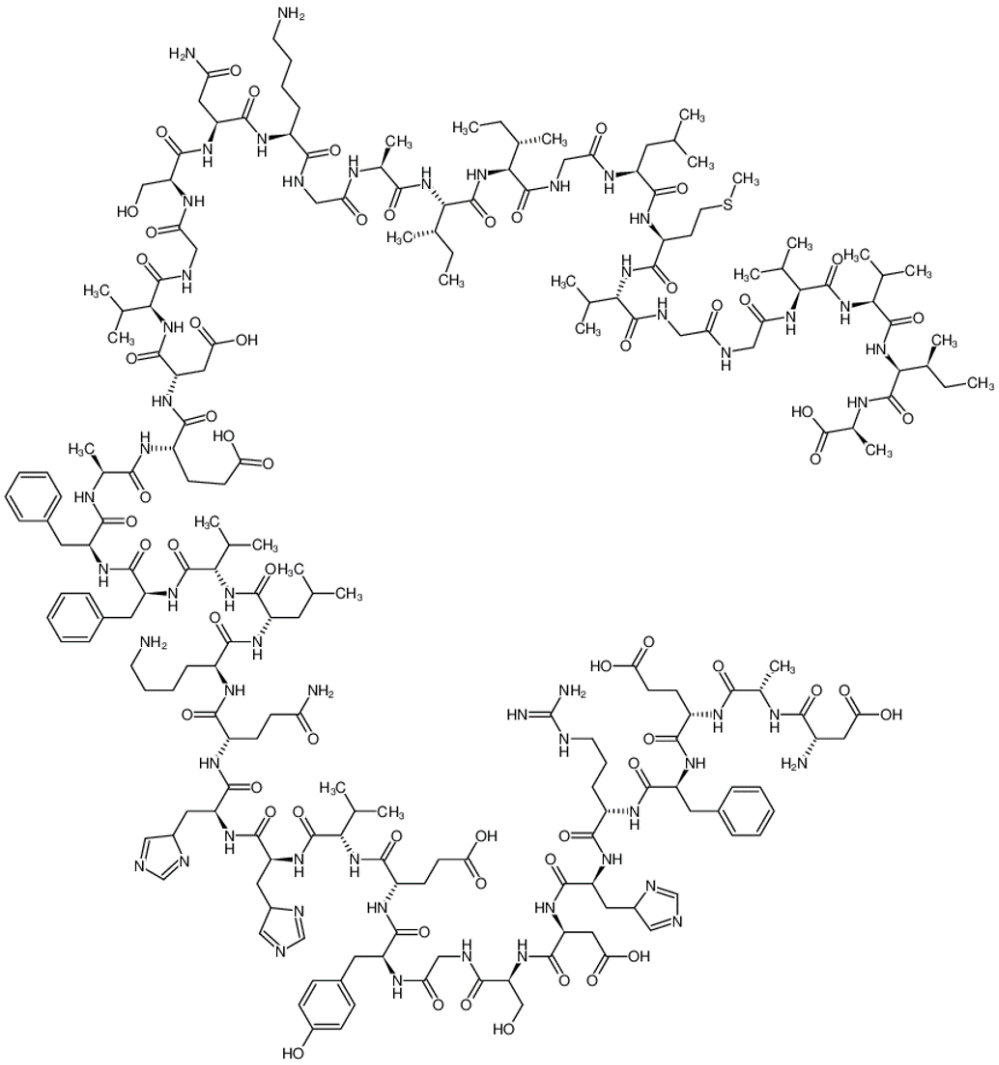

Figure 8: Chemical structure of Amyloid-beta 42 (Echelon Biosciences, 2024).

In the healthy brain, $A\beta_{42}$ production involves the enzymatic cleavage of APP through amyloidogenic and non-amyloidogenic pathways (Findeis, 2007). The soluble form of $A\beta_{42}$ plays role in synaptic plasticity and neuronal signalling, however when the balance is disrupted and the production of $A\beta_{42}$ is overwhelmed, $A\beta_{42}$ begins to accumulate (Azargoonjahromi, 2024). The accumulation of $A\beta_{42}$ leads to the aggregation to form oligomers and then aggregates into insoluble fibrils and plaques. the neuronal connectivity is disrupted by $A\beta_{42}$ aggregation, and it activates the glial cells leading to chronic inflammation (Lansdall, 2014; Sadigh-Eteghad et al., 2014). Oligomeric $A\beta_{42}$ is

specifically harmful as it damages synaptic transmission and promotes calcium dysregulation in neurons (Azargoonjahromi, 2024; Findeis, 2007). By triggering the inflammatory responses, oxidative stress and disruption in the synaptic functions the $A\beta_{42}$ disturbs the homeostasis of neurons (Sadigh-Eteghad et al., 2014).

The goal of this thesis is to analyse the proliferative, antioxidant, and neuroprotective properties of these bioactive peptides and to pinpoint the intracellular pathways via which they exert these effects (De La Monte, 2009). Apelin is crucial in the treatment of neurodegenerative disorders. Numerous investigations concluded that apelin is similarly distributed throughout the central nervous system and that apelin expression levels in the CNS have significantly changed in response to neurological injuries. Studies showed that the CNS has APJ receptors and that apelin binds to the APJ and activates protein kinase B (Akt) and extracellular signal-regulated kinase (ERK) in a variety of cell proliferation or migration processes (Aminyavari et al., 2019).

1.12. Aim and objectives

The project aims to investigate the neuroprotective effects of a novel stable Apelin-13 analogues on neuronal cell protection, proliferation, and differentiation. By inducing cellular stress, we seek to evaluate how apelin-13 amide and (Lys^{8}GluPAL)apelin-13 amide modulates key pathways involved in the neuroprotection. This research is focused to determine whether apelin-13 analogues can mitigate the neuronal dysfunction and apoptosis triggered by the stressors, providing insights into its therapeutic potential for AD.

The key objective of the proposed research is to:

1) Evaluate the effects of novel stable apelin-13 amide and (Lys^{8}GluPAL)apelin-13 amide) peptide in neuronal stem cell proliferation and differentiation in *in-vitro* SH-SY5Y neuroblastoma cells.

2) Evaluate the neuroprotective effects of apelin-13 amide and (Lys^{8}GluPAL)apelin-13 amide against oxidative stress, lipotoxicity, ER stress and apoptosis *in-vitro* in SH-SY5Y neuroblastoma cells.

3) Evaluate the effects of apelin-13 amide and (Lys^{8}GluPAL)apelin-13 amide on beta-amyloid aggregation.

Chapter 2

Materials and Methods

2.1. Materials

Most of the reagents mentioned in this study, unless specified , were purchased from Sigma Aldrich Co Ltd, Fisher Scientific UK, Abcam plc, biorad, cell signalling, and Scientific Laboratory Supplies. SH-SY5Y cells were donated by Ulster University, Belfast, UK and pCS2+MLS-HyPer7 Plasmid (136470) was shared by the colleagues from University of Derby.

2.1.1. Thermo fisher scientific UK

Gibco™ DMEM/F-12 (11320033),), Gibco™ Opti-MEM™ Reduced Serum Medium

10149832), Foetal bovine serum (FBS – 15517589), Gibco™ Trypsin-EDTA (0.25%), Phenol red (11560626), Gibco Penicillin-Streptomycin (10,000 U/mL) (15140122), Invitrogen™ JC-1 Dye (Mitochondrial Membrane Potential Probe) (2524157), Lipofectamine™ 2000 Transfection Reagent (10696153), Lipofectamine™ RNAiMAX Transfection Reagent (13778030), bovine serum albumin (BSA – BP9702-100), Paraformaldehyde, 4% w/v aq. soln., methanol free (047392.9M), BrdU (5-Bromo-2´-Deoxyuridine) (B23151), Formic Acid 99%+ 10x 1mL ampules (28905), Thapsigargin ≥98% (HPLC), solid film (T9033-1MG), Triton X-100, Thermo Scientific™(11488696), Pierce Protease and Phosphatase Inhibitor (15624189), Glycine (White Crystals or Crystalline Powder (10061073), Tris(hydroxymethyl)aminomethane (10424521), Sodium dodecyl sulphate, for molecular biology, ≥98.5% (GC) (10593335), Page Ruler™ Plus Prestained Protein Ladder, 10 to 250 kDa (11852124), Hoechst 33342 Solution (20 mM)(10150888), Ethanol, 70%, for molecular biology (BP8201-500ml), CyQUANT™ LDH Cytotoxicity Assay (C20300), CyQUANT™ MTT Cell Viability Assay (V13154), Invitrogen™Nuclease-Free Water (10429224) , siRNA custom-made AMPK,AMPKa1 sequence 5'->3' Sense (GGUUGGCAAACAUGAAUUGtt) Antisense (CAAUUCAUGUUUGCCAACCtt), Goat anti-Rabbit IgG (H+L) Cross-Adsorbed

Secondary Antibody, Alexa Fluor™ 568 (A-11011), Goat anti-Mouse IgG (H+L) Cross-Adsorbed Secondary Antibody, Alexa Fluor™ 568 (A-11004), Pierce™ BCA Protein Assay Kit (23225).

2.1.2. Sigma Aldrich Co Ltd

Goat Serum (G9023-10ML), Flourosheild (F618-20ML), DAPI (D9542), Protease and Phosphatase Inhibitor Cocktail (PPC1010), AMPK Inhibitor, Compound C (171260-5MG), Palmitic acid (P0500), Lipopolysaccharides from Escherichia coli O111:B4 (L2639-25MG), Sodium Acetate (S2889), Calcium chloride dihydrate (C7902), sodium borohydride (452882-25g), potassium chloride (P5405-500g), magnesium chloride (208337-100g), potassium phosphate monobasic (P5655-500g), magnesium sulphate heptahydrate (M2773-500g), Hexafluoro isopropanol (HFIP) (920-66-1), Chloroform (2186011), Lipid Peroxidation (MDA) Assay Kit (MAK085-1KT), Immobilon-FL PVDF Membrane (IPFL00010), Hydrogen peroxide solution (H1009), Monoclonal Anti-MAP2 antibody produced in mouse (M4403).

2.1.3. Cell signalling Technology

GAPDH XP® Rabbit mAb (5174S) (WB dilution 1:3000), BiP Rabbit mAb (3177) (WB dilution 1:1000), Calnexin Rabbit mAb (2679) (WB dilution 1:1000), Ero1-Lα (3264) (WB dilution 1:1000), IRE1α Rabbit mAb (3294) (WB dilution 1:1000), PDI Rabbit mAb (3501) (WB dilution 1:1000), PERK Rabbit mAb (5683) (WB dilution 1:1000), Atg5 Rabbit mAb (12994) (WB dilution 1:1000), Atg7 Rabbit mAb (8558) (WB dilution 1:1000), Atg3 Antibody (3415) (WB dilution 1:1000), Bcl-2 mouse mAb (51071) (WB dilution 1:750), Bax Mouse mAb (89477) (WB dilution 1:750), Caspase-12 Antibody (58208) (1:750), ATF-6 Rabbit mAb (65880) (ICC dilution 1:250), NRF2 XP® Rabbit mAb (12721) (WB dilution 1:750, ICC dilution 1:250), AMPKα Antibody (2532) (WB dilution 1:1000), Phospho-

AMPKα (Thr172) Rabbit mAb (2535) (WB dilution 1:1000), AMPK Control Cell Extracts (9158), Anti-rabbit IgG, HRP-linked Antibody (7074) (WB dilution 1:1000), Anti-mouse IgG, HRP-linked Antibody (7076) (WB dilution 1:1000).

2.1.4. Abcam plc and Scientific Laboratory Supplies

MTT Assay Kit (Cell Proliferation) (ab211091), Anti-BrdU antibody [IIB5] (ab8152).

2.1.5. 2B scientific

Impact DAB substrate kit Peroxidase (Z J0714), ImmPRESS HRP Goat Anti- Mouse IgG Polymer kit (Z J1012), Goat serum (Z J0412).

2.1.6. Bio-Rad

4–15% Mini-PROTEAN™ TGX Stain-Free™ Protein Gels, 15 well, 15 µl (4568086), 4–15% Mini-PROTEAN® TGX™ Precast Protein Gels, 12-well, 20 µl (4561085), Trans-Blot Turbo Mini 0.2 µm PVDF Transfer Packs (1704156).

2.1.7. Scientific laboratory Supplies (SLS) Ltd

COOMASSIE BRILLIANT BLUE G 250 (1154440025), Acrylamide/Bis-acrylamide, 30% solution (A3699-5X100ML), Immobilon® Forte Western HRP substrate 500 mL (WBLUF0500), 2-Mercaptoethanol (M3148-25ML).

2.1.8. BACHEM

Amyloid beta-42 (4014447)

2.1.9. Promega Corporation

CytoTox 96® Non-Radioactive Cytotoxicity Assay (G1780), CytoTox™ Green Cytotoxicity Assay (G8741), ROS-Glo™ H2O2 Assay (G8820), GSH/GSSG-Glo™ Assay (V6611), Caspase-Glo® 3/7 Assay (G8091), CellTiter-Glo® Luminescent Cell Viability Assay (G7570).

2.1.10. Synpeptide

Apelin-13 amide (JT-97733), (Lys8GluPAL) apelin-13 amide (JT-87479).

2.1.11. Li-Cor biosciences (Cambridge, UK)

Revert 700 Total Protein Stain (926-11021),Revert 700 Wash Solution (926-11012)

2.1.12. Alfa Aesar

Retinoic acid (44540)

2.2. Methods

This research study is designed and conducted at the University of Derby and the experiments will be performed in the university laboratories. This research study is 100% practical, and no participants are required. All the training for the research methods will be provided by the laboratory technician on how to perform the different techniques for the experiments like measuring cell proliferation, neutrit outgrowth, and oxidative stress.

2.2.1. Ethical Considerations

Before conducting the study, ethical approval has been obtained. As there are no participants involved, there is no need for the consent forms, and debriefing forms. No animals have been used in this study. The risk assessment and COSHH form have been provided for all the laboratory experiments.

2.2.2. Cell Treatments

The apelin-13 analogues were saved at -20 °C in dry powder form. The apelin-13 analogues were dissolved in ultra-pure water and diluted in cell culture media to have the desired concentration. To check the purification of peptides, high performance liquid chromatography was performed using Phenomenex Gemini C18 reverse column. Apelin-13 amide (MW- 1550.9) and (Lys^{8}GluPAL)apelin-13 amide (MW- 1534.8) was used at the concentration of 1000 nM.

The cells were treated with five different stressors to create an AD like environment in SH-SY5Y cells. Palmitate (MW-278.41) was obtained in white powder, and the stock was prepared in warm ethanol at 50 mM concentration. It was stirred at 50 °C until dissolved and stored at -20 °C. The working solution (0.6 nM and 1.0 nM) was prepared by dissolving into warm culture media.

LPS was bought as lyophilised powder and sterile PBS was used to dissolve to make stock concentration of 1 mg/mL. it was aliquoted into small amounts and stored at 4 °C. For cell treatments the stock was diluted with cell culture medium at final working concentration of 30 μg and 50 μg.

H_2O_2 was bought in solution at 30% concentration and was diluted in deionised water to make stock of 0.3%. To treat the cells, it was further diluted with cell culture medium to get 50 μM and 100 μM concertation.

Thapsigargin was received in colorless solid film, and it was dissolved in 20% DMSO at concentration of 1 mM. The stock was aliquoted and stored at -20 °C until use. For the cell treatments the thapsigargin stock was further diluted with cell culture medium at final working concentrations of 10 nM and 100 nM.

$A\beta_{42}$ was received in a lyophilised form and was dissolved in 100% HFIP to a final concentration of 1 mM. HFIP is used to break down pre-formed aggregates and keep the peptide in monomeric form. The powder was vortexed and left overnight for HFIP to evaporate. The powder next day was resuspended in DMSO to prepare 5 mM stock and stored at -20 °C until used. To prepare the working solution of 20 μM the $A\beta_{42}$ stock was diluted in culture media.

2.2.3. Maintenance and Sub-culturing of SHSY-5Y cell line

The SH-SY5Y cells were kindly donated by Dr Irundika Dias, translation medicine research group, Aston University, Birmingham and stored in liquid nitrogen at University of Derby. The SH-SY5Y cells thawed and were cultured in 25 cm^2 in monolayers of DMEM/F12 (Dulbecco's Modified Eagle Medium/Nutrient Mixture F-12) with L-glutamine, phenol Red, and supplements of 1% penicillin and streptomycin (100 units/ml), 5% (v/v), Fetal bovine serum (FBS), and incubated for 2 to 5 days in a humidified environment of 95% air/5-10% CO_2 at 37 °C and transferred to 75 cm^2 flask.

After reaching 60–80% confluence, the cells were passaged once a week with a 1:10, 1: 20 split ratios by discarding the growth medium from 75 cm^2 the flask. The cells were washed with 1x phosphate buffer saline (PBS) before adding 5 mL of Trypsin to cells. Trypsin was incubated for 3 minutes at 37 °C and cells were observed under the microscope for detachment and when the 90% cells were detached from the flask surface, added 10 mL of pre warmed growth medium and tapped the flask gently. The cells were collected in the 15 mL falcon tube and centrifuged at 12000 RPMI for 5 minutes. The supernatant was discarded after centrifugation and fresh 1 mL of growth medium was added to resuspend the cell pellet. A sterile Pasteur pipette was then used to repeatedly pass over the cell pellet to break it up. After that, the cell suspension was divided by 1/3 or 1/5 and distributed evenly between two brand-new 75 cm^2 flasks that each contained at least 15 mL of DMEM/F12 medium. To prevent genetic drift, most of the experiments were conducted in passaging numbers 7-20.

2.2.4. SH-SY5Y cell cryopreservation

The cells were kept in 1 mL cryovials in liquid nitrogen for longer-term preservation and storage until needed. When cells from a 75cm^2 flask reached 90-100% confluence, the cells were washed with PBS and trypsin was added for 5 minutes for cells to detach from the surface at 37 °C. After 5 minutes, fresh DMEM/F12 media was added, and the cells were collected in the new 15 mL Eppendorf and to collect the cell pallet we spin at 12000 RPMI for 5 minutes. The cells were then resuspended in 5 mL of freezing medium (DMEM/F12, supplemented with 5% v/v DMSO), which was then transferred to cryovials for storage. When cells freeze, the use of DMSO in the medium aids in preventing the growth of intracellular and extracellular crystals. These cryovials can should be kept at -20 °C for 2 hours before it is kept at -80 °C for a maximum of 24 hours, if they are used right away or Liquid nitrogen for long term storage.

2.2.5. Cell recovery and thawing from liquid nitrogen

Pre warmed DMEM/F12 medium was added to the 25 cm^2 flask before the cell vials were removed from the liquid nitrogen to avoid the abrupt osmotic shock. The vials were thawed with the hand heat for 1-2 minutes and immediately added to the medium. The surface was cleaned with 70% ethanol to avoid any contamination. The 25 cm^2 flask incubated at 37 °C until it reached 80-90% confluency and the cells were passaged to 75 cm^2 flask and managed until use.

2.2.6. MTT- colorimetric Cell Viability assay

MTT (3-(4,5-dimethylthiazol-2yl)-2,5-diphenyltetrazolium bromide) assay was used to measure the effects of apelin analogues and stressors (Palmitate, H_2O_2, Thapsigargin, and amyloid beta-42) on the viability of SHSY-5Y cells by using CyQUANT ^{TM} MTT Cell Viability Assay Kit (Thermofisher Scientific, UK). This technique was used to assess the cellular enzyme activities, growth, and survival in-vitro in response to peptides and stressors. This assay relies on the conversion of light yellow MTT into purple formazan crystals, which is primarily accomplished by succinate dehydrogenase.

To perform this assay 10,000 cells per well were seeded in 96 well plate and incubated for 24 hours at 37 °C. After 24 hours of seeding the cells were treated with different treatments at different timepoints. The cells were incubated with treatments for 2 hours, 4 hours and 24 hours at 37 °C. After the completion of the time of the treatments 10ul of MTT labeling reagent was added for 4h at 37 °C. Later, 100 μL of solubilisation solution was added to stop the reaction for 4h at 37°C.

An absorbance microplate reader (SPECTROstar Omega) at an absorbance of 570 nm was used to detect the MTT assay, a colorimetric-based analysis in which the capacity of the cells to reduce MTT indicates metabolic activity. By taking the average of the

untreated control (cells without treatment), the percentage of cell viability was calculated. When the sample's absorbance was higher than the control, it indicated cell proliferation, and when it was lower than the control, it indicated cell proliferation inhibition. We used one-way ANOVA where N=3.

2.2.7. Luminesce cell viability assay

The CellTiter-Glo® Luminescent Cell Viability Assay is a straightforward technique used to quantify the number of living cells in a culture by measuring the amount of ATP, which indicates the existence of metabolically active cells. For Luminescent cell viability assay, we seeded 10k cells per well in opaque-walled 96 well plates for 24 hours to grow at 37 °C. After 24 hours the cells were treated with different treatments for 4-24 hours at 37 °C. Following the treatments, the plates were equilibrated at room temperature for 30 minutes and 100 μL of Celltiter-Glo reagent was added to the well and mixed the content on orbital shaker for 2 minutes to induce cell lysis. The plate was incubated at room temperature for 10 minutes to stabilise the luminescent signal and recorded the luminescence at an integration time of 0.25-1 second per well.

2.2.8. Cell toxicity assays

CyQUANT ™ LDH Cytotoxicity Assay Kit by Thermofisher Scientific was used to perform the assay which offers simple and dependable approach for measuring LDH release in the media. LDH is an intracellular enzyme found in several cell types, and it is released into the cell culture medium when the plasma membrane is damaged. The LDH assay was based on the conversion of pyruvate to lactate alongside oxidation of NADH to NAD+. The cells were seeded into 96-well plates at a density of 10k cells/well for 24 hours at 37 °C and after the incubation the treatments were added to the appropriate wells. After the treatment incubations for 2 hours, 4 hours, and 24 hours transferred the supernatant to new 96 well plate in triplicates for each treatment. Then 50 μL of reaction mixture (600 μL

of assay buffer stock solution and 11.4 mL of substrate stock solution) added for 30 minutes at room temperature protected from light. Later, 50 μL of stop solution was added to each well and mixed by gentle pipetting. LDH absorbance was measured using the microplate reader at 490 nm within 1-2 hours. The following formula was used to calculate cytotoxicity (percent): cytotoxicity (percent) = (sample OD-low control OD)/(high control OD-low control OD) 100 (OD: optical density). Each OD value was calculated by subtracting the absorbance value from the background value.

For The CytoTox 96® Non-Radioactive Cytotoxicity Assay we used same number of cells seeding above for 24 hours and treated for 4-24 hours depending on treatments. The assay quantitatively detects the concentration of LDH, and the quantification of LDH released in culture supernatants is conducted by measuring the conversion of a tetrazolium salt into a red formazan product. Production of a red formazan product is proportionate to the amount of LDH released and hence the number of lysed cells. After the treatments the test compound is transferred into new plate and 50 μL of CytoTox 96® reagent is added to each and incubated at RT for 30 minutes. After 30 minutes added 50 μL of stop solution and read the absorbance at 490 nm within 1 hour after adding stop solution.

2.2.8. CellTox™ Green cytotoxicity assay

This assay measures the changes in the membrane integrity due to cell damage or death. The assay uses a unique asymmetric cyanine dye that can't be taken up by living cells but selectively stains the DNA of dead cells. When the dye attaches to DNA in cells that are in a damaged state, the dye's fluorescent properties are significantly increased. Living cells do not cause significant increases in fluorescence. Thus, the intensity of the fluorescent signal generated by the dye's interaction with DNA from dead cells is directly related to the level of cytotoxicity. The cells were seeded for 24 hours and treated for 24 hours at 37 °C. prepared and added 100 μL of CellTox Green Reagent (2X) per well

(Transfer CellTox Green dye to Assay buffer Bottle). To ensure the homogeneity the plate was placed on orbital shaker for 1 minute at 700-900 rpm. Then the plate was incubated at RT for 15 minutes protected from light and fluorescence was read at 485-500 nm_{Em}. The background was corrected, and the untreated control was used to take the average, and the graph was plotted using One-way ANOVA analysis.

2.2.10. Differentiation of SH-SY5Y cells

Cultured SH-SY5Y cells were seeded and incubated according to the experimental design for up to 24 hours and 10 μM Retinoic acid (RA) (add 10 μL of 1 mM stock in 1 mL of media) was added for cell differentiation for 3 days at 37 °C. After 3 days of incubation with retinoic acid the cells were washed with 1X PBS and treated with different treatments for 24 hours and 48 hours at 37 °C.

2.2.11. Neurite outgrowth assay

The cells were seeded at the density of $1X10^5$ /well and differentiated for 24 hours with RA. After the differentiation the cells were treated with treatment for 6-48 hours. Following the treatment incubation, the cells were washed with 1X PBS and fixed with 300 μL of 4% paraformaldehyde for 3-5 minutes. After 3 minutes cells were washed again with 1X PBS twice and stained with Coomassie brilliant Blue 250 (for 500 mL add 1 g of dye, 232.5 mL of methanol, 35 mL of acetic acid in 232.5 mL of diH_2O) for 3 minutes. The wells were washed with 1X PBS 3 times to wash excessive dye. Added 1X PBS to keep cells hydrated and imaged under upright microscope at 20x magnification. The double the body of cell neurite outgrowths were counted, and software Image J was used to analyze the neurite outgrowth data under different treatments. We performed statistical analysis using one-way ANOVA, n=3, 10-15 images per treatment.

2.2.12. Reactive oxygen species measurement (ROS) assay

Cell was seeded at the density of 10,000/well in 96-well white plates to investigate the effect of peptide on the ROS levels using the ROS-Glo™ H_2O_2 Assay by Promega. It is a homogenous, fast and sensitive luminescent assay that measure the levels of H_2O_2, directly in the media. H_2O_2 substrate buffer was thawed and 25 μL of H_2O_2 substrate was added to 2 mL H_2O_2 substrate buffer. H_2O_2 substrate solution was added to each well for 4 hours at 37 °C CO_2. A H_2O_2 substrate is used that directly reacts with H_2O_2 to produce a luciferin precursor. After 4-hour incubation the ROS-Glo detection reagent (Transfer the contents of one bottle of thawed Reconstitution Buffer to the amber bottle of lyophilised Luciferin Detection Reagent to produce Reconstituted Luciferin Detection Reagent) was added to each well and incubated for 20 minutes at RT and luminescence was recorded. By adding the detection reagent, the precursor is converted to luciferin and produce luminescent signal which is proportional to the H_2O_2 present in sample.

2.2.13. GSH/GSSH assay

It is a luminescence-based assay that measure the total and oxidised glutathione in cells. Both measurements of total glutathione and GSSG rely on the reaction in which a GSH probe, Luciferin-NT, is converted to luciferin by a glutathione-S-transferase enzyme, coupled with a firefly luciferase reaction. The intensity of light emitted by luciferase is contingent upon the quantity of luciferin generated, which is, in turn, contingent upon the quantity of GSH present. This results in a luminous signal that is directly proportional to the quantity of GSH present. Both reduced glutathione (GSH) and oxidised glutathione (GSSG) are present in healthy cells, with the majority being in the reduced (GSH) form. Assessing toxicological responses requires monitoring changes in GSH and GSSG levels, which serve as indicators of oxidative stress. These changes can potentially lead to apoptosis or cell death. The cells are seeded 10k/well in 96 well plate and designed in

three sets, for total glutathione, oxidised glutathione and standard curve to optimise cell densities.

After treatment incubation removed the cell culture content and added 50ul of Total glutathione lysis reagent (for volume per reaction add 1 μL of luciferin-NT, 10 μL of passive Lysis buffer, 5X and 39 μL of water) and oxidised Glutathione lysis reagent (for volume per reaction add 1ul of luciferin-NT, 0.5 μL of NEM, 25 mM, 10 μL of passive Lysis buffer, 5X and 38.5 μL of water) to designated wells. Added 50 μL of total glutathione lysis reagent to standard wells as well. Incubated the plate at RT on shaker for 5 minutes and followed by adding Luciferin generation reagent (1.25 μL of 100 mM DTT, 3 μL of Glutathione-S-Transferase and 45.75 μL of Glutathione reaction buffer per well) to all wells. The plate was left on shaker for 30 minutes at RT and 100 μL of Luciferin detection reagent was added to each well. The plate was shaked again for 15 minutes and measured the luminescence.

2.2.14 .Caspase-glo 3/7 assay

Caspase-Glo 3/7 assay is used to detect the caspase-3 and caspase-7 activities in the cells treated with different components. Caspase-Glo reagent is prepared by adding the caspase-Glo buffer in caspase-glo 3/7 substrate. And by adding the reagent the cells undergo lysis which is then followed by the cleavage of the substrate by caspase and the production of a luminous signal by the action of luciferase. Cells were seeded in white-walled 96- well plate for 24 hour and treated for different treatments. The plates were equilibrated at RT and 100 μL of Caspase-Glo 3/7 reagent was added and incubated at RT for 1 hour and measured the luminescence.

2.2.15. Cell proliferation by BrdU staining

All the solutions for this assay were made using a 0.1 M concentration of sodium cacodylate and 0.1 M concentration of sucrose, with a pH of 7.4. The washes were done using sodium cacodylate buffer, unless specified otherwise. The sterile 18mm glass coverslips were coated with poly-D-Lysin and added to the 12 well plate, followed by three washes with the distilled water. SH-SY5Y cells were seeded at the density of 5 x 10^4 cells per well for 24 hours to attach. After 24 hours the cells were treated with the appropriate treatments for 4-24 hours in serum free media. Following the treatments, the cells were washed twice for 5 minutes each with sodium cacodylate and added 10uM of BrdU label (add 10 μL of 10 mM BrdU stock in 10 mL media were added) for 24 hours at 37°C CO_2. The cells were then rinsed twice and fixed with 0.25% glutaraldehyde for 20 minutes. After undergoing two washes, the cells were exposed to 100 mM glycine for a duration of 5 minutes. This was followed by an additional 5 minutes in 10% FBS. Finally, the cells were washed twice and added 0.2% Triton X-100 for a duration of 20 minutes to permeabilize, followed by two washes. Subsequently, the cells were incubated four times with a 1 mg/mL of sodium borohydride. Following two further washes, the cells were subsequently blocked overnight at 4 °C with a 3% BSA solution. Afterward, the cells were incubated with primary antibody Mouse Anti-BrdU antibody (1:250) for a 1 hour at room temperature. Two washed with the sodium cacodylate and the cells were incubated for 1 hour at room temperature protected from light with Anti-Mouse AlexaFluro ® 568 (1:400) fluorescent antibody. After Two washes, the coverslips were placed on glass slides suing vectasheild hard set mounting media with DAPI. The images were captured using Olympus XI83 Inverted fluorescence microscope at magnification 20X and analysed using Image J.

2.2.16. Mitochondrial membrane potential (ΔΨm) measurement

JC-1 dye by Thermofisher was used to measure the membrane potentials in SH-SY5Y cells. SHSY5Y cells at density $5x10^4$ cells/well were seeded into 12 well plate on Poly-D lysin coated 18 mm coverslips followed by washing with 1xPBS twice for 48 hours at 37 °C. Following the 48-hour incubation the cells were exposed to different treatments from 6 hours-24 hours at 37 °C CO_2. After treatment incubation the cells were washed with 1XPBS, and cells were incubated with JC-1 dye (2 μM) (add 1.30 μL of 5 mg/mL stock in 1 mL of media) for 30 minutes and incubate at 37 °C CO_2 in dark. After two washes, cells were fixed with 4% paraformaldehyde for 20 minutes and wells were rinsed twice with 1XPBS. The coverslips were taken out on the glass slides with flourosheild mounting media protected from light. Fluorescent images were captured under the 20X and 40X magnification, enabling the acquisition of images for both green (monomers) (excitation 470 nm, emission 525 nm) and red (aggregates) (excitation 560 nm, emission 595 nm) fluorescence, were taken by using Olympus XI83 Inverted fluorescence microscope and analysed using Image J.

2.2.17. Immunohistochemistry (IHC) for Microtubule Associated Protein-2 (MAP2)

The sterile 22 mm glass coverslips were coated with Poli-D-Lysin for 20 minutes and washed twice with 1x PBS and added to 6 well plates. The cells were seeded at the density of 1 x 10^5 for 48 hours alongside with 10 μM retinoic acid to differentiate the cells. Following the two washed with PBS for 5 minutes the treatments were added for 24 hours at 37 °C CO_2. After the treatments the cells were washed again and fixed with 4% paraformaldehyde for 10 minutes at room temperature. The cells were then rinsed twice with PBS and added 0.1% triton-X-100 for 10 minutes at room temperature with was then followed with washing and quenching with 0.3% hydrogen peroxide for 5 minutes. After

quenching the cells were washed and blocked with 5% goat serum for 1 hour at room temperature. Following the blocking the cells were incubated with mouse Monoclonal Anti-MAP2 antibody in goat serum at 4 °C overnight. Next, the coverslips were washed and incubated with Impress Goat anti Mouse Igg Polymer at 37 °C in dark for 30 minutes. The cells were then incubated with Peroxidase substrate solution for 5 minutes until the desired staining and washed and coverslips were removed to the glass slides to image. Zeiss upright microscope was used to take the images at 20x magnification and analysed using Image J.

2.1.8. Hyper7 Imaging

HyPer7 is a genetically engineered fluorescence sensor that can quickly identify hydrogen peroxide within cells. The composition includes a circularly permuted yellow-fluorescent protein (cpYFP) that has been genetically modified into the N. meningitidis OxyR protein, which contains an extremely sensitive domain for detecting H_2O_2 (Pak et al., 2020).

The 18mm glass coverslips were coated with Poly-D-Lysin for 20 minutes and washed with ultrapure water before seeding cells. Cells were seeded at the density of $5x10^4$ cells/well in 12-well plate for 24 hours at 37 °C and 5% CO_2. After 24 hours the cells were transfected with DNA plasmid pCS2+MLS-HyPer7(mitochondrial). LipofectamineTM 2000 and DNA plasmid were diluted in Opti-MEM in individual tubes, mixed to a 1:1 dilution, and incubated for 5 minutes at Room temperature.

After 5 minutes the tubes were mixed and 0.5 μg of plasmid was added and incubated again for 5 minutes. Fresh media was added to each well and 12 μL of transfection was added cells and incubated for 96 hours with a media change 24 hours after transfection. Before 6 hours to the 96 hours completion, the cells were treated with the 100 μM H_2O_2 at 37 °C and 5% CO_2. Following the treatments, washed the cells with 1 x PBS added 15 μg/mg Hoechst 33342 for 5 minutes, washed and fixed with 4% paraformaldehyde for 20 minutes at room temperature. The wells were washed twice, and coverslips were taken

out on the slides and imaged using Olympus XI83 Inverted fluorescence microscope on GFP channel (excitation 470 nm, emission 525 nm).

2.2.19. Cell viability and cell toxicity with AMPK inhibitor Compound C

Compound C is cell-permeable pyrazolopyrimidine compound that has been used to inhibit against AMPK kinase activity. It has been used in combination with the stressors and the peptides to look at the impact of the peptides on cell viability and cell toxicity with and without compound C. For this assay we seeded 1 x 10^4 cells/well in 96-well white walled plate for 24 hours. Following the incubation 5 μM compound C was added to the designated wells and their set of treatments was left without compound C for 30 minutes at 37°C and 5% CO_2. The cells were then treated with different treatments in triplicates twice for 6 hours and incubated at 37 °C and 5% CO_2. After the treatments the CellTiter-Glo viability assay (2.2.7.) and CellTox Green assay (2.2.9.) was used and the viability and cell toxicity were measured by spectrophotometer.

2.2.20. AMPK-siRNA knockdown with Lipofectamine RNAiMAX

For the knockdown of AMPK, 5 nm of siRNA was used and prepared according to the manufacturer's guide. For cell viability and cell toxicity 60 k/well cells were seeded in 24 well plate with and without transfections for 24 hours at 37 °C and 5% CO_2. After 24h, Lipofectamine™ RNAiMAX was added in Opti-MEM and incubated for 5 minutes at room temperature. After 5 minutes the siRNA was added to the tube and incubated again for 5 minutes. After incubation 300 μL of the transfection was added to each well and incubate for 5 minutes and followed by adding 1 mL of fresh media and incubated for 96 hours in total with treatments. Media was changed 24 hours after transfection and treatments were added 24 hours before the 96 hours completion. After the incubation, Abcam cell

proliferation assay kit was used for cell viability plate and the other plate was used to look for cell toxicity by using the CellTox-96 non-radioactive CellTox kit.

For western blot 120k cells were seeded for 24 hours in 12 well plate. The cells were transfected with 5 nM siRNA for 96 followed by the 24-hour treatment with 20 μM Amyloid beta-42 alone and with transfection. After the treatment the protein was extracted using the methods mentioned before (2.2.) and western blot was performed using AMPKα (2532) (1:1000), Phospho-AMPKα (Thr172) Rabbit mAb (2535) (1:1000) antibodies. AMPK Control Cell Extracts (9158) were used as positive controls for both antibodies.

2.2.21. Protein extraction and Quantification using BCA assay

The Protocol for BCA assay was obtained from Thermofisher Pierce™ BCA Protein Assay Kit protocol. To extract the protein 1 $x10^6$ cells were seeded in 6-well plate for 24 hours at 37 °C and 5% CO_2. After incubation cells were treated with treatments for 24h at 37 °C and 5% CO_2. Later the medium was removed and pre warmed PBS added to wash the cells. 0.25% trypsin was added to cells for 2 minutes to detach the cells from the walls and taken out in 1.5 mL Eppendorf. The cell lysate was centrifuged at 6000 RPMI for 5 minutes and cell supernatant was discarded. Lysis buffer RIPA buffer (25 mM Tris, 150 mM NaCl, 1 mM EDTA, 0.5 mM EGTA, 1 mM NaF, 1 mM PMSF, 1X protease inhibitor cocktail (50-80 mL), 0.01% Triton X-100, pH 7.6), was added to the cell pallet and mixed gently and saved at -20°C.

The total protein concentration in SHSY-5Y cell lysates was determined by BCA assay. The proteins were thawed on ice and centrifuged at 15000 RPMI for 10 minutes before use. Protein standards were created by dilutions of blank, 0.2, 0.4, 0.6, 0.8, and 1mg/ml of bovine serum albumin (BSA) in distilled water to create a linear curve (Figure 2.1). The Total protein was diluted with diH_20 to the ratio of 1:2, and 5 mL of each sample were added to 96 well plate. The working solution was prepared by mixing 50 parts of BCA reagent A in 1 part of reagent B (50:1) and 200 mL of the working solution was added to

each well and left at room temperature for 30 minutes to 1 hour covered in light. The absorbance was recorded at 562 nm on plate reader within 1 hour of incubation. The standard curve was plotted, and protein concertation was determined for each sample.

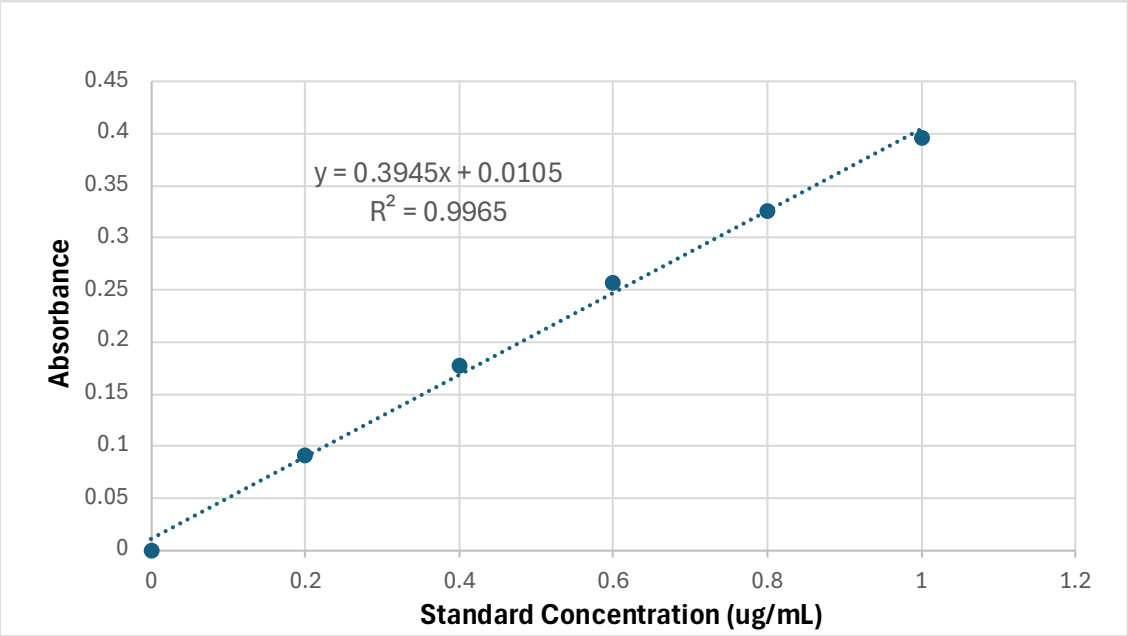

Table 2. Standard Curve for BCA.

2.2.22. Western Blot

The cells were cultured, treated and protein extraction was done as mentioned above (section 2.2.). Following the protein quantification the protein samples were prepared in loading buffer (Bromophenol blue, 8% SDS, 40% glycerol, 0.7 M β-mercaptoethanol, 200 mM Tris, pH 6.8) and heated at 95 °C for 10 minutes. The BIO-RAD Mini Protean TGX Precast gels (4-15%, 12- well comb, 15-20ul) were used for the western blot (BIO-RAD Laboratories, UK).

After taking the precast gel from the bag and the plate was fitted in the electrophoresis chamber in the tank and the comb was removed. In the first row 3ul Page Ruler™ Plus Prestained Protein Ladder, 10 to 250 kDa (11852124) was added and then followed by

10 μg/well of protein samples were loaded. After loading samples, the gel tank was filled with the running buffer (Tris 250 mM, Glycine 1.9M, SDS 1% and 1000 mL diH_2O). The electrophoresis was initially conducted at 100V for 20 minutes and later changed to 160V for 60 minutes.

Following SDS-PAGE gel electrophoresis to separate the proteins, a semi-dry transfer was performed using Trans-Blot Turbo Mini 0.2 μM PVDF Transfer Packs (1704156) pre-wet in transfer buffer (0.25 M Tris, 1.92 M Glycine, 20% (v/v) methanol). The bottom side with the PVDF membrane of the pack was placed on the cassette of Trans-Blot Turbo Transfer System and on top the filter paper given. The system protocol for mini TGX gel (2.5A, 25V for 3 minutes) was performed to transfer. After the transfer of proteins to the PVDF membrane, the membrane was blocked with 5% BSA in TBST on rotary shaker for 2 hours at room temperature to block any non-specific binding of antibodies. The primary antibodies were added to each blot after blocking and then incubated at 4 °C overnight.

After overnight incubation the blots were washed three times with 1 x TBST (0.1% Tween, 200 mM NaCl, 2 mM Tris, pH 7.5). Following washing, secondary Anti-rabbit IgG, HRP-linked Antibody (7074) (1:1000), Anti-mouse IgG, HRP-linked Antibody (7076) (1:1000) in 5% BSA was used for 2 hours at Room temperature covered from light. Afterward, the blots were again washed with 1XTBST (3x5 minutes). The membrane was placed in the Black Li-COR box and 1ml if Immobilon® Forte Western HRP substrate was added for 30 seconds. The membrane was placed in tray and imaged with Li-COR software (Empiria studios Software). GAPDH (1:3000) is used as a loading control for normalizing the expression.

2.2.23. Image Analysis

Image J (v X; National Institutes of Health, Bethesda, MD, USA) was used for image analysis in this research to quantify the intensity of the bands from western blot analysis to ensure the accurate measurement of protein expression, and to measure the intensity

of ICC. Densitometry analysis was used to normalises the band against the loading control. The band intensity of each protein band was normalised to the loading control (GAPDH) and the graph was plotted in the GraphPad PRISM.

Fluorescence intensity of the ICC images was also measured by selecting regions of interest (ROIs) corresponding to individual cells to subtract the background fluorescence. All the images were processed using a standard thresholding and background subtraction method to ensure accuracy and consistency in the samples. The intensity mean was calculated and plotted as a graph. For MAP2 analysis the images were first converted into 8-bit grayscale to standardise intensity measurements. The background intensity was subtracted, and the mean intensity of DAB staining was measured and quantified as optical density (OD).

2.2.24. Statistical analysis

The statistical software PRISM (v.10.0, GraphPad Software Inc., San Diego, CA, USA) is used to analyse the results of the research. One-way (Analysis of Variance) followed by the Bonferroni post-hoc test was used to analyse the statistical significance of difference among experimental groups. All the results were conducted in triplicate to ensure consistency and data were expressed as mean ± standard deviation (SD). Results were graphically represented using bar charts, with error bars denoting SD. A p value of less than 0.05 will be considered as statistically significant.

Chapter 3

Effects of apelin-13 analogues on cell survival proliferation, differentiation and cell growth in Palmitate-induced stress in SH-SY5Y cells in-vitro.

3.1. Introduction

Epidemiological research shows that free fatty acids (FFAs) play a crucial role in the risk of developing AD. PA is a saturated long-chain free fatty acid that contains 16 carbons and is the most common lipid in the human body (Patil & Chan, 2005). It can be found naturally in animals and plants. It is used as an energy source for the cells, regulation of membrane fluidity, and acts as a precursor for signalling molecules and membrane-associated proteins (Panov et al., 2014). Whilst PA serves the physiological roles in the brain, its excessive buildup leads to a detrimental effect on the neuronal cells and leads to lipotoxicity (Naumenko & Ponimaskin, 2018).

Lipotoxicity refers to the toxic effect of these fatty acids, especially saturated fatty acids, on adipose tissues resulting in cellular damage and cellular death (Hauck & Bernhard, 2016). Palmitate-induced lipotoxicity has been demonstrated to aggravate neuronal damage through multiple pathways, including oxidative stress, inflammation, and impaired protein clearance in AD (Vesga-Jiménez et al., 2022). Studies showed that it is prevalent in western diets and is known to induce lipotoxicity, which leads to cellular damage in various tissues including the brain (Kien et al., 2014). The evidence indicates that inflammation caused by lipotoxicity is a critical factor involved in the progression of AD (Glass et al., 2010).

PA produces stress primarily through the activation of ER stress. Palmitate disrupts the folding of proteins in the ER, causing the buildup of misfolded proteins and triggering the unfolded protein response (UPR) (Yuan et al., 2013). The persistent ER stress can contribute to impaired functioning and programmed cell death in neurons, which are closely associated with the development of AD (Hashimoto et al., 2018). Furthermore, palmitate produces oxidative stress by increasing the generation of reactive oxygen species (ROS) (Baldwin et al., 2012). Increased amounts of ROS result in oxidative damage to cellular components, such as lipids, proteins, and DNA (Schieber & Chandel, 2014). The oxidative stress is worsened by stress induced by palmitate on mitochondrial activity, resulting in the loss of mitochondrial membrane potential and increased production of ROS. Oxidative stress has been implicated in the pathology of various

diseases like diabetes, inflammatory diseases, neurodegenerative disease, and cancer (Zhang et al., 2023).

Apelin-13, a biologically active peptide, and its analogue (Lys8GluPAL)apelin-13, have the potential for protecting the nervous system (Masoumi et al., 2018). Apelin have been observed to bind with the APJ receptor, resulting in many physiological outcomes such as cardiovascular control, maintenance of fluid balance, and modulation of metabolic equilibrium (Hu et al., 2021). Recent research has investigated the neuroprotective properties of apelin and its analogues specifically in relation to oxidative stress, inflammation, and apoptosis, all of which are relevant to the development of AD (Than et al., 2014). Apelin-13 amide has proved anti-apoptotic properties in neural cells (Liu et al., 2019).

Hence, the aims of this chapter are to investigate therapeutic potential of apelin-13 amide and (Lys^{8}GluPAL)apelin-13 amide aimed at reducing the palmitate-lipotoxicity in the brain. It will also discuss the role of apelin-13 analogues on the pathways involved in ER stress, inflammation, mitochondrial dysfunction and inflammatory responses.

Objectives:

1. The effects of apelin-13 amide and (Lys^{8}GluPAL)apelin-13 amide on cell viability, cell toxicity and neuronal cell differentiation under palmitate exposure in SH-SY5Y cells.
2. The effects of apelin-13 amide and (Lys^{8}GluPAL)apelin-13 amide on to understand the protein expressions of BAX, Bcl-2 and NRF2. To determine ethe influence of apelin-13 amide and (Lys^{8}GluPAL)apelin-13 amide on apoptotic pathways.

3.2. Results

3.2.1 Effects of novel stable apelin-13 analogues on cell viability in SH-SY5Y cells in-vitro.

A significant increase in cell viability was observed in SH-SY5Y cells treated with stable apelin-13 analogues compared to untreated control. After incubation with peptides cell viability was significantly increased by 13% when treated with apelin-13 amide (1000 nM) (Figure 3.1A, $p<0.0001$) at 2 hours, 18% (Figure 3.1B, $p<0.01$) at 4 hours and 13% increased at 2 hours incubation when treated with (Lys^{8}GluPAL)apelin-13 amide (1000 nM) (Figure 3.1A, $p<0.0001$) compared to untreated control. No significant changes were seen when cells were treated with Apelin-13 amide (1000 nM) (Figure 3.1C, $p>0.05$) at 24 hours and (Lys^{8}GluPAL)apelin-13 amide (1000 nM) (Figure 3.1B, $p>0.05$) at 4 hours and 24 hours (Figure 3.1C, $p>0.05$) compared to control.

Conversely, time and dose dependent reduction in cell viability was by 22% (Figure 3.1A, $p<0.0001$) was observed in cells treated with 0.6 mM palmitate and 30% when treated with 1.0 mM (Figure 3.1A, $p<0.0001$) palmitate at 2 hours, compared to untreated control. Furthermore, at 4 hours 22% reduction was seen when treated with 0.6 mM palmitate (Figure 3.1B, $p<0.0001$), and 30% (Figure 3.1B, $p<0.01$) when treated with 1.0 mM palmitate at 4 hours compared to the untreated control. At 24 hours, 0.6 mM palmitate reduced cell viability by 32% (Figure 3.1C, $p<0.0001$), and 34% by 1.0 mM palmitate (Figure 3.1C, $p<0.0001$), compared to untreated control.

Cells concurrently treated with apelin-13 analogues and palmitate shows significant restoration of cell viability compared to palmitate alone at different timepoints and concentrations. Apelin-13 amide combined with 0.6 mM palmitate significantly improved cell viability at 2 hours by 21% (Figure 3.1A, $p<0.0001$), but no significant changes were seen at 4 hours (Figure 3.1B, $p>0.05$) and 24 hours (Figure 3.1C, $p>0.05$) compared to palmitate alone. However, at the concentration of 1.0 mM palmitate, apelin-13 analogues have significantly increased the cell viability compared to palmitate alone, apelin-13

amide by 20% (Figure 3.1B,p<0.001) and (Lys8GluPAL)apelin-13-amide by 13% (Figure 3.1B,p<0.05) at 4 hours and when treated with 1.0 mM palmitate in combination to apelin-13 amide, viability increased by 23% (Figure 3.1C, p<0.001) and by 11% (Figure 3.1C, p<0.05) with (Lys^{8}GluPAL)apelin-13 amide at 24 hours compared to palmitate alone. When cells were treated with 1.0 mM palmitate combined with Apelin-13 analogues at 2 hours it did not show any changes (Figure 3.1A, p>0.05) compared to 1.0 mM palmitate alone.

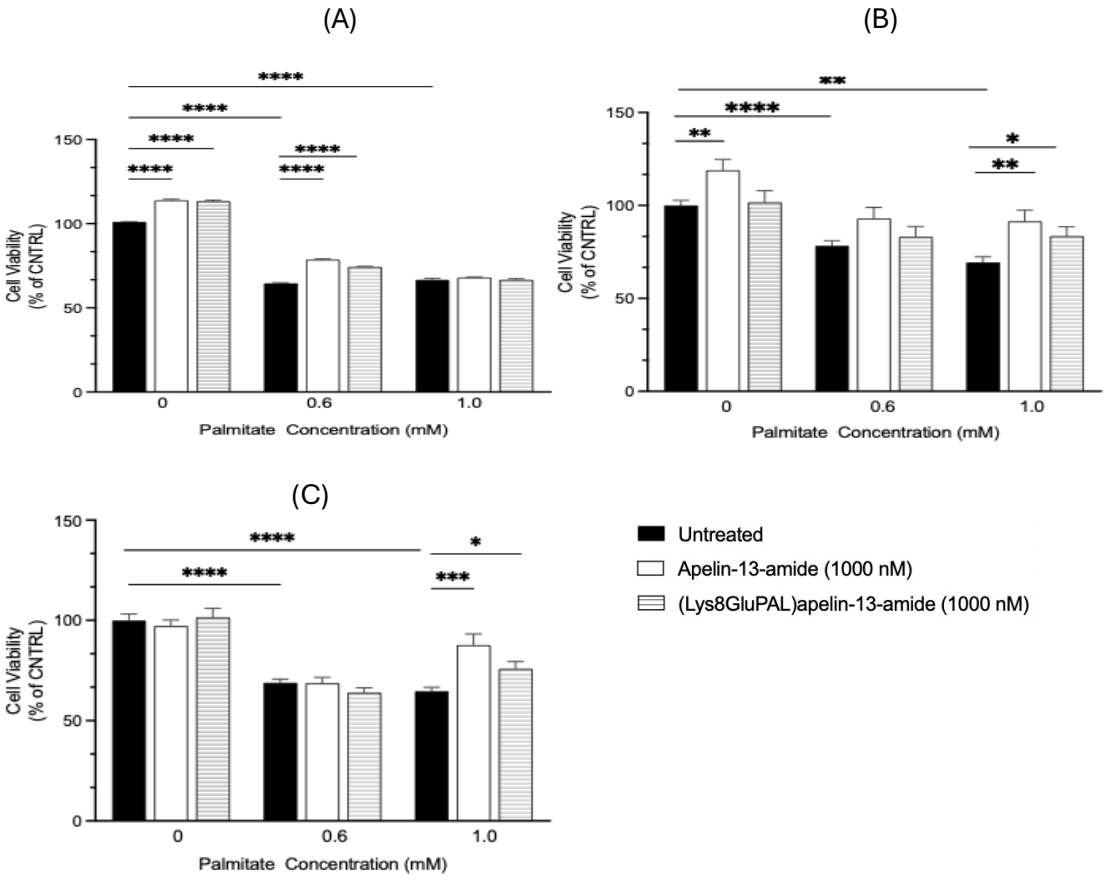

Figure 3.1 Effects of novel stable apelin-13 analogues on cell viability in SH-SY5Y cells in-vitro. Time dependant treatment with apelin-13 analogues impacts on neuronal viability of SH-SY5Y cells with and without 0.6 mm and 1 mM palmitate in –vitro, using MTT reagent to measure the viability based on the reduction of MTT to formazan. Cells were treated with treatments for (A) 2 hours (B) 4 hours and (C) 24 hours. Values represents mean ±SEM (one-way ANOVA, n=3 where *p<0.05, **p<0.01,***p<0.001, and ****p<0.0001 compared to control.

3.2.2 Effect of apelin-13 analogues on ATP based cell viability under palmitate-induced in cell toxicity.

The cell viability observed by measuring the ATP levels using luminescent assay. The results shows that apelin-13 amide-treated cells had non-significant increase in viability by 16% (Figure 3.2A, $p>0.05$), and (Lys8GluPAL)apelin-13-amide-treated cells by 8% (Figure 3.2A, $p<0.01$), compared to untreated control. On the other hand, cell viability was significantly reduced by 28% (Figure 3.2A ,$p<0.01$) when exposed to the 0.6 mM palmitate and by 38% (Figure 3.2A, $p<0.0001$) when exposed to a dose of 1.0 mM palmitate compared to untreated control. Co-treatment of cells with 0.6 mM palmitate and apelin-13 amide improved cell viability by 16% (Figure 3.2A, $p>0.05$) and 26% (Figure 3.2A, $p<0.01$) for 1.0 mM palmitate compared to palmitate alone. Co-treatment of cells with 0.6 mM palmitate and (Lys^{8}GluPAL)apelin-13 amide improved cell viability by 14% (Figure 3.2A, $p>0.05$) and 26% (Figure 3.2A, $p<0.01$) for 1.0 mM palmitate compared to palmitate alone.

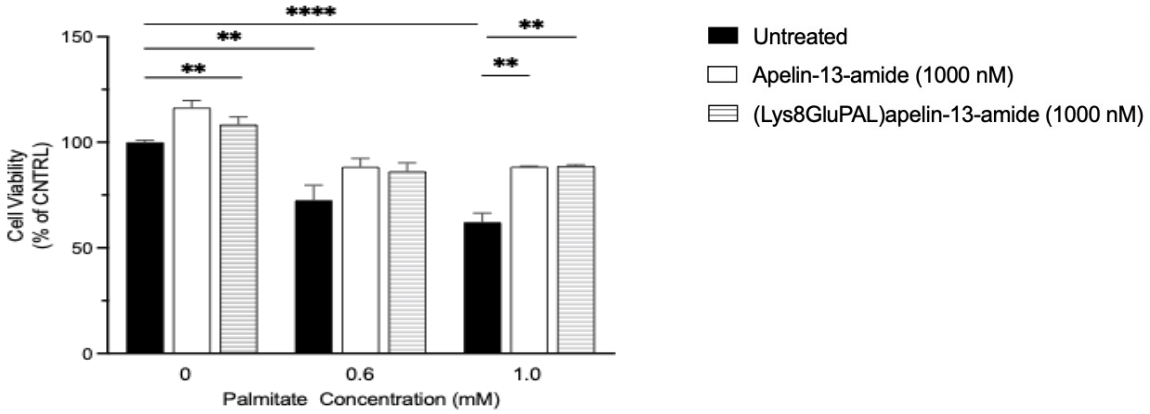

Figure 3.2 Effect of apelin-13 analogues on ATP based cell viability under palmitate-induced in cell toxicity. Dose dependant effects of apelin-13 amide and (Lys^{8}GluPAL)apelin-13 amide on viability using Celltiter-Glo reagent to measure the viability based on the luminescence produced by ATP present in viable cells at 6 hours. Cells were treated for 6 hours with treatments and Promega Celltiter-Glo luminescent kit was used to measure the cell viability. Values represents mean ±SEM for n=3 where **p<0.01, ****p<0.0001.

3.2.3. Effect of apelin-13 analogues on cell proliferation in SH-SY5Y cells.

Evaluation of cell proliferation was done by assessing incorporation of BrdU in SH-SY5Y cells. Compared to untreated control, no significant difference in the number of BrdU positive cells were seen when treated with apelin-13 amide (Figure 3.3B, $p>0.05$), and (Lys^{8}GluPAL)apelin-13-amide showed non-significant increase by 20% (Figure 3.3B, $p>0.05$) compared to untreated control. Treatment with 0.6 mM palmitate reduced cell proliferation by 47% (Figure 3.3B, $p<0.01$) compared to untreated control. Non-significant increases in BrdU positive cells were found when cells co-treated with 0.6 mM palmitate and apelin-13 amide by 14% (Figure 3.3B, $p>0.05$) and 14% (Figure 3.3B, $p>0.05$) for (Lys^{8}GluPAL)apelin-13-amide, compared to palmitate alone.

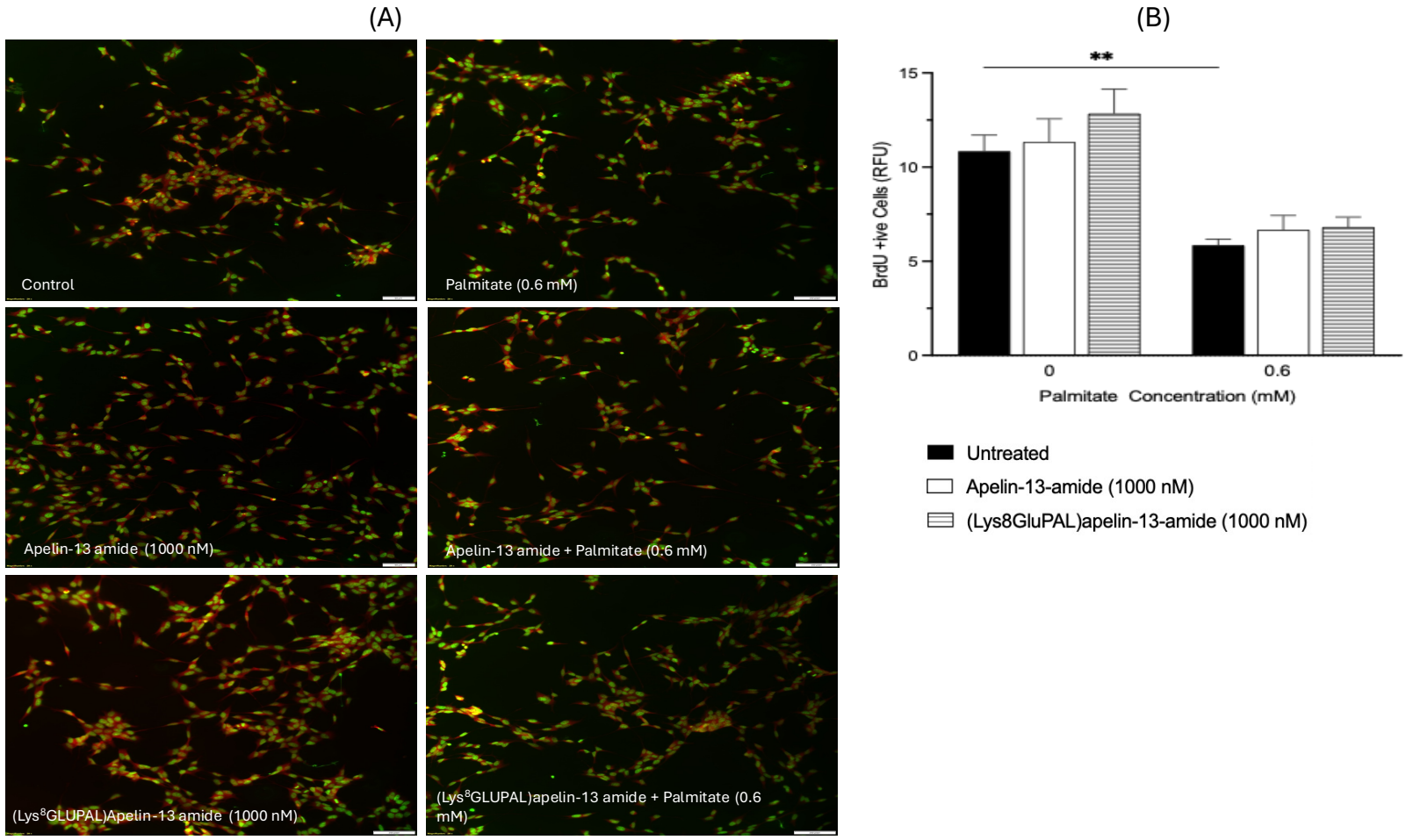

Figure 3.3 Effect of apelin-13 analogues on cell proliferation in SH-SY5Y cells. BrdU incorporation assay was used to assess cell proliferation. (A) Representative images of SH-SY5Y cells stained with BrdU and DAPI are shown (20x magnification). The DAPI is shown in a pseudo colour green instead of blue and BrdU incorporated in red colour. (B) Graph of quantification of BrdU positive cells treated with apelin-13-amide, (Lys^{8}GluPAL)apelin-13-amide measured by Image J. Values represent mean ±SEM for n=3 where $^{**}p<0.01$.

3.2.4. Effect of apelin-13 analogues on neurite outgrowth in SH-SY5Y cells.

Representative images showing neurite outgrowth in SH-SY5Y when differentiated by RA (10 μM) and stained with cells Coomassie brilliant blue (Figure 3.4A). Compared to untreated control, a slight non-significant increase in neurite extensions was seen when treated with both apelin-13 amide by 16% (Figure 3.4B, $p>0.05$) and (Lys^8GluPAL)apelin-13-amide by 18% (Figure 3.4B, $p>0.05$). Neurite outgrowth was significantly reduced by 46% (Figure 3.4B, $p<0.0001$) when cells were treated with palmitate (0.6 mM) compared to untreated control. When treated co-currently with palmitate (0.6 mM), Apelin-13 amide restored and improved neurite outgrowth significantly by 74% (Figure 3.4B, $p<0.0001$) and (Lys^8GluPAL)apelin-13-amide improved neurite extension by 38% (Figure 3.4B, $p<0.001$) compared to palmitate alone.

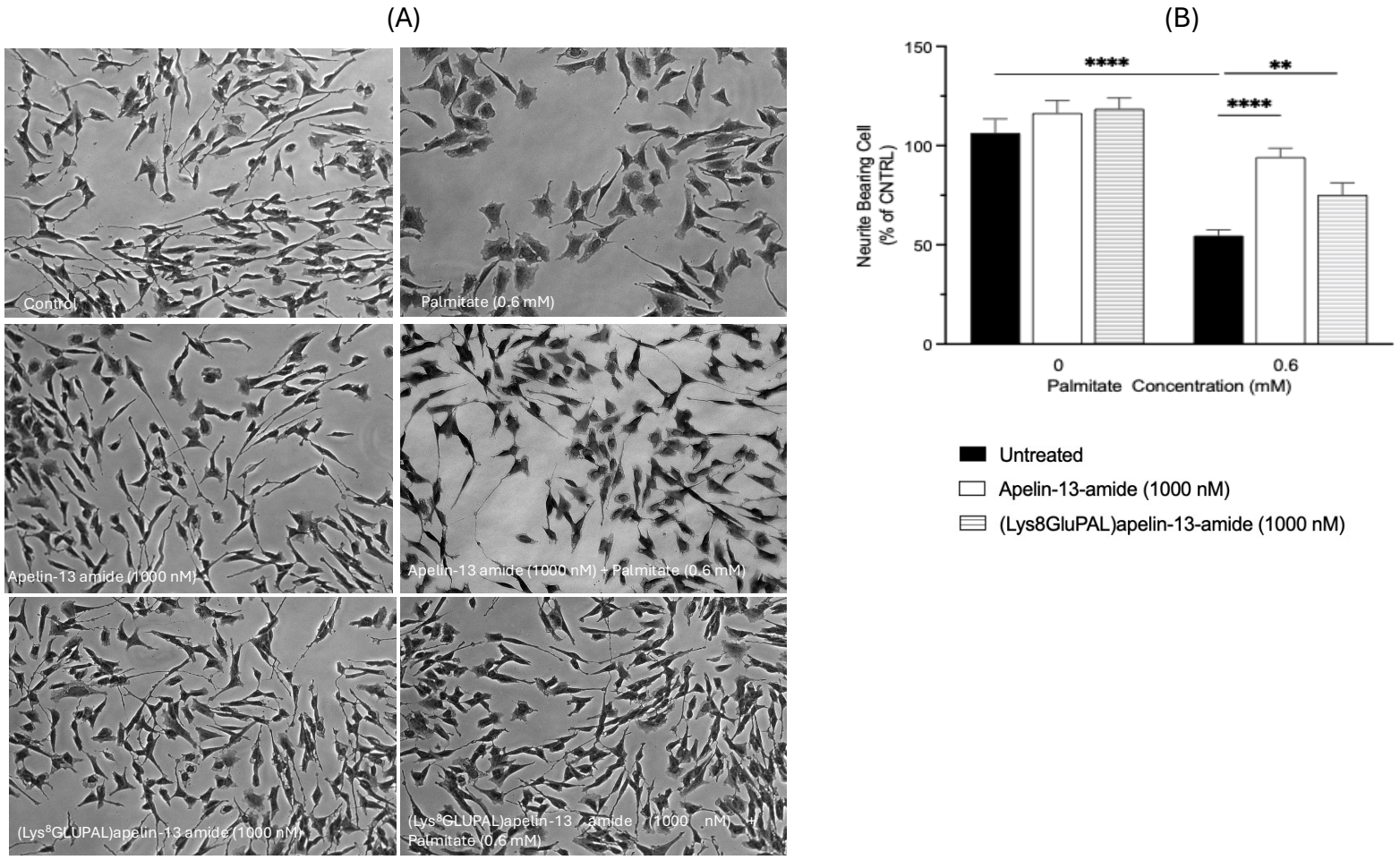

Figure 3.4 Effect of apelin-13 analogues on neurite outgrowth in SH-SY5Y cells. Effects of apelin-13 amide and (Lys^{8}GluPAL)apelin-13 amide on neurite outgrowth length of SH-SY5Y cells *in-vitro*. (A) shows represented images of stained cells with Coomassie brilliant blue and (B) shows the graph for neurite bearing cells. Cells were treated for 48h, and cells were stained with Coomassie brilliant blue and imaged under the light microscope at 20x magnification. Value represents mean ±SEM for n=3 where **p<0.01, and ****p<0.0001.

3.2.5. Effect of apelin-13 analogues on neuronal differentiation in SH-SY5Y cells under palmitate-induced stress.

Evaluation of neuronal cell differentiation was measured using MAP2 expression in SH-SY5Y cells, where Figure 3.5A shows representative images. Apelin-13 amide treatment resulted in a significant (Figure 3.5B, 12%, $p<0.01$) increase in MAP2 expression, whereas (Lys^{8}GluPAL)apelin-13-amide showed no significant change in expression levels compared to untreated control (Figure 3.5B, $p>0.05$). In contrast, cells treated with (0.6 mM) palmitate, exhibited a significant reduction in MAP2 expression by (Figure 3.5B, 32%, $p<0.01$) compared to the untreated control. Co-treatment of cells with 0.6 mM palmitate and apelin-13 amide led to a non-significant (Figure 3.5B, 12%, $p>0.05$) increase in MAP2 expression, and comparably, (Figure 3.5B, 14%, $p>0.05$) increase was observed with (Lys^{8}GluPAL)apelin-13-amide, compared to palmitate alone.

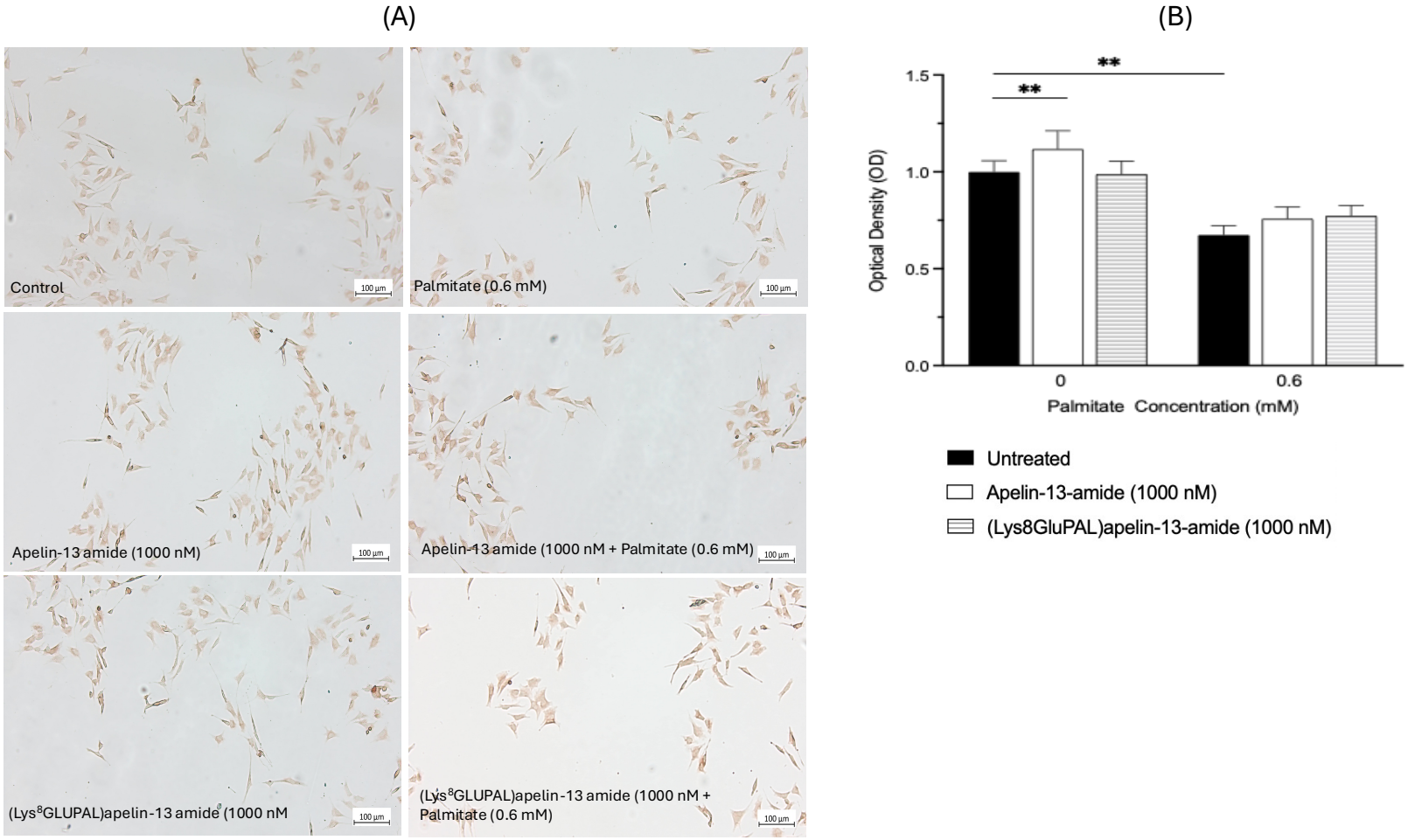

Figure 3.5 Effect of apelin-13 analogues on neuronal differentiation in SH-SY5Y cells under palmitate-induced stress. MAP2 a neuronal differentiation marker was used in SH-SY5Y cells to look at the effect of apelin-13 analogues on neuronal differentiation where (A) images of MAP2 staining with DAB substrate and (B) graph of optical density. Cells were differentiated with retinoic acid (10 µM) for 24 hours and treated with apelin-13-amide, (Lys^{8}GluPAL)apelin-13-amide with or without palmitate. Values represents mean ±SEM for n=3 where *p<0.05 **p<0.01.

3.2.6. Effect of apelin-13 analogues on cell toxicity-induced by palmitate in SH-SY5Y cells.

Apelin-13 amide and (Lys^{8}GluPAL)apelin-13-amide significantly reduced cell toxicity induced by the 0.6 mM and 1.0 mM palmitate (Figure 3.6). Treatment with apelin-13 amide alone reduced cell toxicity by 10% (Figure 3.6A, $p<0.01$) after 2 hours, 11% (Figure 3.6B, $p>0.05$) after 4 hours and showed no change at 24 hours, compared to untreated control. When treated with (Lys^{8}GluPAL)apelin-13-amide toxicity was reduced by 11% (Figure 3.6A, $p<0.01$) after 2 hours, 14% (Figure 3.6B, $p<0.001$) after 4 hours, and 7% (Figure 3.6C, $p<0.05$) after 24 hours compared to untreated control.

However, the cell toxicity had no significant change at 0.6 mM (Figure 3.26A, $p>0.05$) concentration of palmitate and increased by 35% (Figure 3.6A, $p<0.0001$) at 1.0 mM after 2 hours compared to untreated control. the cell toxicity was reduced by 30% (Figure 3.6B,$p<0.0001$) at 0.6 mM, and 17% (Figu6e 3.2B, $p<0.0001$) at 1.0 mM after 4 hours and by 33% (Figure 3.6C, $p>0.05$) at 0.6 mM and 31% (Figure 3.6C, $p<0.001$) at 1.0 mM after 24 hours, compared to untreated control. When the cells were concurrently treated with apelin-13 amide and 0.6 mM palmitate, the cell toxicity reduction was 3% (Figure 3.6A, $p>0.05$) at 2 hours , by 4% (Figure 3.6A, $p<0.05$) at 4 hours and 17% (Figure 3.6C, $p<0.05$) at 24 hours compared to 0.6 mM palmitate. Co-treatment of apelin-13 amide with 1.0 mM palmitate reduced cell toxicity by 20% (Figure 3.6A, $p<0.01$) after 2 hours, 11% (Figure 3.6B, $p>0.05$) after 4 hours and 12% (Figur6 3.2C, $p>0.05$) after 24 hours for 1.0 mM palmitate. Co-treatment with (Lys^{8}GluPAL)apelin-13-amide and 0.6mM palmitate reduced cell toxicity by 6% (Figure 3.6A, $p>0.05$) after 2 hours, 23% (Figure 3.6B, $p<0.001$) after 4 hours and 17%(Figure 3.6C, $p>0.05$) by 24 hours at, and 12% (Figure 3.6A, $p<0.05$) after 2 hours, 26% (Figure 3.6B, $p<0.0001$) after 4 hours and, 6% (Figure 3.6C, $p<0.05$) after 24 hours at 1.0 mM palmitate, compared to palmitate alone.

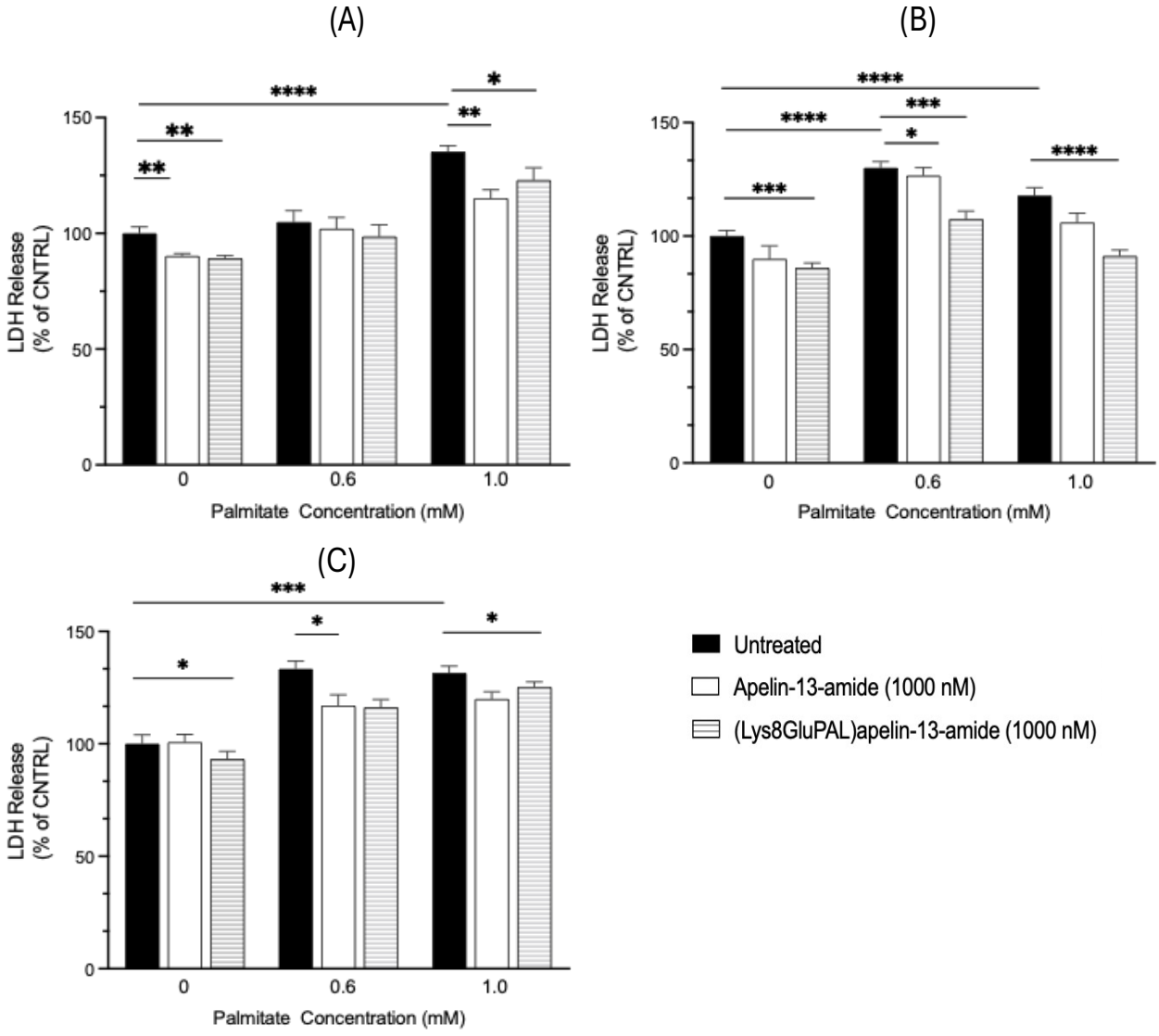

Figure 3.6 Effect of apelin-13 analogues on cell toxicity-induced by palmitate in SH-SY5Y cells. Time-dependant effects of apelin-13 on toxicity of SH-SY5Y cells *in-vitro* using lactate dehydrogenase (LDH) assay to measure the release of LDH enzyme from damaged cells. Cells were treated with the treatments for (A) 2-hour (B) 4-hour (C) 24-hour. Values represents mean ±SEM (one-way ANOVA, n=3 where *p<0.05, **p<0.01,***p<0.001, and ****p<0.0001.

3.2.7. Effect of apelin-13 analogues on DNA damage induced by Palmitate in SH-SY5Y cells.

Reduced cell toxicity was seen when the cells were treated with apelin-13 amide, by 20% (Figure 3.7B, $p<0.001$), and 22% (Figure 3.7B $p<0.001$) with (Lys^{8}GluPAL)apelin-13-amide, compared to the untreated control. Palmitate (0.6 mM) treatment showed no significant change in cell toxicity, however a significant increase of 18% (Figure 3.7B $p<0.001$) was observed at a concentration of 1.0 mM palmitate, compared to untreated control. Co-treatment of apelin-13 analogues and 0.6 mM palmitate, there was no observed change in cell toxicity, for 1.0 mM palmitate, cell toxicity reduced non significantly by 8% (Figure 3.7B, $p>0.05$) with apelin-13 amide and significantly by 28% (Figure 3.7B $p<0.0001$), with (Lys^{8}GluPAL)apelin-13-amide, compared to palmitate alone.

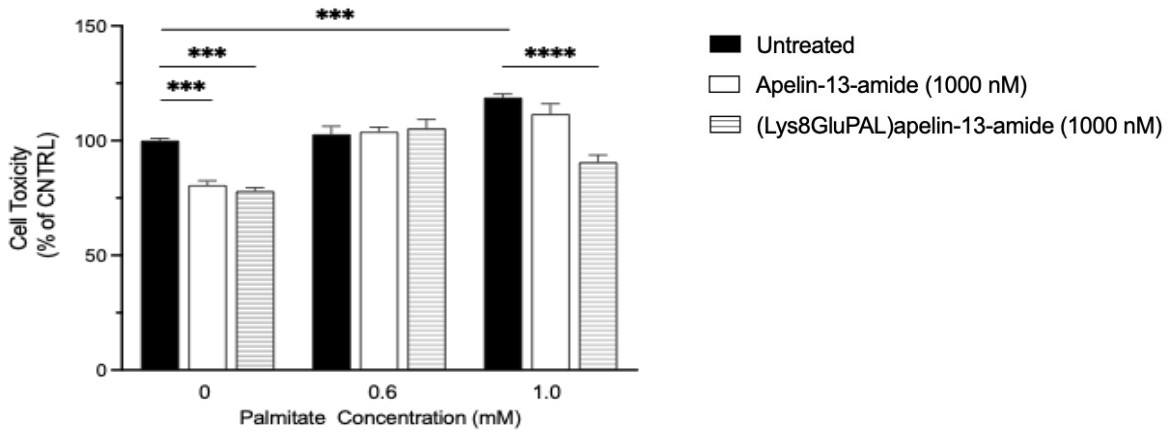

Figure 3.7 Effect of apelin-13 analogues on DNA damage induced by Palmitate in SH-SY5Y cells. Cells were treated for 6 hours with apelin-13 analogues in presence or absence of palmitate and Promega CellTox Green cytotoxicity Kit was used to measure the DNA damage. CellTox green reagent to utilize a fluorescent dye that binds to DNA released from damaged cell. Values represents mean ±SEM for n=3 where ***$p<0.001$, ****$p<0.0001$.

3.2.8 Effect of apelin-13 analogues on Glutathione/Oxidized Glutathione ratio levels and ROS in SH-SY5Y cells.

Evaluation of ROS production was done by Luminescence end point assay. Reduction in ROS production compared to untreated control was observed with both peptides, apelin-13 amide (Figure 3.6B, 5%, $p>0.05$) and (Lys^{8}GluPAL)apelin-13-amide (Figure 3.6B, 6%, $p>0.05$) compared to untreated control. Treatment with 0.6 mM palmitate increased ROS levels by 30% (Figure 3.8B, $p<0.05$) and 23% (Figure 3.8B, $p>0.05$) for 1.0 mM palmitate compared to untreated control. Co-treatment with apelin-13 amide showed non-significant reduction in ROS levels (Figure 3.8B, 23%, $p>0.05$) for 0.6 mM palmitate, and slight decline by 2% (Figure 3.8B, $p>0.05$) for 1.0 mM palmitate, compared to palmitate alone. Likewise, when cells were co- treated with (Lys^{8}GluPAL)apelin-13-amide, ROS reduced by 19% (Figure 3.8B, $p>0.05$) for 0.6 mM palmitate , and 7% ($p>0.05$) for 1.0 mM palmitate, compared to palmitate alone.

The intracellular redox stability of SH-SY5Y cells was measured by analysing the GSH/GSSG ratio. The GSH/GSSG ratio was significantly increased when treated with apelin-13 amide by 36% (Figure 3.8A, $p<0.01$) and, by 35% (Figure 3.8A, $p<0.01$) with (Lys^{8}GluPAL)apelin-13 amide, compared to untreated control. On the other hand, treatment with palmitate showed significant reduction in the GSH/GSSG ratio by 36% (Figure 3.8A, $p<0.01$), compared to the untreated control. Co-treatment of 0.6 mM palmitate with Apelin-13 amide showed significant increase by 31% (Figure 3.8A, $p<0.01$) and with (Lys^{8}GluPAL)apelin-13-amide by 37% (Figure 3.8A, $p<0.05$), compared to palmitate alone.

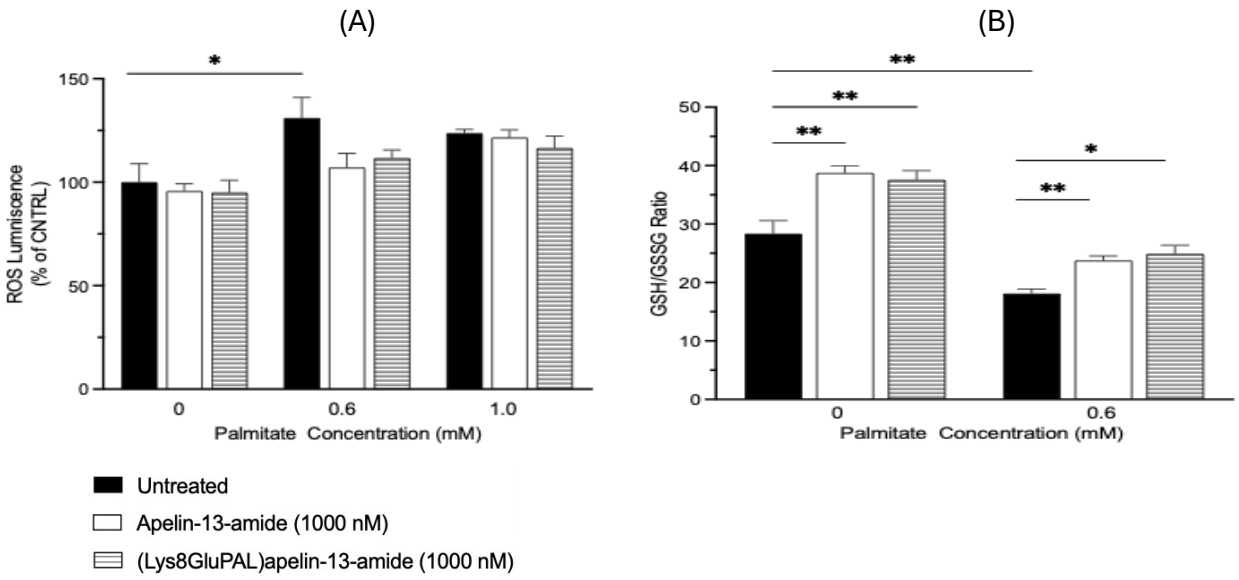

Figure 3.8 Effect of apelin-13 analogues on Glutathione/Oxidized Glutathione ratio levels and ROS in SH-SY5Y cells. (A) ROS (Reactive Oxygen Species) measurement, (B) ratio of reduced and total glutathione in SHSY5Y cells when treated with apelin-13 amide and (Lys^{8}GluPAL)apelin-13 amide under stress induced by palmitate. Values represent mean ±SEM for n=3 where *p<0.05,**p<0.01, ***p<0.001.

3.2.9. Effect of apelin-13 analogues on restored mitochondrial membrane potential in SH-SY5Y under palmitate-induced stress.

To measure the mitochondria potential ($\Delta\Psi_m$), cells were stained with J aggregate forming cationic dye JC-1. Figure 3.9A shows the representative fluorescent images of JC-1 stain under the microscope at 20x magnification. The fluorescent intensity was measured using Image J and graph was plotted using GraphPad PRISM. JC-1 is a fluorescent dye that produces green light in its monomeric form and red light when it aggregates in mitochondria. This change in colour indicates the presence of membrane potential. A drop in membrane potential leads to a decrease in red fluorescence and an increase in green fluorescence. Which indicates mitochondrial depolarisation and loss of mitochondrial membrane potential, which is often linked with apoptosis.

Compared to untreated control, apelin-13 amide treatment led to significant increase in mitochondrial membrane potential by 82% (Figure 3.9B, $p<0.05$) and non-significant by 60% ($p>0.05$) for (Lys^8GluPAL)apelin-13-amide, compared to untreated control. Significant reduction in membrane potential was seen when cells treated with 0.6mM palmitate (Figure 3.9B, 82%, $p<0.01$), compared to untreated control. Co-treatment of 0.6 mM palmitate with apelin-13 amide led to an increase in $\Delta\Psi_m$ by 128% (Figure 3.9B, $p<0.01$) and 32% non-significant increase when treated with (Lys^8GluPAL)apelin-13-amide (Figure 3.9B, $p>0.05$), compared to palmitate alone.

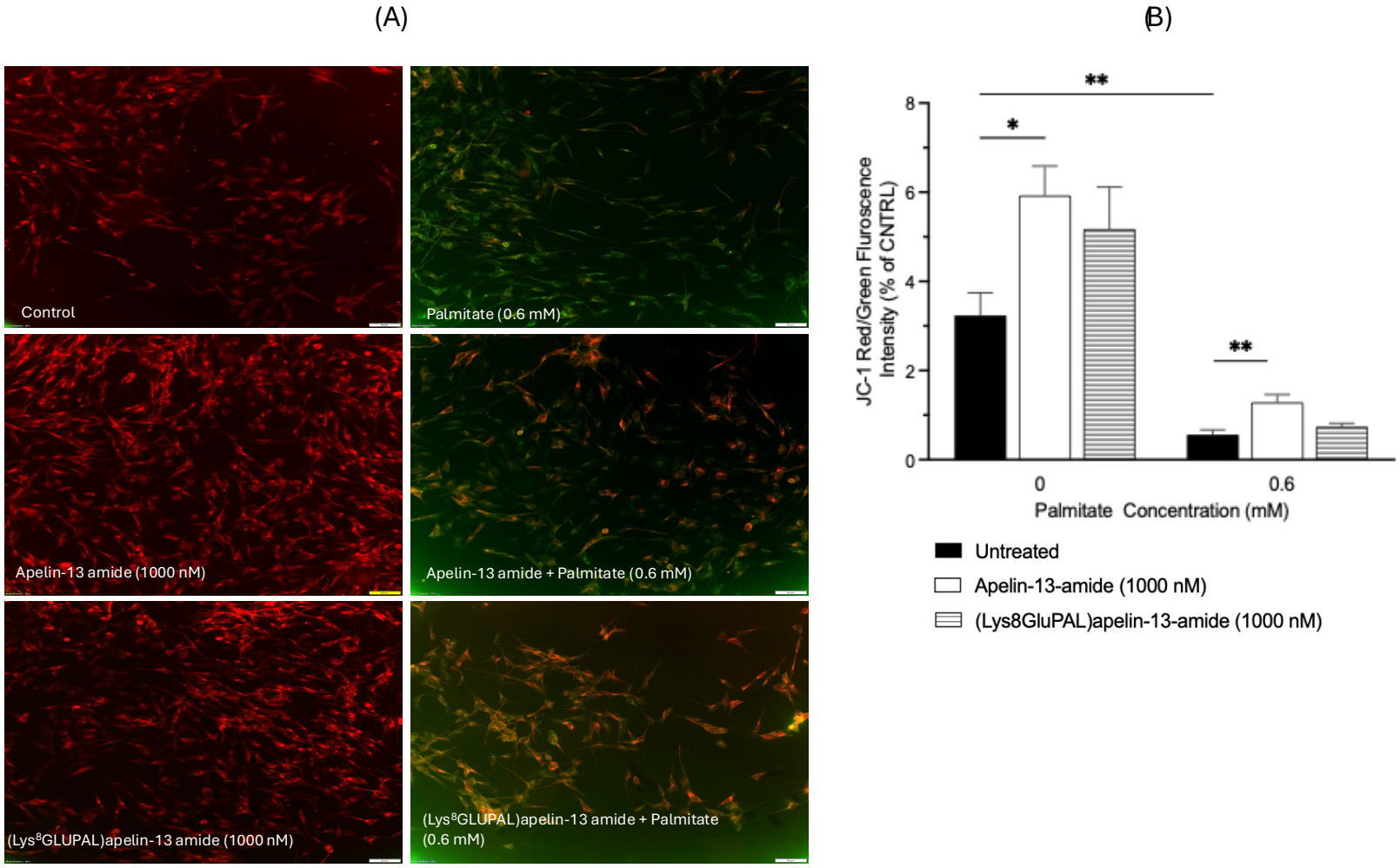

Figure 3.9 Effect of apelin-13 analogues on restored mitochondrial membrane potential in SH-SY5Y under palmitate-induced stress. Shows ΔΨm using JC-1 staining (A) Representative images of SH-SY5Y cells stained with JC-1 on two different channels, and merge (20x magnification). (B) Graph of JC-1 Red/Green fluorescence ratio of cells treated with apelin-13-amide, pGlu(Lys^{8}GluPAL)apelin-13-amide and palmitate. Values represents mean ±SEM for n=3 where *p<0.05, **p<0.01.

3.2.10. Effects of apelin-13 analogues on apoptosis induced by palmitate in SH-SY5Y cells.

The caspse-3/7 activity in SH-SY5Y cells was measured to evaluate the apoptosis levels. The luminescent signal produced by the cleavage of the caspase-3/7 substrate was directly related to the activity of caspase 3/7. The caspase 3/7 activity was significantly reduced when the cells were treated with apelin-13 amide by (Figure 3.10A, 23%, $p<0.05$) and (Lys^{8}GluPAL)apelin-13-amide (Figure 3.10A, 30% $p<0.01$), compared to untreated control. The treatment with 0.6 mM palmitate significantly increased apoptosis by 41% (Figure 3.10A, $p<0.001$) and by 4266% (Figure 3.10B, $p<0.0001$) for 1.0 mM palmitate, compared to untreated control. Co-treatment of palmitate with apeli-13 amide reduced activity by 36% (Figure 3.10A, $p<0.0001$) for 0.6 mM palmitate and 90% (Figure 3.10B, $p<0.0001$) for 1.0 mM palmitate, compared to palmitate treatments alone. Co-treated with (Lys^{8}GluPAL)apelin-13-amide, reduced cell apoptosis by 36% (Figure 3.10A, $p<0.0001$) for 0.6 mM palmitate and 95% (Figure 3.10B, $p<0.0001$) for 1.0 mM palmitate, compared to palmitate treatments alone.

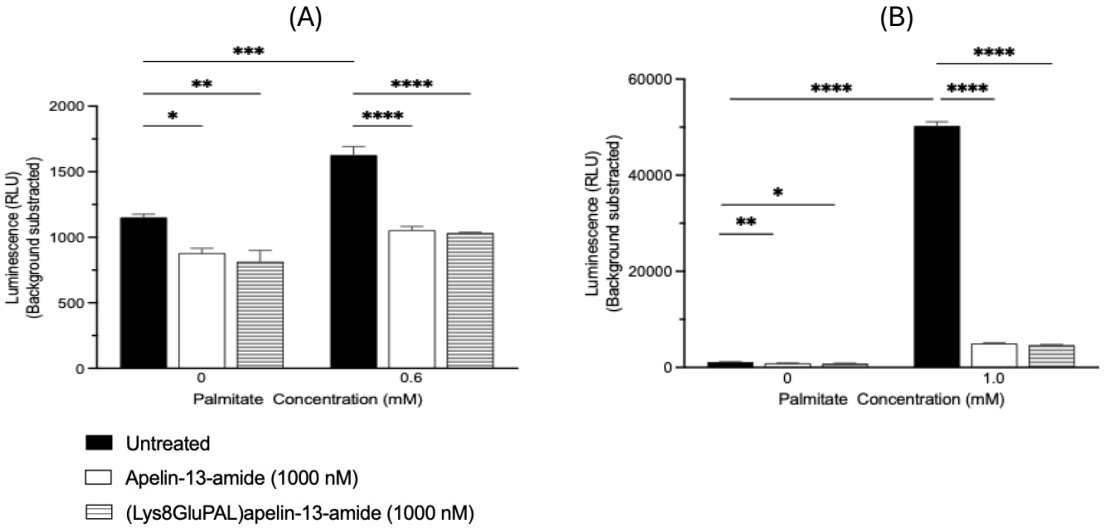

Figure 3.10 Effects of apelin-13 analogues on apoptosis induced by palmitate in SH-SY5Y cells. Dose dependant effects of palmitate with and without apelin-13 amide and (Lys^{8}GluPAL)apelin-13 amide on Caspase 3/7 activity of SH-SY5Y cells *in-vitro.* (A) palmitate 0.6mM (B) Palmitate 1mM. Values represents mean ±SEM for n=3 where *p<0.05, **p<0.01, ***p<0.001 , ****p<0.0001.

3.2.11 Effect of apelin-13 analogue on the expression of NRF-2 protein under palmitate-induced cellular stress.

To evaluate the impact of apelin-13 analogues on oxidative stress response, western blot analysis was utilized to measure the NRF-2 protein expression. NRF-2 is a key transcription factor, plays crucial role in regulating the expression of antioxidant proteins. Apelin-13 amide treatment led to a non-significant reduction in NRF-2 expression suggesting the downregulation of the oxidative stress response pathway (Figure 3.11, $p>0.05$) and (Lys^{8}GluPAL)apelin-13-amide showed no impact (Figure 3.11, $p>0.05$), compared to untreated control. However, the 0.6 mM palmitate increased the expression non-significantly by 86% (Figure 3.11, $p>0.05$), compared to untreated control. Co-treatment of 0.6 mM palmitate with apelin-13 amide reduced the NRF-2 expression by 27% (Figure 3.11, $p>0.05$) and with (Lys^{8}GluPAL)apelin-13-amide by 18% (Figure 3.11, $p>0.05$) but it's not significant, compared to palmitate alone.

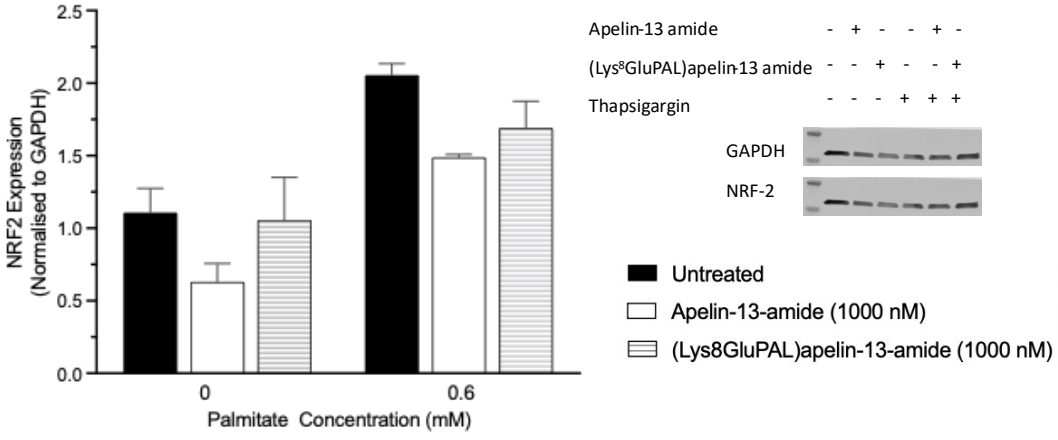

Figure 3.3.11 Effect of apelin-13 analogue on the expression of NRF-2 protein under palmitate-induced cellular stress. NRF-2 protein expression was normalized using GAPDH protein expression. Data was analysed using Image J and GraphPad Prism version 10. Values represents mean ±SEM for n=3 where *$p<0.05$.

3.3.12 Effect of apelin-13 analogues on apoptosis-related factors pro-apoptotic (BAX) and anti-apoptotic (Bcl-2) protein expressions.

To evaluate the effect of apelin-13 analogues on palmitate induced apoptosis, western blot analysis was utilised to assess the expression of Bax and Bcl-2 proteins. The results illustrated apelin-13 analogues showed no significant change in BAX expression, compared to untreated control (Figure 3.12A, $p>0.05$). However, the BAX expression was significantly increased by 20% (Figure 3.12A, $p<0.05$) when treated with 0.6 mM palmitate, compared to untreated control. Co-treatment of palmitate reduced BAX expression by 17% (Figure 3.12A, $p<0.05$) for apelin-13 amide and 16% (Figure 3.12A, $p<0.05$) for (Lys^{8}GluPAL)apelin-13-amide, compared to palmitate alone.

No change in anti-apoptotic Bcl-2 protein was observed when treated with Apelin-13 amide, and non-significant rise by 23% (Figure 3.12B, $p>0.05$) in Bcl-2 was seen when treated with (Lys^{8}GluPAL)apelin-13-amide, compared to untreated control. Treatment with 0.6mM palmitate led to non-significant 12% decline (Figure 3.12B, $p>0.05$) in Bcl-2 expression, compared to untreated control. Co-treatment of palmitate with apelin-13 amide increased Bcl-2 expression non-significantly by 30% ($p>0.05$) and significantly by 80% (Figure 3.12B, $p<0.05$) when treated with (Lys^{8}GluPAL)apelin-13-amide, compared to palmitate alone.

The Bax/Bcl-2 ratio was calculated from quantified protein band intensities. The treatment with 0.6 mM palmitate resulted in non-significant rise by 32% (Figure 3.12C, $p>0.05$), and (Lys^{8}GluPAL)apelin-13-amide reduced by 22% (Figure 3.12C, $p>0.05$), compared to untreated control. No change was observed with apelin-13 amide treatment. Co-treatment of 0.6 mM palmitate reduced BAX/Bcl-2 significantly by 33% (Figure 3.12C, $p<0.05$) with apelin-13 amide and 52% (Figure 3.12C, $p<0.01$) with (Lys^{8}GluPAL)apelin-13-amide, compared to palmitate alone. This suggests an anti-apoptotic effect by apelin-13 analogues and promoting cell survival.

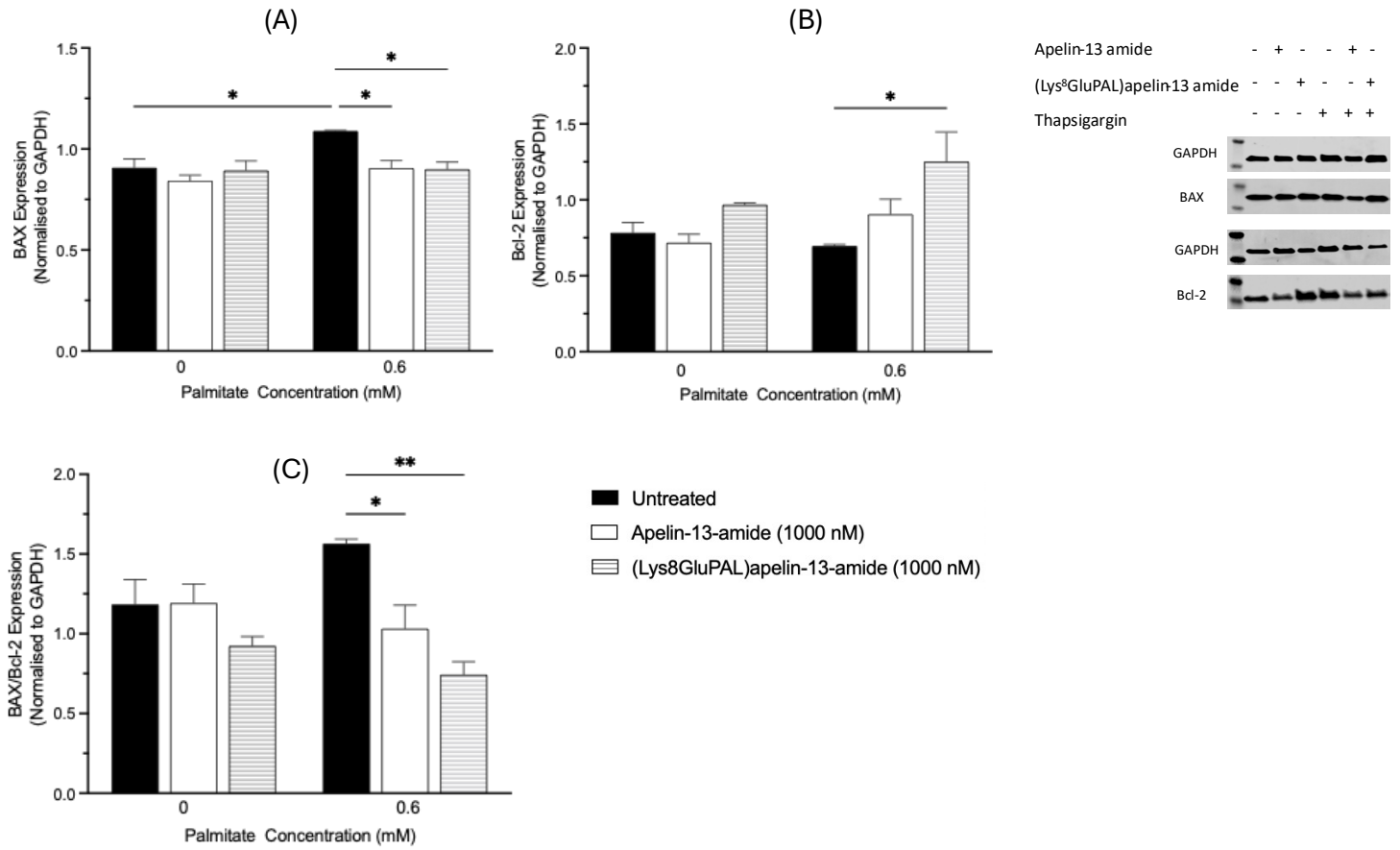

Figure 3.12. Effect of apelin-13 analogues on apoptosis-related factors BAX and Bcl-2 protein expressions. (A) Graph representation and blot images of Protein BAX, (B) Graph representation and blot images of protein Bcl-2, and (C) is graph representation of ratio of BAX/Bcl-2. The BAX and Bcl-2 expression was normalised to GAPDH protein expression. Data was analysed using Image J and GraphPad Prism version 10. Values represents mean ±SEM for n=3 where *p<0.05.

3.3. Discussion

In this chapter, we have looked at the role of free fatty acids on induction of oxidative stress, cell toxicity, cell differentiation and apoptosis in neuroblastoma cell line. Palmitate can induce stress and can lead to oxidative stress, inflammation and ROS production which contributed to neuronal cell death (Hsiao et al., 2014). Palmitate triggers apoptosis by multiple routes, such as the stimulation of caspases and the mitochondrial apoptotic pathway (Hsiao et al., 2014). Apelin-13 amide counteracts these effects by regulating crucial indicators of cell death, such as decreasing the presence of proteins that promote cell death, such as Bax, and increasing the amounts of proteins that prevent cell death, such as Bcl-2 (Mlyczyńska et al., 2021). Apelin-13 amide improves the ability of cells to defend against oxidative stress by increasing the production and effectiveness of antioxidant which helps in the neutralisation of ROS (Fang et al., 2002). It also has shown to enhance the autophagy and helps in clearing misfolded proteins and maintain the homeostasis. Apelin can be a promising therapeutic target in the treatment of AD (Than et al., 2014). Palmitate induces apoptosis via mitochondrial dysfunctions and ROS generation and can cause activation of caspase leading to cell death (Wei et al., 2006). Palmitate is showed to activate the endoplasmic reticulum (ER) stress pathways which lead to the apoptosis in pancreatic beta-cells and suggesting that cell death induced by palmitate led to the type 2 diabetes (Korsakov et al., 2006). Our study then explored the dose dependent effect of the stable apelin analogues and their function in restoring and counteracting the deleterious effects of free fatty acids.

Cell Viability

This study has shown the apelin-13 amide and (Lys^{8}GluPAL)apelin-13-amide significantly mitigated the palmitate- induced reduction in cell viability *in-vitro*. Apelin-13 analogues improved cell survival when treated alone compared to the untreated control. The positive effects of the stable analogues were both time dependent and dose dependent in MTT

Assay. When we looked at the ATP production from metabolic active cells, apelin showed only dose dependent.

In our studies apelin-13 amide was more potent compared to (Lys^{8}GluPAL)apelin-13-amide both when used individually or when combined with palmitate. This corroborates previous findings showing similar drug action where modified versions were more stable but did not perform as well in activating the APJ receptors as apelin-13 amide (O'Harte et al., 2018). Apelin has previously shown to improve cell survival in various other in-vitro studies including oxygen glucose deprivation cell models (Zhang et al., 2022). Xia et al, has also showed protective effects of apelin in skeletal muscles cells (2020).

A study done by Parthsarathy et al, had previously indicated that apelin-13 analogues functions as a growth inhibitor (2017). Our study has used a higher concentration and a modified stable analogue which has improved bioavailability (half-life), increased affinity and increase potency (O'Harte et al., 2018). This confirms that apelin functions like a growth factor in improving cell viability and survival on its own and it has protective functions against palmitate action (Kamińska et al., 2024) .

Studies showed that palmitate inhibits the mTOR signalling pathway. Stress signals like the oxidative damage activates AMPK activation and led to reduced mTORC1 activity. By the reduced protein synthesis and increased autophagy, mTORC1 suppression will worsen the cell death (Korsakov et al., 2006). On the other side apelin-13 analogues have shown to promote cell survival by activation of PI3K/Akt pathway. It is well known for the regulation cell growth and survival. The mTORC1 is activated by the Akt phosphorylation which stimulates the protein synthesis and inhibits autophagy (Long et al., 2021).

Cell Proliferation and differentiation

Apelin-13 and its analogues have shown to significantly improve the cell proliferation and differentiation (Lopez-Suarez et al., 2022). The importance of Apelin-13 in neurogenesis is linked to its potential to influence key signalling pathways, such as PI3K/Akt and

MAPK/ERK, which are responsible for controlling cell growth and survival (Chen et al., 2020). Studies have shown that apelin activates the PI3K/Akt signalling pathway and promote the phosphorylation of Akt, cell proliferation, differentiation and reduce apoptosis (Ramasubbu & Devi Rajeswari, 2022). Apelin is also known to regulate the MAPK/ERK pathway and promoting the synaptic plasticity and cell survival. It is the most important pathway in the proliferation and differentiation in neuronal cells (Masoumi et al., 2018). However, studies shows that palmitate might block the PI3K/Akt pathway, an essential pathway for cellular differentiation and proliferation. Palmitate enhances oxidative stress and impaired mitochondrial function, resulting in the inhibition of PI3K/Akt signalling. This leads to impaired phosphorylation of Akt, resulting in heightened apoptosis and lower cell viability (Calvo-Ochoa et al., 2017).

Cell proliferation in SH-SY5Y cells is promoted by activating the PI3K/Akt pathway. When the apelin-13 bind to the APJ receptor it activates PI3K (phosphoinositide 3-kinase) which leads to the phosphorylation of Akt (Protein kinase B), which then regulates the cell growth, divisor and protein synthesis Via mTORC1 activation. The mTORC1 is the key regulator pathway for cell growth and protein synthesis, and palmitate activated the AMPK that suppresses the mTORC1 activity which results in the cell death (Zheng et al., 2021). Our results have shown that the apelin-13 analogues have shown non-significant improvement in cell proliferation when treated in combination to the palmitate in SH-SY5Y cells. The non-significant increase can be due to the severity of the stress induced by palmitate or the short half-life of the apelin-13 analogues.

The results from the neurite outgrowth assay demonstrated that apelin-13 amide and (Lys8GluPAL)apelin-13-amide promoted significant increase in neurite extension and palmitate reduced neurite extension significantly. When the cells were treated with palmitate alongside with apelin-13 analogues it improved the neurite extensions significantly suggesting that impact of apelin on the reduction of oxidative stress, improving mitochondrial function, inhibiting apoptosis, and activation the key signalling pathways.

Studies suggested that consumption of hight fat diets with saturated fatty acids like palmitic acid trigger ER stress and oxidative stress and disrupting the cytoskeletal

dynamics, which are essential for neurite extensions (Jo et al., 2021). Study by Hao et al, illustrated that palmitate suppressed the ERK1/2 pathway which is involved in neuronal differentiation and neurite outgrowth (2015). Although the inhibition of mTORC1 by AMPK activation plays essential role in impaired neurite outgrowth by limiting the synthesis of essential proteins for neurite extensions (Duan et al., 2019). Apelin-13 and its analogues have shown to improve neuronal development and outgrowth by stimulating pathways involved in enhancing the structural proteins. Apelin-13 activate the ERK1/2 and PI3/Akt pathway crucial for promoting cytoskeletal remodelling and growth formation facilitating neurite extensions (Deng et al., 2022).

Apelin-13 amide and (Lys8GluPAL)apelin-13-amide promoted neuronal differentiation and increased MAP2 expression, a marker of neuronal maturation (Zhang et al., 2011). The differentiation and maintenance of the neuronal cells is critical for the cognitive health and the results have shown that palmitate induced cell death and reduced neuronal cell differentiation. Studies suggest that apelin-13 may activate the signalling pathways that promote neuronal growth and connectivity (García-Cruz & Arias, 2024). Apelin-13 activated the ERK1/2 pathway which are essential for differentiation and synaptic plasticity (Lv et al., 2020). Our results shows that apelin-13 and its analogue improved the MAP2 expression significantly when treated alone and non-significantly when combined with palmitate. These findings suggest the key pathways that apelin-13 can promote to increase the cell proliferation differentiation and neuronal development.

Cell Toxicity

We employed two different assays to measure the cell toxicity, one is to look at the LDH release from damaged or lysed cells in the media both at time and dose dependant. And other one is to detects the membrane integrity loss in dead or dying cells where apelin-13 only showed dose dependant. Previous studies have shown that apelin-13 analogues have protective effect, and it should mitigate the effect of palmitate (Chen, 2014). Studies

by Yin et al, have shown that apelin-13 reduced cell toxicity induced by cisplatin an anticancer drug (2020).

Our results illustrated that cytotoxicity was significantly reduced in cells treated with apelin-13 amide and (Lys^{8}GluPAL)apelin-13-amide when treated with higher concertation of palmitate at all time points. And the reduction in cell toxicity was consistently seen at 4 hour for both concentration of palmitate suggesting the early protective effect. This suggest that both analogues provide the protection but it various with the concentration of the palmitate and the timepoint which can be due to the difference in stability of the analogues.

However, the results from the assay to measure the DNA damage have shown that apelin-13 analogues did not significantly make any impact when treated with 0.6 mM palmitate but at 1.0 mM palmitate (Lys^{8}GluPAL)apelin-13-amide significantly reduced the cells toxicity. The lack of protection by the apelin-13 analogues at the 0.6 mM palmitate can be due stronger activation of the cell survival pathways PI3/Akt/mTOR and AMPK under severe stress.

Oxidative Stress

Oxidative stress plays crucial part in the pathogenesis of AD. Palmitate elevated ROS levels in SH-SY5Y cells which led to oxidative stress (Baldwin et al., 2012). In our study, we measured oxidative stress by GSH/GSSG ratio, ROS levels and JC-1 mitochondrial membrane potential along with NRF-2 expression via western blot. Our results shows that GSH/GSSG ratio was significantly enhanced by treatment with Apelin-13 amide and (Lys^{8}GluPAL)apelin-13-amide alone and combined with palmitate indicating the antioxidant capacity. The reduction of GSH/GSSG ratio indicates the oxidative stress caused by palmitate as the conversion of GSH to GSSG is response to the elevated ROS levels. GSH is a major antioxidant that protect neurons from oxidative stress and neutralises the ROS. GSH/GSSG is the key indicator of cellular redox balance

(Fernández-Sánchez et al., 2011). The reduced GSH/GSSG ratio suggest reduced antioxidant defence and high oxidative stress in AD (Ansari & Scheff, 2010).

The recent studies have suggested the role of apelin-13 in the redox balance is really critical as it promotes the synthesis and regeneration of the GSH and minimize the oxidative stress induced by palmitate treatments (Than et al., 2014) (Fernández-Sánchez et al., 2011). This is also supported by the increased activity of antioxidant enzymes which are important to neutralize the ROS and protect cells from oxidative stress (Fang et al., 2002). To further analyses we used ROS assay where it showed that the treatment with apelin-13 amide and (Lys^{8}GluPAL)apelin-13-amide reduced the ROS levels but not significantly for lower concertation of palmitate and made slight difference to the cells treated with higher concentrations. Suggests that apelin-13 analogues can mitigate the oxidative stress, but it may be less effective under the higher concertation of the palmitate. The increased ROS levels trigger pro-apoptotic signalling via JNK (c-jun N-terminal kinase) and p38 MAPK pathways contributing to cellular damage and apoptosis (Yin et al., 2020).

We have shown that the palmitate treatment led to the mitochondrial damage in SH-SY5Y cells that has increased ROS production and causing increased mitochondrial membrane depolarisation which cased cell apoptosis (Ng & Say, 2018) (Fernández-Sánchez et al., 2011). Previous studies have shown the protective effect of apelin-13 on the $\Delta\Psi_m$ by reducing oxidative stress markers, and inhibiting apoptotic pathways (Liu et al., 2023). Studies have shown that cytochrome C is released in response to the stress to cytoplasm and it triggers intrinsic apoptotic pathway. which then activates caspase proteins which are responsible for dismantling the cell during apoptosis (Xu et al., 2017). Our results shows that palmitate treated cells showed a significant loss of mitochondrial membrane potential and apelin-13 analogues have improved the mitochondrial potential induced by palmitate but not significantly. However, the lack of the significant change can be used to the severe oxidative stress caused by palmitate treatment.

Furthermore, our results showed an increase in NRF-2 a transcriptional factor by palmitate alone and reduction in NRF-2 protein expression when cells co-currently treated with apelin-13 analogues also suggest that apelin-13 can enhance the cellular antioxidant

defence system. NRF-2 regulates the expression of antioxidant genes to detoxify ROS and to maintain a balance in the redox homeostasis and protects neurons against oxidative stress by activating PI3K/Akt and AMPK pathways (Wan et al., 2021). Study by Ma et al have shown that oxidative stress can rise the formation and ROS by downregulating the NRF-2 activity (Ramyaa et al., 2014).

Apoptosis

To further elucidate the mechanism of apoptosis linked with oxidative stress we have examined caspase 3/7 activity and expression of BAX and Bcl2 proteins. Our results demonstrated marked activation of caspase-3/7 in palmitate-treated cells, reflecting the induction of intrinsic apoptotic pathway, mediated by mitochondrial collapse and oxidative stress. This is in accordance with previous evidence showing that mitochondrial membrane depolarization, cytochrome c and caspases activation are involved in palmitate-induced apoptosis (Xu et al., 2017) (Takeo et al., 2024). Treatment with apelin-13 markedly decreased caspase-3/7 activity, indicating an anti-apoptotic effect that is likely mediated through the rescuing of mitochondrial function and boosting antioxidant defence mechanisms via NRF-2 pathway discussed above (Yin et al., 2020).

Our western blot analysis showed that palmitate increased a pro-apoptotic protein BAX expression, which reducing anti-apoptotic protein Bcl-2. The balance between the BAX and Bcl-2 Bax promotes mitochondrial outer membrane permeabilization which results in release cytochrome c and activation of caspase. Apelin-13 and analogues have improved the expression of Bcl-2 by reducing the BAX expression suggesting the protective effect. The reduction in caspase 3/7 activity and alteration of the apoptosis related protein BAX and Bcl-2 illustrates that apelin-13 have been useful to hinder the apoptotic pathways triggered by palmitate (Shao et al., 2021).

3.4. Conclusion

Apelin-13 amide and (Lys^{8}GluPAL)apelin-13-amide is a neuroprotective peptide that be used for targeting different pathological pathways including, oxidative stress, inflammation, apoptosis, synaptic function and autophagy. Effect of apelin-13 to reduce cell toxicity, improve cell proliferation, reduce oxidative stress make the possibilities for the development of novel therapeutic strategies for AD (Shown in Table 3). The importance of apelin-13 in neurogenesis is linked to its potential to influence key signalling pathways, such as PI3K/Akt and MAPK/ERK, which are responsible for controlling cell growth and survival (Chen et al., 2020). This research has shown that the apelin-13 analogues have been able to mitigate the effect of palmitate induced oxidative stress and apoptosis and improving the cell viability, proliferation, and differentiation in SH-SY5Y cells.

Experiments	Assays Used	Palmitate Effect	Apelin Effect	Pathway Impact
Cell Viability	MTT, CellTiter-Glo	↓ cell viability	↑ viability under palmitate induced stress	PI3K/Akt activation for survival signalling
Proliferation & Differentiation	BrdU, MAP2, Neurite Outgrowth	↓ cell proliferation and neurite outgrowth	↑ cell proliferation and neurite outgrowth	PI3K/Akt for proliferation, ERK1/2 for promoting cytoskeletal remodelling
Cell Toxicity	LDH, CellTox Green	↑ cell toxicity	↓ cell toxicity induced by palmitate	AMPK activation, NRF-2-linked antioxidant response
Mitochondrial & Oxidative Stress	JC-1, ROS-Glo, GSH/GSSG	↓ MMP, ↑ ROS, disturbed redox balance	↑ MMP, ↓ ROS, normalized redox balance	AMPK/NRF-2 pathway activated, mitochondrial membrane potential improvement
Apoptosis	Caspase 3/7, BAX, Bcl-2	↑ apoptosis, ↑ pro-apoptotic and ↓ anti-apoptotic protein expression	↓ caspase activity, ↓ pro-apoptotic and ↑ anti-apoptotic protein expression	PI3K/Akt inhibits apoptosis,

Table 3: Collective summary effect of apelin-13 and its analogues on SH-SY5Y cells under palmitate-induced stress.

This table shows the protective effect of apelin-13 and its analogues on the oxidative stress, apoptosis, ER stress, mitochondrial membrane potential in SH-SY5Y cells. Apelin-13 analogues improved cell viability, inhibited apoptosis via PI3/K/Akt and reduced oxidative stress via AMPK-NRF-2 pathways, proving its potential for AD therapeutics.

Chapter 4

Protective effect of apelin-13 analogues against Hydrogen Peroxide-induced oxidative stress.

4.1. Introduction

AD is characterised by the cognitive decline and the synaptic dysfunction. There are number of factors that impact on the progression of AD like age, genetics, lifestyle and environment (Pistollato et al., 2018). Oxidative stress is the critical factor in the neuronal death and the progression of the disease. Oxidative stress rises due to the imbalance between the ROS production and cellular antioxidant defence system leading to lipid peroxidation, toxicity, DNA damage, disrupting cell functions and membrane integrity (Zhao et al., 2019).

H_2O_2 is a byproduct of the normal cellular metabolism, and it is naturally occurring ROS in the brain. It plays a key role in the regulation of neuronal plasticity, antioxidant defence and synaptic formation (Konno et al., 2021). Excessive exposer to H_2O_2 leads to neuronal damage and oxidative stress (Chen et al., 2009). As Mitochondria has high metabolic activity it is known as the primary source of H_2O_2. H_2O_2 levels are shown to be elevated in the brain of AD in several studies, as mitochondrial dysfunction increases the production of ROS, Aβ plaques and inflammation (Misrani et al., 2021). Number of studies used H_2O_2 as a stress induced to mimic the disease like environment to study neurodegenerative diseases caused by oxidative stress. Neuronal dysfunction is caused by H_2O_2 through number of mechanisms like mitochondrial impairment, disruption of redox homeostasis and activating apoptotic pathway (Misrani et al., 2021).

Apelin-13 analogues has been studied for various pathological condition due to its protective effects against the cellular stress. It is a bioactive peptide and endogenous ligand of APJ receptor, which is found in various tissues in the body (O'Harte et al., 2017). Recent studies have shown that apelin-13 and its analogues modulated oxidative stress, inflammation, reduced apoptosis and promoted cell survival and proliferation (Li et al., 2024). Number of key pathways are activated when apelin binds to APJ, like AMPK, ERK and PI3K/Akt pathway (Li et al., 2024; Senturk & Manfredi, 2012). ERK is involved in cell proliferation and differentiation, AMPK regulates cellular energy homeostasis and reduce oxidative stress and PI3K/Akt pathway is critical for cell survival by inhibiting pro-apoptotic

factors (Savova et al., 2023). Studies have showed that apelin-13 analogues improve the mitochondrial function by reducing the oxidative stress. Study by Wang et al, have showed that apelin-13 analogues activated the PI3K/Akt pathway and reduce the ROS levels and protect against the cytotoxicity (2020). Apelin-13 is known to maintain the cellular homeostasis and alleviates the apoptosis and ER stress (Cheng et al., 2021).

The aim of this chapter is to explore the neuroprotective effect of apelin-13 amide and (Lys^{8}GluPAL)apelin-13 amide on cellular stress induced by the H_2O_2. We explored the effects of apelin-13 via cell viability, toxicity, proliferation, differentiation, apoptosis, ROS quantification, GSH/GSSG ratio, caspase activity and western blot assays. We looked at the key pathways involved in the oxidative stress, inflammation and ER stress and illustrated that apelin-13 and its analogues have a protective effect against the stress induced by H_2O_2.

Objectives:

1. Evaluate the role of apelin-13 amide and (Lys^{8}GluPAL)apelin-13 amide in modulation oxidative stress and apoptosis.
2. Investigate the protective effect of apelin-13 and it analogue on the ER stress and proteostasis.
3. Explore the protective effect of apelin-13 amide and (Lys^{8}GluPAL)apelin-13 amide on cell survival and cell growth under H_2O_2 induced stress.

4.2. Results

4.2.1: Effect of apelin-13 analogues on improved cell viability upon persistent H_2O_2 induced stress.

Apelin-13 analogues restored cell viability of SH-SY5Y cells when stress induced by H_2O_2 (50 μM and 100 μM). The cells were treated at different timepoints alone with H_2O_2 in presence or absence of apelin-13 amide and (Lys^{8}GluPAL)apelin-13 amide. The CyQUANT ™ MTT Cell Viability Assay Kit was used to measure the cell viability based on the conversion of yellow MTT tetrazolium dye to purple formazan crystals by metabolic active cells. At 2 hours cell viability was significantly enhanced by 22% with apelin-13 amide (Figure 4.1A, $p<0.01$) and 26% by (Lys^{8}GluPAL)apelin-13 amide (Figure 4.1A, $p<0.001$), however reduced by 29% (Figure 4.1A, $p<0.001$) for 50 μM H_2O_2 and 40% by 100 μM H_2O_2 (Figure 4.1A, $p<0.0001$), compared to untreated control. Compared to H_2O_2 alone, co-treatment of apelin-13 amide with 50 μM H_2O_2 restored cell viability by 28% (Figure 4.1A, $p<0.05$), and with 100 μM H_2O_2 by 51% (Figure 4.1A, $p<0.0001$). And co-treatment of (Lys^{8}GluPAL)apelin-13 amide with 50 μM H_2O_2 led to 45% (Figure 4.1A, $p<0.0001$) restoration and 52% at 100 μM H_2O_2 (Figure 4.1A, $p<0.001$).

The cell viability was significantly enhanced by 25% at 4 hours treatment with apelin-13 amide (Figure 4.1B, $p<0.0001$) and 17% by (Lys^{8}GluPAL)apelin-13 amide (Figure 4.1B, $p<0.01$), however reduced by 29% for 50 μM H_2O_2 (Figure 4.1B, $p<0.0001$), and 36% by 100 μM H_2O_2 (Figure 4.1B, $p<0.0001$), compared to untreated control.

Compared to H_2O_2 alone, co-treatment of 50 μM H_2O_2 with apelin-13 amide increased cell viability by 32% (Figure 4.1B, $p<0.0001$), and 30% (Figure 4.1B, $p<0.0001$), with (Lys^{8}GluPAL)apelin-13 amide. Co-treatment of 100 μM H_2O_2 restored the cel viability by 31% (Figure 4.1B, $p<0.0001$), and 25% (Figure 4.1B, $p<0.01$), for apelin-13 amide and (Lys^{8}GluPAL)apelin-13 amide respectively.

The results revealed that compared to untreated control, apelin-13 amide and (Lys^{8}GluPAL)apelin-13 amide alone at 6 hours increased the cell viability by 22% (Figure 4.1C, $p<0.01$) and 26% (Figure 4.1C, $p<0.001$) respectively. The cell viability was reduced by 34% (Figure 4.1C, $p<0.0001$) with 50 μM H_2O_2, and 51% (Figure 4.1C, $p<0.0001$) for 100 μM H_2O_2, compared to untreated control. Co-treatment of 50 μM H_2O_2 with apelin-13 amide restored cell viability by 30% (Figure 4.1C, $p<0.05$) and 43% (Figure 4.1C, $p<0.0001$) when treated with (Lys^{8}GluPAL)apelin-13 amide, compared to H_2O_2. Co-treatment of 100 μM H_2O_2 with apelin-13 amide restored cell viability by 42% (Figure 4.1C, $p<0.01$) and 51% (Figure 4.C, $p<0.001$) when treated with (Lys^{8}GluPAL)apelin-13 amide, compared to H_2O_2.

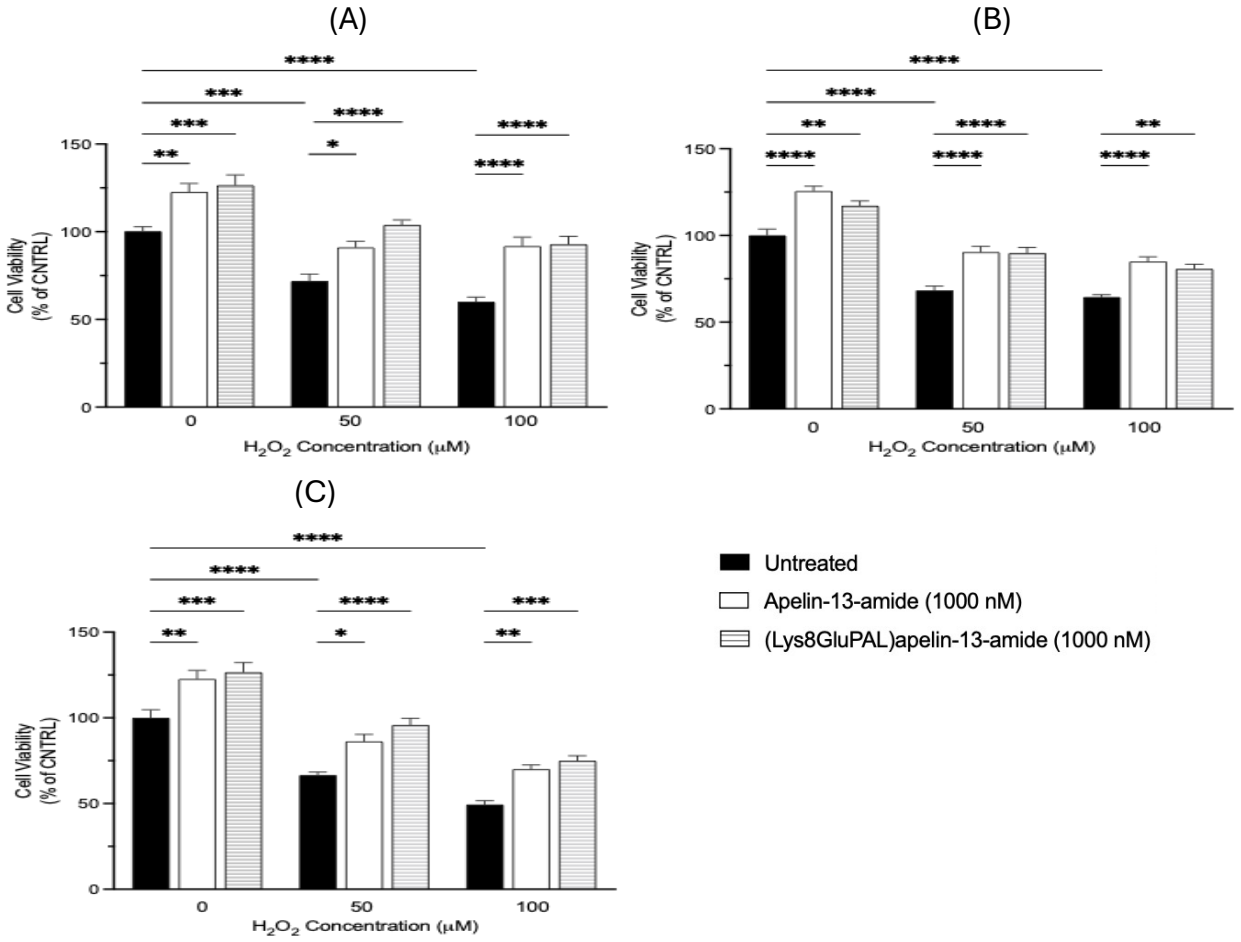

Figure 4.1: Effect of apelin-13 analogues on improved cell viability upon persistent H_2O_2 induced stress. Time dependent effect of apelin-13 analogues on neuronal viability of SH-SY5Y cells with and without H_2O_2 *in-vitro*. Cells were treated with treatments for (A) 2 hours. (B) 4 hours and (C) 6 hours. Values

represent mean ±SEM (one-way ANOVA, n=3 where *p<0.05, **p<0.01, ***p<0.001, and ****p<0.0001 compared to control.

4.2.2: Effect of apelin-13 analogues against dose dependant deterioration of cell viability by H_2O_2-induced stress in SH-SY5Y cells.

The cells were treated for 6 hours and CellTiter-Glo viability kit was used to measure the cell viability based on the ATP release from metabolic active cells in SH-SY5Y cells in-vitro. The results showed that the cell viability was significantly improved by apelin-13 amide by 16% (Figure 4.2, p<0.001) and by 8% (Figure 4.2, p>0.05) with (Lys^{8}GluPAL)apelin-13 amide, compared to untreated control. H_2O_2 (50 μM) reduced cell viability by 15% (Figure 4.2, p<0.001), and H_2O_2 (100 μM) by 20% (Figure 4.2, p<0.0001), compared to untreated control. Co-treatments 50 μM H_2O_2 with apelin-13 amide led to 5% increase in cell viability (Figure 4.2, p>0.05) and 9% (Figure 4.2, p<0.05) by (Lys^{8}GluPAL)apelin-13 amide, compared to H_2O_2 treatment alone. However, the treatment with 100 μM H_2O_2 and apelin analogues had no change, compared to H_2O_2 alone.

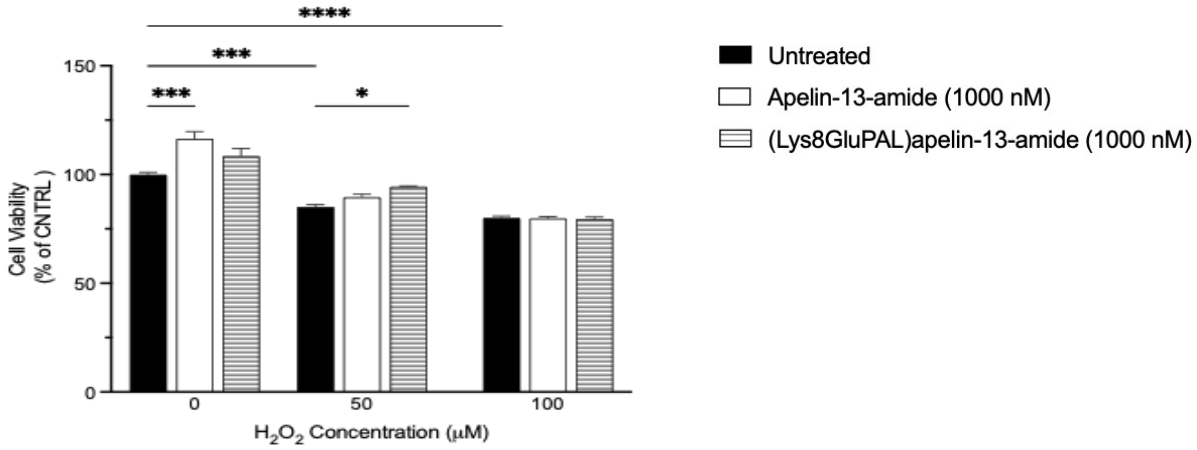

Figure 4.2: Apelin-13 analogues protect against dose dependant deterioration of cell viability by H_2O_2-induced stress in SH-SY5Y cells. The cells were exposed to H_2O_2 in presence or absence of apelin-13 amide and (Lys^{8}GluPAL)apelin-13 amide for 6 hours. Prior to the treatment the cells were incubated with 5 μM Compound C for AMPK pathway involvement. Celltiter-Glo luminescent assay was used to measure

the viability by ATP production. Cell values represent mean ±SEM for n=3 where *p<0.05, ***p<0.001, ****p<0.0001.

4.2.3: Effect of apelin-13 analogues on improved cell proliferation against H_2O_2-induced stress.

BrdU incorporation assay was used to measure the cell proliferation in SH-SY5Y cells, where BrdU binds to the newly synthesized DNA. The cells were treated for 6 hours with peptides in presence or absence of H_2O_2 and representative images of BrdU immunofluorescent under Olympus Inverted Microscope at 20X magnification are shown Figure 4.3A and the graph analysis is showed in Figure 4.3B. The results showed that compared to untreated control, apelin-13 amide and (Lys^8GluPAL)apelin-13 amide improved cell proliferation by 5% (Figure 4.3B, p>0.05) and 13% (Figure 4.3B, p>0.05) respectively and 50 μM H_2O_2 reduced the cell proliferation by 55% (Figure 4.3B, p<0.01). Co-treatment of 50 μM H_2O_2 with apelin-13 amide improved cell proliferation by 31% (Figure 4.3B, p>0.05) and (Lys^8GluPAL)apelin-13 amide by 9% (Figure 4.3B, p>0.05), compared to H_2O_2 alone.

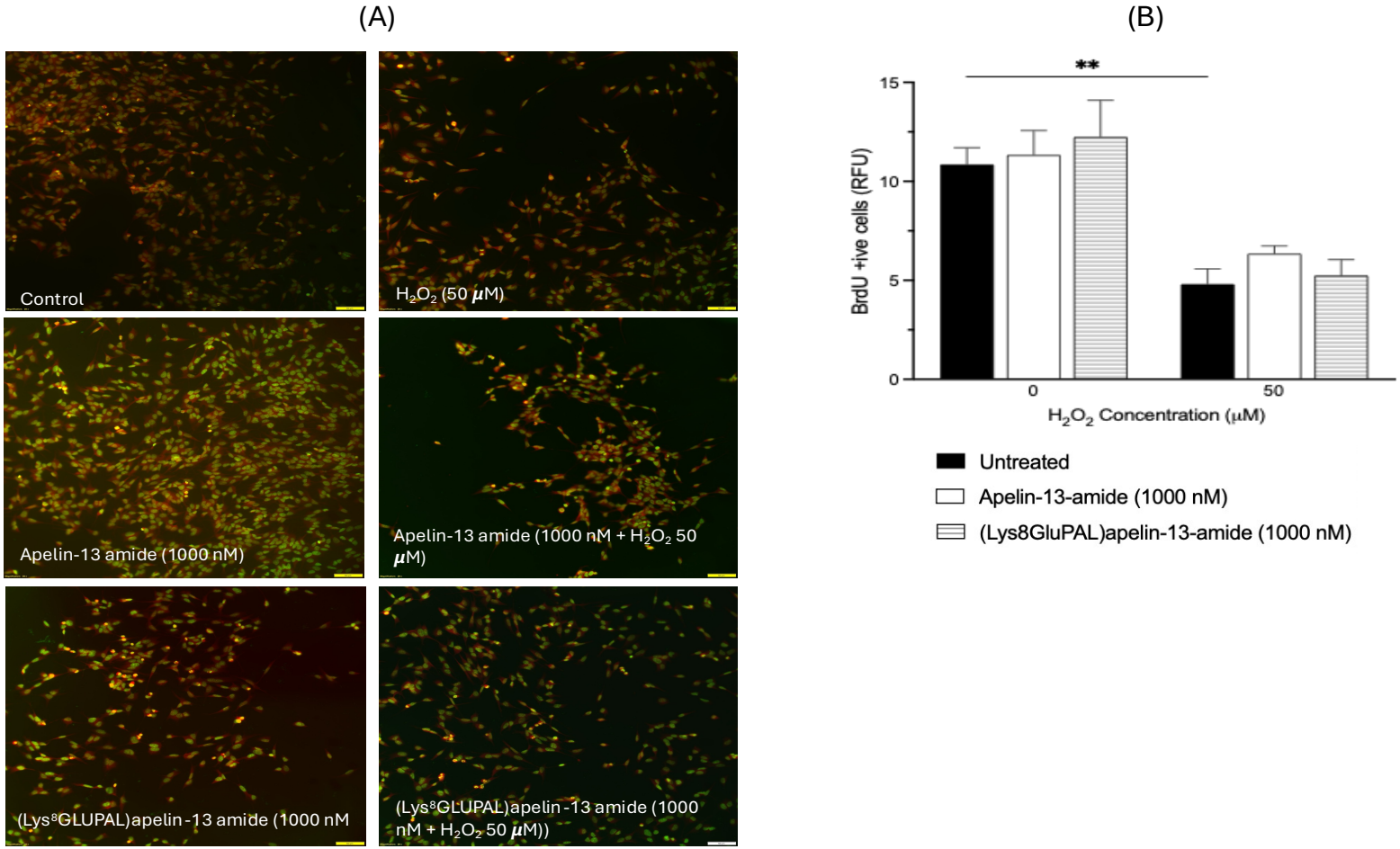

Figure 4.3: Effect of apelin-13 analogues on improved cell proliferation against H_2O_2-induced stress. Cells were treated with H_2O_2 in presence or absence of apelin-13 analogues to look at the cell proliferation. BrdU incorporation assay was used to assess cell proliferation in SH-SY5Y cells. (A) Representative images of SH-SY5Y cells stained with BrdU and DAPI are shown (20x magnification). (B) Graph of quantification of BrdU positive cells treated with Apelin-13-amide, and (Lys^{8}GluPAL)apelin-13-amide with and without H_2O_2. Values represents mean ±SEM for n=3 where **p<0.01.

4.2.4: Effect if of apelin-13 analogues on neurite outgrowth under stress induced by H_2O_2.

The SH-SY5Y cells were incubated with RA for 72 hours and treated for 24 hours with apelin-13 analogues in presence or absence of H_2O_2. The cells were stained with Coomassie brilliant blue stain and upright light microscope at 20X magnification was used to look at the neurite extensions and were counted manually by observing neurites double the size of the cell body. The data showed that compared to the untreated control, apelin-13 amide increased the neurite extensions by 26% (Figure 4.4 B, $p<0.05$), and (Lys^8GluPAL)apelin-13 amide by 29% (Figure 4.4 B, $p<0.01$), however H_2O_2 reduced neurites by 56% (Figure 4.4B, $p<0.0001$). When the cells were co-treated with H_2O_2 and apelin-13 amide the neurite growth improved by 38% (Figure 4.4B, $p>0.05$) and 28% (Figure 4.4B, $p<0.01$) by (Lys^8GluPAL)apelin-13 amide, compared to H_2O_2 alone.

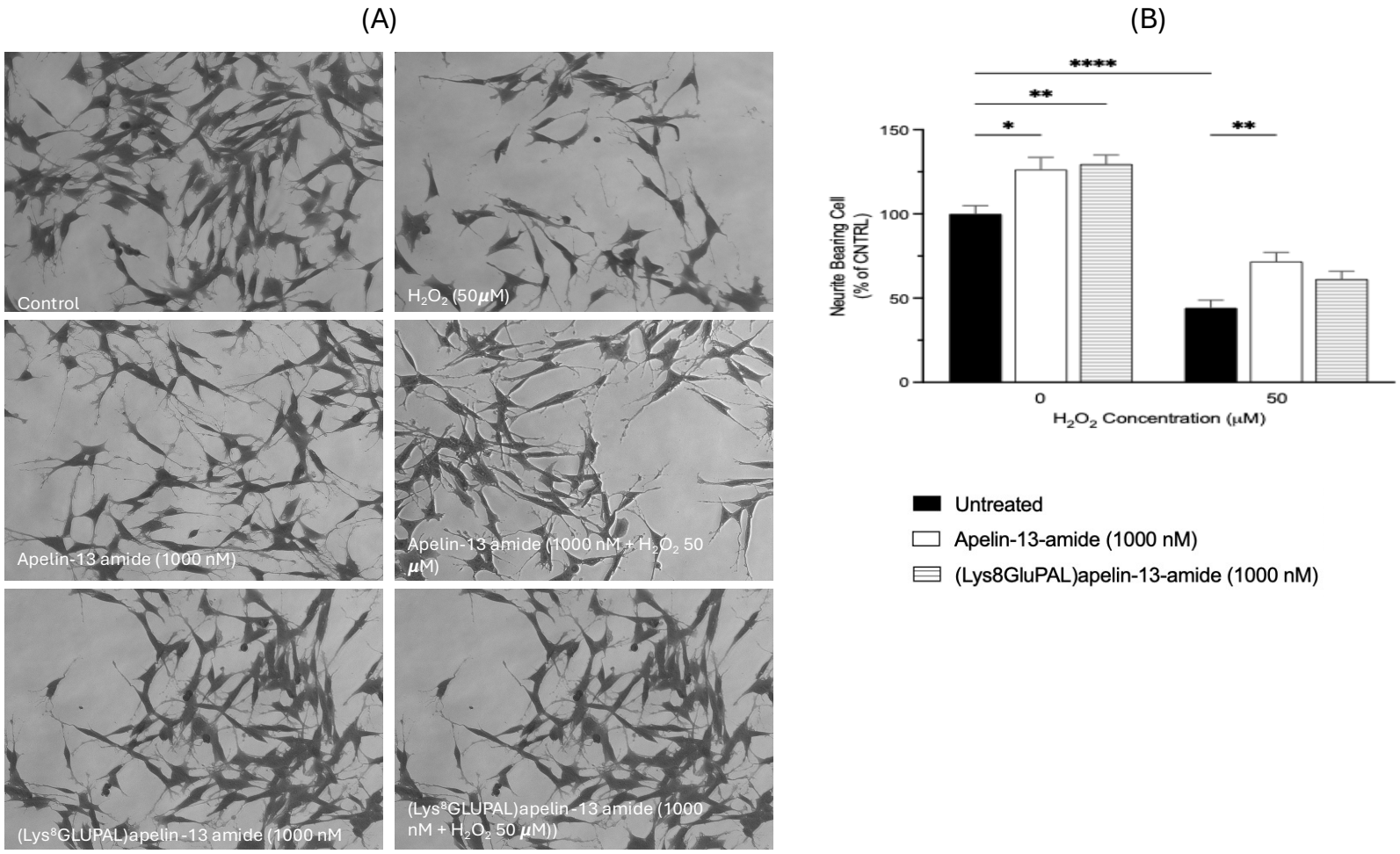

Figure 4.4: Effect of apelin-13 analogues on neurite outgrowth under stress induced by H_2O_2. The cells were pre-incubated in retinoic acid for 24 before treatments of H_2O_2 in presence or absence of apelin-13 analogues for 6 hours. Coomassie brilliant blue staining was used to stain the cells and images under upright microscope at 20X magnification. Neurite growth was quantified as the percentage of cells bearing axodendritic processes longer than two times cell diameters in length for cells treated with H_2O_2. Values represents mean ±SEM for n=3 where **p<0.01.

4.2.5: Effect of apelin-13 analogues on improved neuronal differentiation under H_2O_2 induced stress.

MAP2, a marker for differentiation was used to measure the neuronal integrity and differentiation in SH-SY5Y cells under H_2O_2-induced stress. The cells were captured under upright microscope at 20X magnification and image J was used to quantify the intensity where (A) is representative images and (B) graph of the optical density. The results showed that treatment with apelin-13 amide (12%; Figure 4.5B, $p>0.05$) and (Lys^{8}GluPAL)apelin-13-amide (25%; Figure 4.5B, $p>0.05$) increased MAP2 expression non significantly, compared to untreated control. However, the treatment with H_2O_2 reduced the neuronal differentiation by 46% (Figure 4.5B, $p>0.05$), compared to untreated control. The co-treatment of apelin-13 amide and (Lys^{8}GluPAL)apelin-13-amide with H_2O_2 improved the differentiation by 32% (Figure 4.5B, $p>0.05$) and 48% (Figure 4.5B, $p>0.05$) respectively, compared to H_2O_2 alone.

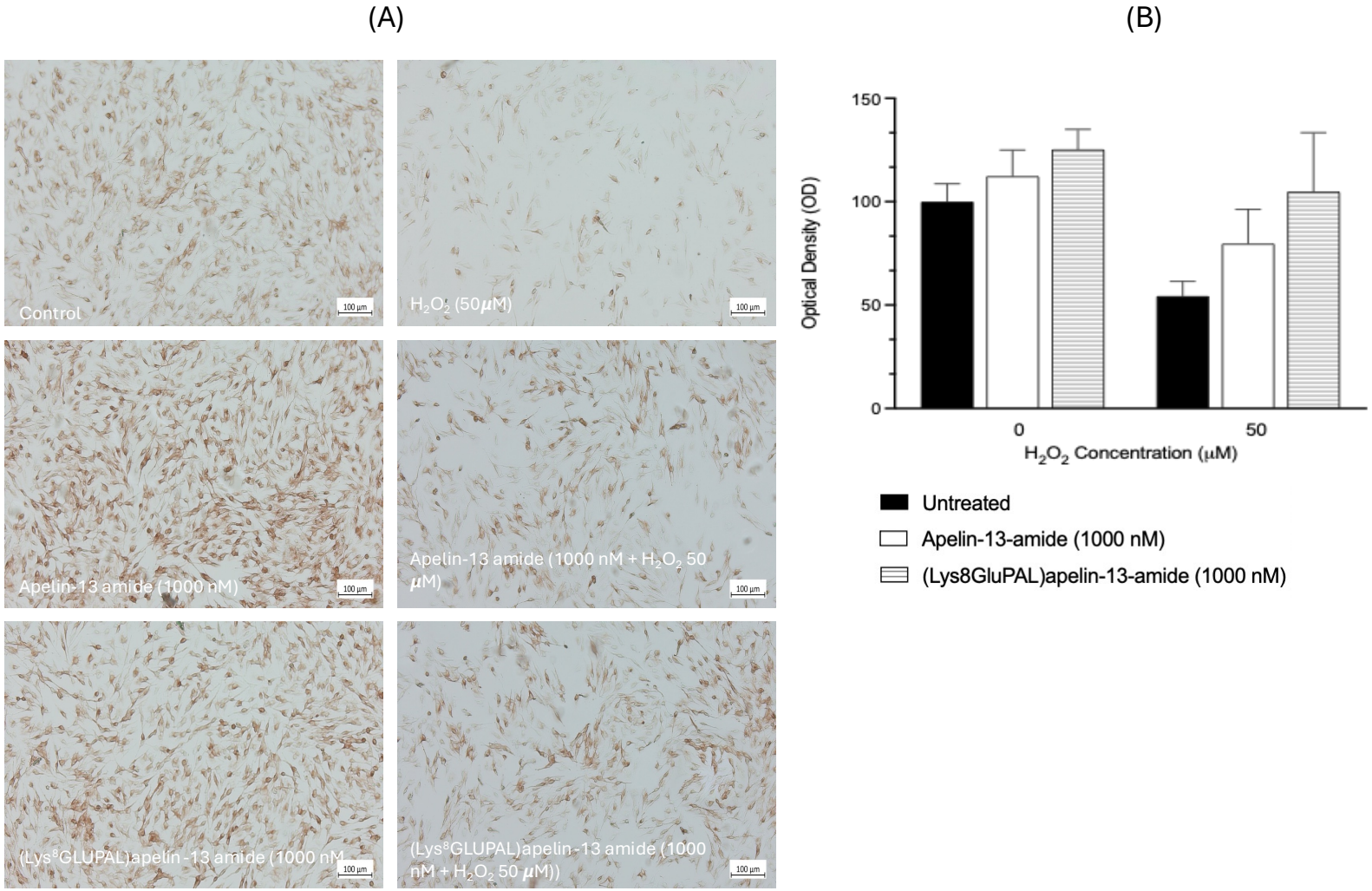

Figure 4.5: Effect of apelin-13 analogues on improved neuronal differentiation under H_2O_2 induced stress. The cells were pre-incubated in retinoic acid for 24 before treatments of H_2O_2 in presence or absence of apelin-13 analogues for 6 hours. (A) Representative photographs depicting MAP2 expression in SHY-SY5Y cells (B) graph showing quantification of MAP2 expression under Light microscope. Values represent mean ±SEM for n=3 where **p<0.01.

4.2.6: Effect of apelin-13 analogues against H_2O_2 -induced cell toxicity at different timepoints.

The cells were treated with apelin-13 analogues in presence or absence of H_2O_2 for 2-6 hours and cell toxicity was measured using LDH assay. At 2 hours apelin-13 amide and (Lys^{8}GluPAL)apelin-13-amide significantly reduced cell toxicity induced by 50 μM H_2O_2 (30%, Figure 4.6A, $p<0.001$) and 100 μM H_2O_2 (26%, Figure 4.6A, $p<0.01$), compared to untreated control. However, H_2O_2 treatment led to increase of LDH release by 22% (Figure 4.6A, $p<0.01$) for 50 μM and 41% (Figure 4.6A, $p<0.0001$) for 100 μM, compared to untreated control. Apelin-13 amide co-treatment with 50 mM H_2O_2 reduced cell toxicity by 24% (Figure 4.6A, $p<0.001$) and 30% (Figure 4.6A, $p<0.0001$) with 100 μM H_2O_2, compared to H_2O_2 alone. And (Lys^{8}GluPAL)apelin-13-amide reduced toxicity by 22% (Figure 4.6A, $p<0.0001$) for 50 μM H_2O_2 and 32% (Figure 4.6A, $p<0.0001$) for 100 μM H_2O_2.

At 4 hours, the treatments with apelin-13 amide and (Lys^{8}GluPAL)apelin-13 amide showed significant reduction in cell toxicity by 25% (Figure 4.6B, $p<0.0001$) and 27% (Figure 4.6B, $p<0.0001$) respectively and increased by 32% (Figure 4.6B, $p<0.0001$) with 50 μM H_2O_2 and 47% (Figure 4.6B, $p<0.0001$) with 100 μM H_2O_2, compared to untreated control. The cell toxicity was reduced when cells were co-currently treated with apelin-13 amide and 50 μM H_2O_2 by 13% (Figure 4.6B, $p<0.001$) and by 20% for 100 μM H_2O_2 (Figure 4.6B, $p<0.0001$). (Lys^{8}GluPAL)apelin-13 amide co-treatment with 50 μM H_2O_2 and 100 μM H_2O_2 led to reduction in cell toxicity by 20% (Figure 4.6B, $p<0.001$) and 25% (Figure 4.6B, $p<0.001$) respectively, compared to H_2O_2, treatment alone.

Compared to untreated control, the cell toxicity at 6 hours was reduced by 18% (Figure 4.6C, $p<0.001$) for apelin-13 amide and 32% (Figure 4.6C, $p<0.01$) for (Lys^{8}GluPAL)apelin-13 amide, however increased by 40% (Figure 4.6C, $p<0.0001$) for 50 μM H_2O_2. The co-treatment of 50 μM H_2O_2 with apelin-13 amide reduced cell toxicity y 27% (Figure 4.6C, $p<0.001$) and with (Lys^{8}GluPAL)apelin-13 amide by 16% (Figure 4.6C,

p<0.05), compared to H_2O_2 treatment alone. There was no significant change by apelin-13 analogues or 100 μM H_2O_2 on cell toxicity (Figure 4.6C, p>0.05).

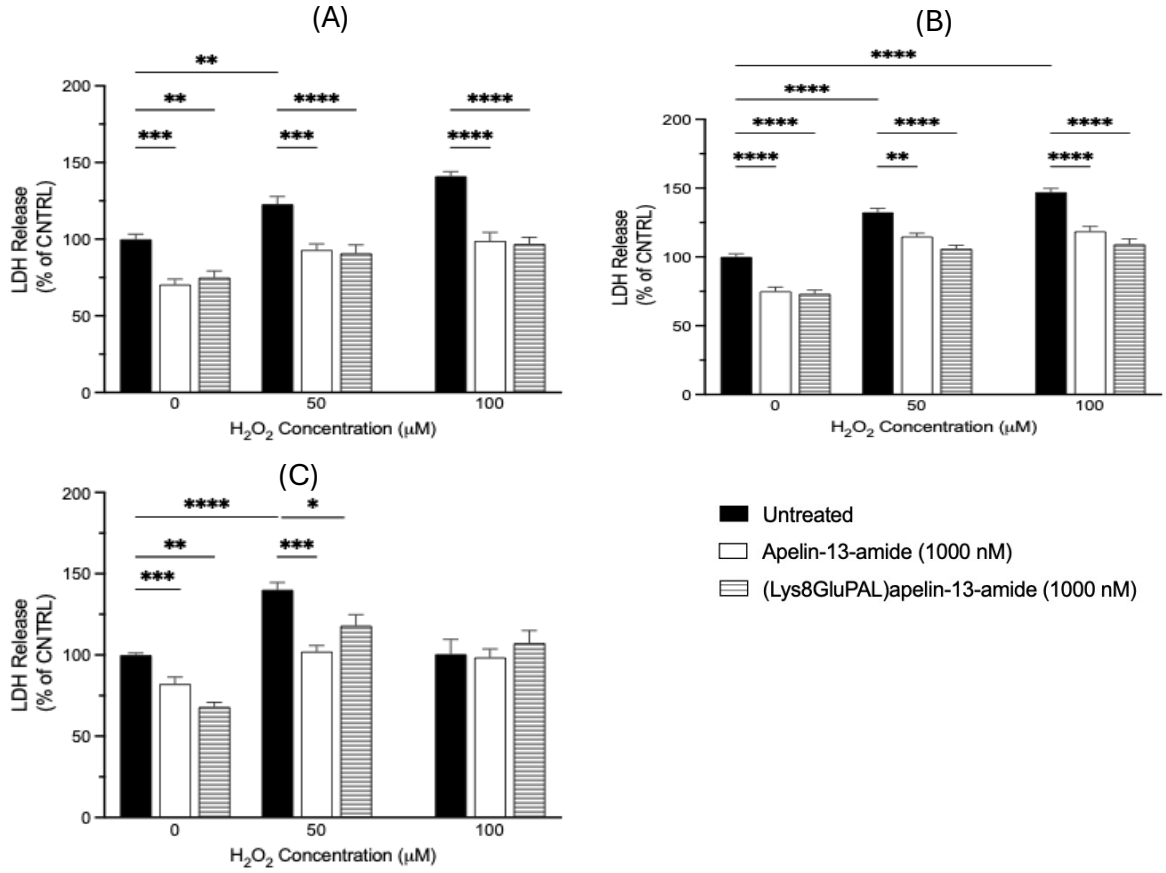

Figure 4.6: Effect of apelin-13 analogues against H_2O_2-induced cell toxicity at different timepoints. Following 24-hour cell seeding and 8-hour serum starvation, cells were exposed to H_2O_2 in presence or absence of apelin-13 amide and (Lys^{8}GluPAL)apelin-13-amide for (A) 2-hour (B) 4-hour (C) 6-hour. The Lactate dehydrogenase (LDH) release presented as percentage of control. Values represents mean ±SEM (one-way ANOVA, n=3 where *p<0.05, **p<0.01, ***p<0.001, and ****p<0.0001.

4.2.7: Effect of apelin-13 analogues on mitigating cell toxicity induced by H_2O_2 measured by DNA damage .

The cells were treated with apelin-13 analogues for 6 hours in presence or absence of H_2O_2 (50 and 100 μM) and CellTox Green cytotoxicity assay kit was used to measure DNA damage for cell toxicity in SH-SY5Y cells in-vitro. The results showed that the cell toxicity was significantly reduced by 20% (Figure 4.7, $p<0.001$) by apelin-13 amide and 22% (Figure 4.7, $p<0.001$) by (Lys⁸GluPAL)apelin-13 amide at 6 hours, however H_2O_2 (50 and 100 μM) increased the cell toxicity by 10% and 37% (Figure 4.7, $p<0.05$), compared to untreated control. The co-treatments of H_2O_2 (100 μM) with apelin-13 amide showed reduction in cell toxicity by 21% (Figure 4.7, $p<0.05$) and by 28% (Figure 4.7, $p<0.05$) for (Lys⁸GluPAL) pelin-13 amide, compared to H_2O_2 treatment alone. However, there was no significant change seen when treated with apelin-13 analogues and H_2O_2 50 μM.

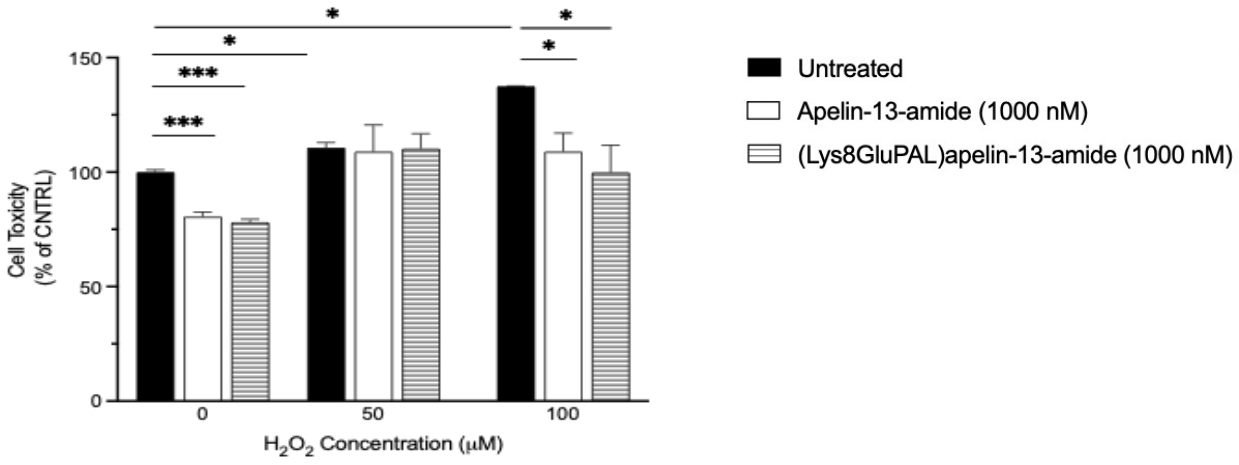

Figure 4.7: Effect of apelin-13 analogues on mitigating H_2O_2-induced cell toxicity induced by H_2O_2. Dose dependent effects of apelin-13 amide and (Lys⁸GluPAL)apelin-13 amide on toxicity induced by H_2O_2 was seen using CellTox Green cytotoxicity assay. Cells were exposed for 6 hours to in the presence or absence of apelin-13 amide and (Lys⁸GluPAL)apelin-13-amide. Values represents mean ±SEM for n=3 where *p<0.05, ***p<0.001.

4.2.8: Effect of apelin-13 analogues on the ROS production and improved cellular redox balance in SH-SY5Y cells.

The cells were treated with the apelin-13 analogues in presence or absence H_2O_2 of for 6 hours and ROS kit and GSH/GSSG kit was used to measure the ROS levels and the GSH/GSSG balance is in SH-SY5Y cells in-vitro. The results revealed that compared to untreated control, the ROS levels had no significant change when cells were treated with apelin-13 amide and (Lys^{8}GluPAL)apelin-13 amide (Figure 4.8A, $p>0.05$), however 50 μM H_2O_2 and 100 μM H_2O_2 treatment led to a significant rise in ROS% by 52% (Figure 4.8A, $p<0.01$) and 724% (Figure 4.8A, $p<0.0001$) respectively. Co-treatment of apelin-13 amide with 50 μM H_2O_2 reduced ROS by 20% (Figure 4.8A, $p>0.05$) and 10% for 100 μM H_2O_2 (Figure 4.8A, $p>0.05$), compared to H_2O_2 alone. Compared to H_2O_2 alone, (Lys^{8}GluPAL)apelin-13 amide co-treatment with 50 μM H_2O_2 reduced the ROS% by 18% (Figure 4.8A, $p>0.05$) and 32% for 100 μM H_2O_2 (Figure 4.8A, $p<0.0001$).

The GSH/GSSG ratio was reduced non significantly by apelin-13 amide (10%, Figure 4.8B, $p>0.05$) and (Lys^{8}GluPAL)apelin-13 amide (11%, Figure 4.8B, $p>0.05$) treatment alone and 50 μM H_2O_2 reduced significantly by 92% (Figure 4.8B, $p<0.0001$), compared to untreated control. Compared to H_2O_2, the GSH/GSSG ratio had no significant change of co-treatment with apelin analogues (Figure 4.8B, $p>0.05$).

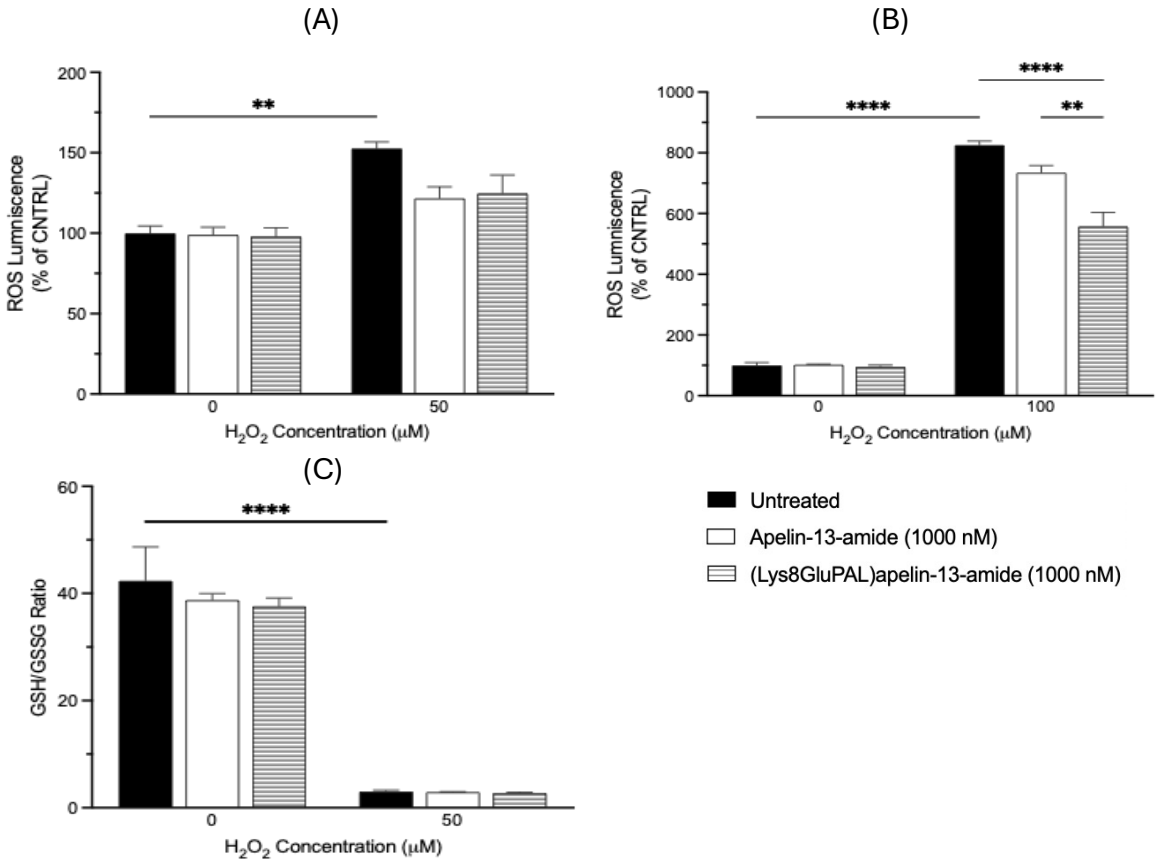

Figure 4.8: Effect of apelin-13 analogues on the ROS production and improved cellular redox balance in SH-SY5Y cells. The oxidative stress induced by H_2O_2 for 6 hours and treated in presence or absence of apelin-13 analogues. (A-B) ROS% measurement of SH-SY5Y cells induced by H_2O_2 (B) represents ratio of reduced and total glutathione in SHSY5Y cells. Values represents mean ±SEM for n=3 where **p<0.01,****p<0.0001.

4.2.9: Effect of apelin-13 analogues on mitochondrial membrane potential in H_2O_2-induced SH-SY5Y cells.

The mitochondrial membrane potential in SH-SY5Y cells in-vitro was measured using JC-1 dye. The cells were treated with apelin-13 analogues in presence or absence of 50 μM H_2O_2, for 6 hours before adding the JC-1 dye. The JC-1 is generally used to study the mitochondrial health and when it enters in the mitochondria and forms aggregates in healthy cells emitting red fluorescence. It remains in monomers forms in damages form and emit green light. Fluorescent microscope was used to visualised cell at 20X magnification, and the intensity was measured using Image j and analysed by One-way ANOVA. The representative images are shown in Figure 4.7A and the results presented that Apelin-13 amide and (Lys^{8}GluPAL)apelin-13 amide increased the intensity of JC-1 Red/Green ratio by 20% (Figure 4.9B, $p<0.05$) and 33% (Figure 4.9B, $p>0.05$) respectively, indicating slightly improved Mitochondrial membrane potential, however 50 μM H_2O_2 reduced it by 80% (Figure 7.9B, $p<0.05$), compared to untreated control. Compared to H_2O_2 treatment alone, the co-treatment H_2O_2 with apelin-13 amide improved the mitochondrial membrane potential by 266% (Figure 4.9B, $p>0.05$), and by 133% (Figure 4.9B, $p<0.01$), with (Lys^{8}GluPAL)apelin-13 amide.

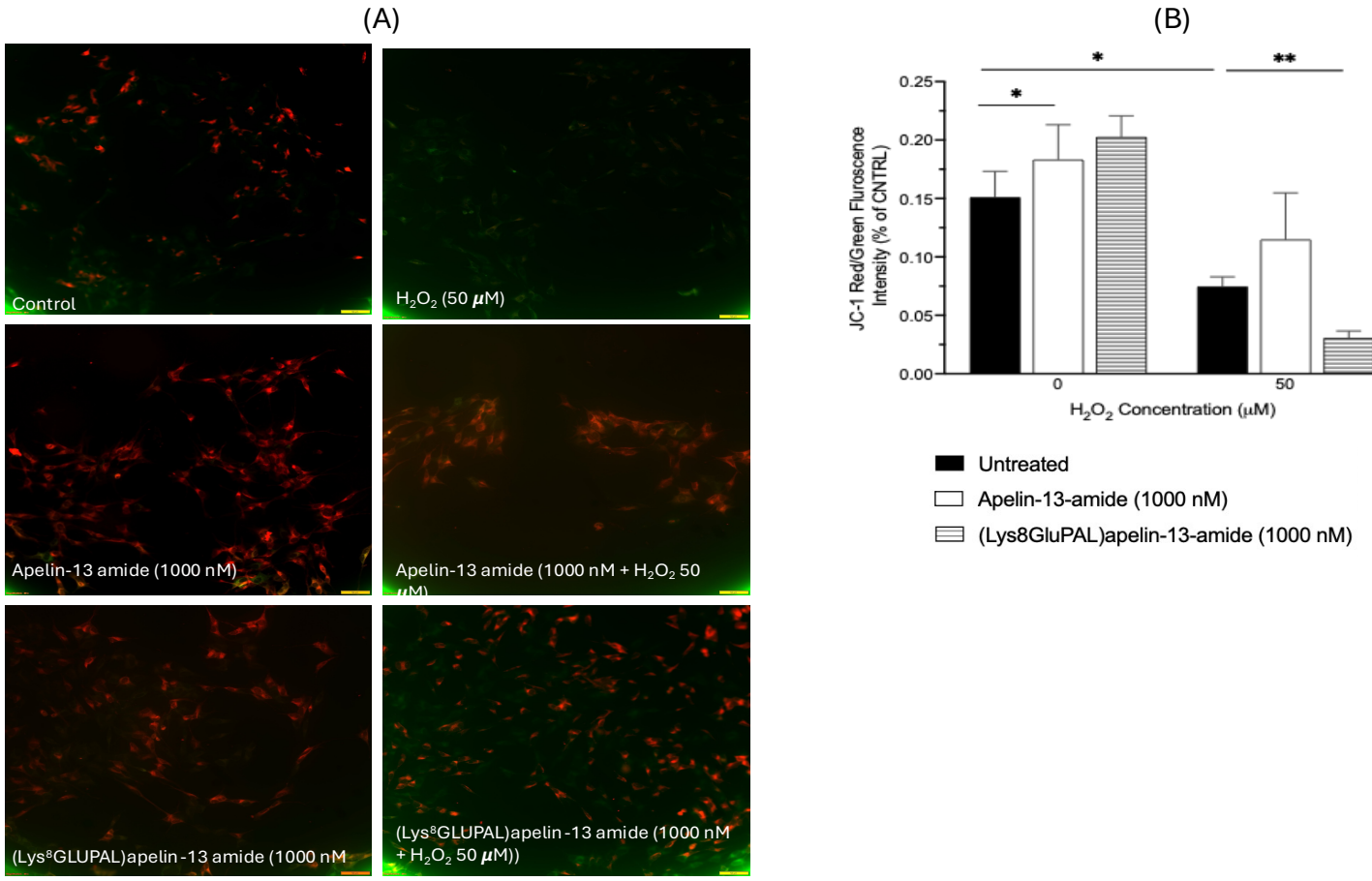

Figure 4.9: Effect of apelin-13 analogues on mitochondrial membrane potential in H2O2-induced SH-SY5Y cells. Mitochondrial membrane potential (ΔΨm) of SH-SY5Y cells under H_2O_2-induced stress was measured using JC-1 staining. (A) representative images of SH-SY5Y cells stained with JC-1 (20x magnification) and (B) graph of JC-1 Red/Green fluorescence ratio of cells treated with Apelin-13-amide, pGlu(Lys^{8}GluPAL)apelin-13-amide and H_2O_2. Values represents mean ±SEM for n=3 where *p<0.05, ***p<0.001.

4.2.10: Effect of apelin-13 analogues on apoptosis induced by H_2O_2 in SH-SY5Y cells.

The cells were treated for 6 hours with H_2O_2 in presence or absence of apelin-13 analogues and apoptosis was measured by caspase3/7-Glo activity kit in SH-SY5Y cells in-vitro. Compared to untreated control, apelin-13 amide was able to reduce the apoptosis by 23% (Figure 4.10, $p<0.01$) and (Lys^{8}GluPAL)apelin-13 amide by 30% (Figure 4.10, $p<0.05$) for 50 μM H_2O_2, however, the apoptosis was increased significantly by 1000% (Figure 4.10, $p<0.0001$) for 50 μM H_2O_2, and 1896% (Figure 4.10, $p<0.0001$) for 100 μM H_2O_2. Compared to H_2O_2 alone, co-treatment of apelin-13 amide reduced caspase 3/7 activity significantly by 26% (Figure 4.10, $p<0.001$) for 50 μM H_2O_2 and by 30% (Figure 4.10, $p<0.0001$) for 100 μM H_2O_2. Lys^{8}GluPAL)apelin-13 amide co-treatment with 50 μM H_2O_2 reduced apoptosis by 60% (Figure 4.10, $p<0.0001$) and 32% for 100 μM H_2O_2, compared to H_2O_2 alone.

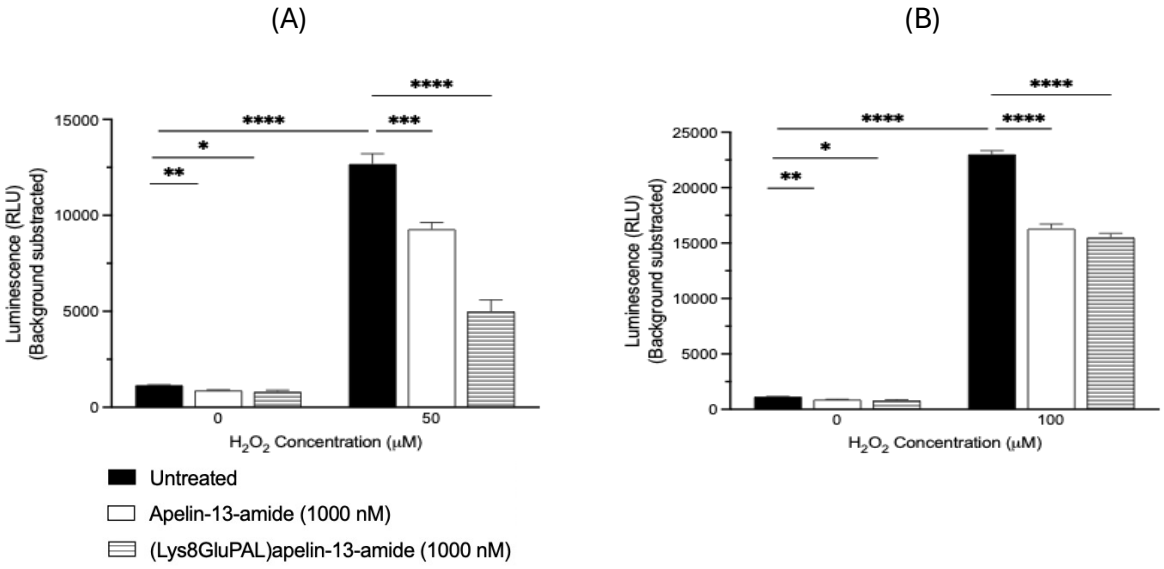

Figure 4.10: Effect of apelin-13 analogues on apoptosis induced by H_2O_2 in SH-SY5Y cells. SH-SY5Y cells were treated for 6 hours with H_2O_2 in presence or absence of apelin-13 analogues and caspase activity was measured by Caspase-Glo® 3/7 assay where (A) H_2O_2 50 μM (B) H_2O_2 100 μM. The data is represented in relative luminescence unit (RLU) and values represents mean ±SEM for n=3 where *p<0.05, **p<0.01, ***p<0.001 , ****p<0.0001.

4.2.11: Effects of apelin-13 analogues to mitigates H_2O_2-induced mitochondrial ROS generation in SH-SY5Y cells transfected with Hyper7.

To further assess the mitochondrial oxidative stress, cells were transfected with pCS2+MLS-HyPer7, before 6 hours of treatment with apelin-13 analogues in presence or absence of H_2O_2. SH-SY5Y cells were observed under fluorescent microscope and image J was used to quantify the intensity. Treatment with apelin-13 alone resulted in 17% (Figure 4.11B, $p>0.05$), reduction in mitochondrial ROS, (Lys^{8}GluPAL)apelin-13-amide had no change but H_2O_2 treatment led to 70% (Figure 4.11B, $p<0.05$), rise in Hyper-7 intensity indicating the ROS production by H_2O_2. The co-treatment of H_2O_2 with apelin-13 amide reduce the mitochondrial ROS by 40% (Figure 4.11B, $p<0.05$), and (Lys^{8}GluPAL)apelin-13-amide by 48% (Figure 4.11B, $p<0.01$), compared to H_2O_2 alone.

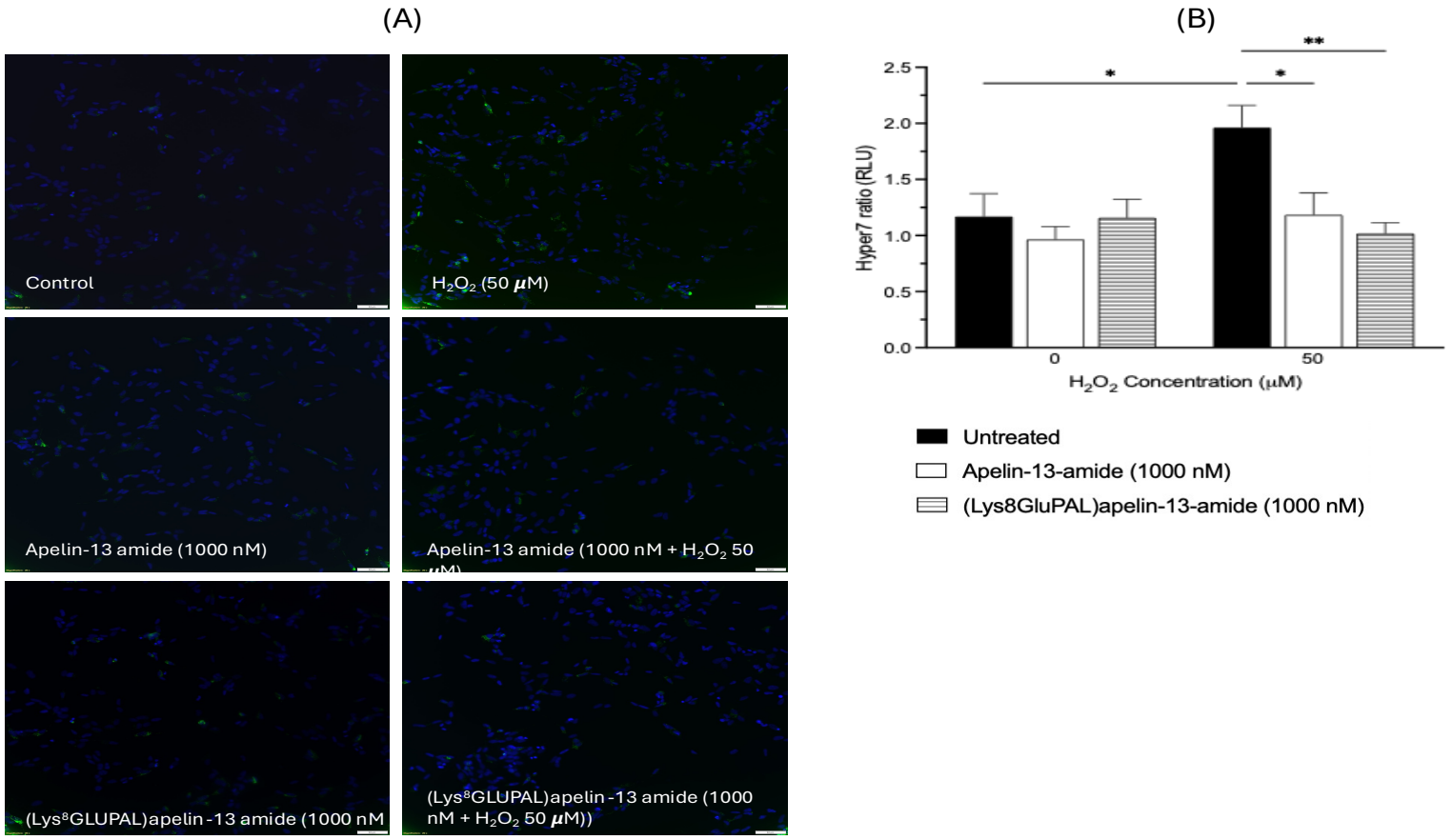

Figure 4.11: Effects of apelin-13 analogues to mitigates H_2O_2-induced mitochondrial ROS generation in SH-SY5Y cells transfected with Hyper7. The cells were transfected for 72 hours before treatment with peptides in presence and absence of H_2O_2. Mitochondrial Hyper Probe pCS2+MLS-HyPer7 was chosen to show the increase in mitochondria derived H_2O_2. (A) Fluorescence images illustrate H_2O_2 generation relative to control cells at 20X magnification and (B) is graph analysis of Hyper ratio measured by Image J. Values represents mean ±SEM for n=3 where *p<0.05, **p<0.01.

4.2.12: Effect of apelin-13 analogues to reduced oxidative stress damage induced by H_2O_2.

Nuclear factor erythroid 2-related factor 2 (NRF-2) is a transcription factor and its expression in SH-SY5Y cells was measured by western blot. The cells were treated for 6 hours with apelin-13 analogues in presence or absence of 50 μM H_2O_2 prior to the harvesting and GAPDH is used as a loading control. The results for NRF-2 expression showed that no significant change when treated with apelin-13 amide and (Lys^{8}GluPAL)apelin-13 amide (Figure 4.12, $p>0.05$) but reduced by 72% (Figure 4.12, $p<0.05$) when treated with 50 μM H_2O_2, compared to untreated control. The NRF-2 expression was increased by 100% (Figure 4.12, $p>0.05$) when the cells were co-currently treated with apelin-13 analogues, compared to H_2O_2 treatment alone.

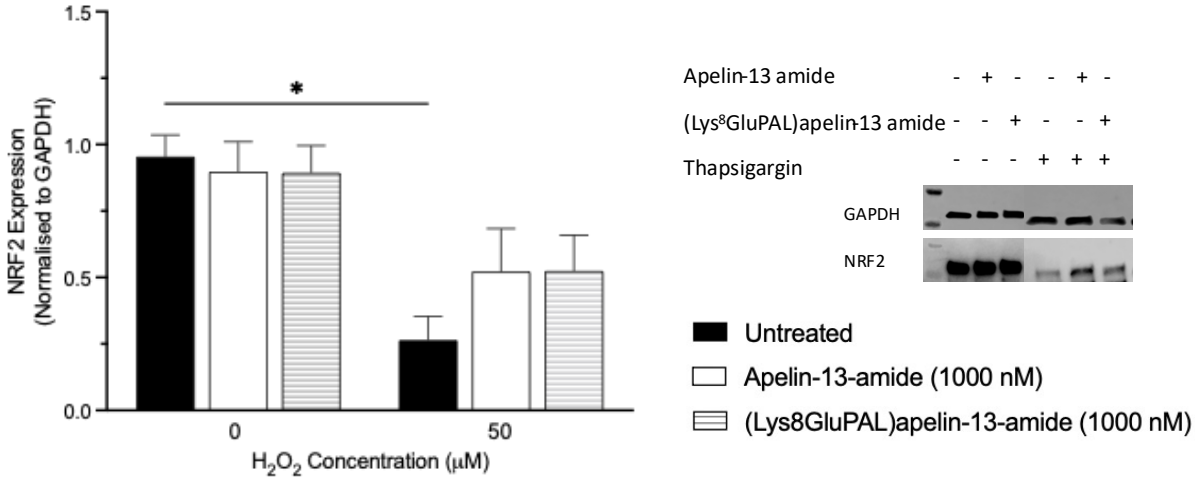

Figure 4.12: Effect of apelin-13 analogues to reduced oxidative stress damage induced by H_2O_2. The SH-SY5Y cells were treated with apelin-13 analogue in presence or absence of H_2O_2 for 6 hours to measure NRF-2 protein levels. Western blot analysis was performed to detect NRF-2 expression, with GAPDH used as the loading control for normalization. Densitometric analysis was carried out to quantify protein expression, and the results are presented as mean ± SEM from three independent experiments where n = 3, *$p<0.05$.

4.2.13: Effect of apelin-13 analogues on expression levels of apoptotic proteins in H_2O_2-stressed SH-SY5Y cells.

The cells were treated for 6 hours with apelin-13 amide and (Lys^{8}GluPAL)apelin-13 amide with and without 50 μM H_2O_2 following seeding and harvested to run western blot to look at the expression of apoptotic proteins. Apelin-13 analogues had non-significant change on the expression of pro-apoptotic protein BAX (Figure 4.13A, $p>0.05$) but increased by 8% (Figure 4.13A, $p>0.05$) , compared to untreated control. However, co-treatment of apelin-13 amide and (Lys^{8}GluPAL)apelin-13 amide with 50 μM H_2O_2 led to a decline in expression by 4% (Figure4.13A, $p>0.05$), and 27% (Figure 4.13A, $p>0.05$), respectively, compared to 50 μM H_2O_2 alone. However, the expression of anti-apoptotic protein Bcl-2 was reduced by 8% (Figure 4.13B, $p>0.05$) when treated with 50 μM H_2O_2, and increased by 14% (Figure 4.13B, $p>0.05$) with apelin-13 amide and 19% (Figure 4.13B, $p>0.05$) with (Lys^{8}GluPAL)apelin-13 amide, compared to untreated control. Compared to H_2O_2 treatment alone, the expression of Bcl2 was increased by 21% (Figure 4.13B, $p>0.05$) and 57% (Figure 4.13B, $p>0.05$) when treated with apelin-13 amide and (Lys^{8}GluPAL)apelin-13 amide respectively.

The BAX/Bcl-2 ratio was quantified to analyse the balance between the pro-apoptotic and anti-apoptotic proteins. (Lys^{8}GluPAL)apelin-13 amide and 50 μM H_2O_2 co-treatment led to no significant change but increased slightly by 11% (Figure 4.13C, $p>0.05$) for apelin-13 amide, compared to untreated control. The co-treatment of 50 μM H_2O_2 with apelin-13 amide had no significant change and (Lys^{8}GluPAL)apelin-13 amide reduced by 23% (Figure 4.13C, $p>0.05$), compared to H_2O_2 treatment alone.

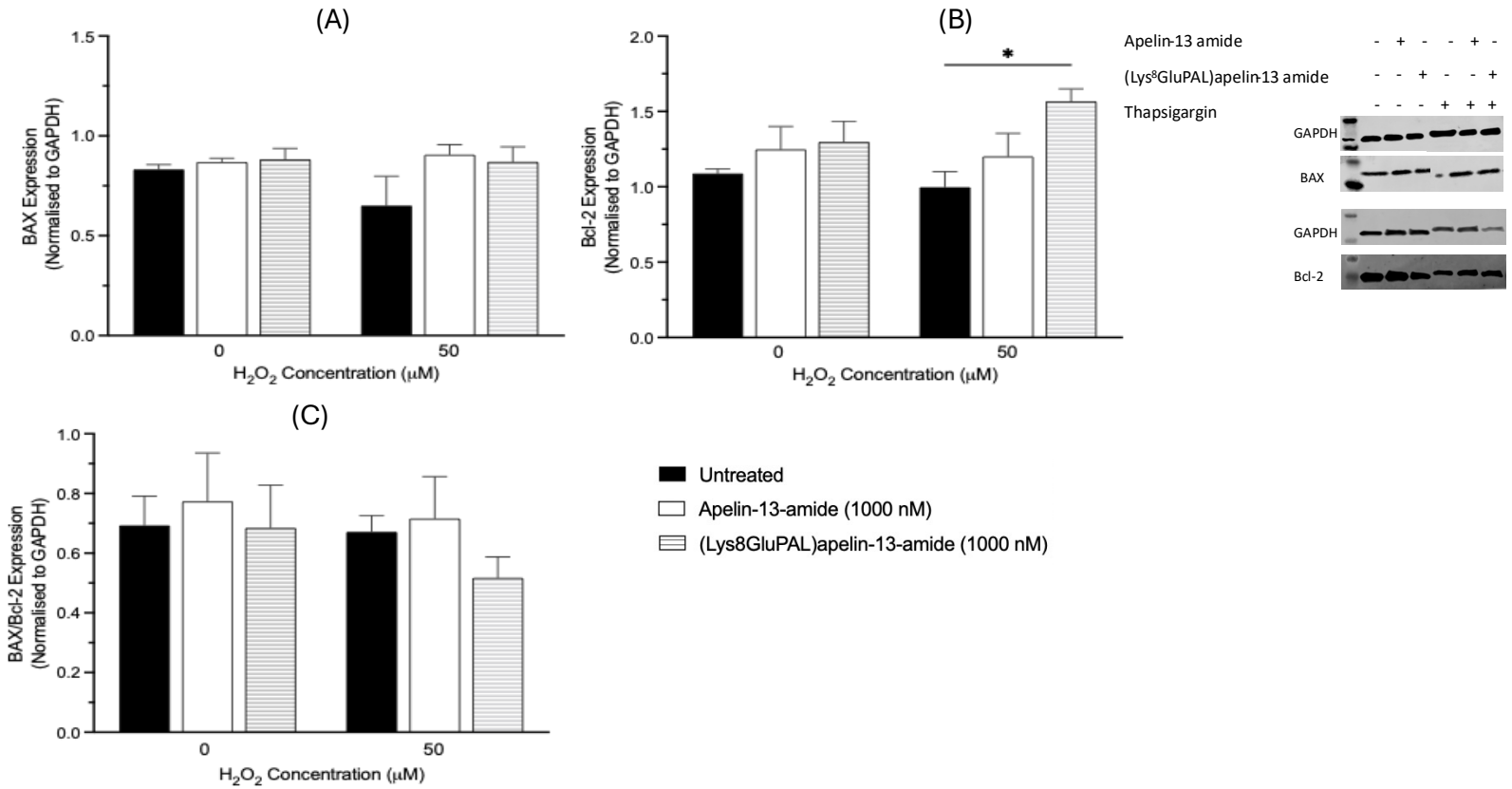

Figure 4.13: Effect of apelin-13 analogues on expression levels of apoptotic proteins in H_2O_2-stressed SH-SY5Y cells. Apoptotic markers BAX and Bcl-2 expression in SH-SY5Y cells was seen after 6 hours treatment with apelin-13 analogue with or without H_2O_2 for 6 hours. Representative Western blot images and graph show the protein levels of (A) pro-apoptotic BAX, (B) anti-apoptotic Bcl-2 and (C) BAX/Bcl-2 ratio was calculated to assess the balance between pro-apoptotic and anti-apoptotic signalling. The protein expression was normalised by loading control GAPDH. Quantitative analysis was performed using densitometry, and data were analysed using One-Way ANOVA. Values are presented as mean ± SEM for n = 3, where *p<0.05.

4.2.14: Effect of apelin-13 analogues on ER stress markers under H_2O_2 -induced stress.

The expression ER stress markers, IRE1a and BiP in SH-SY5Y cells with 50 μM H_2O_2 exposure led to increase by 22% (Figure 4.14A, p>0.05) and 9% (Figure 4.14B, p>0.05) respectively. Apelin-13 amide and (Lys^{8}GluPAL)apelin-13 amide treatments increased IRE1 expression by 19% (Figure 4.14A, p>0.05) and 11% (Figure 4.14A, p>0.05) respectively and there was no change seen in expression of BiP, compared to untreated control.

However, when co-treated with H_2O_2 and apelin-13 amide, IRE1α expression was reduced by 12% (Figure 4.14A, p>0.05) and BiP by 22% (Figure 4.14B, p>0.05) , compared to H_2O_2 alone. And co-treatment with (Lys^{8}GluPAL)apelin-13 amide reduced IRE1 expression by 32% (Figure 4.14A, p>0.05) and BiP by 30% (Figure 4.14B, p>0.05), compared to H_2O_2 alone.

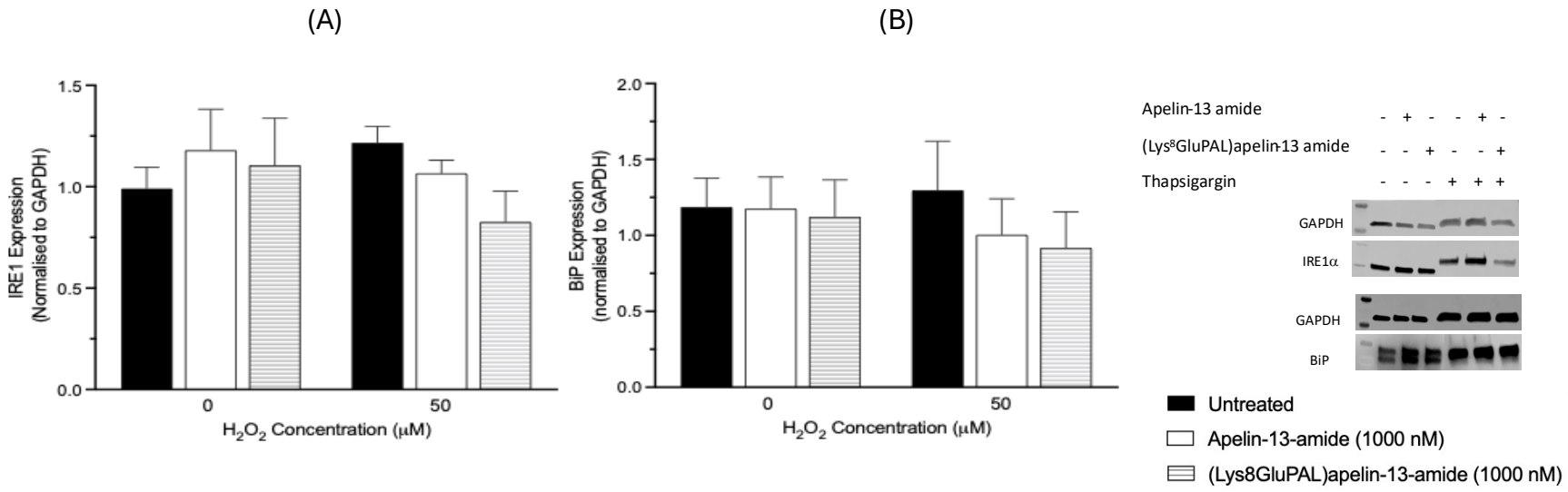

Figure 4.14: Effect of apelin-13 analogues on ER stress markers under H_2O_2 -induced stress. Expression of ER stress markers IRE1 and BiP in SH-SY5Y cells treated with apelin-13 analogue in presence or absence of H_2O_2 for 6 hours. The western blot analysis showing the protein levels of (A) IRE1 and (B) BiP. GAPDH was used as a loading control for normalization. Quantitative analysis was performed using densitometry, and data were analysed using One-Way ANOVA. Values are presented as mean ± SEM for n = 3.

4.2.15: Effect of apelin-13 analogues on ER stress response induced by H_2O_2 in SH-SY5Y cells.

The activation of ER tress response pathway under H_2O_2-induced stress was measured by western blot analysis of the protein expression of ER stress markers. Apelin-13 analogues and (Lys^{8}GluPAL)apelin-13-amide increased the expression of Ero1-Lα by 16% (Figure 4.15A, $p>0.05$) and 10% (Figure 4.15A, $p>0.05$) respectively, however calnexin, PDI and PERK had no significant change, compared to untreated control. The H_2O_2 treatment led to increase in calnexin by 20% (Figure 4.15A, $p>0.05$), Ero1-Lα by 28% (Figure 4.15B, $p>0.05$) and PERK by 15% (Figure 4.15D, $p>0.05$) and reduced PDI expression by 7% (Figure 4.15C, $p>0.05$), compared to untreated control.

Compared to H_2O_2, the co-treatment of H_2O_2 with apelin-13 amide increased calnexin expression by 14% (Figure 4.15A, $p>0.05$), PDI by 7% (Figure 4.15C, $p>0.05$) and reduced Ero1-Lα expression by 11% (Figure 4.15B, $p>0.05$) and PERK by 35% (Figure 4.15D, $p<0.01$). And co-treatment of H_2O_2 with (Lys^{8}GluPAL)apelin-13-amide increased PDI expression by 8% (Figure 4.15C, $p>0.05$) and reduced calnexin by 12% (Figure 4.15A, $p>0.05$), Ero1-Lα by 14% (Figure 4.15B, $p>0.05$) and PERK by 31% (Figure 4.15A, $p<0.01$), compared to H_2O_2 alone.

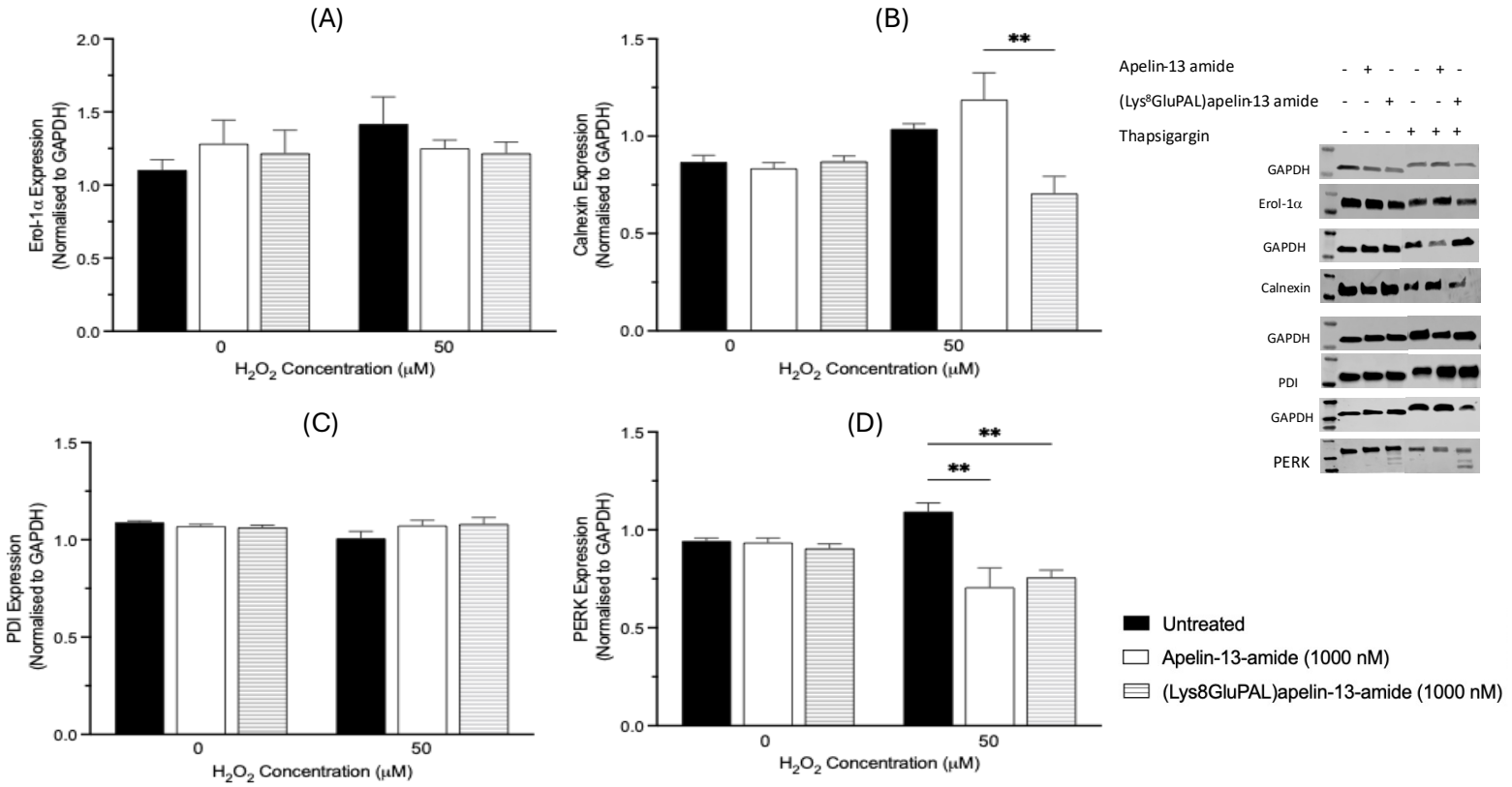

Figure 4.15: Effect of apelin-13 analogues on ER stress response induced by H_2O_2 in SH-SY5Y cells. ER stress-related protein expression in SH-SY5Y cells treated with apelin-13 analogue in presence or absence of H_2O_2 for 6 hours. Representative Western blot images showing the expression levels of and graphs of analysis (A) Calnexin, (B) Ero1-Lα, (C) PDI, and (D) PERK. GAPDH was used as a loading control for normalization. Quantitative analysis was performed using densitometry, and data were analysed using One-Way ANOVA. Values are presented as mean ± SEM for n=3 where **p<0.01.

4.2.16: Effect of apelin-13 analogues on autophagy related proteins under H_2O_2 -induced stress in SH-SY5Y cells.

Autophagy related proteins expression of ATG3, ATG7 and ATG5 under ER stress induced by H_2O_2 in SH-SY5Y cells was measured by western blot analysis to determine the effect of apelin-13 analogues. Apelin-13 amide and (Lys^8GluPAL)apelin-13-amide had no significant change in expression of ATG7 and ATG5, but ATG3 expression was increased by 22% and 32% (Figure 4.16A, $p>0.05$), respectively, compared to untreated control. The co-treatment of H_2O_2 and apelin-13 amide increased the expression of ATG3 by 17% (Figure 4.16A, $p>0.05$), ATG7 by 13% (Figure 4.16B, $p<0.01$), and ATG5 by 12% (Figure 4.16C, $p>0.05$), compared to H_2O_2 alone. The (Lys^8GluPAL)apelin-13-amide co-treatment with H_2O_2 led to rise in expression of ATG3 by 39% (Figure 4.16A, $p>0.05$), ATG7 by 12% (Figure 4.16B, $p<0.01$), and ATG5 by 10% (Figure 4.16C, $p>0.05$), compared to H_2O_2 alone.

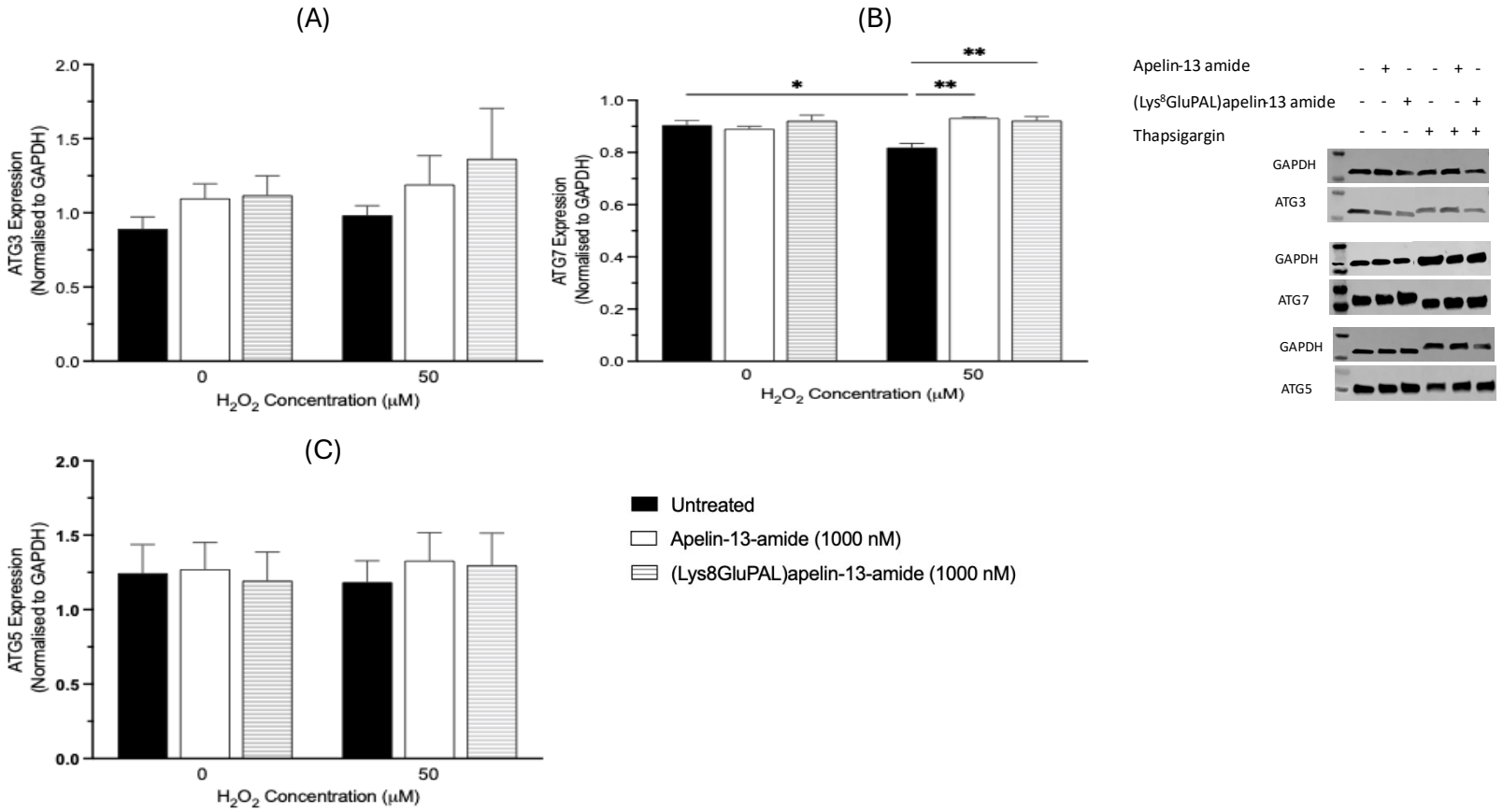

Figure 4.16: Effect of apelin-13 analogues on autophagy related proteins under H_2O_2 -induced stress in SH-SY5Y cells. The cells were treated with apelin-13 analogues in presence or absence of H_2O_2 and autophagy-related protein expression in SH-SY5Y cells was seen via western blot analysis (A) ATG3 (B) ATG7, and (C) ATG5. GAPDH was used as a loading control for normalization. Quantitative analysis was performed using densitometry, and data were analysed using One-Way ANOVA. Values are presented as mean ± SEM (n = 3).

4.2.17: Effect of apelin-13 analogues on cell viability and cell toxicity induced by H_2O_2 after AMPK inhibition.

Compound C was used to examine that AMPK is involvement in apelin-13' role in promoting cell survival and death in SH-SY5Y. The cells were pre-treated with compound C for 30 minutes and followed by treatment with apelin-13 analogues in presence or absence of H_2O_2 and determined cell viability and cell toxicity. The apelin-13 analogues showed 20-23% (Figure 4.17A, $p<0.05$) rise in cell viability, however reduced by 20% (Figure 4.17A, $p>0.05$) with 50 μM H_2O_2, compared to untreated control. Compared to H_2O_2 treatment alone, the cell viability was increased in co-treatment of H_2O_2 with Apelin-13 amide by 25% (Figure 4.17A, $p>0.05$) and (Lys^8GluPAL)apelin-13 amide by 30% (Figure 4.17A, $p>0.05$).

On the other hand, compound C treated cells showed no significant change in viability for apelin-13 analogues in presence or absence of H_2O_2 (Figure 4.17A, $p>0.05$), and 50 μM H_2O_2 reduced cell viability 12% (Figure 4.17A, $p>0.05$), compared to untreated control.

The cells toxicity without the compound C was reduced by 11% (Figure 4.17B, $p>0.05$), with apelin-13 amide and 15% (Figure 4.17B, $p>0.05$), by (Lys^8GluPAL)apelin-13 amide, however increased by 19% (Figure 4.17B, $p>0.05$) when treated with 50 μM H_2O_2 reduced, compared to untreated control. The co-treatment of H_2O_2 with apelin-13 amide reduced cell toxicity by 22% (Figure 4.17B, $p<0.01$), and with (Lys^8GluPAL)apelin-13 amide by 18% (Figure 4.17B, $p<0.05$), compared to H_2O_2 alone. Whereas when treated with compound c, there was no change in cell toxicity by apelin-13 analogues and increased by 19% (Figure 4.17B, $p>0.05$), H_2O_2. The cell toxicity was increased by 22%-33% (Figure 4.17B, $p<0.0001$) when co-treated with apelin-13 analogues and H_2O_2, indicating the role of AMPK in apelin's protecting effect.

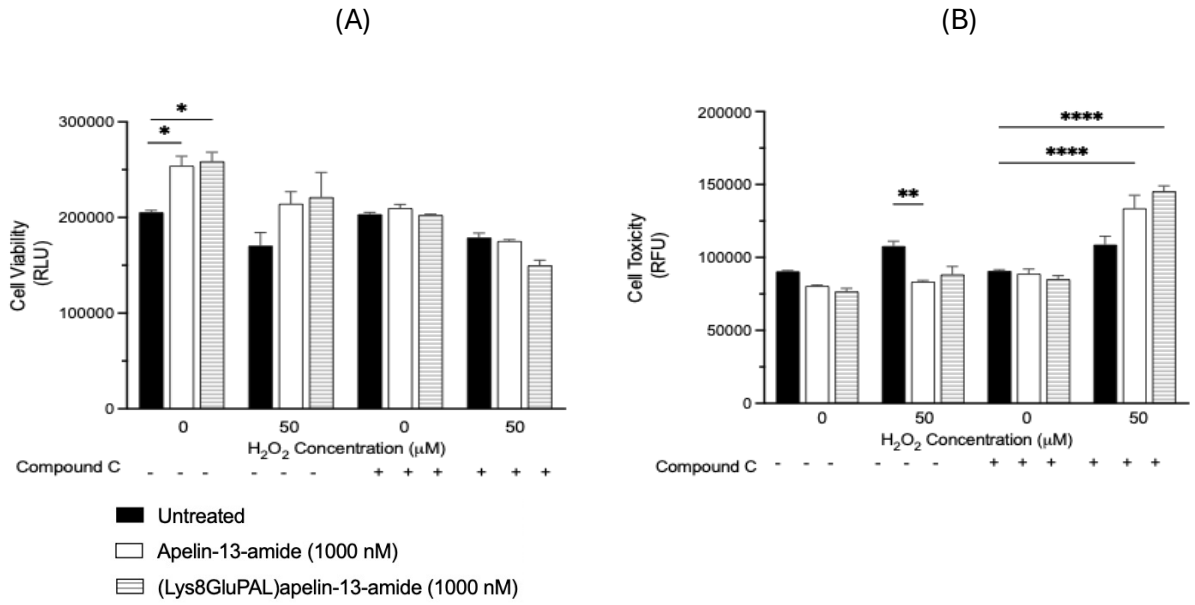

Figure 4.17: Effect of apelin-13 analogues on cell viability and cell toxicity induced by H_2O_2 after AMPK inhibition. The AMPK pathway mediated the protective effect of H_2O_2 in SH-SY5Y cells. The cells were pre-treated with 5 μM Compound C and then treated with peptides in the presence or absence H_2O_2. (A) cell viability measured ATP production was assessed using CellTiter-Glo® viability assay kit and (B) CellTox™ Green cytotoxicity assay was used to measure the toxicity. Cell values represent mean ±SEM for n=3 where *p<0.05, **p<0.01, ****p<0.0001.

4.3. Discussion

This chapter findings determine the protective effects of apelin-13 analogues under oxidative stress-induced by H_2O_2 in SH-SY5Y cells. The data highlighted that apelin-13 analogues can improve cell viability, support proliferation, decrease toxicity, and regulate critical cellular processes such as mitochondrial function, apoptosis, ER stress, and autophagy. Apelin-13 analogues are known to regulate various biological processes like inflammation, oxidative stress, and energy metabolism. Apelin-13 amide and (Lys^{8}GluPAL)apelin-13-amide have been shown to have longer half-life and bioavailability (O'Harte et al., 2017). Recent research has shown that apelin-13 analogues can be used as a therapeutic agent for obesity-diabetes (O'Harte et al., 2017). H_2O_2 is a ROS and it's a byproduct of a cellular mechanism. It is generated in mitochondria during oxidative phosphorylation (Konno et al., 2021). In normal brain antioxidant system tightly regulate the production and clearance of H_2O_2, however during the oxidative stress in mitochondrial the ROS production is increased including H_2O_2 in brains of AD (Tönnies & Trushina, 2017). The results of this chapter suggest that apelin-13 analogues can be used as a therapeutic agent for AD.

Cell viability

Apelin-13 analogues significantly improved cell viability when the cells were treated at different timepoints in presence or absence of H_2O_2. The treatment of H_2O_2 led to significant decrease in cell viability due to the due to oxidative stress that damage the biomolecules and disrupts the cellular homeostasis (Tönnies & Trushina, 2017). H_2O_2 is a ROS that causes protein oxidation, DNA damage and lipid peroxidation by producing very reactive hydroxyl radicals through Fenton reactions (Yang et al., 2023). It also impairs mitochondria, disrupting ATP production and triggering a self-perpetuating cycle of increased ROS generation (Yang et al., 2023). The co-treatment of apelin-13 analogues with H_2O_2 improved the cell viability for all timepoints. This protecting effect can be attributed to apelin-13's role in activating cellular pathways that mitigate oxidative

stress. Previous studies have determined apelin's is involved in activation of the PI3K/AKT signalling pathway and upregulation of the NRF-2 antioxidant response, which possibly contributed to the detected improvement in cell survival (Duan et al., 2019). These results support apelin-13 analogue's function as an anti-inflammatory agent by being consistent with previous studies that demonstrate its capacity to reduce oxidative stress in cardiovascular and neuronal models (Wysocka et al., 2018).

Cell proliferation and differentiation

Cellular proliferation and differentiation impacted by cellular stress is key to understand the progression of the disease (Saha et al., 2020). Studies have showed that apelin-13 have positive role in cell proliferation and differentiation (Lu et al., 2013). Apelin-13 is known to inhibit apoptosis and stimulate cell proliferation in glial and other cell lines (O'Donnell et al., 2007). In our study we have used BrdU as a proliferation marker and MAP2 as a differentiation marker. The results showed that H_2O_2 treatments significantly reduced the cell proliferation and Apelin-13 analogues promotes cell proliferation, even under oxidative stress conditions induced by H_2O_2. DNA damage caused by H_2O_2 treatments activate the ATM/ATR-p53 pathway, which leads to cell cycle arrest through p21 upregulation, and stops progression in G1 or G2 phases. It is also involved in suppressing the protein synthesis by inhibiting the PI3K/AKT/mTOR pathway and dysregulates ERK/MAPK pathway, which e lead to senescence or apoptosis (Reinhardt et al., 2007; Senturk & Manfredi, 2012).

Our study aligns with the recent finding, showed that apelin-13 analogues activate the AMPK pathway which is involved in restoring energy balance and homeostasis. Apelin-13 analogues activate PI3K/AKT signalling, increasing mTOR activity to promote cellular differentiation and proliferation (Yang et al., 2014). The ERK/MAPK pathway is modulated by apelin-13 analogues which ensure appropriate activation to promote cell cycle progression and differentiation. This suggests that apelin-13 analogues support recovery

after H_2O_2 induced stress by stimulating new DNA synthesis and cellular repair mechanisms (Peng et al., 2023).

Additionally, the MAP2 expression was enhanced by apelin-13 analogues in SH-SY5Y cells under oxidative stress and it demonstrate the role of apelin in neuronal differentiation, which is critical for restoring cellular function. H_2O_2 treatments alone led to reduced MAP2 expression in SH-SY5Y cells. These findings align with studies that report Apelin's involvement in neuronal repair and its ability to enhance neurogenesis in models of brain injury (Zhang et al., 2011). Studies have showed that H_2O_2 disrupts the cellular signalling pathways required for cellular integrity and stability. MAP2 protein levels are reduced under H_2O_2 stressed cells as it disrupts microtubule stability levels by oxidising cytoskeletal proteins (Wilson & González-Billault, 2015).

Results also showed that apelin-13 analogues mitigate the negative effect of H_2O_2 on neurite outgrowth and enhanced the neurite extensions. H_2O_2 damages the cytoskeletal components by inhibiting essential pathways for neuronal growth like PI3K/AKT and Wnt/β-catenin. Apelin-13 mitigate the effect of H_2O_2 on the neurite outgrowth to restore cytoskeletal integrity by activating these pathways. These results focus on the potential of apelin-13 analogues to mitigate neuronal stress and enhance connectivity in oxidative stress-related neurodegenerative conditions.

Cell toxicity

The results demonstrated that apelin-13 analogues significantly reduced the cell toxicity induced by H_2O_2 in SH-SY5Y cells across all time points. H_2O_2 treatments increased the cellular stress significantly indicating that excessive ROS production leads to neurodegeneration. Excessive ROS production overwhelms the antioxidant defence system and cause lipid peroxidation, oxidative stress, inflammation and ER stress (Xin et al., 2022). Mitochondrial dysfunction by H_2O_2 leads to the energy deficit and eventually cell death. ROS production activates the pro-apoptotic pathways and the excessive

apoptosis results in cell death (Qu et al., 2022). Cellular homeostasis and neuronal functions are impaired by the prolonged cellular stress (Qu et al., 2022).

Apelin-13 showed to mitigate the cellular stress in various studies and improved the cellular homeostasis (Yang et al., 2014). As mentioned earlier that apelin-13 analogues activates AMPK and it maintains ATP levels to maintain cell viability. Apelin-13 analogues are involved in caspase activation by which it reduces the programmed cell death and maintain cell integrity (Tochigi et al., 2013). Studies showed that apelin-13 analogues regulate UPR and PI3K/AKT pathway activation to promote cell survival and protein folding (Chen et al., 2011). By modifying NF-κB signalling, apelin-13 reduce the production of pro-inflammatory cytokines, which protect the cells from cytotoxicity by alleviating inflammation-induced damage (Zhang et al., 2016).

Mitochondrial and oxidative stress

Mitochondrial plays key role in the cell survival and mitochondrial dysfunction is the key progression factor in AD (Lin & Beal, 2006). Mitochondria is responsible for number of cellular process and major source of energy providing ATP via oxidative phosphorylation to main the normal function of the cells and homeostasis (Lin & Beal, 2006). Number of studies have shown the AD brains have extensive mitochondrial abnormalities (Swerdlow, 2018). Studies have showed that 90% of cellular ROS production is contributed by mitochondria, as ROS is generated in the mitochondrial as a byproduct during electron transport of aerobic respiration (Balaban et al., 2005; Ngo & Duennwald, 2022).

We have used ROS assay and molecular probe to measure the ROS produced by H_2O_2 and GSH/GSSG assay to estimate the redox balance, JC-1 assay to look at the mitochondrial membrane potential and NRF-2 expression under H_2O_2 induced stress. The results showed that H_2O_2 treatment for 6 hours led to increased ROS production in SH-SY5Y cells as H_2O_2 induce oxidative stress that leads to mitochondrial dysfunction and leads to excessive production of ROS (Wang et al., 2020). However, the treatment with

apelin-13 amide and (Lys^{8}GluPAL)apelin-13-amide mitigated H_2O_2 induced oxidative stress and reduced the ROS production significantly. The molecular probe with Hyper-7 a genetically encoded H_2O_2 sensor, was used to evaluate the intracellular ROS levels in response to oxidative stress in SH-SY5Y cells. The results demonstrated that H_2O_2 treatment led to significant increase in Hyper-7 fluorescence intensity, indicating the increased intracellular H_2O_2. However, co-treatment of H_2O_2 with apliein-13 analogues effectively reduced the Hyper-7 intensity suggesting the role of apelin-13 analogues in mitigating the oxidative stress induced by H_2O_2.

Furthermore, the mitochondrial membrane potential was reduced significantly by H_2O_2 treatments, and the apelin-13 analogues showed to improve the mitochondrial membrane potential significantly. This indicates the apelin-13 analogues have a therapeutic potential in treatment of AD. Our results align with the previous research has showed that apelin-13 analogues can reduce the ROS production and improve the mitochondrial function (Li et al., 2024).

Similarly, the GSH/GSSG ratio an indicator of redox balance was also reduced dramatically due to the H_2O_2 induced oxidative stress. However, apelin-13 analogues were unable to make a significant change which can be due to the excessive oxidative stress overwhelms the antioxidant response. The limited availability of NAPDH due to the severe oxidative stress which is required for GSSG conversion to GSH. Studies have proved that apelin-13 can mitigate the H_2O_2 induced intracellular oxidative stress and improved GSH/GSSG ratio (Li et al., 2024). Research data also demonstrated that apelin-13 inhibits apoptosis induced by H_2O_2 and effectively reduce the ROS generation and restore the mitochondrial membrane potential (Pouresmaeili-Babaki et al., 2018; Li et al., 2024).

Apoptosis

The pro and anti-apoptotic proteins play crucial role in the regulating the mitochondrial apoptotic pathway (Yao et al., 2005). Our result illustrated that the expression of pro-

apoptotic protein BAX under H_2O_2 induced stress is elevated and the anti-apoptotic Bcl-2 is reduced. However, the Bax expression under co-treatment of H_2O_2 and apelin-13 amide was reduced indicating the protective effect but the (Lys^{8}GluPAL)apelin-13-amide was unable to mitigate ethe effect of H_2O_2. The bcl-2 expression was improved by the apelin-13 analogues showing its protective effect against the H_2O_2 induced apoptosis by activating PI3K/Akt and Akt pathways.

Moreover, the caspase 3/7 results showed that H_2O_2 treatment led to significant increase in the caspase activity, however the apelin-13 analogues reduced the caspase activity significantly indicating the protective effect against apoptosis by activating the AMPK, MAPK, intrinsic apoptotic pathway and PI3K/Akt pathways. These pathways inhibit the caspase activation in various stress conditions and improve the cell survival (Xing et al., 2011; Tochigi et al., 2013).

The primary mechanism of apoptosis is the intrinsic mitochondrial pathway and caspase-dependant cell death caused by H_2O_2 is linked to reduced mitochondrial membrane potential and caspase 3/7 activation (Tochigi et al., 2013). Apelin-13 is shown to shield SH-SY5Y cells from apoptosis by blocking cytochrome C release, caspase-3 activation and mitochondrial depolarisation (Pouresmaeili-Babaki et al., 2018). Li et al have showed that apelin-13 analogues supress the apoptosis and regulate cell proliferation, antioxidant effect and inflammatory inhibition (2024). These results demonstrate the therapeutic potential of apelin-13 analogues in decreasing this damage and highlight the crucial roles played by the Bcl-2/Bax pathway and caspase-3/7 in oxidative stress-induced apoptosis.

ER stress and UPR pathway

To look at the effect of aplen-13 analogues protection against ER stress induced by H_2O_2 and activation of UPR pathway we looked at the protein expression of IRE1α, PERK, PDI, BiP, ERO1α and calnexin. ER is responsible for protein folding, lipid synthesis, calcium storage and protein synthesis (Yang et al., 2020). The accumulation of misfolded protein in the ER overwhelms the capacity and lead to ER stress. ER stress can be resulted from

number of factors like oxidative stress, calcium dysregulation, genetic mutation and protein load (Ozcan & Tabas, 2012). Under the stress induced by multiple factors like increased H_2O_2, cells activate the UPR signalling to restore the ER homeostasis. If the stress is prolonged it leads to apoptosis and cell death (Ozcan & Tabas, 2012). The key UPR pathways like PERK, IRE1 and ATF6 are activated to halt protein translation, upregulation of gene involved in protein folding and degradation and translocation to the Golgi for activation of chaperons like BiP (Tsai & Weissman, 2010).

The results from our study showed that the under H_2O_2 induced stress the PERK, IRE1α, calnexin, ERO1α and BiP expression were increased and apelin-13 analogues managed to reduce the expression of these proteins. The PDI and IRE1α expression was reduced under H_2O_2 induced stress and apelin-13 analogues improved the expression. These results align with the previous studies looked at the effect of ER stress markers by activating the PI3K/Akt pathway and suggesting a potential therapeutic use of apelin-13 analogues for ER stress-related disorders (Chen et al., 2011; Zito et al., 2010). Study by Chen et al, showed that apelin-13 analogues inhibit IRE1α and JNK activation, suggesting that apelin modulates JNK-regulated cell death pathways and IRE1α-associated ER stress (2011). It illustrated that apelin-13 analogues alleviates ER stress by inhibiting the expression of PERK, IRE1α, ERO1α-L, calnexin and BiP and increases the expression of PDI (Chen et al., 2011). These results indicate that apelin-13 mitigates ER stress by increasing protein-folding capacity and reducing the accumulation of misfolded proteins.

Autophagy

NRF-2 is a transcription factor that regulates antioxidant defence systems against the stress (Li et al., 2004). Under physiological condition, NRF-2 is mainly localised to cytoplasm in a complex with Keap1 (Kelch-like ECH-associated protein 1) and under stress NRF-2 dissociates from Keap1 and rapidly translocate into nuclease where it initiates its transcriptional activity (Wan et al., 2021). The NRF-2 expression is significantly reduced by H_2O_2 induced stress and the treatment of apelin-13 analogues led to the

improvement of NRF-2 expression. Studies have investigated NRF-2 in disease contexts and it has shown to control a wide range of antioxidant enzymes involved in the detoxification and removal of oxidative stress (Ngo & Duennwald, 2022; Tönnies & Trushina, 2017).

A key adaptive response to oxidative stress is autophagy, which allow cells to degrade damaged proteins and organelles (Guo et al., 2017). To look at the effect of apelin-13 analogues on the autophagy we looked at the expression of autophagy related protein via western blot method. Our results showed that H_2O_2 treatment led to reduced autophagy-related proteins ATG3, ATG7, and ATG5. ATG3, ATG5, and ATG7 are essential autophagy related proteins and involved in the cellular homeostasis and stress response. ATG7, an E1-like activating enzyme, conjugates autophagosome-forming proteins ATG12 and LC3. ATG3, an E2-like conjugating enzyme, lipidates LC3 (microtubule-associated protein 1 light chain 3) to create LC3-II, which integrates into the autophagosome membrane and allows elongation (Li et al., 2020). ATG5, together with ATG12 and ATG16L1, is essential for autophagosome development and membrane closure before fusion with lysosomes for destruction (Wang et al., 2023). These proteins help autophagosomes form and function, removing damaged components and preserving cellular homeostasis, especially under ER stress and oxidative damage (Wang et al., 2023). The induce of ER stress and NRF-2 pathway suppression by H_2O_2 leads to impaired autophagy. However, apelin-13 analogues upregulated the expression of these protein when treated co-currently with the H_2O_2, indicating its role in enhancing autophagic flux.

The apelin-13 analogues promoted autophagy by activating NRF-2 and reduce ER stress (Duan et al., 2019). This data aligns with studies showing that apelin-13 analogues promote autophagy in models of ischemic injury and metabolic disorders (Cheng et al., 2021). By increasing autophagy, apelin-13 analogues are prone to facilitates the elimination of impaired components and supports cellular recovery, further contributing to its protective effects (Cheng et al., 2021). Apelin-13 analogues promote the autophagy by AMPK pathway, a key pathway for the restoration and it inhibits the mTOR signalling pathway (Wang & Jia, 2023).

Mechanism action of apelin-13 analogues

In addition to observing the protective effects of apelin-13 analogues on cell viability under oxidative stress induced by H_2O_2, we also investigated the role of AMPK in mediating protective effect of apelin analogues. We used compound C, a known AMPK inhibitor and the cells were treated with and without compound C prior to treatments. AMPK is a crucial energy sensor and cellular homeostasis regulator. It is frequently triggered in response to stress to improve cell survival and restore metabolic balance (Liu et al., 2014).

In our study, we looked at the cell viability with and without AMPK inhibition. the results showed that the apelin-13 analogues were able to reduce oxidative stress induced by H_2O_2 and improve cell viability in absence of compound C. However, the inhibition of AMPK by compound C shown a significant reduction in cell viability, suggesting that AMPK plays a crucial role in mediating the protective effects of apelin-13 analogues. These results prove that AMPK is preserving mitochondrial function and reducing oxidative stress (Zeng et al., 2024).

To further analyse the role of apelin-13 in AMPK activation and its effect on the cell toxicity we used compound C an AMPK inhibitor. The cells treated without the compound c showed that apelin-13 analogues were able to mitigate the effect of H_2O_2 induced oxidative stress and led to reduce the cell toxicity. However, the cells with AMPK inhibiting did not show any improvement but led to increased cell toxicity. These findings indicate that apelin-13 plays protective role against the cellular stress induced by H_2O_2 and it is involved in the activation of the AMPK.

4.4. Conclusion

To conclude, H_2O_2 was used as a cellular stress model to mimic the neurotoxicity in AD brains. This chapter provide compelling evidence that apelin-13 analogues have therapeutic potential against the H_2O_2 induced oxidative stress and can be useful to treat AD. The study demonstrated that apelin-13 analogues significantly improved the cell viability, survival, proliferation and reduce cytotoxicity and improve the mitochondrial function, inhibit apoptosis and reduce ER stress by activating the key signalling pathways like AMPK, NRF-2, UPR and PI3K/AKT pathway (shown in table 4). Apelin-13 analogues reduce ROS and lipid peroxidation in SH-SY5Y cells and protect from H_2O_2-induced oxidative damage. Therefore, apelin-13 analogues have the potential to be a novel peptide to treat and prevent AD.

Experiments	Assays Used	H_2O_2 Effect	Apelin-13 Effect	Pathway Impact
Cell Viability	MTT, CellTiter-Glo	↓ cell viability	↑ viability under H_2O_2-induced stress	PI3K/Akt activation for cell survival signalling
Proliferation & Differentiation	BrdU, MAP2, Neurite Outgrowth	↓ cell proliferation and neurite outgrowth	↑ cell proliferation and ↑ neurite outgrowth	PI3K/Akt/mTOR for proliferation, ERK/MAPK for differentiation
Cell Toxicity	LDH, CellTox Green	↑ cell toxicity	↓ toxicity	AMPK activation, NRF-2-linked and UPR regulation
Mitochondrial & Oxidative Stress	JC-1, ROS-Glo, GSH/GSSG, Hyper-7	↓ MMP, ↑ ROS, disturbed redox balance	↑ MMP, ↓ ROS, normalized redox balance	AMPK/NRF-2 pathway activated, mitochondrial support
Apoptosis	Caspase 3/7, BAX, Bcl-2	↑ apoptosis, ↑ pro-apoptotic and ↓ anti-apoptotic protein expression	↓ caspase activity, ↓ BAX and ↑ Bcl-2 expression	PI3K/Akt inhibits apoptosis, AMPK/MAPK inhibit caspase activation
ER Stress & UPR	ATF6, PERK, BiP, PDI, Calnexin	↑ ER stress markers	↓ ATF6, PERK, BiP, and calnexin	Reduced ER stress via AMPK and PI3K/Akt modulation and UPR pathway
Autophagy	ATG3, ATG5, ATG7	↓ autophagy related proteins	↑ expression of autophagy proteins	AMPK inhibits mTOR and promotes autophagy
AMPK Role Confirmation	Compound C, AMPK siRNA	↓ cell viability and increased cell toxicity	Loss of protection when AMPK inhibited and AMPK knockdown	AMPK plays a central role in regulating neuroprotection

Table 4: Collective summary effect of apelin-13 and its analogues on SH-SY5Y cells *H_2O_2*-induced stress.

Collective summarise table shows protective effect of apelin-13 and its analogues on the oxidative stress, apoptosis, ER stress, mitochondrial membrane potential in SH-SY5Y cells against ROS generated by *H_2O_2*.

Chapter 5

Effects of apelin-13 analogues on cell proliferation, differentiation and apoptosis induced by Lipopolysaccharides in SH-SY5Y cells *in-vitro*.

5.1 Introduction

Alzheimer's is complex neurodegenerative disorder characterised by memory loss, cognitive decline and behaviour changes. It is most common type of dementia affecting people above the age of 55 years old. Number of factors are responsible for the progression of the disease. After decades of research there is still no cure for Alzheimer's.

In this chapter we used Lipopolysaccharides (LPS) to mimic AD-like pathology in-vitro. LPS is a potent endotoxin derived from the outer protective membrane of Gram-negative bacteria (Yuan et al., 2022). LPS are big molecules essential for shielding the microbes from specific types of chemical attacks and preserving the integrity of their structure. The lipid A, the core polysaccharide, and the O antigen are the three components of LPS. Lipid A is the chemically active component that has the potential to stimulate an intense immune reaction (Bertani & Ruiz, 2018). LPS are present in a wide range of conditions, including the gastrointestinal tract of humans, soil, water, and vegetation, where Gram-negative bacteria are predominant (Munford, 2008). When microbes die and breakdown, they may be released into the organism that is the host, potentially resulting in reactions against the host's immune system leading to inflammation. LPS has the ability for binding to toll-like receptor 4 (TLR4) on immune system cells upon entering the bloodstream, thereby initiating a signalling cascade that leads to the generation of pro-inflammatory cytokines, including TNF-α, IL-1β, and IL-6. If left unchecked, this inflammatory response is crucial for combating infections, but it can also result in pathological conditions (Azzam et al., 2023).

Recent studies have revealed that apelin-13 analogues play a vital role in the reducing the inflammatory responses stimulated by LPS (He et al., 2020). A natural occurring apelin-36 have been shown to supress the ASK1\MAPK signalling pathway activated by LPS (He et al., 2020). A study by fan et al stated that apelin-13 analogues could reduce LPS-induced lung injury (Fan et al., 2015). An animal study showed that apelin-13 decreased neuroinflammation and enhanced the cognitive function when exposed to LPS. Apelin-13 inhibited microglial activation and reduced production of pro-inflammatory cytokines (Hu et al., 2022).

In this chapter we aimed to find whether apelin-13 analogues inhibit the neuroinflammation, oxidative stress induced by LPS and look at the impact of apelin-13 analogues on the cell proliferation and cell survival.

Objectives:

1. To analyse the protective effect of apelin-13 analogues on the cell viability and toxicity induced by LPS.
2. To investigate the impact of apelin-13 analogues on the expression of apoptotic and antiapoptotic markers.

5.2. Results

5.2.1: Effect of apelin-13 analogues in time dependent manner on the cell viability in SH-SY5Y cells.

One-way ANOVA revealed that cells treated with apelin-13 amide (1000 nM) showed an increase in cell viability (13%; $p>0.05$, Figure 5.1A) at 2 hours, (29%; $p<0.001$, Figure 5.1B), and (2%; $p>0.05$, Figure 5.1C) for 24 hours. Treatments with (Lys^{8}GluPAL)apelin-13-amide showed significant increase for 4 hours (16%; $p<0.001$, Figure 5.1B), 2 hours (17%; $p>0.05$, Figure 5.1A) and 24 hours had no change, compared to untreated control. On the other hand, there was an evident cytotoxic effect of LPS, it considerably decreased cell viability for LPS 30 μg by (28%, $p<0.01$, Figure 5.1A) at 2 hours, (31% $p<0.001$, Figure 5.1B) at 4h, and (31%, $p<0.001$, Figure 5.1C). For LPS 50 μg the cells viability declines by (41%; $p<0.0001$, Figure 5.1A) at 2 hours, (40%; $p<0.0001$, Figure 5.1B) at 4 hours, and (57%; $p<0.0001$, Figure 5.1C) at 24 hours, compared to untreated control.

When cells were co-treated with apelin-13 amide and LPS, a significant restoration of cell viability was observed for 30 μg LPS (13%; $p<0.01$, Figure 5.1A) at 2 hours, (33%; $p<0.001$, Figure 5.1B) at 4 hours, and (13%; $p>0.05$, Figure 5.1C) at 24 hours compared to LPS 30 μg alone. For LPS 50 μg, the combined treatment with apelin-13 amide led to an increase of 9% ($p>0.05$) for 2 hours, 31% ($p<0.001$) for 4 hours, and 23% ($p>0.05$) for 24 hours compared to LPS 50 μg alone. Correspondingly, the combined treatment with 30 μg LPS and (Lys^{8}GluPAL)apelin-13-amide resulted in a 14% ($p>0.05$), 12% ($p<0.01$), and 9% ($p>0.05$) increase, and co-treatment with 50 μg led to an increase of 11% for 2 hours, 13% for 4 hours, and 36% for 24 hours ($p>0.05$) compared to LPS 50 μg alone.

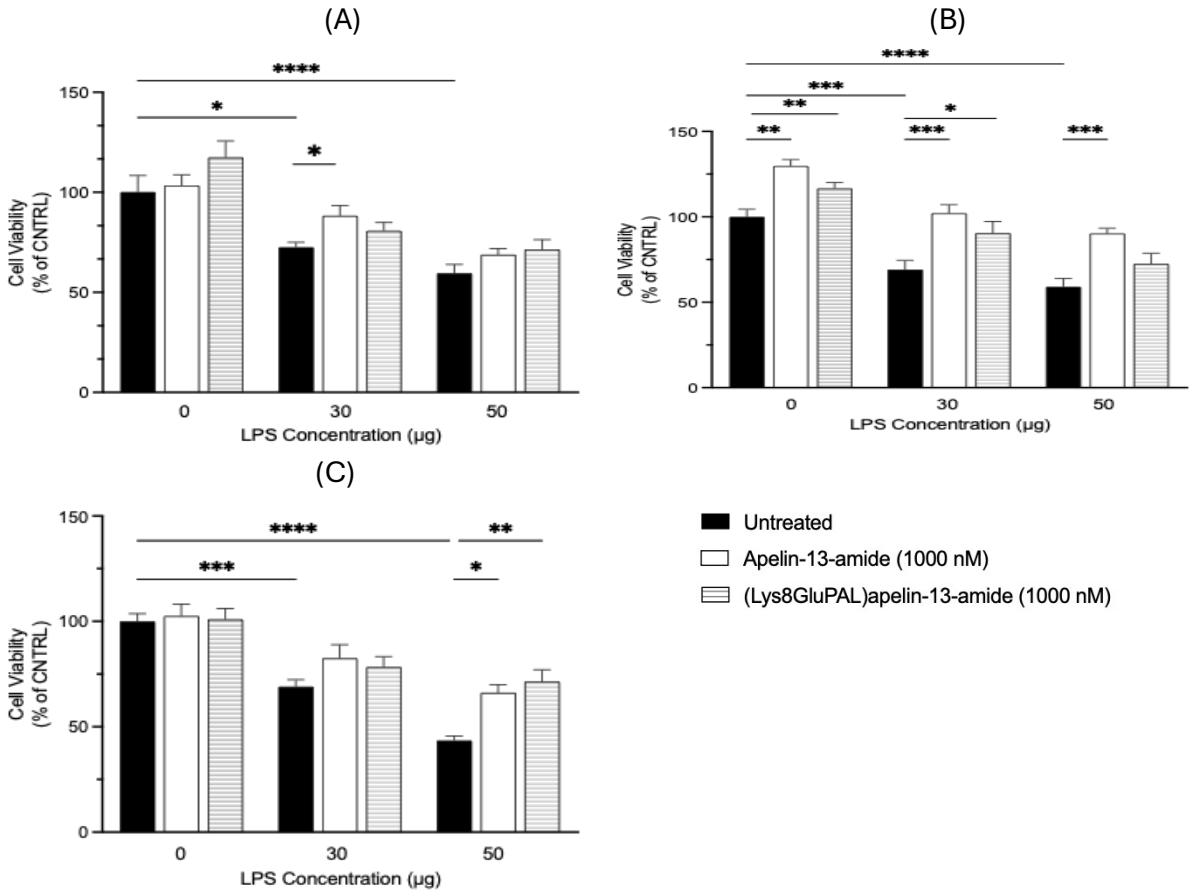

Figure 5.1 Effect of apelin-13 analogues in time dependent manner on the cell viability in SH-SY5Y cells. Time dependant treatment with apelin-13 analogues impacts on neuronal viability of SH-SY5Y cells with and without 30 μg and 50 μg of LPS *in-vitro*, using MTT reagent to measure the viability based on the reduction of MTT to formazan. Cells were treated with treatments for (A) 2h. (B) 4h and (C) 24h. values represents mean ±SEM (one-way ANOVA, n=3 where *p<0.05, **p<0.01,***p<0.001, and ****p<0.0001 compared to control.

5.2.2 Effect of apelin-13 analogues cell viability under LPS-induced stress in SH-SY5Y cells.

In comparison to untreated controls, treatment with apelin-13 amide increased cell viability by 16% (Figure 5.2; $p<0.05$), treatment with (Lys^8GluPAL)apelin-13-amide increased it by 8% (Figure 5.2; $p>0.05$). However, cell viability was significantly decreased by LPS at 30 µg (Figure 5.2; 30%; $p<0.0001$) and 50 µg (Figure 5.2; 43%; $p<0.0001$) compared to untreated control. Furthermore, co-treatment of apelin-13

amide with LPS 30 μg and increased cell viability by 32% (Figure 5.2; $p<0.001$) and with LPS 50 μg by 21% (Figure 5.2; $p<0.0001$). And co-treatment of (Lys^{8}GluPAL)apelin-13-amide with LPS 30 μg increased cell viability by 19% (Figure 5.2; $p>0.05$) and 36% (Figure 5.2; $p<0.01$) for LPS 50 μg, compared to stressors alone.

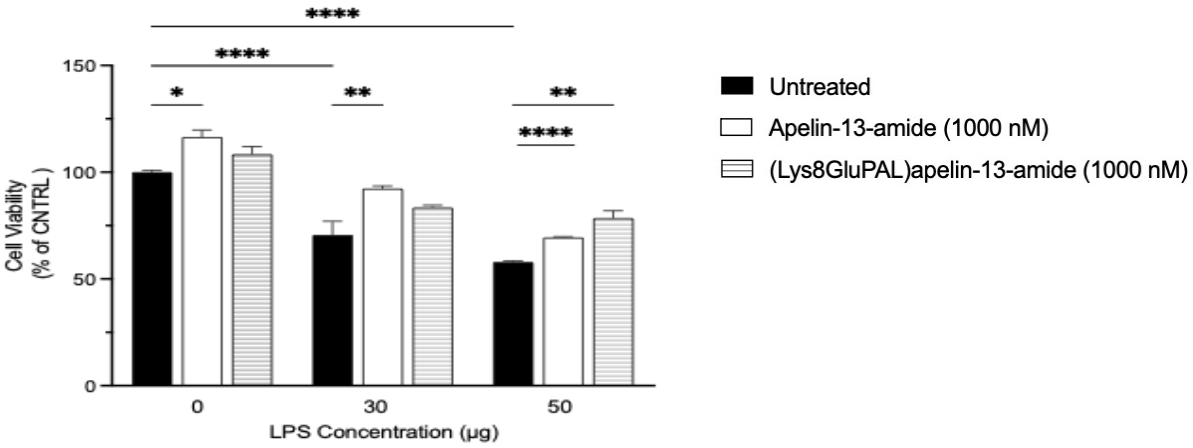

Figure 5.2: Effect of apelin-13 analogues cell viability under LPS-induced stress in SH-SY5Y cells. Dose dependent effects of apelin-13 amide and (Lys^{8}GluPAL)apelin-13 amide on viability of SH-SY5Y cells *in-vitro*. Cells were treated for 6h and the Celltiter-Glo luminescent assay and was used to measure the viability. Values represents mean ±SEM for n=3 where *p<0.05, **p<0.01, ****p<0.0001.

5.2.3.Effect of apelin-13 analogues on cell proliferation in SH-SY5Y cells.

The images depict the distribution of BrdU immunoreactive SH-SY5Y cells at a magnification of 20X where DAPI is displayed in a green pseudo colour instead of blue, while BrdU inclusion is represented in red (Figure 5.3A). The Figure 5.3B is the quantitative representative graph of the total number of BrdU positive cells measured by Image J. After treatment with apelin-13 amide, the assay quantitatively shows a little rise in the number of BrdU-positive cells, marking a 3% (Figure 5.3B; $p>0.05$), and treatment with (Lys^{8}GluPAL)apelin-13-amide led to a 7% (Figure 5.3B; $p>0.05$) rise in cell proliferation. However, treatment with LPS 30 µg led to 45% (Figure 5.3B; $p<0.05$) reduction, and a 54% reduction at 50 µg (Figure 5.3B; $p<0.01$), compared to the untreated control.

As compared to cells treated with LPS alone, co-treatment with apelin-13 amide and LPS at concentrations of 30 µg and 50 µg increased proliferation by 16% (Figure 5.3B; $p>0.05$), and 40% (Figure 5.3B; $p>0.05$), respectively. The proliferation rates were further increased by co-treatment with (Lys^{8}GluPAL)apelin-13-amide and LPS, showing increases of 43% (Figure 5.3B; $p>0.05$) and 40% (Figure 5.3B; $p>0.05$) at 30 µg and 50 µg LPS doses, respectively.

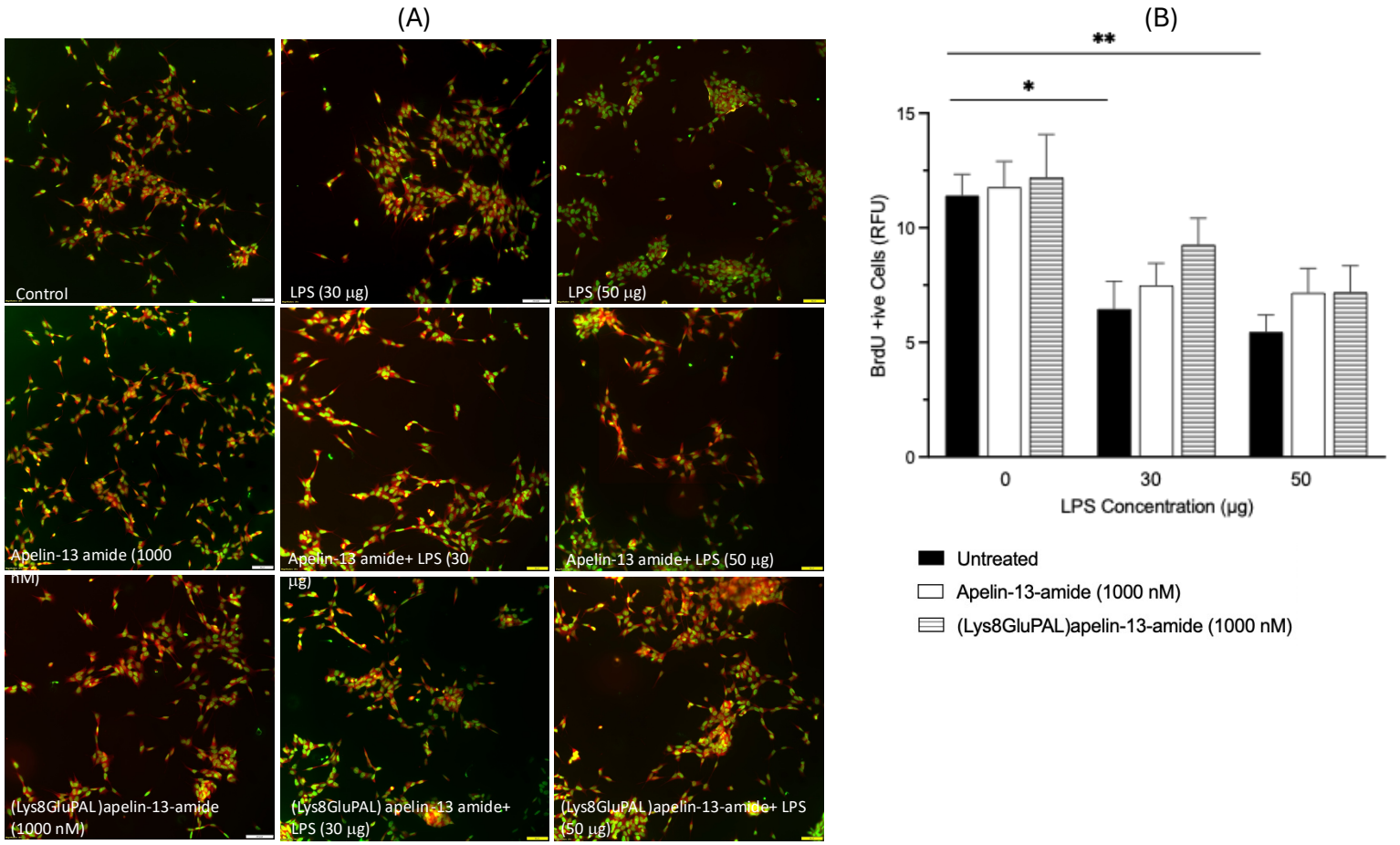

Figure 5.3: Effect of apelin-13 analogues on cell proliferation in SH-SY5Y cells. BrdU incorporation assay was used to assess cell proliferation. (A) Representative images of SH-SY5Y cells stained with BrdU and DAPI are shown (20x magnification). (B) Graph of quantification of BrdU positive cells treated with apelin-13-amide, (Lys^{8}GluPAL)apelin-13-amide. Values represents mean ±SEM for n=3 where *p<0.05, **p<0.01, ***p<0.001, ****p<0.0001.

5.2.4. Effect of apelin-13 analogues on neurite outgrowth in SH-SY5Y cells.

Representative images showing SH-SY5Y cells stained with Coomassie brilliant blue to identify the neurite outgrowth shown in Figure 5.4A.
The corresponding graph quantifies the neurite outgrowth observed in Figure 5.4B. The treatment with apelin-13 amide increased outgrowth by 45% ($p<0.001$), and by 50% ($p<0.0001$) when treated with (Lys^8GluPAL)apelin-13 amide, demonstrating strong neurite extension in comparison to control. On the other hand, there were significant reductions in neurite outgrowth of 44% ($p<0.001$) with LPS 30 µg and 66% ($p<0.0001$) with 50 µg compared to untreated control.

However, neurite outgrowth increased significantly when cells were co-treated with apelin-13 amide and LPS 30 µg by 55% ($p<0.05$) and 20% ($p>0.05$) for LPS 50 µg, indicating a restorative or protective impact of apelin-13 amide on neurite development. Moreover, treatment with (Lys^8GluPAL)apelin-13-amide and LPS 30µg improved neurite outgrowth by 89% ($p<0.0001$) and 88% ($p<0.05$) when combined with LPS 50 µg compared to LPS alone.

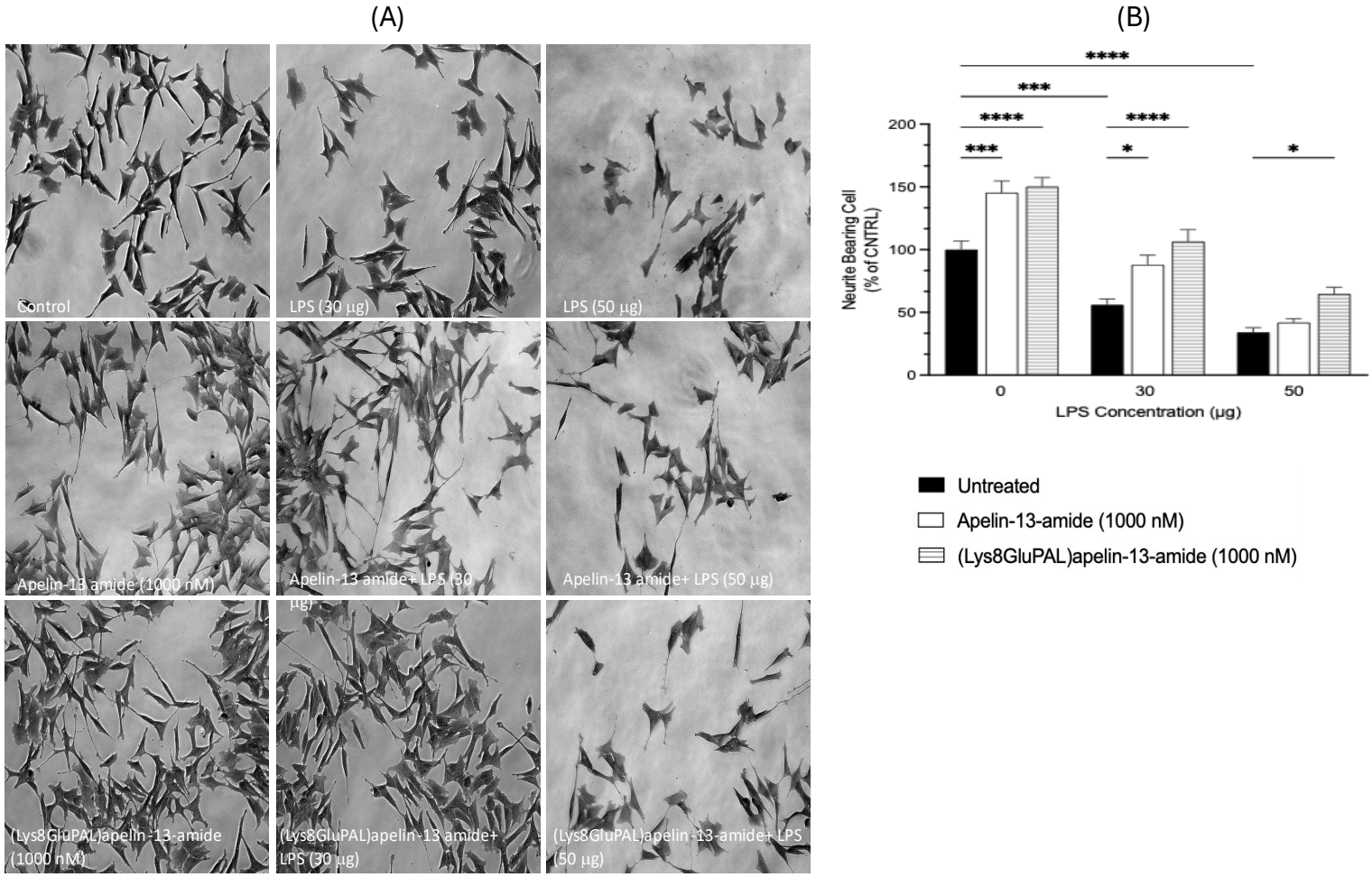

Figure 5.4: Effect of apelin-13 analogues on neurite outgrowth in SH-SY5Y cells. Illustrates the expression of MAP2 in SH-SY5Y cells (A) images of MAP2 staining with DAB substrate and (B) graph of optical density. Cells were differentiated with retinoic acid (10 μM) for 24 hours and treated with apelin-13-amide, (Lys^{8}GluPAL)apelin-13-amide with and without LPS. Values represents mean ±SEM for n=3.

5.2.5 Effect of apelin-13 analogues on neuronal differentiation in SH-SY5Y cells under LPS-induced stress.

Figure 5.5A presents illustrative images of MAP2 antibody with HRP substrate of SH-SY5Y cells to visualize the expression of Microtubule-associated protein 2 (MAP2). Figure 5.5B provides a graphical representation of the optical density measurements by Image J. Apelin-13 amide and (Lys^{8}GluPAL)apelin-13-amide increased MAP2 expression by 12% ($p>0.05$) compared to untreated control. However, the MAP2 expression was reduced by 46% ($p<0.05$) with LPS 30 μg and 53% ($p<0.05$) by LPS 50 μg compared to untreated control.

Co-treatment of apelin-13 amide with LPS 30 μg led to increase by 16% ($p>0.05$), and (10%; $p>0.05$) for 50 μg, compared to LPS alone. When cells were co-treated with (Lys^{8}GluPAL)apelin-13-amide and LPS 30 μg, neurite outgrowth increased by 33% ($p>0.05$) and 25% ($p>0.05$) for LPS 50 μg, compared to LPS alone.

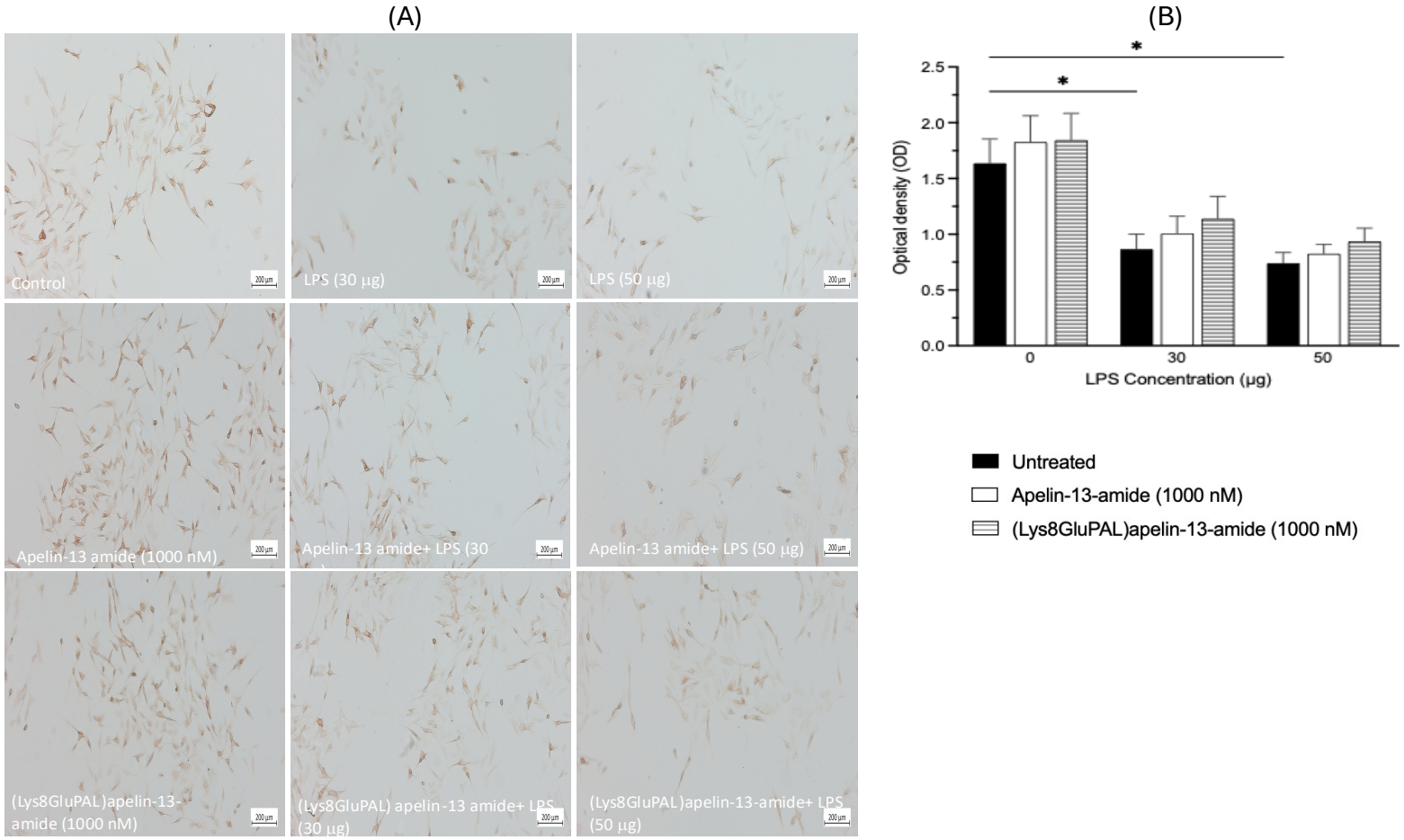

Figure 5.5: Effect of apelin-13 analogues on neuronal differentiation in SH-SY5Y cells under LPS-induced stress. Effects of apelin-13 amide and (Lys^{8}GluPAL)apelin-13 amide on neurite outgrowth length of SH-SY5Y cells *in-vitro*. (A) shows represented images of stained cells and (B) shows the graph for neurite bearing cells. Cells were treated for 48 hours, and cells were stained with Coomassie brilliant blue and imaged under the light microscope at 20x magnification. Value represents mean ±SEM for n=3 where *p<0.05, **p<0.01, ***p<0.001, ****p<0.0001.

5.2.6 Effect of apelin-13 analogues on cell toxicity of SH-SY5Y cells in time dependent manner.

SH-SY5Y cells showed time-dependent changes in toxicity after being treated with LPS and analogues of apelin-13 in a colorimetric cell toxicity experiment. Different reactions to the treatments were seen over three time points, 2 hours (Figure 5.6A), 4 hours (Figure 5.6B), and 24 hours (Figure 5.6C).

After treatment with apelin-13 amide, there was a non-significant (Figure 5.6A; 5%; $p>0.05$) decrease in cell toxicity at 2 hours, (Figure 5.6B; 14%; $p>0.05$) at 4 h hours and (Figure 5.6C; 7%; $p>0.05$) at 24 hours compared to untreated control. Cell toxicity with LPS 30 μg was increased by (Figure 5.6A; 19%; $p<0.001$) for 2 hours, (Figure 5.6B; 44%; $p<0.001$) for 4 hours, and (Figure 5.6C; 17%; $p>0.05$) for 24 hours, and for LPS 50 μg the toxicity was elevated by (Figure 5.6A; 20%; $p<0.001$) for 2 hours, (Figure 5.6B; 51%; $p<0.0001$) for 4 hours and (Figure 5.6C; 25%; $p>0.05$) for 24 hours compared to untreated control. When treated with (Lys^8GluPAL)apelin-13-amide cell toxicity was declined by 1% (Figure 5.6A; $p>0.05$) at 2 hours, 17% (Figure 5.6B; $p>0.05$) at 4 hours, and 3% (Figure 5.6C; $p>0.05$) at 24 hours compared to untreated control.

A notable reduction in cell toxicity was observed when cells were concurrently treated apelin-13 amide with LPS 30 μg (Figure 5.6A; 19%, $p<0.0001$) at 2 hours, 27% (Figure 5.6B; $p<0.001$) at 4 hours and (Figure 5.6C; 10%; $p>0.05$) at 24 hours compared to LPS 30 μg alone. When cells concurrently treated with (Lys^8GluPAL)apelin-13-amide and LPS 50 μg the cells toxicity declined by (Figure 5.6A; 10%; $p<0.05$) at 2 hours, (Figure 5.6B; 31%; $p<0.001$) at 4 hours and no change at 24 hours compared to LPS 50 μg alone. Co-treatment with (Lys8GluPAL)apelin-13-amide and LPS 30 μg mitigated the cell toxicity by 22% (Figure 5.6A; $p<0.0001$) at 2 hours, 29% (Figure 5.6B; $p<0.01$) at 4 hours, and 4% (Figure 5.6C; $p>0.05$) at 24 hours compared to LPS 30 μg alone. When treated with (Lys^8GluPAL)apelin-13-amide and LPS 50 μg there was no change seen at 2 hours and 24 hours, but the cells toxicity dropped (Figure 5.6B; 23%; $p<0.05$) at 4 hours compared to LPS 50 μg alone.

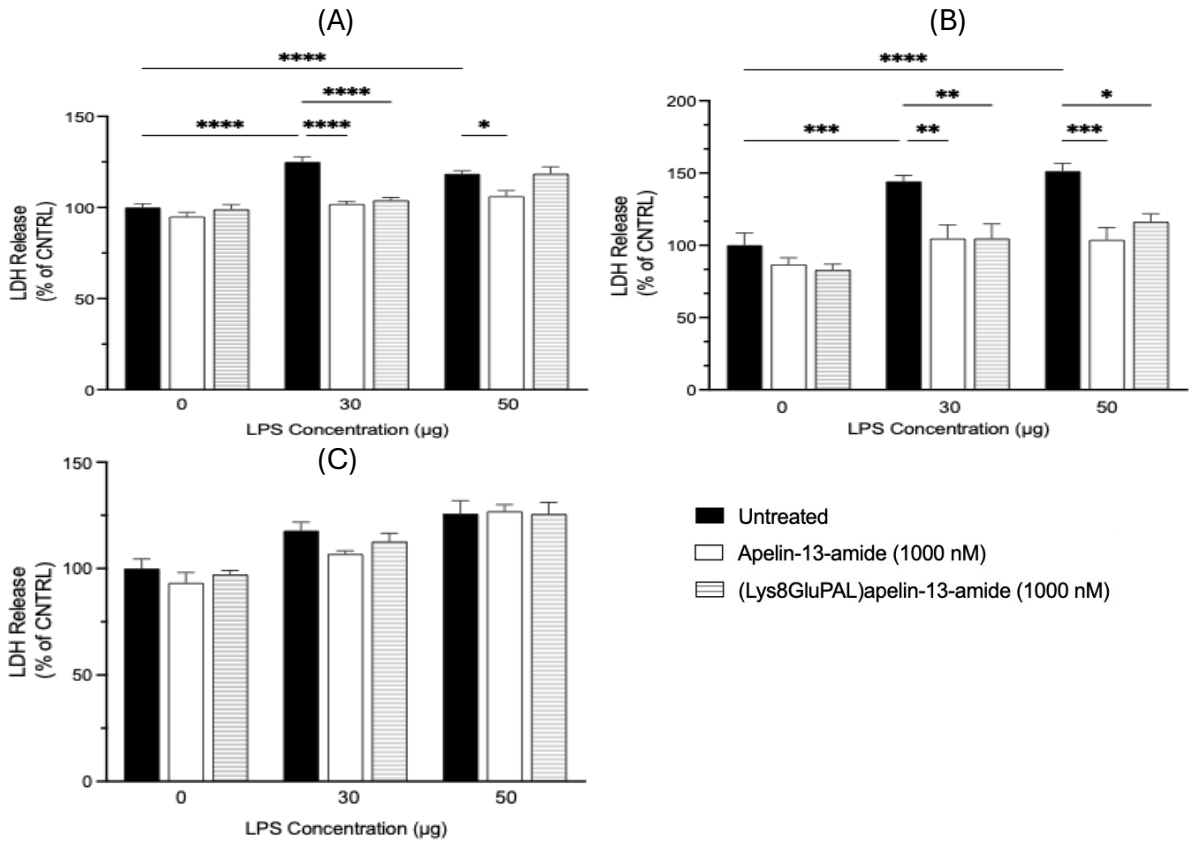

Figure 5.6: Effect of apelin-13 analogues on cell toxicity of SH-SY5Y cells in time dependent manner. Time-dependent effects of apelin-13 on toxicity of SH-SY5Y cells *in-vitro* using lactate dehydrogenase (LDH) assay to measure the release of LDH enzyme from damaged cells. Cells were treated with the treatments for (A) 2-hour (B) 4-hour (C) 24-hour. Values represents mean ±SEM (one-way ANOVA, n=3 where *p<0.05, **p<0.01, ***p<0.001, and ****p<0.0001 compared to control.

5.2.7 Effect of apelin-13 analogues cell toxicity induced by LPS in SH-SY5Y cells.

Cell toxicity assay showed that apelin-13 amide treatment alone reduced toxicity by 20% (Figure 5.7; p<0.001), while (Lys^{8}GluPAL)apelin-13-amide treatment lowered by 22% (Figure 5.7; p<0.001), compared to untreated control. When compared to the untreated control, cell toxicity raised 15% (Figure 5.7; p<0.01) with LPS 30 µg and 30% (Figure 5.7; p<0.01) with LPS 50 µg. Apelin-13 amide co-treatment reduced LPS-induced toxicity by 15% (Figure 5.7; p>0.05) for LPS 30 µg 10% (Figure 5.7; p>0.05) for LPS 50 µg. Similarly, toxicity reduction of 27% for LPS 30 µg and 26% (Figure 5.7;

p<0.05) for LPS 50 µg was observed upon co-treatment with (Lys^{8}GluPAL)apelin-13-amide compared to LPS alone.

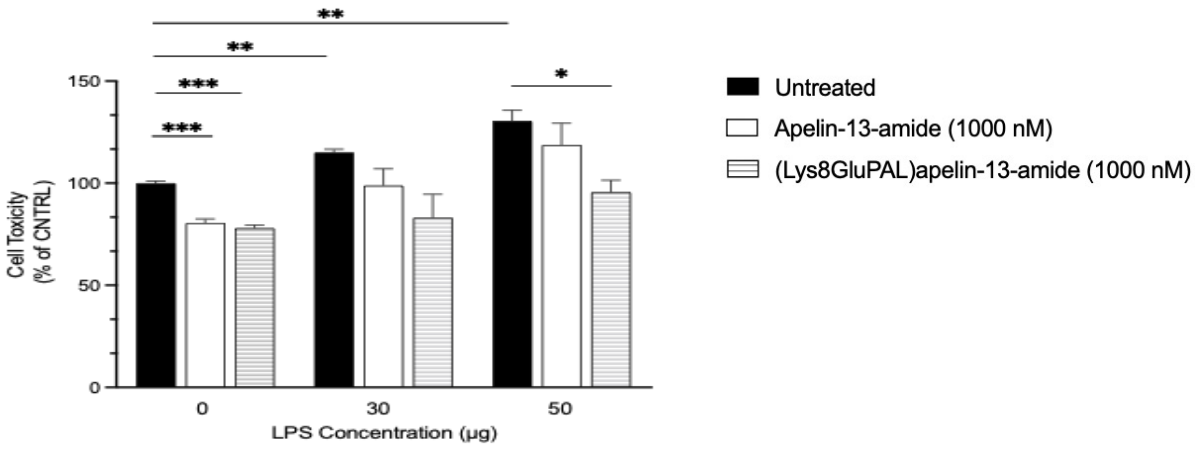

Figure 5.7: Effect of apelin-13 analogues cell toxicity induced by LPS in SH-SY5Y cells. Dose dependent effects of apelin-13 amide and (Lys^{8}GluPAL)apelin-13 amide on viability (A) and toxicity (B) of SH-SY5Y cells *in-vitro*. Cells were treated for 6h and the Celltiter-Glo luminescent assay and CellTox Green cytotoxicity assay were used to measure the viability and toxicity. Values represents mean ±SEM for n=3 where *p<0.05, **p<0.01, ***p<0.001, ****p<0.0001.

5.2.8. Effect of apelin-13 analogues LPS-induced ROS and reduction in GSH/GSSG.

Figure 5.8 A presents the results from a reactive oxygen species (ROS) luminescence assay evaluating the effects of apelin-13 amide, (Lys^{8}GluPAL)apelin-13-amide, and LPS on ROS production in SH-SY5Y cells. The assay showed that there was no statistically significant change in ROS levels following treatment with apelin-13 amide. But the use of (Lys^{8}GluPAL)apelin-13-amide resulted in a 6% decrease in ROS (Figure 5.8A; p<0.01) compared to untreated control. On the other hand, in comparison to the untreated control, treatment with LPS at dosages of 30 µg and 50 µg markedly elevated ROS levels by 33% (Figure 5.8A; p<0.05) and 87% (Figure 5.8A; p<0.0001), respectively. Co-treatment of apelin-13 amide and LPS 30 µg showed a significant 28% (Figure 5.8A; p<0.001) decrease in ROS, while at 50 µg of LPS, there was only a 12% (Figure 5.8A; p>0.05) reduction. Similarly, co-treatment with

(Lys^{8}GluPAL)apelin-13-amide and LPS 30 µg decreased ROS levels by 37% (Figure 5.8A; p<0.001), but only a 9% reduction was observed with LPS 50 µg (Figure 5.8A; p>0.05) compared to LPS alone.

Figure 5.8B illustrates the changes in the GSH/GSSG ratio, an important indicator of oxidative stress and cellular redox balance. The GSH/GSSG ratio rose by 35% (Figure 5.8B; p<0.01) when treated with apelin-13 amide and 34% (Figure 5.8B; p<0.01) when treated with (Lys^{8}GluPAL)apelin-13-amide compared to untreated control. Conversely, when compared to the untreated control, LPS at 30 µg concentration significantly decreased the GSH/GSSG ratio by 42% (Figure 5.8B; p<0.001). When the cells were treated LPS 30 µg in combination to apelin-13 amide and (Lys^{8}GluPAL)apelin-13-amide, the GSH/GSSG ratio increased significantly by 43% (Figure 5.8B; p<0.05) and by 56% (Figure 5.8B; p<0.01) respectively.

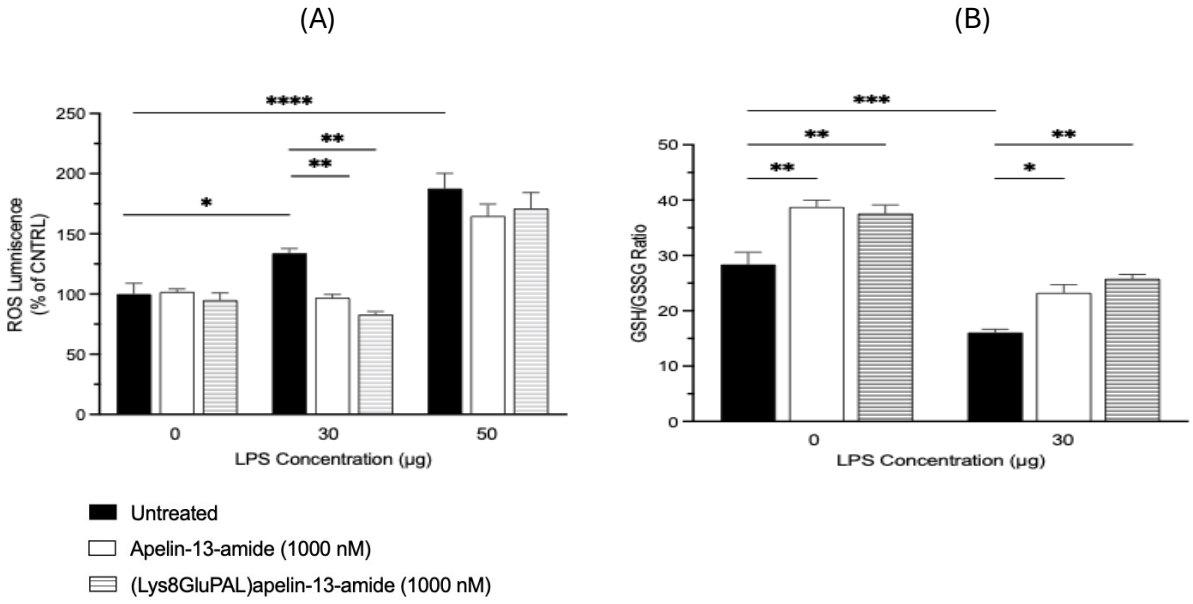

Figure 5.8: Effect of apelin-13 analogues LPS-induced ROS and reduction in GSH/GSSG. (A) ROS (Reactive Oxygen Species) measurement, (B) represents ratio of reduced and total glutathione in SHSY5Y cells when treated with apelin-13 amide and (Lys^{8}GluPAL)apelin-13 amide of SH-SY5Y cells induced by LPS. Values represents mean ±SEM for n=3 where *p<0.05, **p<0.01, ***p<0.001.

5.2.9. Effect of apelin-13 analogues on mitochondrial membrane potential in SH-SY5Y.

Figure 5.9A illustrates the demonstrative fluorescence microscopy images of SH-SY5Y at 20X magnification stained with JC-1 dye and Figure 3.9B graph is measurement of the optical density. Apelin-13 amide treatment alone resulted in an 84% (Figure 5.9B; $p<0.01$) rise in JC-1 aggregates, which are a marker of enhanced mitochondrial membrane potential. In addition, treatment with (Lys^8GluPAL)apelin-13-amide increased membrane potential by 60% (Figure 5.9B; $p<0.01$) compared to untreated control. On the other hand, in comparison to the untreated control, treatment with LPS at doses of 30 µg and 50 µg resulted in a significant drop in membrane potential of 92% (Figure 5.9B; $p<0.001$) and 81% (Figure 5.9B; $p<0.01$), respectively. A significant 520% (Figure 5.9B; $p<0.05$) rise in membrane potential was observed upon co-treatment with Apelin-13 amide with 30 µg LPS, and 105% (Figure 5.9B; $p<0.01$) with LPS 50 µg compared to LPS alone. Furthermore, in comparison with LPS treatment alone, 395% (Figure 5.9B; $p<0.05$) increase was observed upon co-treatment of (Lys^8GluPAL)apelin-13 amide with LPS 30 µg and 111% (Figure 5.9B; $p<0.01$) for (Lys^8GluPAL)apelin-13-amide with LPS 50 µg.

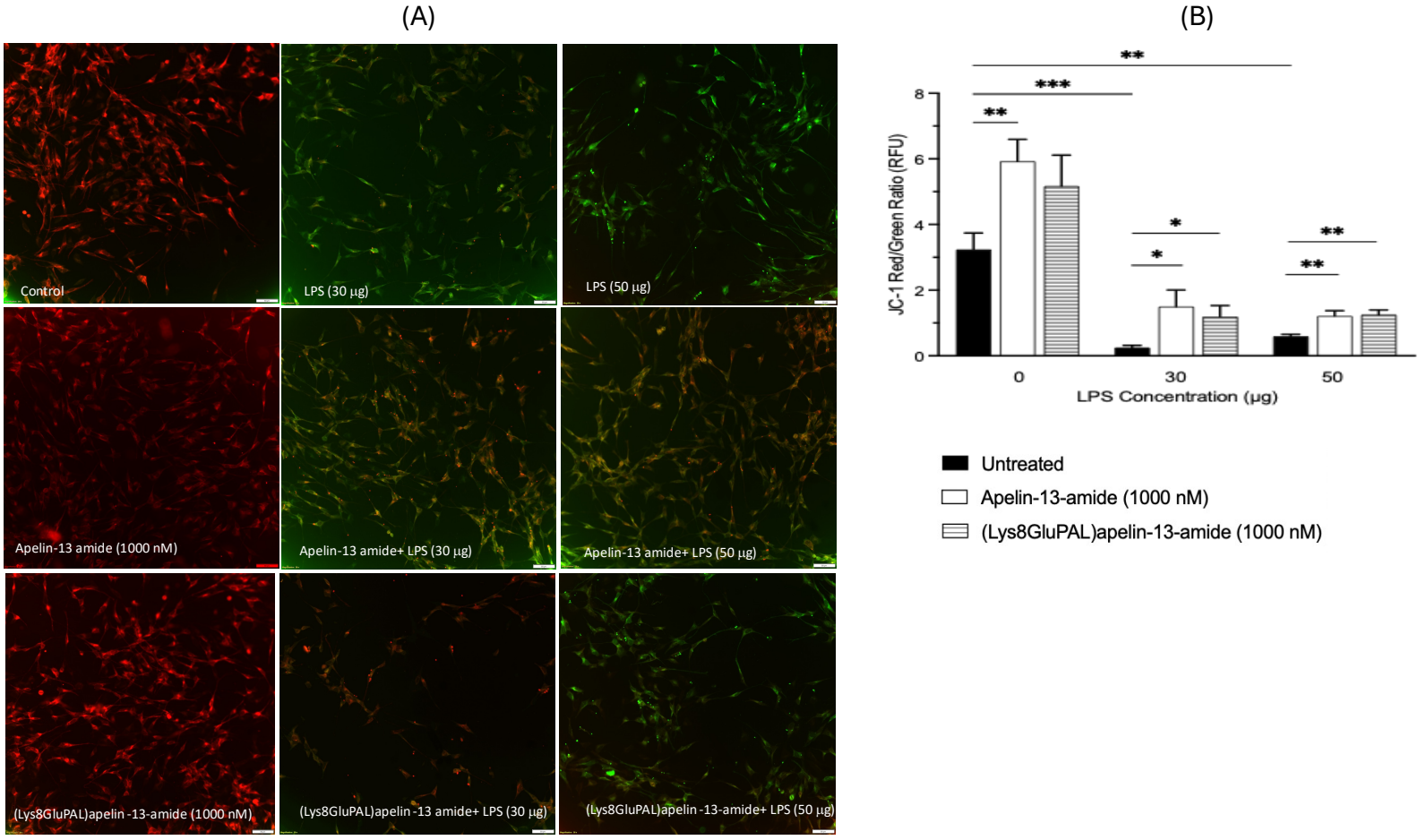

Figure 5.9: Effect of apelin-13 analogues on mitochondrial membrane potential in SH-SY5Y. Displays mitochondrial membrane potential (ΔΨm) using JC-1 staining. (A) Representative images of SH-SY5Y cells stained with JC-1 on two different channels and merge (20x magnification). (B) Graph of JC-1 Red/Green fluorescence ratio of cells treated with apelin-13-amide, (Lys^{8}GluPAL)apelin-13-amide and LPS. Values represents mean ±SEM for n=3 where *p<0.05, **p<0.01, ***p<0.001 , ****p<0.0001.

5.2.10 Effect of apelin-13 analogues on LPS-induced apoptosis in SH-SY5Y cells.

The dose-dependent effects of LPS on caspase-3/7 activity, a marker of apoptosis in SH-SY5Y cells, are shown LPS 30 µg (Figure 5.10A) and for LPS 50 µg (Figure 5.10B). When compared to untreated cells, treatment with apelin-13 amide resulted in a 23% drop in caspase-3/7 activity (Figure 5.10A, B; $p<0.05$), while (Lys^{8}GluPAL)apelin-13 amide caused a more significant decrease (Figure 5.10A, B; 30%; $p<0.01$) compared to untreated control. On the other hand, caspase 3/7 activity was considerably increased by 30 µg and 50 µg of LPS treatment, respectively, by 7% (Figure 5.10A; $p<0.05$) and 1000% (Figure 5.10B; $p<0.0001$), suggesting significant stimulation of apoptotic processes at these higher dosages of LPS.

When cells were co-treated with apelin-13 amide and LPS at both 30 µg and 50 µg caspase activity was dramatically reduced by approximately 17% (Figure 5.10A; $p>0.05$), and 56% (Figure 5.10B; $p<0.0001$), respectively. Like this, co-treatment at the same dosages of LPS and (Lys^{8}GluPAL)apelin-13-amide significantly reduced caspase activity by 56% (Figure 5.10A; $p<0.0001$), and 60% (Figure 5.10B; $p<0.0001$), respectively compared to LPS alone.

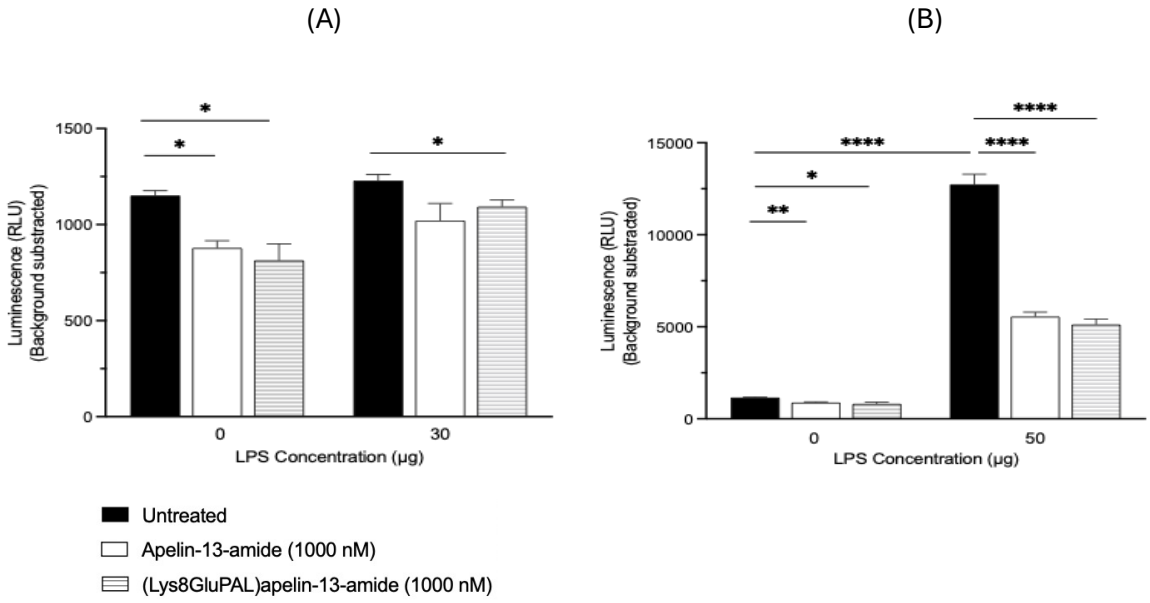

Figure 5.10 Effect of apelin-13 analogues on LPS-induced apoptosis in SH-SY5Y cells. Dose dependent effects of apelin-13 amide and (Lys^{8}GluPAL)apelin-13 amide on Caspase 3/7 activity of SH-SY5Y cells *in-vitro.* (A) LPS 30 µg (B) 50 µg. Values represents mean ±SEM for n=3 where *p<0.05, **p<0.01, ***p<0.001 , ****p<0.0001.

5.2.11 Effect of apelin-13 analogues on reduced expression of Nrf-2 in SH-SY5Y cells.

Figure 5.11 shows the impact of apalin-13 analogues and LPS treatment on the NRF-2 protein expression analysis. Apelin-13 amide reduced expression (Figure 5.11; 28%; p>0.05), and (Lys^{8}GluPAL)apelin-13-amide showed no effect in NRF-2 expression compared to control. However, LPS 30 µg had increased expression by 71% (Figure 5.11; p>0.05), compared to untreated control. Co- treatment of LPS led to non-significant reduction in NRF-2 expression by 22% (Figure 5.11; p>0.05) for apelin-13 amide and 5% (Figure 5.11; p>0.05) for (Lys^{8}GluPAL)apelin-13-amide compared to LPS 30 µg alone.

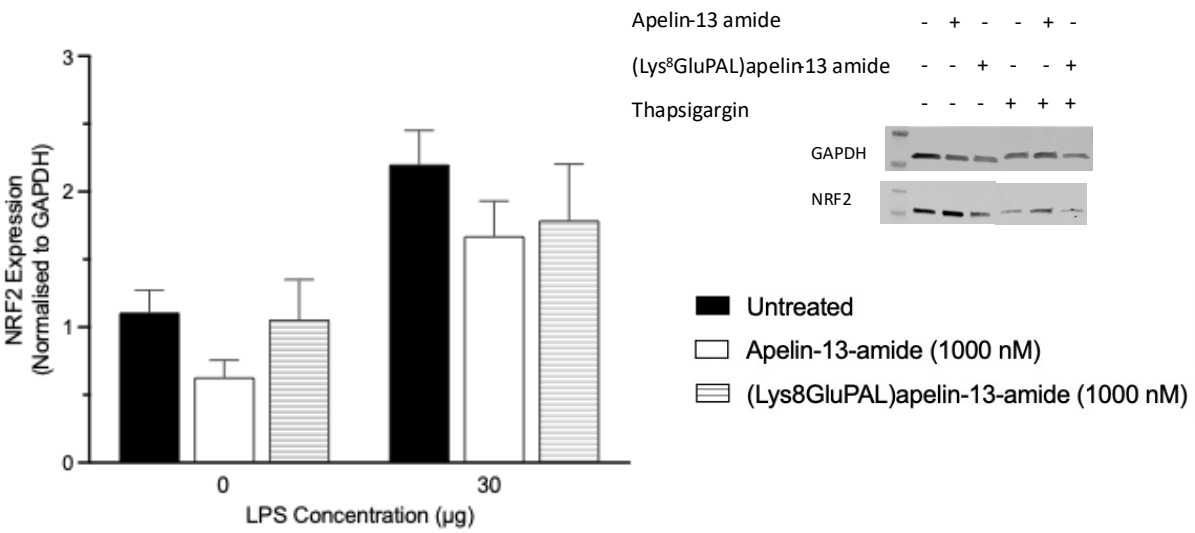

Figure 5.11: Effect of apelin-13 analogues on reduced expression of NRF-2 in SH-SY5Y cells. For LPS treatments NRF-2 protein expression was normalized using GAPDH protein expression. Data was analysed using Image J and GraphPad Prism version 10. Values represents mean ±SEM for n=3 where *p<0.05.

5.2.12 Effect of apelin-13 analogues on ER stress related protein expression under LPS-induced stress.

The changes in protein expression of BAX, Bcl2 and ration of BAX/bcl-2 by LPS induced apoptosis is demonstrated in Figure 3.3.12. The BAX expression was reduced by 7% (Figure 5.12 A; p>0.05) when treated with apelin-13 amide and showed no effect with for (Lys^{8}GluPAL)apelin-13-amide. Whereas the LPS 30 µg increased BAX expression by 35% (Figure 5.12 A; p<0.01) compared to untreated control. Co-treatment of LPS 30 µg declined expression by 35% (Figure 5.12 A; p<0.01) for both apelin-13 analogues, compared to LPS alone (Figure 3.11A).

apelin-13 amide treatment had no significant impact on the expression of Bcl-2 but the (Lys^{8}GluPAL)apelin-13-amide increased the Bcl-2 expression by 23% (Figure 5.12 B; p>0.05) compared to untreated control. However, LPS treatment led to 10% (Figure 5.12 B; p>0.05) decline in Bcl-2 expression. Co-treatment of LPS with apelin-13 amide increased expression by 27% (Figure 5.12 B; p<0.01) for and 26% (Figure 5.12 B; p<0.05) for (Lys^{8}GluPAL)apelin-13-amide compared to LPS alone (Figure 3.11B).

Apelin-13 amide had no impact on the Bax/Bcl-2, but (Lys^{8}GluPAL)apelin-13-amide reduced the expression by 22% (Figure 5.12 C; $p>0.05$), and LPS 30 µg increased by 51% ($p<0.01$), compared to untreated control. Co-currently treatment of LPS reduced ratio significantly by 48% (Figure 5.12 C; $p<0.001$) for apelin-13 amide and 55% (Figure 5.12 C; $p<0.0001$) for (Lys^{8}GluPAL)apelin-13-amide compared to LPS alone.

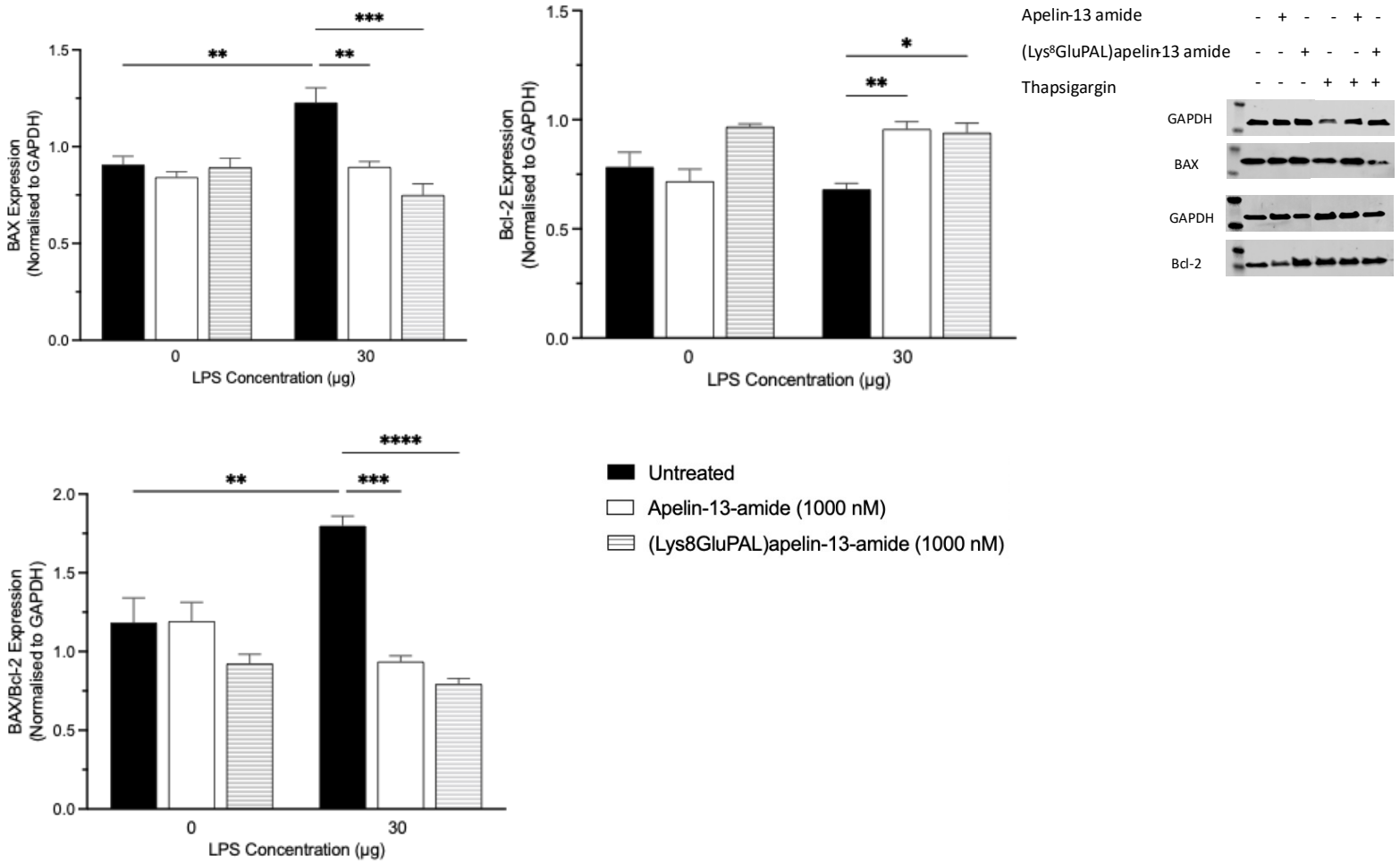

Figure 5.12: Effect of apelin-13 analogues on ER stress related protein expression under LPS-induced stress. (A) Graph representation and blot images of Protein BAX, (B) Graph representation and blot images of protein Bcl-2 and (C) is graph representation of ration of BAX/Bcl-2. The BAX and Bcl-2 expression was normalised to GAPDH protein expression. Data was analysed using Image J and GraphPad Prism version 10. Values represents mean ±SEM for n=3 where *p<0.05.

5.2.13 Effects of apelin-13 analogues on compound C-induced AMPK inhibition on cells viability and cell toxicity.

The results in Figure 3.2.13A shoes the impact of compound C on cell viability by inhibiting the AMPK pathway. The cells were incubated with and without compound C prior to the treatments for 6 hours with LPS 30 µg. The results show that without compound C SH-SY5Y cells improved cell viability 23% (Figure 5.13 A; $p>0.05$) with apelin-13 amide, 24% (Figure 5.13 A; $p<0.05$) with (Lys^8GluPAL)apelin-13 amide, however reduced by 39% when treated with LPS 30 µg, compared to untreated control. Co-treatment of LPS 30 µg with apelin-13 amide improved cell viability by 95% (Figure 5.13 A; $p<0.0001$) and 62% (Figure 5.13 A; $p<0.0001$) for (Lys^8GluPAL)apelin-13 amide, compared to LPS alone. On the other hand, when the cells were incubated with compound C, there was no significant change was seen when treated with apelin-13 analogues, but the cell viability was reduced by 11% with LPS 30 µg compared to control. When co-treated with LPS the cell viability was further reduced by 8% (Figure 5.13 A; $p>0.05$) for apelin-13 amide and 11% (Figure 5.13 A; $p>0.05$) for (Lys^8GluPAL)apelin-13 amide compared to LPS alone.

The results shows that the cell toxicity without compound C is reduced when treated with apelin-13 amide (Figure 5.13 B; 11%; $p>0.05$) and (Lys^8GluPAL)apelin-13 amide (15%; $p<0.05$) but increased when treated with LPS 30 µg (Figure 5.13 B; 16%; $p<0.01$) compared to untreated control. Co-treatment of LPS 30 µg reduced cell toxicity by 21% (Figure 5.13 B; $p<0.0001$) with apelin-13 amide and 22% (Figure 5.13 B; $p<0.0001$) with (Lys^8GluPAL)apelin-13 amide compared to LPS alone. For the cells treated with Compound C there is no significant impact by the apelin-13 analogues and LPS 30 µg increased toxicity by 16% (Figure 5.13 B; $p<0.01$) compared to untreated control. when co treated LPS 30 µg with apelin-13 amide and (Lys^8GluPAL)apelin-13 amide toxicity was increased by 2% for both (Figure 5.13 B; $p>0.05$) compared to LPS alone.

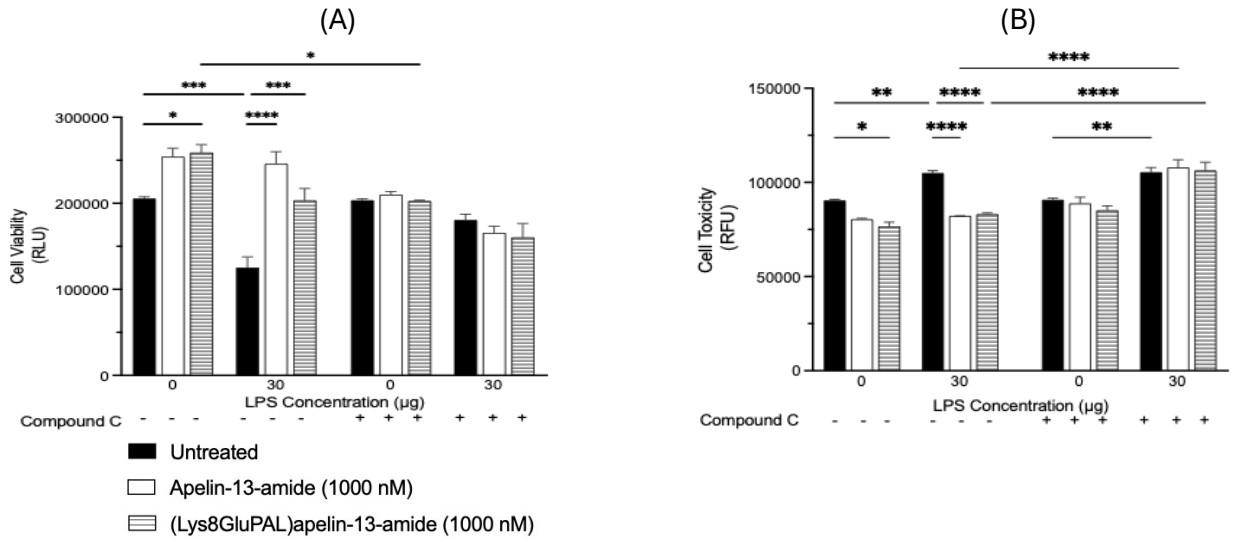

Figure 5.13 Effects of apelin-13 analogues on compound C-induced AMPK inhibition on cells viability and cell toxicity. Effect of apelin-13 amide and (Lys^{8}GluPAL)apelin-13 amide on viability (A) and toxicity (B) of SH-SY5Y cells *in-vitro* with and without the compound C. Cells were treated for 30 minutes with compound C to inhibit the AMPK prior to the treatments for 6 hours and the Celltiter-Glo luminescent assay and CellTox Green cytotoxicity assay were used to measure the viability and toxicity. Values represents mean ±SEM for n=3 where *p<0.05, **p<0.01, ***p<0.001, ****p<0.0001.

5.3. Discussion

In this chapter effect of apelin-13 amide and (Lys^{8}GluPAL)apelin-13-amide in AD were investigated by induced neuroinflammation and oxidative stress in SH-SY5Y cells. An apelin-13 analogues have played a major role in cell proliferation and cell differentiations. LPS, an active endotoxin, can cross the blood-brain barrier and cause neurological inflammation (Brown, 2019). This process has been suggested that plays a significant role in the development of AD. LPS triggers ROS production and lead to oxidative stress, lipid peroxidation and ER stress. Oxidative stress activates UPR in response to the ROS production as a part of the immune response to the presence of the gram-negative bacterial cell wall LPS, which plays an important role in the elimination of the bacteria (Maitra et al., 2009). However, the uncontrolled activation of ROS leads to the inflammation and tissue damage (Kratzer et al., 2012).

Research has revealed that patients with AD have a higher level of LPS in their brains, which implies a potential correlation between the aggravation of neurodegeneration processes, infections caused by bacteria, and LPS-induced inflammation (Zhan et al., 2018).

This study illustrated the impact of apelin-13 amide and (Lys^{8}GluPAL)apelin-13-amide on the cell viability, toxicity, neuronal differentiation, proliferation, Map2 expression and apoptotic and pro-apoptotic protein expression when treated with stressor called LPS. The results suggest the potential of apelin-13 analogues as a treatment in AD.

Cell Viability

The results showed that treatment with LPS significantly reduced cell viability. The co-treatments of apelin-13 amide and (Lys^{8}GluPAL)apelin-13-amide with LPS resulted in a significant improvement in cell survival. This increase was seen at both LPS concentrations after 4 hours, and specifically for LPS 50 µg after 24 hours. The cell

viability was also improved at 2 hours, but it did not show any significance. LPS cause oxidative stress in brain that led to the neuronal damage by activating the microglial to release pro-inflammatory cytokines, mitochondrial dysfunction, neuroinflammation, stimulation of NAPDH oxidase, and blocking antioxidant pathways (Luo et al., 2019). In the central nervous system, microglial are the main immune-system cells. The LPS presence in the brain may activate them, which results in the release of pro-inflammatory mediators. The continued inflammation that may arise from the persistent stimulation of these immune responses is damaging to brain functioning and may speed up the buildup of amyloid-beta plaques and tau tangles, the main hallmark pathologies of Alzheimer's disease (Gao et al., 2023).

The luminescent cell viability assay results indicating the significant decline in ATP levels by LPS treatment and increase in cell viability by apelin-13 analogues confirmed the neuroprotective effect of apelin-13 analogues. These data indicate that the peptides can reduce the toxic effects caused by LPS, therefore improving cell viability. Apelin-13 analogues are known to enhance neuronal survival by activating PI3K/Akt signalling pathway (Kamińska et al., 2024). This aligns with the previous research where apelin-13 analogues have shown protective effect effects against the oxidative stress and apoptosis (Zou et al., 2016; Zhang et al., 2022).

Cell proliferation and differentiation

Our research has also shown that apelin-13 analogues have an ability to improve the cell proliferation and cellular differentiation. The cytoskeletal protein MAP2 is a neuronal component developed in the dendrites and cell bodies which can determine the morphology of the cells. LPS has been significantly reducing the MAP2 density at different concentration of LPS, and apelin-13 amide and (Lys^{8}GluPAL)apelin-13-amide improved the MAP2 alongside with LPS but not significant. LPS leads to the mitochondrial dysfunction by number of pathways like by activating the TLR4 on microglial leading to the production of pro-inflammatory cytokines and production of ROS. Which leads to the

oxidative stress to the proteins of mitochondria, lipids, DNA, and decline in the electron transport and reduces ATP production (Esteves et al., 2023). Apelin-13 stimulate the ERK1/2 and PI3/Akt pathway vital for promoting cytoskeletal remodelling and growth formation facilitating neurite extensions (Deng et al., 2022).

Cell toxicity

To assess the role of apelin-13 analogues toward the cytotoxicity induced by LPS we used LDH and DNA damage assay. Results showed that apelin-13 analogues were able to mitigate the cell toxicity induced by LPS at different time points. LPS a stress model used in this chapter is known to cause the cytotoxicity by several pathways like TLR4, oxidative stress by ROS production and apoptosis. The study by Zhang et al showed that apelin-13 analogues treatment in mice mitigated the LPS induced cytotoxicity by suppressing NF-κB pathway (2018). Apelin-13 analogues led to the reduced production of pro-inflammatory cytokines and reduced the structural damage to the lung tissues (Zhang et al., 2018).

Oxidative stress

ROS and ratio of reduced glutathione to oxidized glutathione plays important role in the cellular signalling, but the excessive ROS production can lead to the oxidative stress contributing to the cellular damage and pathogenesis of many diseases (Schieber & Chandel, 2014). The results indicated that LPS treatments led to the increased number of ROS in SH-SY5Y cells which suggest the pro-inflammatory and oxidative effect of LPS and disruption in the cellular homeostasis. When the cells were co-treated with LPS and apelin-13 analogues the significant reduction in ROS was observed which suggest that an antioxidant effect of apelin and protection against the

The reduced GSH/GSSG ratio indicate the oxidative stress induced by LPS. Which align with the known effect of LPS for activating the inflammatory pathways and production of ROS which reduce the GSH levels and increase GSSG accumulation (Armstrong et al., 2002). The significant improvement in the GSH/GSSG ratio by apelin-13 amide and (Lys8GluPAL) apelin-13-amide with LPS treatment indicate the potential of the apelin-13 to mitigate the oxidative stress induced by LPS. Apelin-13 analogues has a strong antioxidant effect and reduce oxidative stress via AMPK pathway (Huang et al., 2025). Apelin-13 analogues have shown to reduce ROS generation and impairments of glucose transporters and ion channel ATPase (Huang et al., 2025). We observed increase in NRF-2 expression with LPS treatment, which suggest that adaptive cellular response to the oxidative stress. NRF-2 is a transcription factor that regulates that expression of antioxidant proteins that protect against the inflammation and oxidative stress. The activation of NRF-2 leads to the upregulation of various antioxidant genes (Ma, 2013). Co-treatment with apelin-13 amide and (Lys^{8}GluPAL) apelin-13-amide reduced the NRF-2 protein expression, which illustrates the potential of apelin-13 analogues to mitigate the oxidative stress and neuroinflammation. In the treatment of AD, the effect of apelin-13 analogues can be explored further, and it can be potential therapeutic drug.

Apoptosis

The results suggest the LPS treatment leads to the increase in caspase3/7 activity which highlights the pro-apoptotic effect of LPS specifically at higher concentration of LPS. The higher concentration of LPS dramatically increased the apoptosis compared to the lower concentration. When the cells co-treated LPS with apelin-13 amide and (Lys^{8}GluPAL)apelin-13-amide, the aplin-13 analogues have exerted anti-apoptotic effect and reduce the caspase activity significantly. The apelin-13 analogues exert the protective effect by modulating the key apoptotic regulators like by inhibiting the activation of Bax a pro-apoptotic protein or enhancing the anti-apoptotic protein Bcl-2 (Wen et al., 2023; Zhu et al., 2019). The western blot results have shown that LPS led to a significant increase

in the BAX protein expression and non-significant reduction in Bcl-2 protein. The co-treatments of LPS with apelin-13 amide and (Lys^{8}GluPAL)apelin-13-amide led to the significant reduced BAX expression and increased Bcl-2 expression. The BAX/bcl-2 ratio is shown to be significantly increased with LPS treatment and reduced with the apelin-13 analogues co-treatment with LPS. Study by Shao et al showed that apelin-13 analogues protect against the neuronal apoptosis by activating anti-apoptotic pathways. Apelin-13 analogues regulate the activation of AMPK and PI3K/Akt pathways and these pathways are involved in the activation of anti-apoptotic pathways (Vince et al., 2018; Zhu et al., 2019).

Mechanistic study of apelin-13 analogues

In this study we have also looked at the cell viability and cell toxicity with or without the compound C in SH-SY5Y cells. Compound C is an inhibitor of AMP-activated protein kinase (AMPK) also called dorsomorphin. AMPK is the main sensor of the energy in the cells which regulates the metabolic pathways to maintain the energy homeostasis (Dai et al., 2013). The inhibition of AMPK by compound C leads to the cellular stress response and effect the viability and toxicity (Liu et al., 2014). The cell viability in absence of compound C was increased and cell toxicity was reduced when treated with apelin-13 analogues and LPS. However, pre incubation with compound C led to no significance change in the cell viability under LPS induced stress on cell toxicity was increased compared to untreated control. In these findings apelin-13 analogues found to be unsuccessful in reducing the cell toxicity when treated with compound C as the compound C blocks the AMPK pathway and apelin-13 analogues are activated through this pathway. Studies showed that the inhibition of AMPK pathway can also lead to the disruption in various pathway that are important in cell survival (Liu et al., 2014).

5.4. Conclusion

This chapter summarise the protective effect of apelin-13 analogues in the cellular toxicity induced by LPS. LPS is a potent inducer of oxidative stress, apoptosis and neuroinflammation. In this chapter we used LPS as a stress model to mimic the AD-like pathology and study the effect of stable peptide Apelin-13 and its analogues. The results showed that apelin-13 analogues were able to mitigate the cytotoxicity induced by LPS through the activation of PI3K/Akt, ERK1/2, NRF-2 and AMPK pathways (shown in Table 5). Number of studies have highlighted the role of apelin-13 in reducing toxicity in various disease but its role in AD is still undiscovered. Apelin-13 enhances the cell growth, survival, and modulates the neuroinflammation, suggesting its role a therapeutic agent in AD.

Experiments	Assays Used	LPS Effect	Apelin-13 Effect	Pathway Impact
Cell Viability	MTT, CellTiter-Glo	↓ cell viability	↑ viability under LPS-induced stress	PI3K/Akt activation for survival signalling
Proliferation & Differentiation	BrdU, MAP2, Neurite Outgrowth	↓ cell proliferation and neurite outgrowth	↑ cell proliferation and neurite outgrowth	PI3K/Akt for proliferation, ERK1/2 for promoting cytoskeletal remodelling
Cell Toxicity	LDH, CellTox Green	↑ cell toxicity	↓ cell toxicity induced by LPS	AMPK activation, NRF-2-linked antioxidant response
Mitochondrial & Oxidative Stress	JC-1, ROS-Glo, GSH/GSSG	↓ MMP, ↑ ROS, disturbed redox balance	↑ MMP, ↓ ROS, normalized redox balance	AMPK/NRF-2 pathway activated, mitochondrial membrane potential improvement
Apoptosis	Caspase 3/7, BAX, Bcl-2	↑ apoptosis, ↑ pro-apoptotic and ↓ anti-apoptotic protein expression	↓ caspase activity, ↓ pro-apoptotic and ↑ anti-apoptotic protein expression	PI3K/Akt inhibits apoptosis, AMPK promotes cell survival
AMPK Role Confirmation	Compound C, AMPK siRNA	↓ cell viability and increased cell toxicity	Loss of protection when AMPK inhibited and AMPK knockdown	AMPK plays a central role in regulating neuroprotection

Table 5: Collective summary effect of apelin-13 and its analogues on SH-SY5Y cells LPS-induced inflammatory stress.

Summarised table shows protective effect of apelin-13 and its analogues on LPS-induced cell toxicity, oxidative stress, proliferation, apoptosis, ER stress, and mitochondrial membrane potential in SH-SY5Y cells.

Chapter 6

Effects of apelin-13 analogues on cell proliferation, survival, differentiation in Thapsigargin-induced stress in SH-SY5Y cells in-vitro.

6.1: Introduction

Neurodegenerative disease including AD and PD are known for the significant impact on the morbidity and mortality worldwide (Janyou et al., 2015). Progressive neuronal damage is a hallmark of these disorders, which are frequently caused by oxidative stress, protein misfolding, and ER malfunction (Javaid et al., 2024). Many studies have shown the impact of ER stress in the development of neurodegenerative diseases and these disease shares the common pathogenic mechanism of aggregation and deposition of Unfolded proteins (Janyou et al., 2015). ER is the key organelle for controlling calcium signalling and protein folding. Cells experience ER stress when the ER is disrupted because unfolded proteins build up in the ER lumen and Ca2+ is discharged from the ER to the cytoplasm (Kleizen & Braakman, 2004).

Thapsigargin is naturally occurring sesquiterpene lactone derived from the plant Thapsia garganica. It is known as a cytotoxin because of its potent biological activity, specifically, its ability to disrupts the intracellular homeostasis (Askari et al., 2022). By blocking the sarco/endoplasmic reticulum Ca2+-ATPase (SERCA) pump, thapsigargin reduces the amount of calcium stored in the ER. A series of cellular reactions, including as ER stress, unfolded protein response (UPR) activation, and modification of calcium-dependent signalling pathways, are brought on by this disruption (Lindner et al., 2020). The SERCA pump is crucial for the regulation of calcium homeostasis which is essential for cell survival and cell signalling (Sehgal et al., 2017). The SERCA pump is a P-type ATPase that maintains low cytosolic Ca2+ concentration by pumping Ca2+ ions from the cytoplasm into the ER of non-muscle cells and into the sarcoplasmic reticulum (SR) lumen of skeletal and cardiac muscle cells using the energy of ATP hydrolysis (Aguayo-Ortiz & Espinoza-Fonseca, 2020).

The depletion of calcium stores and increases in cytosolic calcium by the inhibition of SERCA leads to the disruption in protein folding’s and lead to accumulation of misfolded proteins. Which activates the UPR, a stress response mechanism but the prolonged exposure to the stress leads to apoptosis. In this chapter, thapsigargin has been used to

trigger ER stress through the UPR, calcium store depletion, and SERCA pump inhibition. This model mimics neurodegenerative stress conditions, allowing evaluation of apelin-13's protective role in mitigating ER stress-induced neuronal damage in SH-SY5Y cells.

Apelin is known for its biological functions in several tissues including controlling blood pressure, angiogenesis, food uptake and apoptosis (Ishida et al., 2004). In 1998, apelin was first discovered as an endogenous ligand of the orphan G-protein-coupled receptor (GPCR) APJ in bovine gastric extracts (Wen et al., 2023). The APJ receptor and Apelin are ubiquitously expressed throughout the body. Apelin is an adipokine and it's secreted by the white adipose tissues (WAT), and have number of subtypes, but apelin-13 is considered the most bioactive (O'Harte et al., 2017). Study by Parthsarathy et al, illustrated that modified apelin-13 analogue, (Lys^{8}Glupal)apelin-13 amide have enhanced stability and bioavailability has enhanced resistance to the enzymatic degradation, making it more effective for in-vivo applications (2017). Studies illustrated that apelin-13, counteracts ER stress to have a neuroprotective effect (Jeong et al., 2014).

Apelin-13 is known to protect the cells in ER stress, and it has been shown to reduce the ER stress-related inflammation and oxidative stress by activating the pathways like AMP-activated protein kinase (AMPK) (Xu et al., 2019). Previous study showed that by promoting cell survival mechanisms and lowering the buildup of misfolded proteins, apelin-13 helps mitigate the negative effects of prolonged ER stress, including apoptosis (Jeong et al., 2014). This makes it potentially beneficial for conditions in which ER stress plays a significant role, such as neurodegenerative disorders.

This chapter investigates the role of stable apelin-13 in modulating cellular stress responses, such as apoptosis and autophagy, in cells experiencing thapsigargin-induced ER stress. This study investigates the molecular pathways, including AMPK and UPR, that underlie the protective role of apelin-13, aiming to elucidate its potential therapeutic applications in neurodegenerative diseases associated with ER stress.

Objectives:

1. Evaluate the effect of apelin-13 amide and (Lys^{8}GluPAL)apelin-13 amide on cell survival, proliferation and differentiation under thapsigargin-induced stress in SH-SY5Y cell.
2. Investigate the impact of apelin-13 on mitochondrial function and oxidative stress to elucidate its protective effects against cellular damage.
3. Evaluate the effect of apelin-13 on thapsigargin-induced endoplasmic reticulum stress by assessing key markers, including IRE1, Bcl-2, Bax, and ATG proteins.

6.2: Results

6.2.1 Effect of novel stable apelin-13 analogue on cell viability under thapsigargin-induces stress in SH-SY5Y cells in-vitro.

To evaluate the effects of the peptides on cell viability, SH-SY5Y cells were treated with or without 10 nM thapsigargin and measured for metabolic active cells post incubation at various time points. Ours results showed no significant changes in cells treated with Apelin-13 amide and (Lys^{8}GluPAL)apelin-13 amide alone at all different timepoints compared to untreated control (Figure 6.1A, B, C, $p>0.05$). The cell viability was significantly reduced at 2 hours by 38% (Figure 6.1A, $p<0.0001$), at 4 hours by 40% (Figure 6.1B, $p<0.0001$) and at 24 hours by 48% (Figure 6.1C, $p<0.0001$) when treated with thapsigargin alone compared to untreated control.

When the cells were co currently treated with 10 nM thapsigargin and Apelin-13 amide or (Lys^{8}GluPAL)apelin-13 amide the cell viability at 2 hours improved by 25% (Figure 6.1A,$p< 0.01$) and 29% (Figure 6.1A,$P<0.01$) respectively, compared to thapsigargin alone. The cell viability was significantly improved at 4 hours when treated 10 nM thapsigargin with apelin 13 amide (34%, Figure 6.1B, $p<0.05$) and (Lys^{8}GluPAL)apelin-13 amide (35%, Figure 6.1B, $p<0.05$), compared to thapsigargin alone. However, the combined treated cells at 24 hours did not show any significant change compared to thapsigargin alone (Figure 6.1C, $p>0.05$).

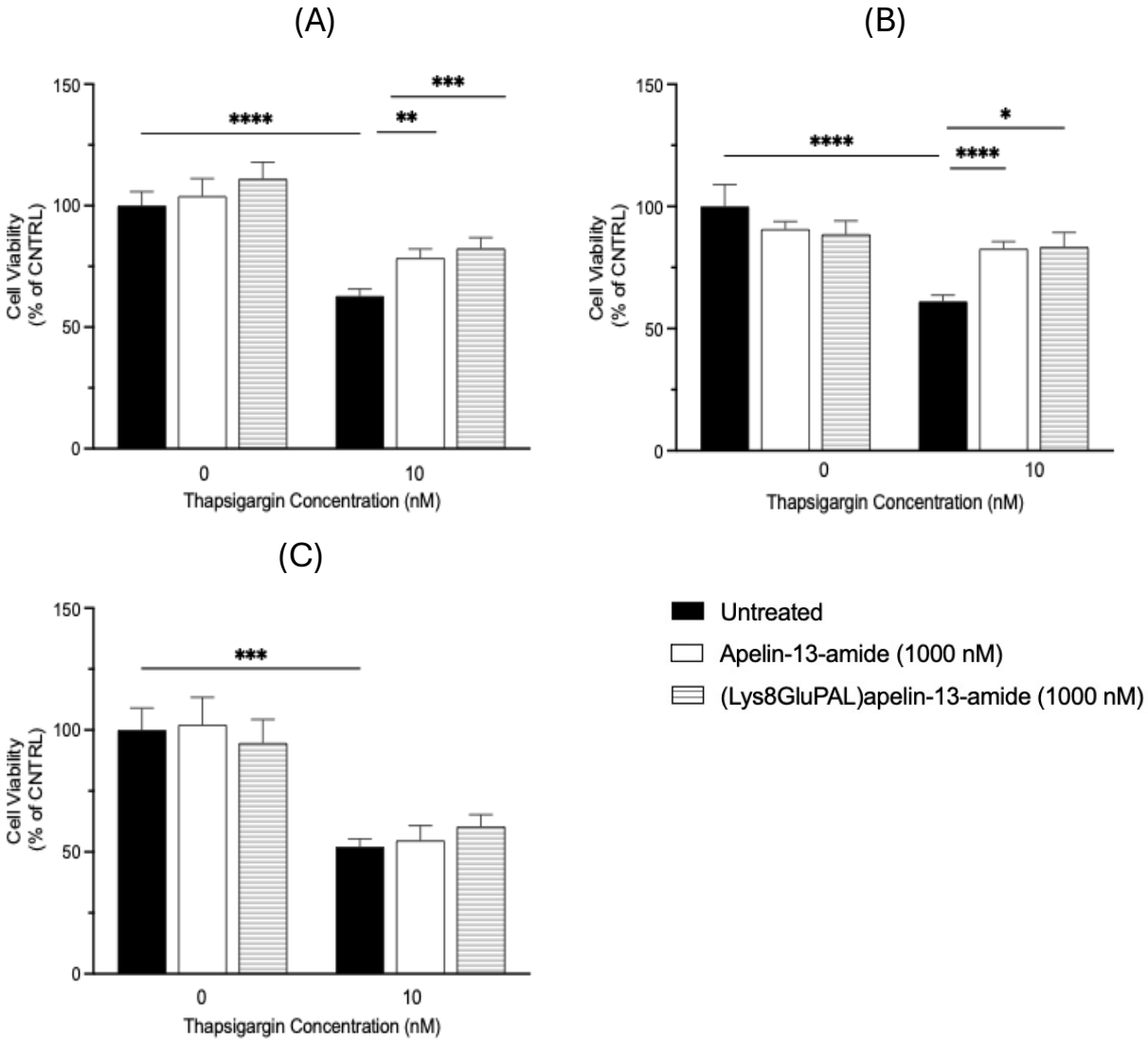

Figure 6.1: Effect of novel stable apelin-13 analogue on cell viability under thapsigargin-induces stress in SH-SY5Y cells in-vitro. Time dependant effect of apelin-13 analogues on SH-SY5Y cells *in-vitro* on cell viability with or without 10 nM Thapsigargin. Cell viability was measured by MTT colorimetric assay based on the reduction of MTT to formazan. Cells were treated at different timepoints (A) 2 hours, (B) 4 hour and (C) 24 hours. Data represents mean ±SEM (one-way ANOVA, n=3 where *p<0.05, **p<0.01,***p<0.001, and ****p<0.0001) compared to control.

6.2.2 Effect of apelin-13 analogues against dose dependant deterioration of cell viability by thapsigargin in SH-SY5Y cells.

To look at the dose dependant impact of thapsigargin with or without the Apelin-13 amide and (Lys^{8}GluPAL) apelin-13 amide on the viability of SH-SY5Y cells in-vitro, measured the levels of ATP released from the viable cells. The results shows that apelin-13 amide treatment significantly increased cell viability by 16% (Figure 6.2, $p<0.001$) but (Lys^{8}GluPAL)apelin-13 amide had no significant effect (Figure 6.2, $p>0.05$), compared to untreated control. However, the cell viability was significantly reduced by 14% (Figure 6.2, $p<0.01$) when treated with 10 nM thapsigargin, and by 35% (Figure 6.2, $p<0.0001$) when treated with 100 nM thapsigargin, compared to untreated control.

Co-treatments of cells with Apelin-13 amide with 10 nM thapsigargin restored cell viability by 5% (Figure 6.2, $p>0.05$) and for 100 nM by 36% (Figure 6.2, $p<0.0001$), compared to the respective thapsigargin alone. Compared to respective thapsigargin treatments alone, the combined (Lys^{8}GluPAL)apelin-13 amide treatments with 10 nM and 100 nM improved cell viability by 4% (Figure 6.2, $p>0.05$) and 35% (Figure 6.2, $p<0.0001$) respectively.

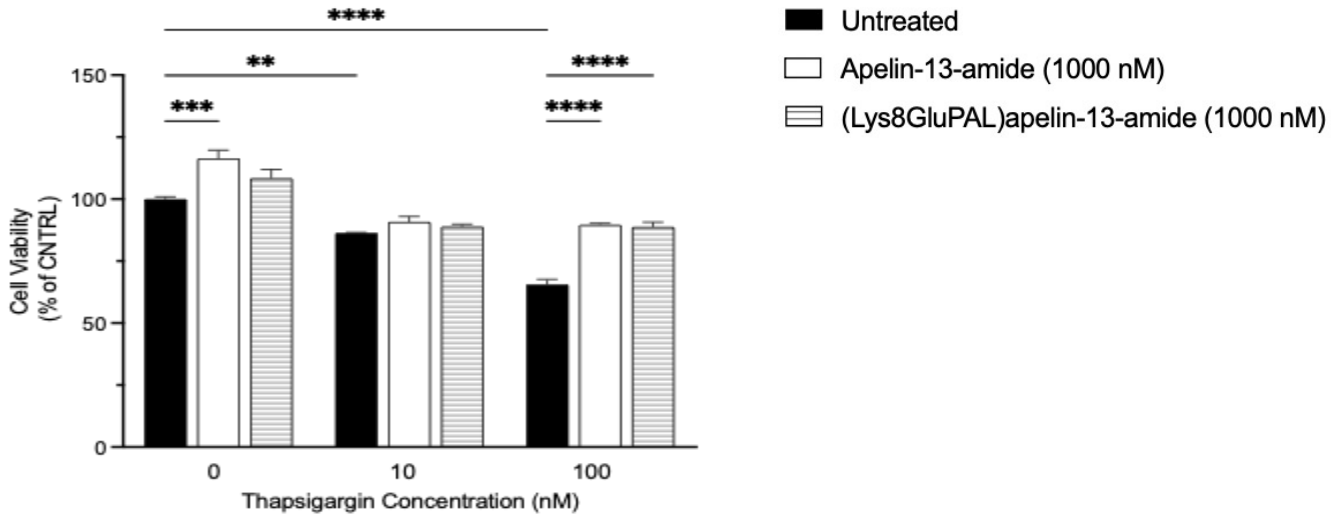

Figure 6.2: Effect of apelin-13 analogues against dose dependant deterioration of cell viability by thapsigargin in SH-SY5Y cells. The protective effect of apelin-13 analogues on cell viability as dose dependent stress-induced by thapsigargin in SH-SY5Y cells *in-vitro*. The cells were treated for 6 hours with

or without the apelin-13 amide and (Lys^{8}GluPAL)apelin-13 amide and the Celltiter-Glo reagent was used to measure the viability based on ATP present in the viable cells. Values represents mean ±SEM for n=3 where **p<0.01, ***p<0.001, ****p<0.0001.

6.2.3: The effect of apelin-13 analogues on cell proliferation in SH-SY5Y cells.

The incorporation of BrdU into newly synthesized DNA was visualised by immunofluorescence to look the impact of apelin-13 analogues on the cell proliferation. The representative immunofluorescent images of BrdU incorporation assay under Olympus Inverted microscope at 20X magnification are presented in Figure 6.3 A. The results illustrated that both peptides were able to improve the cell proliferation slightly but was non-significant (Figure 6.3B, p>0.05) and 10 nM thapsigargin reduced the cell proliferation by 55 % (Figure 6.3B, p<0.01), compared to untreated control. When the cells were co-currently treated with thapsigargin and Apelin-13 amide the cell proliferation improved non significantly by 30% (Figure 6.3B, p>0.05), and 8% (Figure 6.3B, p>0.05) for (Lys^{8}GluPAL)apelin-13-amide, compared to thapsigargin alone.

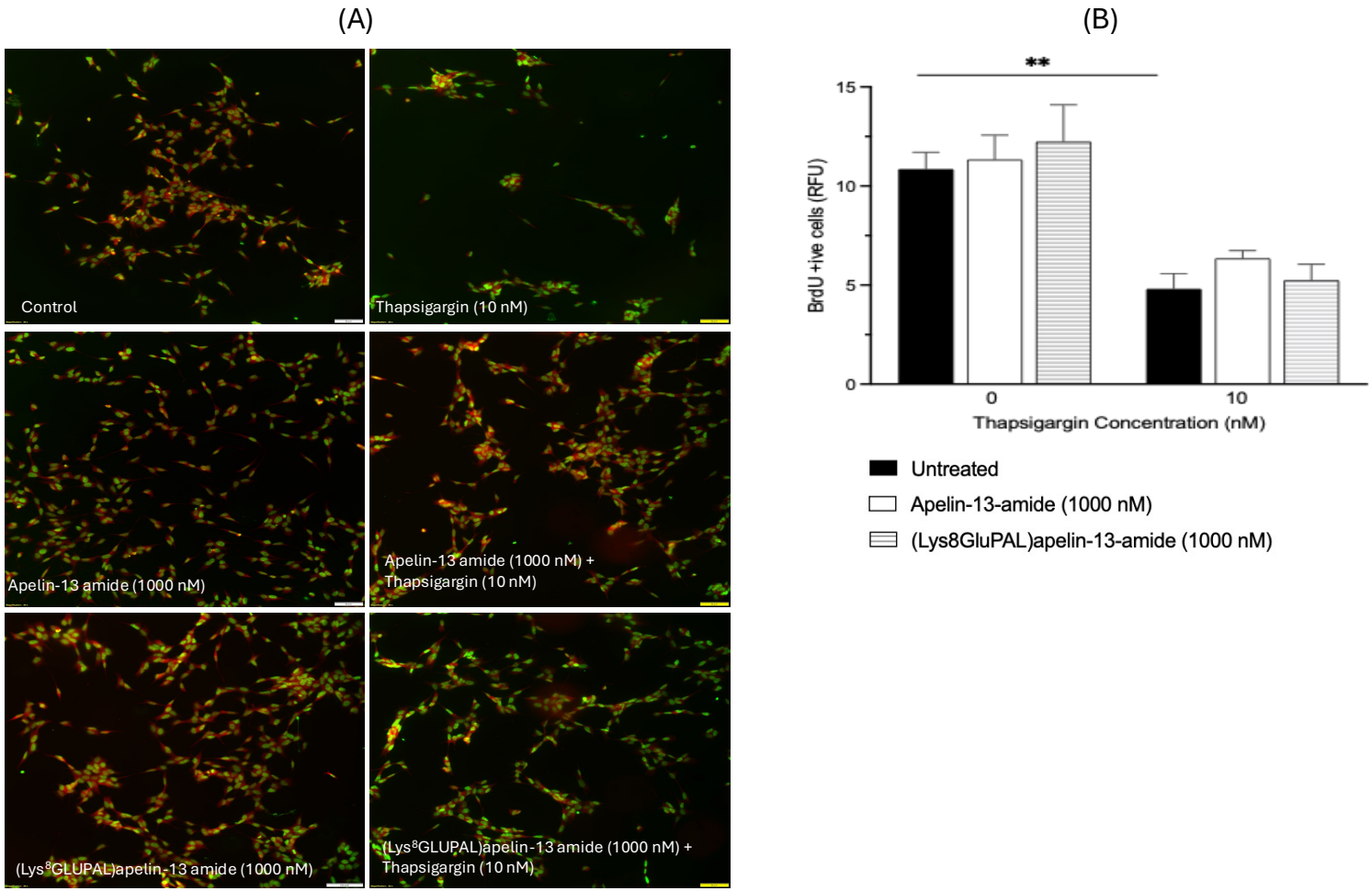

Figure 6.3: The effect of apelin-13 analogues on cell proliferation in SH-SY5Y cells. Images from BrdU immunofluorescence staining were captured using the Olympus inverted microscope and analysed (A) Representative images of SH-SY5Y cells stained with BrdU as pseudo green colour and DAPI as red colour captured at 20X magnification. (B) Quantification of BrdU positive cells as a measure of cell proliferation was analysed using Image J software and expressed in relative fluorescence units (RFU). Values represent mean ±SEM for n=3 where $^{**}p<0.01$.

6.2.4: Effect of apelin-13 amide on neurite outgrowth in SH-SY5Y cells.

The neuronal differentiation was observed in SH-SY5Y cells in-vitro, when the cells were differentiated by retinoic acid (RA) for 72 hours before adding treatments for 24 hours. The changes in morphology of the cells were observed under upright light microscope at 20X magnification and represented in Figure 6.4 A. Coomassie brilliant blue stain was used to look at the neurite extensions and were counted manually by observing neurites double the size of the cell body. The data showed that compared to the untreated control, Apelin-13 amide and (Lys^8GluPAL)apelin-13 amide showed non-significant rise in the neurite extensions (Figure 6.4 B, $p>0.05$), but 10 nM thapsigargin reduced the neurite outgrowth by 60% (Figure 6.4B, $p<0.0001$). When the cells were co-treated with 10 nM thapsigargin and apelin-13 amide the neurite growth improved by 50% (Figure 6.4B, $p<0.01$) and 51% (Figure 6.4B, $p<0.05$) by (Lys^8GluPAL)apelin-13 amide, compared to thapsigargin alone.

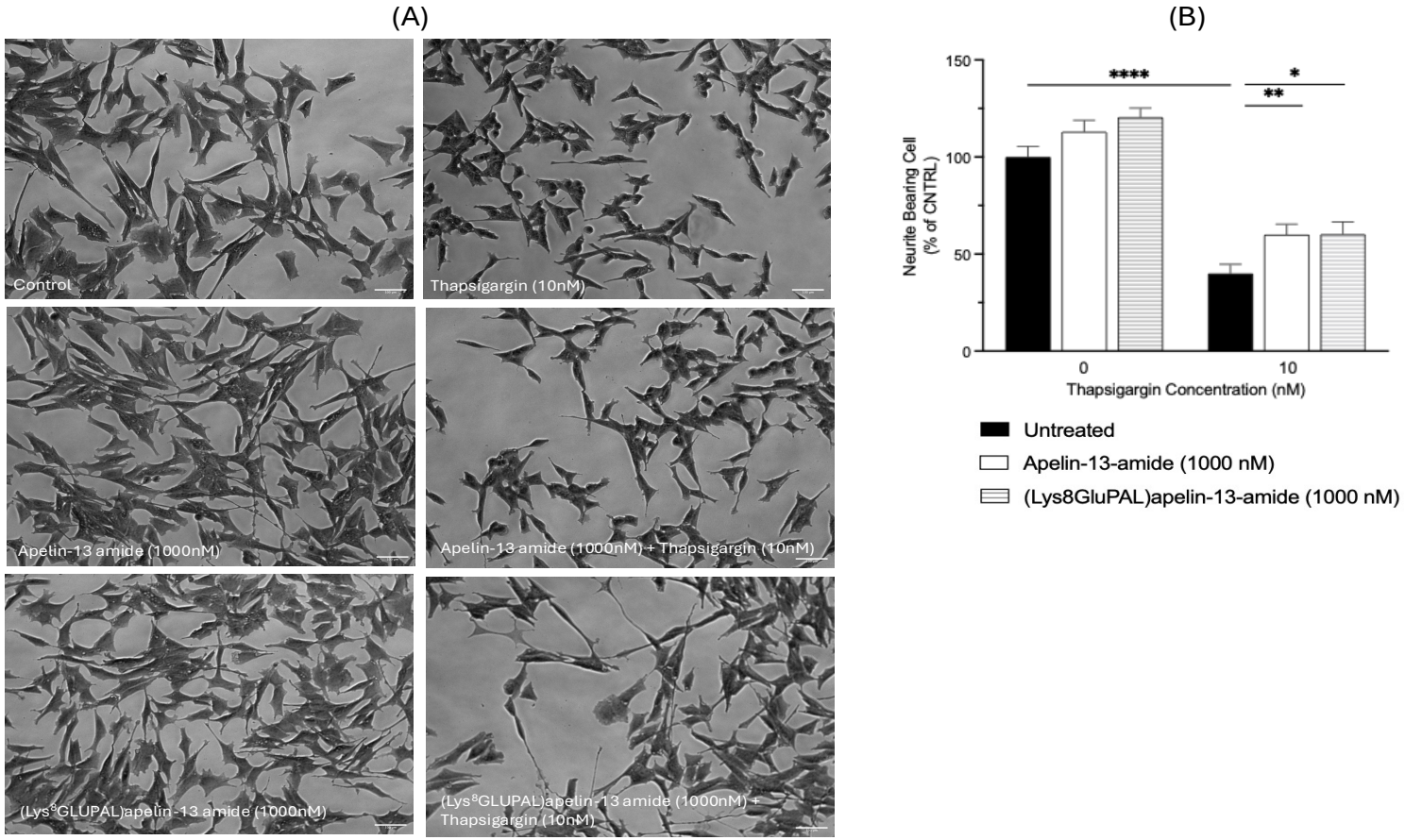

Figure 6.4: Effect of apelin-13 amide on neurite outgrowth in SH-SY5Y cells. Neurite outgrowth was assessed in SH-SY5Y cells in-vitro following treatments with apelin-13 amide and (Lys^{8}GluPAL)apelin-13 amide when the stress was induced by 10 nM thapsigargin. the cells were treated with Retinoic acid (RA) (10 μM) for 24 hours prior to treatments. (A) representative images of Coomassie brilliant blue stained cells and (B) graph of neurite bearing cells analysed by GraphPad PRISM. The cells were treated for 48 hours before staining and imaged under the light microscope at 20X magnification. Values represent mean ±SEM for n=3 where *p<0.05, **p<0.01, and ****p<0.0001.

6.2.5: Effect of stable apelin-13 analogues on neuronal differentiation on SH-SY5Y cells under stress induced by thapsigargin.

To measure the neuronal integrity and differentiation we used MAP2 (Microtubule-Associated protein 2) a marker for differentiation in SH-SY5Y cells in-vitro. Figure 6.5 A shows representative images of MAP2 staining in SH-SY5Y cells under light microscope The results show that the treatment of apelin-13 amide and (Lys^{8}GluPAL) apelin-13 amide compared to the untreated control, increased neuronal differentiation by 17% (Figure 6.5B, $p>0.05$) and 23% (Figure 6.5B, $p>0.05$) respectively. However, thapsigargin reduced the differentiation by 65% (Figure 6.5B, $p<0.0001$), compared to untreated control. The co-treatments of apelin-13 amide with 10 nM thapsigargin restored the differentiation by 57% (Figure 6.5B, $p<0.0001$) and 58% (Figure 6.5B, $p<0.0001$) for (Lys^{8}GluPAL) apelin-13 amide, compared to thapsigargin alone.

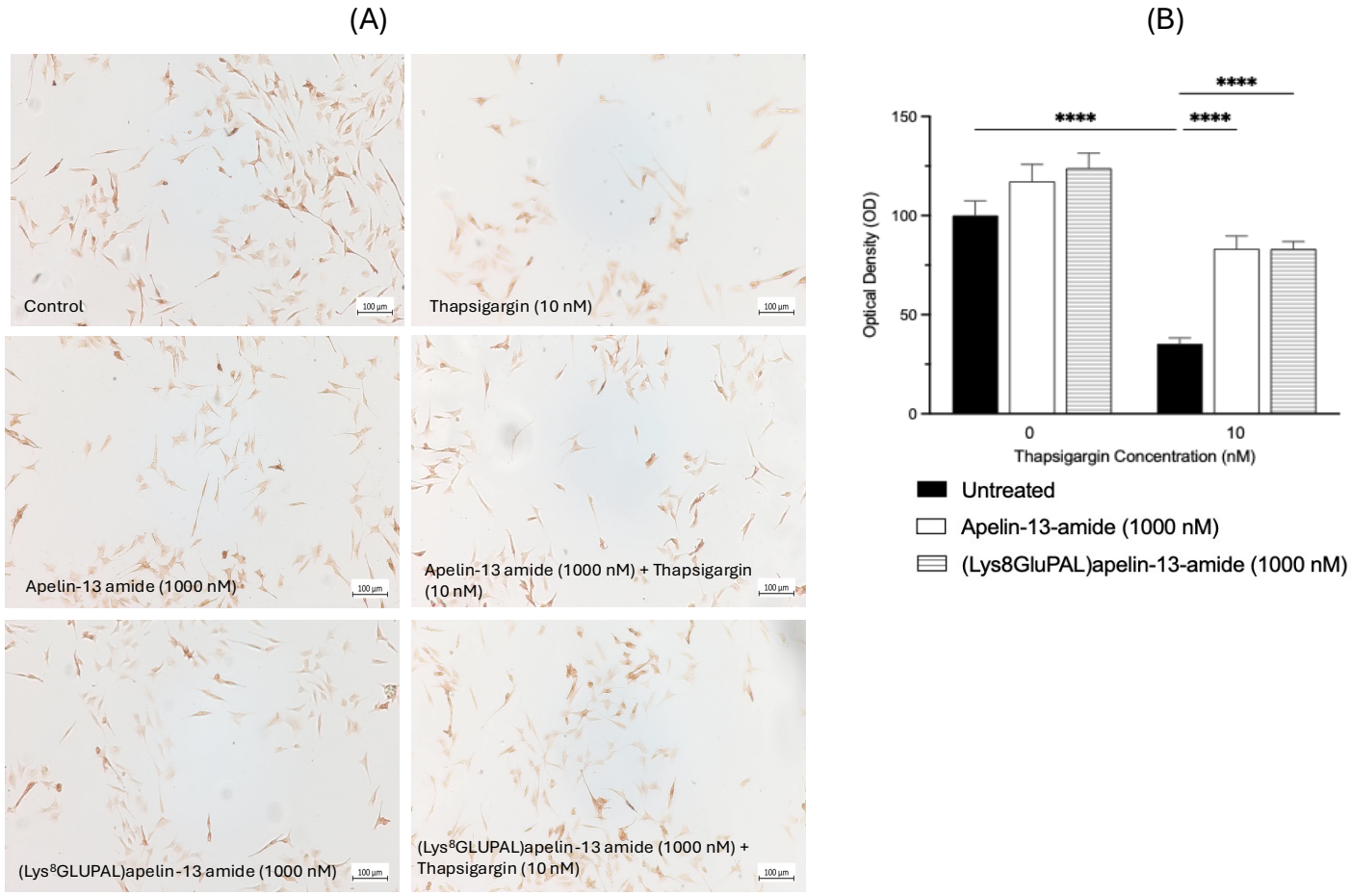

Figure 6.5: Effect of stable apelin-13 analogues on neuronal differentiation on SH-SY5Y cells under stress induced by thapsigargin. MAP2 expression, indicative of neuronal differentiation, has been measured in SH-SY5Y cells following treatment with apelin-13 and (Lys^{8}GluPAL)apelin-13 amide for 24 hours with and without 10 nM thapsigargin. The cells were differentiated with retinoic acid (10μM) prior to treatments. (A) illustrative Immunofluorescence images of MAP2-positive cells, signifying improved neuronal differentiation in the treated groups and (B) is the quantification of MAP2 expression involved the analysis of optical intensity. Values represent mean ±SEM for n=3 where ****p<0.0001.

6.2.6: Effect of stable apelin-13 analogues on cell toxicity induced by thapsigargin at different time-points.

The cell toxicity was induced by 10 nM thapsigargin and the effect of apelin-13 analogues on the cell toxicity was measured using the CyQUANT ™ LDH Cytotoxicity Assay in time-dependent manner. Both apelin-13 amide and (Lys^{8}GluPAL)apelin-13-amide showed no changes to cell toxicity compared to untreated control at 2 and 4 hours ($p>0.05$, Figure 6.6 A&B). After 24 hours (Lys^{8}GluPAL)apelin-13-amide reduced cell toxicity by 15% (Figure 6.6C, $p<0.05$), compared to untreated control. However, the cell toxicity was significantly increased when treated with 10 nM thapsigargin by 26% (Figure 6.6A, $p<0.05$) at 2 hours, by 11 % (Figure 6.6B, $p<0.05$) at 4 hours and no change (Figure 6.6C, $p>0.05$) at 24 hours, compared to untreated control.

Apelin-13 analogues reduced the thapsigargin-induced cell toxicity by 12% (Figure 6.6A, $p>0.05$) at 2 hours. At 4 hours the apelin-13 amide reduced cell toxicity by 36% (Figure 6.6B, $p<0.001$) and 30% (Figure 6.6B, $p<0.001$) by (Lys^{8}GluPAL)apelin-13-amide, compared to the 10 nM thapsigargin. The apelin-13 amide treatment led to 17% (Figure 6.6C, $p>0.05$) reduction in cell toxicity and 6% (Figure 6.6C, $p>0.05$) by (Lys^{8}GluPAL)apelin-13-amide, at 24 hours compared to thapsigargin alone.

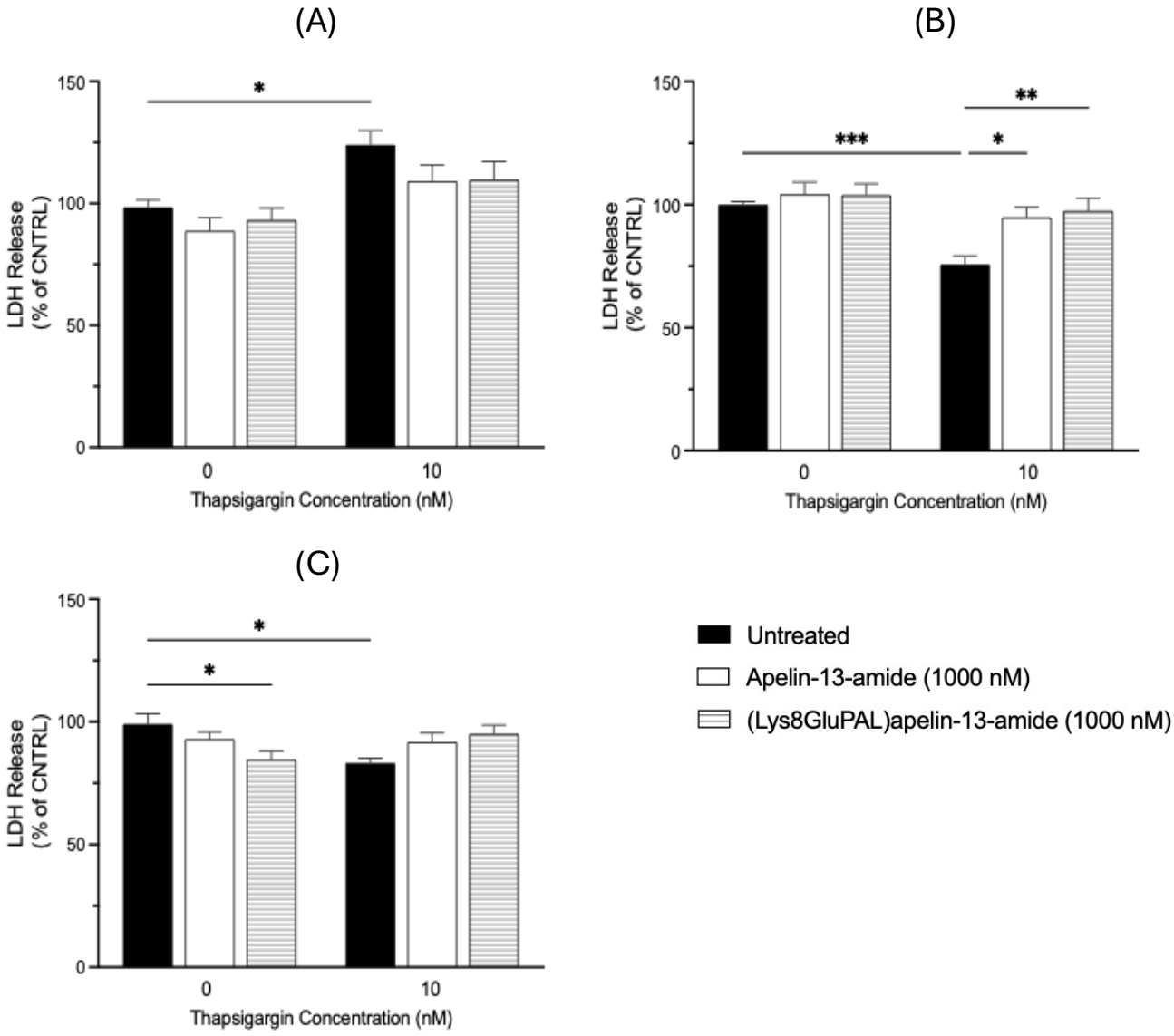

Figure 6.6: Effect of stable apelin-13 analogues on cell toxicity induced by thapsigargin at different time-points. Time dependant effect of apelin-13 amide and (Lys^{8}GluPAL)apelin-13-amide on the cell toxicity induced by 10 nM thapsigargin in SH-SY5Y cells *in-vitro*. The cells were treated for different timepoints (A) 2 hours, (B) 4 hours and (C) 24 hours. The cell toxicity was measured by using LDH assay to measure the release of the LDH enzyme from damaged cells. Values represents mean ±SEM (one-way ANOVA, n=3 where *p<0.05, **p<0.01, and ***p<0.001.

6.2.7: Effect of apelin-13 analogues on cell toxicity induced by different concentration of Thapsigargin in SH-SY5Y cells.

To further confirm the real time cell toxicity, we employed CellTox green cytotoxicity assay, which measures the fluorescence from DNA released from the damaged cells. The results showed that apelin-13 amide and (Lys^{8}GluPAL)apelin-13 amide reduced the cell toxicity in SH-SY5Y cells by 20% (Figure 6.7, $p<0.05$) and 22% (Figure 6.7, $p<0.01$) respectively, compared to untreated control. However, the cell toxicity was increased in cells by 10% (Figure 6.7, $p<0.01$) when treated with 10 nM thapsigargin and 30% (Figure 6.7, $p<0.001$) with 100 nM thapsigargin, compared to untreated control. When looking at the protective effect of apelin-13 analogues against the thapsigargin-induced stress, it shows that at 10 nM concentration Apelin-13 amide did not make any change and (Lys^{8}GluPAL) apelin-13 amide reduced slightly by 10% (Figure 6.7, $p>0.05$), compared to 10 nM thapsigargin alone. At higher concentration of thapsigargin (100 nM), (Lys^{8}GluPAL) apelin-13 amide was able to mitigate the cell toxicity by 14% (Figure 6.7, $p<0.05$) and apelin-13 amide reduced non significantly by 12% (Figure 6.7, $p>0.05$), compared to 100 nM thapsigargin alone.

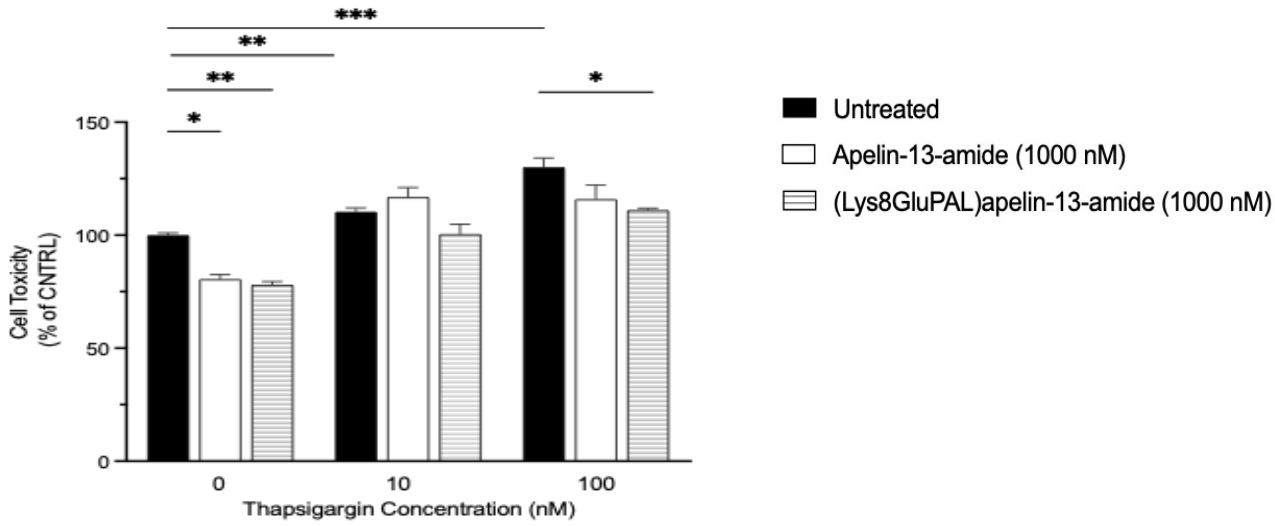

Figure 6.7: Effect of apelin-13 analogues on cell toxicity induced by different concentration of Thapsigargin in SH-SY5Y cells. The dose-dependent impact of apelin-13 analogues on cell toxicity was evaluated in SH-SY5Y cells *in-vitro*, when treated with and without 10 nM and 100 nM thapsigargin for 6 hours. The Cell tox green assay is used to measure the real time cytotoxicity by binding to the DNA released from the compromised membranes. Values represents mean ±SEM for n=3 where *p<0.05, **p<0.01, and ***p<0.001.

6.2.8: Effect of apelin-13 analogues on oxidative stress and redox balance in SH-SY5Y cells.

The ROS assay was used to measure the ROS levels, which are indicative of oxidative stress in cells and GSH/GSSG is used to assess the balance between the reduced glutathione and oxidised glutathione, a key indicator of redox state of the cell. The cells were treated with two different concentrations of thapsigargin (10 nM and 100 nM) to look at the ROS and 10 nM for GSH/GSSG. One-way ANOVA results showed no significant change in ROS levels when cells treated with apelin-13 analogues at both concentration of thapsigargin (Figure 6.8 A and B, p>0.05), compared to untreated control. However, the ROS levels were s significantly increased by 10 nM thapsigargin (Figure 6.8A, 36%

increase, $p<0.01$) 100 nM thapsigargin (Figure 6.8B, 128% increase, $p<0.0001$) compared to untreated control. Apelin-13 amide was able to reduce this increase by 24% (Figure 6.8A, $p<0.05$) and (Lys^{8}GluPAL)apelin-13 amide by 27% (Figure 6.8A, $p<0.01$) when treated combined with 10 nM thapsigargin. for. Similarly, when treated in combination with 100 nM thapsigargin, apelin-13 amide reduced ROS levels by 30% (Figure 6.8B, $p<0.001$) and (Lys^{8}GluPAL)apelin-13 amide by 23% (Figure 6.8B, $p<0.001$) for

The data suggest that GSH/GSSG ratio had no significant change when treated with apelin-13 analogues alone (Figure 6.8C, $p>0.05$), however, the ratio was significantly reduced by 64% (Figure 6.8C, $p<0.001$) when treated with 10 nM thapsigargin. Co-treatments of 10 nM thapsigargin showed non-significant rise in GSH/GSSG ratio with Apelin-13 amide (Figure 6.8C, 7% increase, $p>0.05$) and (Lys^{8}GluPAL)apelin-13 amide, (Figure 6.8C, 10% increase, $p>0.05$).

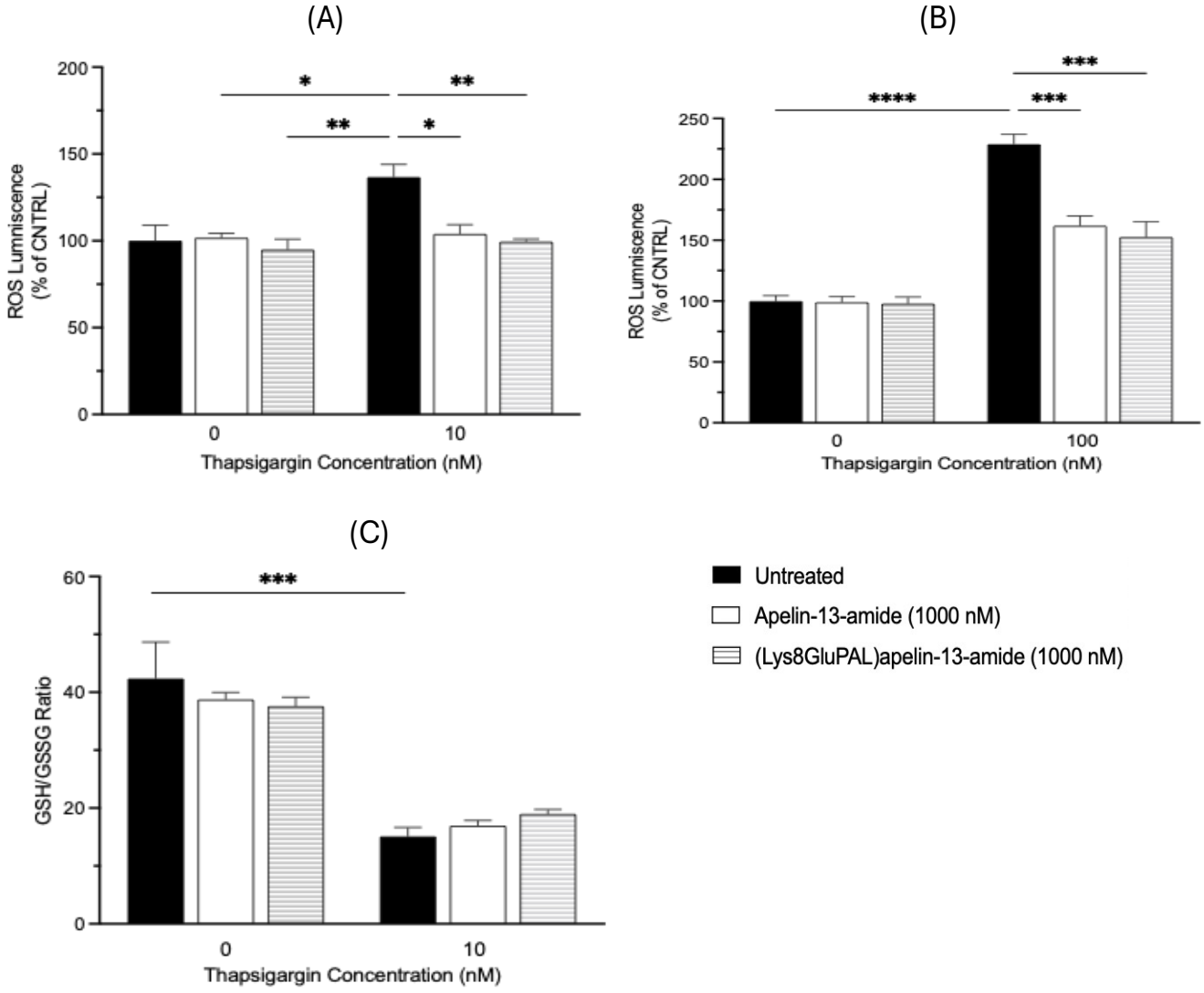

Figure 6.8: Effect of apelin-13 analogues on oxidative stress and redox balance in SH-SY5Y cells. Reactive oxygen species (ROS) levels and oxidative stress balance (GSH/GSSG ratio) were measured in SH-SY5Y cells *in-vitro*, treated with increasing concentrations of thapsigargin (10 nM and 100 nM), with and without apelin-13 amide and (Lys^{8}GluPAL)apelin-13 amide. (A) is ROS measurement at 10 nM thapsigargin treatment, (B) ROS measurement at 100 nM thapsigargin treatment and (C) ratio of reduced and total glutathione. Values represent mean ±SEM for n=3 where *p<0.05,**p<0.01, ***p<0.001, and ****p<0.0001.

6.2.9: Effect of apelin-13 analogues on mitochondrial membrane potential under thapsigargin-induced stress.

The mitochondrial membrane potential is a key indicator of the mitochondrial health and cellular stress, especially in apoptosis or diseases. To measure the mitochondrial membrane potential the cells were seeded and treated with apelin-13 analogues and thapsigargin for 24 hours. The cells were then exposed to the JC-1 dye which enters the mitochondria and forms aggregates in healthy cells emitting red fluorescence. In damaged cells it remains in monomers and emit green light. The red/green ratio indicates mitochondrial health. Figure 6.9 A shows representative images of JC-1 stain under fluorescent microscope (20X magnification)

Our results show improved mitochondrial membrane potential when treated with apelin-13 amide by 82% (Figure 6.9B, $p<0.05$), and (Lys^8GluPAL)apelin-13-amide by 60% (Figure 6.9B, $p>0.05$), compared to untreated control. However, 10 nM thapsigargin reduced the membrane potential by 94% (Figure 6.9B, $p<0.01$), compared to untreated control. Compared to the thapsigargin alone, the mitochondrial membrane potential was restored significantly by combined treatment of apelin-13 amide (563%, Figure 6.9B, $p<0.0001$) and 10 nM thapsigargin and (Lys^8GluPAL)apelin-13-amide and 10 nM thapsigargin (1222%, Figure 6.9B, $p<0.0001$).

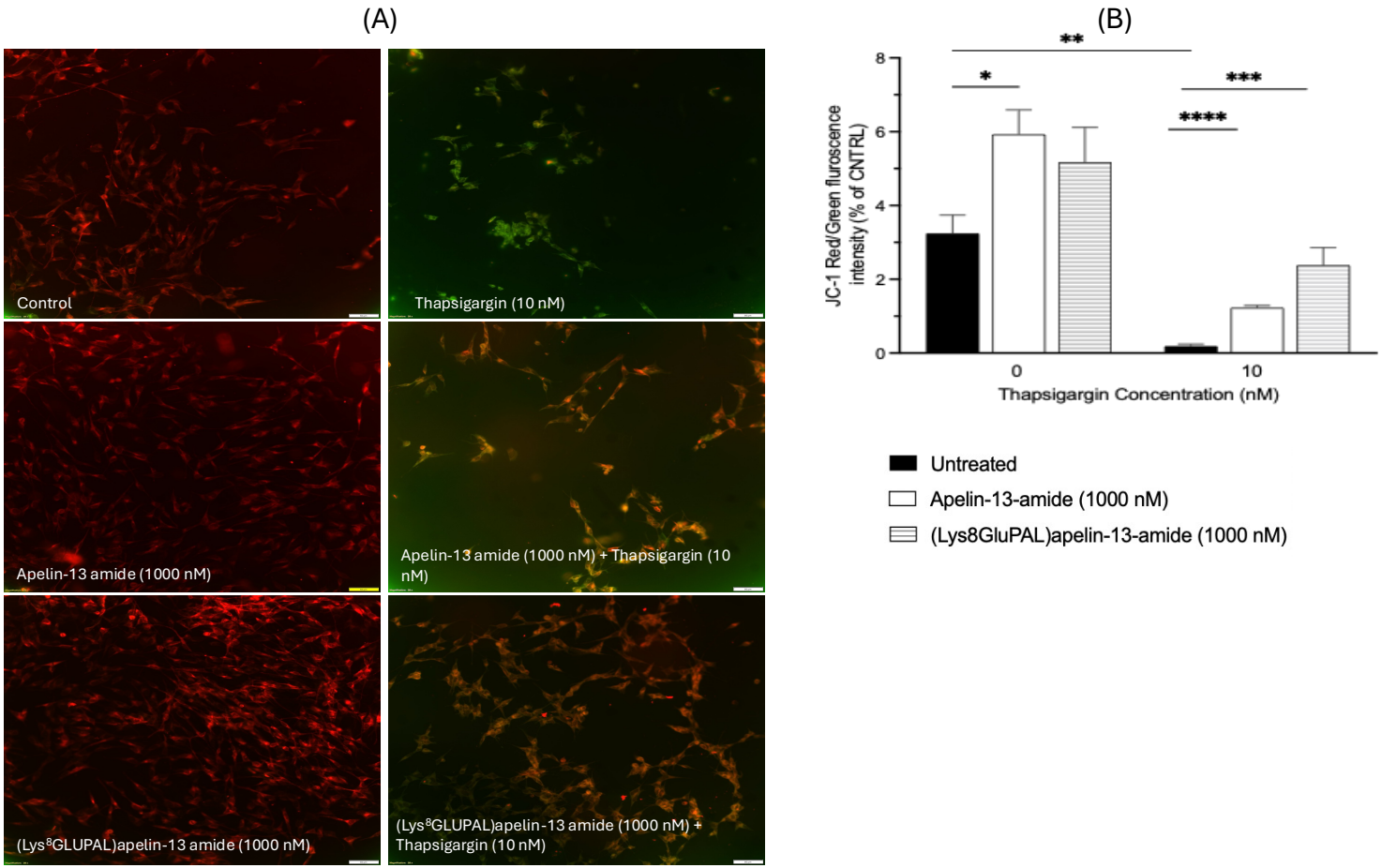

Figure 6.9: Effect of apelin-13 analogues on mitochondrial under thapsigargin-induced stress.

The JC-1 dye assay is used to measure the Mitochondrial membrane potential in SH-SY5Y cells *in-vitro*. The cells were treated with apelin-13 analogues with and without 10 nM thapsigargin 24 hours and then images under fluorescent microscope at 20X magnification. (A) representative images of the stained cell with JC-1 dye and (B) is the graph of the Red/Green florescent ratio. Values represent mean ±SEM for n=3 where *p<0.05,**p<0.01, ***p<0.001, and ****p<0.0001.

6.2.10: Effect of apelin-13 analogues on apoptosis induced by thapsigargin in SH-SY5Y cells.

To evaluate the apoptosis levels induced by thapsigargin in SH-SY5Y cells in-vitro we used caspase-Glo 3/7 detection kit. Both apelin-13 amide and (Lys^{8}GluPAL)apelin-13 amide significantly reduced caspase 3/7 activity by 24% (Figure 6.10A, $p<0.05$) and 30% (Figure 6.10A, $p<0.05$) respectively, compared to untreated control. However, the caspase 3/7 activity was significantly increased by thapsigargin treatments (Figure 6.10A, 23% increase, $p<0.05$) by 10 nM and 1368% (Figure 6.10B, $p<0.0001$) by 100 nM thapsigargin, compared to untreated control.

Compared to 10 nM thapsigargin, caspase 3/7 activity was reduced non significantly by 17% (Figure 6.10A, $p>0.05$) for apelin-13 amide and significantly by 19% (Figure 6.10A, $p<0.05$) for (Lys^{8}GluPAL)apelin-13 amide. For 100 nM thapsigargin treatments with apelin-13 amide the caspase 3/7 activity was reduced significantly by 46% (Figure 6.10B, $p<0.0001$) and by 53% (Figure 6.10B, $p<0.0001$) for (Lys^{8}GluPAL)apelin-13 amide, compared to 100 nM thapsigargin alone.

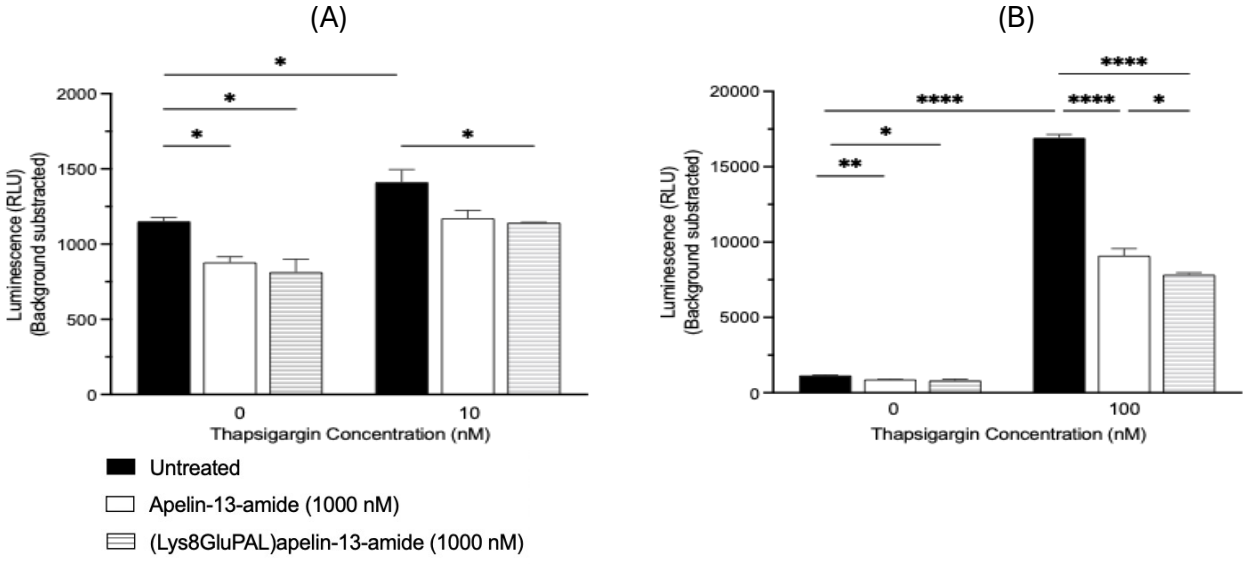

Figure 6.10: Effect of apelin-13 analogues on apoptosis induced by thapsigargin in SH-SY5Y cells. Caspase 3/7 activity was measured in the SH-SY5Y cells *in-vitro* when cells treated with apelin-13 amide

and (Lys8GluPAL)apelin-13 amide alongside two concertation of thapsigargin (10 nM and 100 nM). (A) is 10 nM thapsigargin and (B) is 100 nM thapsigargin. Values represents mean ±SEM for n=3 where *p<0.05, **p<0.01, and ****p<0.0001.

6.2.11: Effect of apelin-13 analogues ATF-6 expression to regulate UPR in SH-SY5Y cells.

The cells were seeded and treated for 24 hours to investigate the effect apelin-13 analogues impact on thapsigargin-induced translocation of the ATF6 during ER stress. The cells were probed with anti-ATF6 antibody and figure 6.11 A shows representative images of ATF6 immunolabeling in SH-SY5Y cells. The results showed that apelin-13 amide and (Lys^{8}GluPAL)apelin-13 amide had no significant change in ATF6 expression when treated alone. Cells when exposed to 10 nM thapsigargin, showed an increase in ATF6 expression (17% increase; Figure 6.11B, $p>0.05$) which was reduced when they were treated with apelin-13 amide (33% reduction, Figure 6.11B, $p<0.01$), or (Lys^{8}GluPAL)apelin-13 amide (41% reduction Figure 6.11B, $p<0.001$).

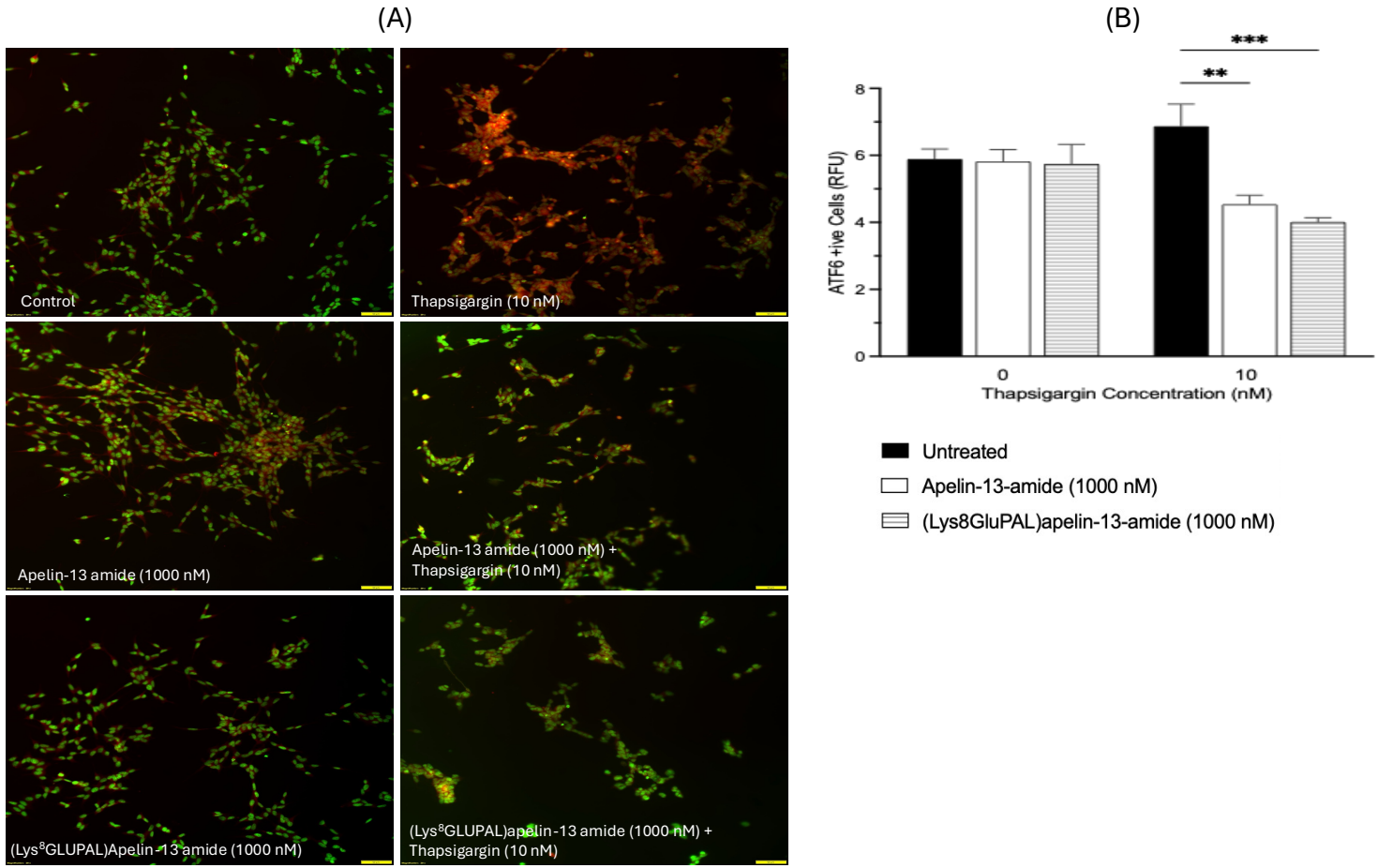

Figure 6.11: Effect of apelin-13 analogues on ATF-6) expression to regulate UPR in SH-SY5Y cells. Apelin-13 amide and (Lys8GluPAL)apelin-13 amide resolves the UPR in the SH-SY5Y cells *in-vitro*. After 24 hours seeding the cells were serum starved and treated with the 10 nM thapsigargin with and without the apelin-13 analogues for 24 hours. The cells were then labelled with ATF6 and imaged under the fluorescent microscope at 20X magnification and scale bar of 50 μM. (A) representative images of the ATF6 immunolabelling and (B) is the graph measuring the ATF6 RFU by image J. Values represents mean ±SEM for n=3 where **p<0.01, and ***p<0.001.

6.2.12: Effect of apelin-13 analogues against thapsigargin-induced oxidative stress on NRF-2 expression in SH-SY5Y cells.

NRF-2 is the key transcription factor involved in cellular defence against oxidative stress. Figure 6.12A shows representative images of NRF-2 immunolabeling under fluorescent microscope (20X magnification). The data from the immunocytochemistry (ICC) shows that apelin-13 amide and (Lys^{8}GluPAL)apelin-13 amide had no impact (Figure 6.12B, $p>0.05$) and 10 nM thapsigargin increased the nuclear NRF-2 expression by double (100%, Figure 6.12B, $p<0.0001$), compared to untreated control. Co-treatment of thapsigargin with apelin-13 amide (30% reduction, Figure 6.12B, $p<0.001$) and (Lys^{8}GluPAL)apelin-13 amide (18% reduction; Figure 6.12B, $p<0.05$) were able to reduce NRF-2 expression, compared to thapsigargin alone.

The western blot analysis showed that apelin-13 analogues alone reduce nuclear NRF-2 expression by 6% (Figure 6.12C, $p>0.05$) and 10 nM thapsigargin increased by 8 % (Figure 6.12C, $p>0.05$), compared to untreated control. The co-treatment of apelin-13 amide and (Lys^{8}GluPAL)apelin-13 amide with thapsigargin led to reduction in NRF-2 expression by 18% (Figure 6.12C, $p>0.05$) and 50% (Figure 6.12C, $p>0.05$) respectively, compared to thapsigargin alone.

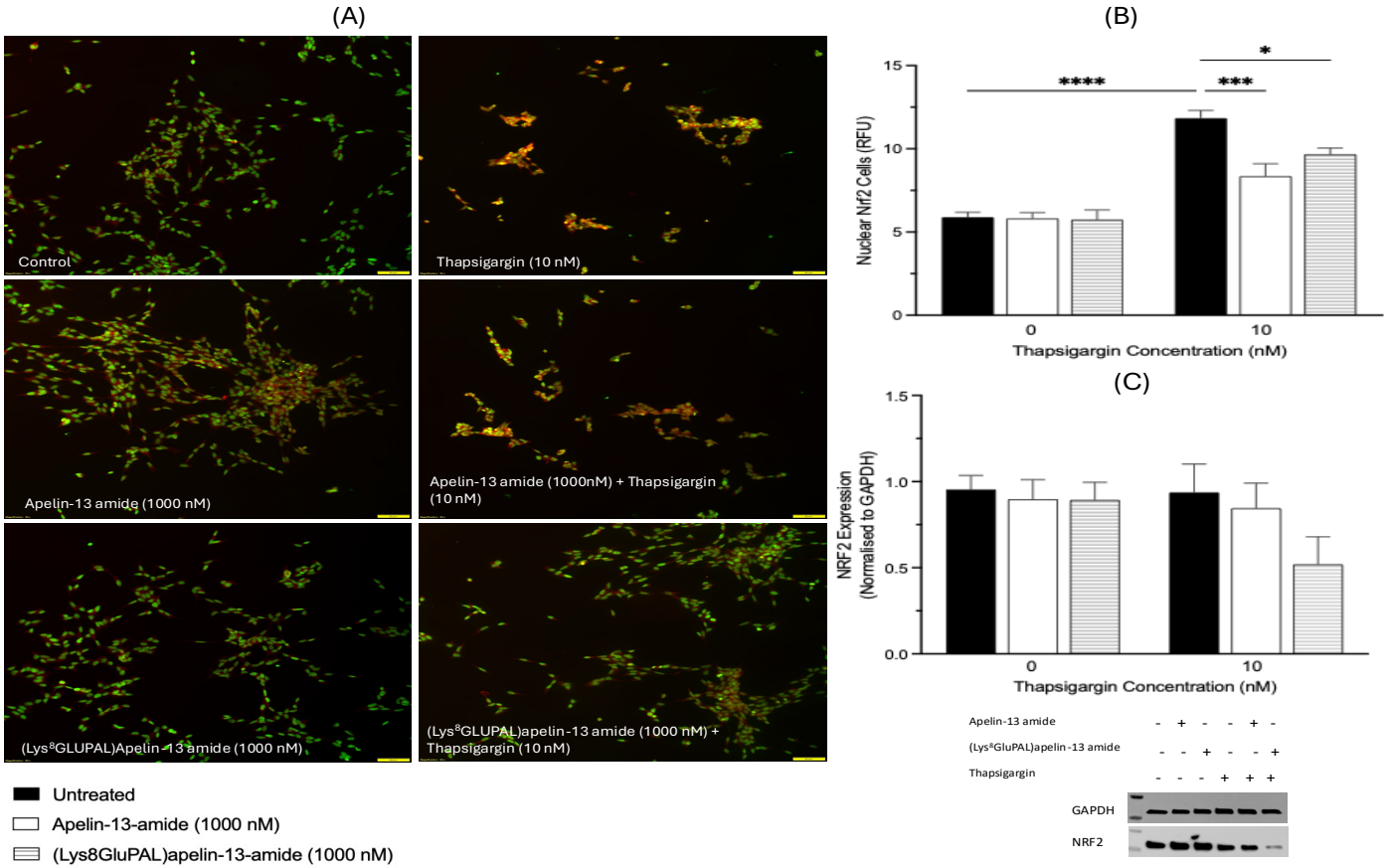

Figure 6.12: Effect of apelin-13 analogues against thapsigargin-induced oxidative stress on NRF-2 expression. The effect of apelin-13 amide and (Lys^{8}GluPAL)apelin-13 amide on the NRF-2 signalling pathway with and without was measured by immunolabeling with NRF-2 a transcription factor and western blot analysis. The cells were then labelled with NRF-2 antibody (1:250) and imaged under fluorescent microscope at 20X magnification, scale bar of 50 μM. (A) representative images of the immunostaining with NRF-2, (B) the graph of the intensity of the nuclear translocation of NRF-2 and (C) is the western blot analysis of NRF-2 when GAPDH was used as a loading control. Values represents mean ±SEM for n=3 where *p<0.05, ***p<0.001, ****p<0.0001.

6.2.13: Effect of apelin-13 amide and (Lys^{8}GluPAL)apelin-13 amide on caspase-12 expression in SH-SY5Y cells.

To assess the impact of apelin-13 analogues on ER stress-induced apoptosis by 10 nM thapsigargin we used caspase 12 immunolabeling. Caspase-12 is localised in the ER and is activated in response to prolonged ER stress, and by detecting its expression and localisation using ICC in SH-SY5Y cells, we evaluated the apoptosis induced by thapsigargin which is directly related to the ER dysfunction. Figure 6.13A shows representative images of ICC immunolabeling of Caspase-12 The results illustrated that apelin-13 analogues did not make significant impact alone, thapsigargin increased the caspase-12 in nucleus by 125% (Figure 6.13B, $p<0.001$), compared to untreated control. The co-treatments of 10 nM thapsigargin with apelin-13 amide reduced caspase-12 by 13% (Figure 6.13B, $p>0.05$) and 26% (Figure 6.13B, $p>0.05$) for (Lys^{8}GluPAL) apelin-13 amide, compared to thapsigargin alone.

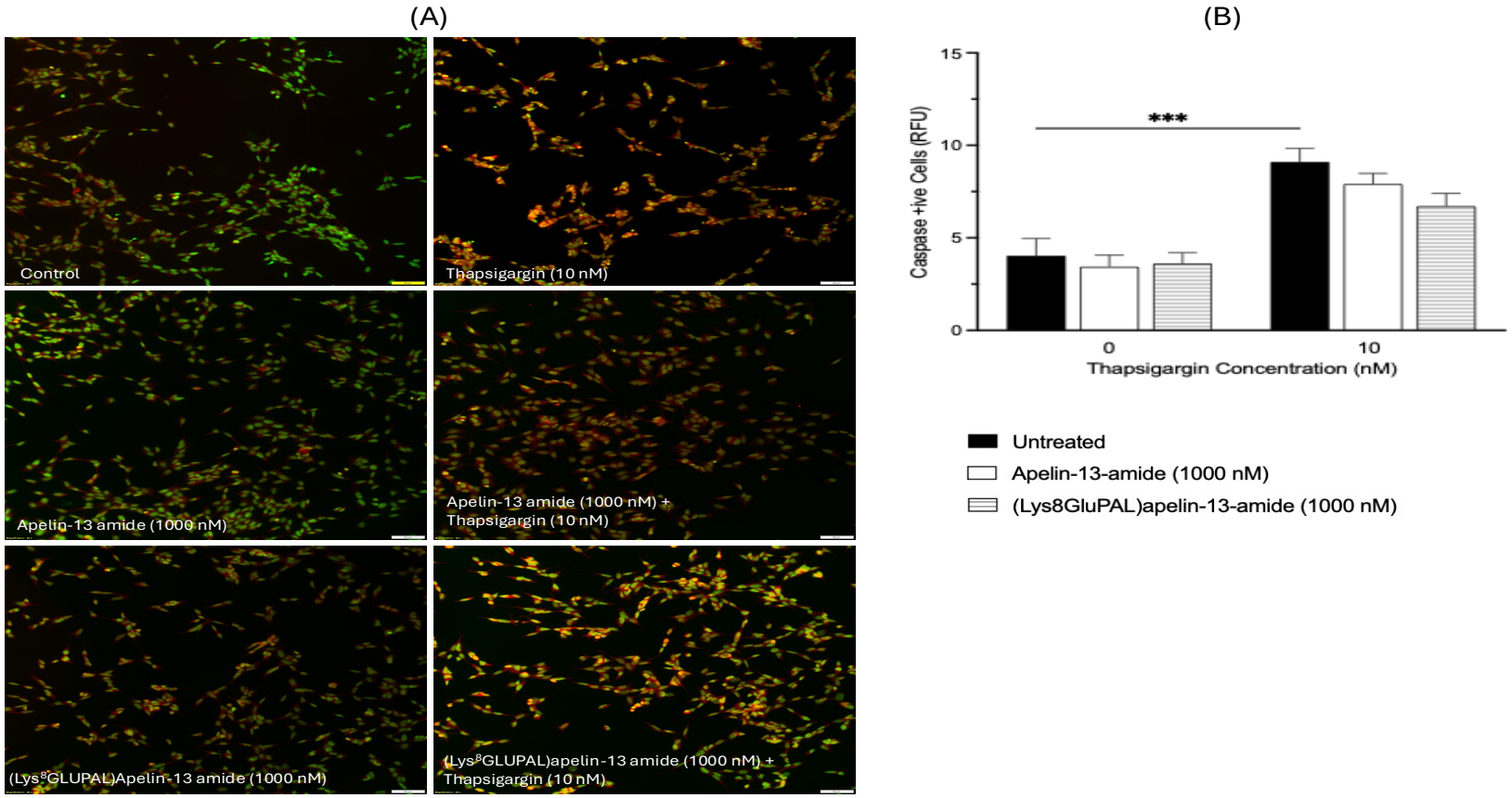

Figure 6.13: Effect of apelin-13 amide and (Lys8GluPAL)apelin-13 amide on caspase-12 expression in SH-SY5Y cells. Caspase-12 expression was visualised by the immunofluorescence staining in SH-SY5Y cells *in-vitro* treated with thapsigargin and apelin-13 analogues. Caspsde-12 activation is highly increased in the cells stress, with fluorescence intensity indicating caspase-12 translocation from the ER to the cytoplasm. (A) representative images of caspase-12 immunostaining at 20X magnification with scale bar 50 uM and (B) is the graph measured intensity in RFU. Values represents mean ±SEM for n=3 where ***p<0.001.

6.2.14: Effect of apelin-13 analogues on apoptotic pathway and protective effect against thapsigargin induced apoptosis.

The protective effect of apelin-13 amide and (Lys^{8}GluPAL)apelin-13 amide on thapsigargin induced apoptosis was measured by assessing the expression of pro-apoptotic BAX and anti-apoptotic Bcl-2 in SH-SY5Y cells. The results demonstrated that there was no significant change seen in pro-apoptotic BAX expression when treated with apelin-13 amide (Figure 6.14A, $p>0.05$) and (Lys^{8}GluPAL)apelin-13 amide (Figure 6.14A, $p>0.05$), and 10 nM thapsigargin increased the BAX expression by 68% (Figure 6.14A, $p>0.05$), compared to untreated control. Apelin-13 amide reduced the 10 nM thapsigargin induced BAX expression by 47% (Figure 6.14A, $p>0.05$) and (Lys^{8}GluPAL)apelin-13 amide by 24% for (Figure 6.14A, $p>0.05$).

The expression of anti-apoptotic Bcl-2 was increased by 9 % (Figure 6.14B, $p>0.05$) when treated alone with apelin-13 analogues. However, thapsigargin reduced the Bcl-2 expression by 16% (Figure 6.14B, $p>0.05$), compared to untreated control. Compared to the 10 nM thapsigargin , the Bcl-2 expression was restored by 43% (Figure 6.14B, $p>0.05$) when treated with apelin-13 amide and by 26% (Figure 6.14B, $p>0.05$) with (Lys^{8}GluPAL)apelin-13 amide.

The BAX/Bcl-2 ratio was quantified to measure the balance between the BAX and Bcl-2 proteins. The higher ratio indicated the shift toward apoptosis while the lower suggest towards a protective state. The results indicated that there was no significant change seen when treated alone with apelin-13 analogues, but BAX/Bcl-2 ratio was increased by 100% (Figure 6.14C, $p>0.05$) with 10 nM thapsigargin treatments, compared to untreated control. compared to the thapsigargin treatments, the combined treatments of thapsigargin with apelin-13 amide reduced the ratio by 64% (Figure 6.14C, $p<0.05$), and by 39% (Figure 6.14C, $p>0.05$), for treatments with (Lys^{8}GluPAL)apelin-13 amide.

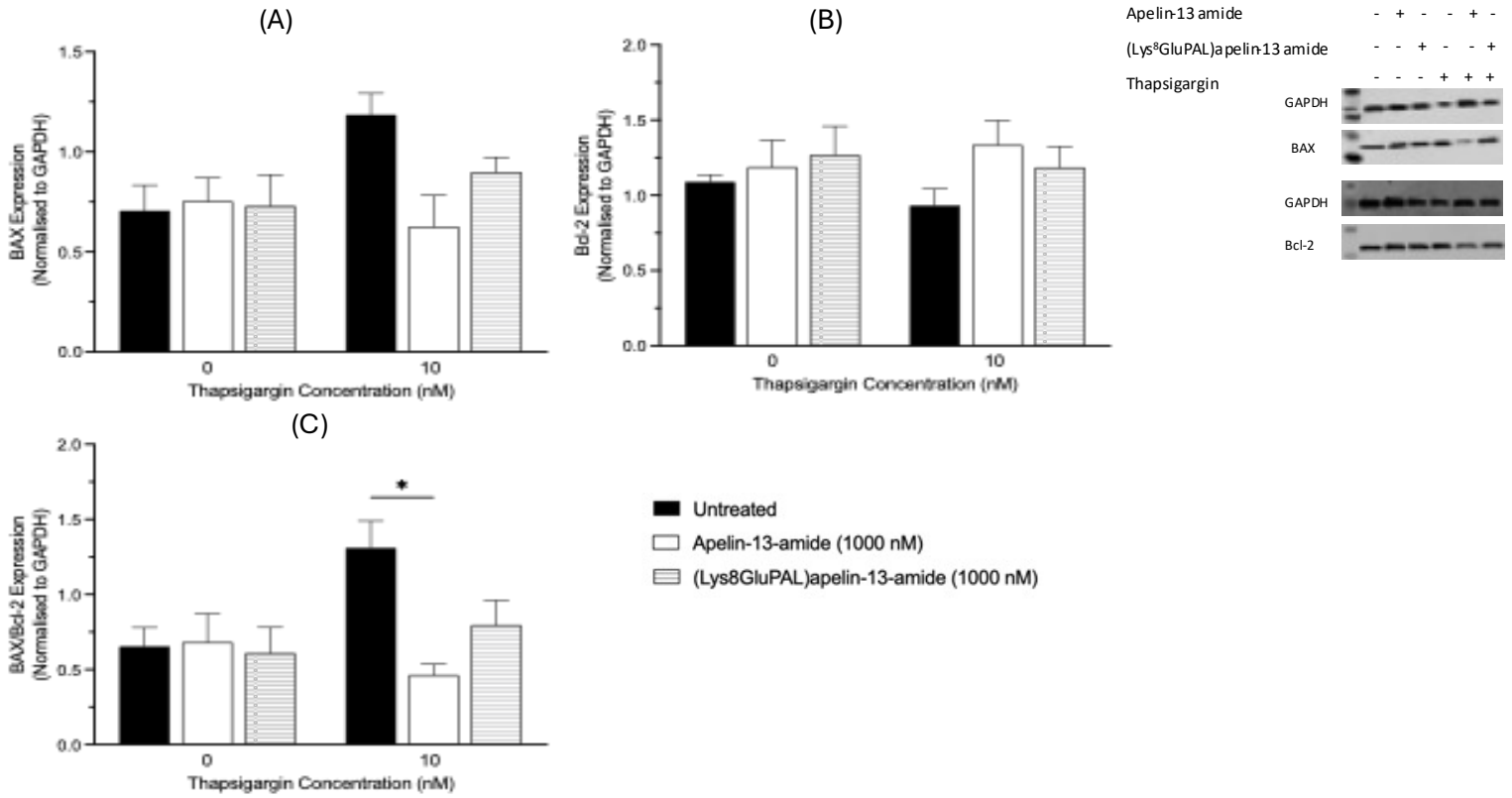

Figure 6.14: Effect of apelin-13 analogues on apoptotic and protective effect against thapsigargin induced apoptosis. The expression levels of the pro-apoptotic protein Bax and the anti-apoptotic protein Bcl-2 were assessed in SH-SY5Y cells *in-vitro* subjected to apelin-13 analogues after thapsigargin-induced endoplasmic reticulum stress. Cells were harvested and expression of (A) BAX and (B) Bcl-2 and (C) BAX/Bcl-2 ratio was determined by western blot. GAPDH was used as a loading control and the band intensity was measured by image J. Data is expressed as fold change to control (Untreated control) and analysed by one-way ANOVA. Values represents mean ±SEM for n=3 where *p<0.05.

6.2.15: Effect of apelin-13 analogues on ER stress response by analysis of BiP and IRE1 expression in SH-SY5Y cells.

To evaluate the activation of UPR pathway in SH-SY5Y cells which is triggered during the ER stress- induced by thapsigargin 10 nM, we analysed the expression of IRE1a and BiP proteins by western blot . The results show slight increase in IRE1 expression by apelin-13 amide (19%, Figure 6.15A, $p>0.05$), (Lys^8GluPAL)apelin-13 amide (19%, Figure 6.15A, $p>0.05$) and 10 nM thapsigargin (40%, Figure 6.15A, $p>0.05$) but not significant, compared to untreated control. When cells were exposed to 10nM thapsigargin, both apelin-13 amide (8% reduction, 6.15A, $p>0.05$) and (Lys^8GluPAL)apelin-13 amide (19% reduction, Figure 6.15A, $p>0.05$) were able to reduce thapsigargin induced increase in IRE1 expression.

On the other hand, there was no significant change seen in BiP expression when treated with apelin-13 analogues (Figure 6.15B, $p>0.05$), though 10 nM thapsigargin increase the expression by 22% (Figure 6.15B, $p>0.05$) though not significant. Compared to thapsigargin, apelin-13 amide combined with thapsigargin reduced the BiP expression by 15% (Figure 6.15B, $p>0.05$), and (Lys^8GluPAL)apelin-13 amide showed no change.

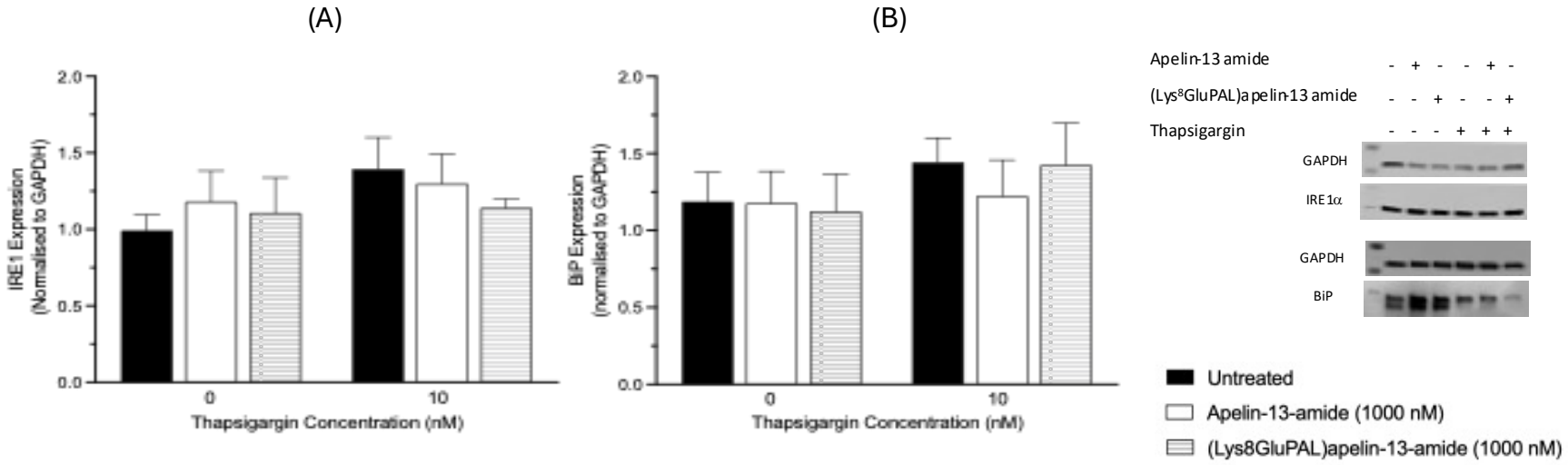

Figure 6.15: Effect of apelin-13 analogues on ER stress response by analysis of BiP and IRE1 expression in SH-SY5Y cells. Western blot analysis was performed to assess the protein expression of the IRE1a (Inositol-Requiring Enzyme 1 alpha) and BiP (Binding immunoglobin Protein) in SH-SY5Y cells *in-vitro*. The cells were treated with and without the 10 nM thapsigargin to look at the protective effect of apelin-13 amide and (Lys^{8}GluPAL)apelin-13 amide. (A) the graph representation of the IRE1a and (B) graph representation of BiP. GAPDH was used as a loading control and the band intensity was measured by image J. Data is expressed as fold change to control (Untreated control) and analysed by one-way ANOVA. Data are presented as mean ±SEM for n=3.

6.2.16: Effect of apelin-13 amide and (Lys^{8}GluPAL)apelin-13-amide on ER stress responses induced by thapsigargin in SH-SY5Y cells.

We evaluated the protein expression of major quality-control chaperons, Ero1-Lα (ER oxidoreductase 1α (Figure 6.16A), Calnexin (Figure 6.16B), PDI (Figure 6.16C), and PERK (Figure 6.16D) proteins to correlate the restorative effect of apelin-13 analogues on the UPR and ER proteostasis. . One way ANOVA revealed that apelin-13 amide and (Lys^{8}GluPAL)apelin-13-amide alone did not make any changes in all protein expression (Figure 6.16A, B, C, D, $p>0.05$), compared to untreated alone. The results showed that 10 nM thapsigargin treatment increased protein expression of Ero1-Lα by 21% (Figure 6.16A, $p>0.05$) of PERK by 16% (Figure 6.16D, $p<0.01$) and reduced expression of calnexin by 21% (Figure 6.16B, $p>0.05$) and PDI by 15% (Figure 6.16C, $p>0.05$), compared to untreated control.

Compared to the thapsigargin alone, the co-treatments of apelin-13 amide and 10 nM thapsigargin reduced protein expression of Ero1-Lα by 15% (Figure 6.16A, $p>0.05$), PDI by 4% (Figure 6.16C, $p>0.05$) and PERK by 26% (Figure 6.16D, $p<0.001$) and increased calnexin expression by 26% (Figure 6.16B, $p>0.05$). Co-treatment of thapsigargin with (Lys^{8}GluPAL)apelin-13-amide reduced protein expression of Ero1-Lα by 19% (Figure 6.16A, $p>0.05$), of PDI by 23% (Figure 6.16C, $p<0.01$) of PERK by 10% (Figure 6.16D, $p<0.05$) and increased calnexin expression by 4% (Figure 6.16B, $p>0.05$), compared to thapsigargin alone.

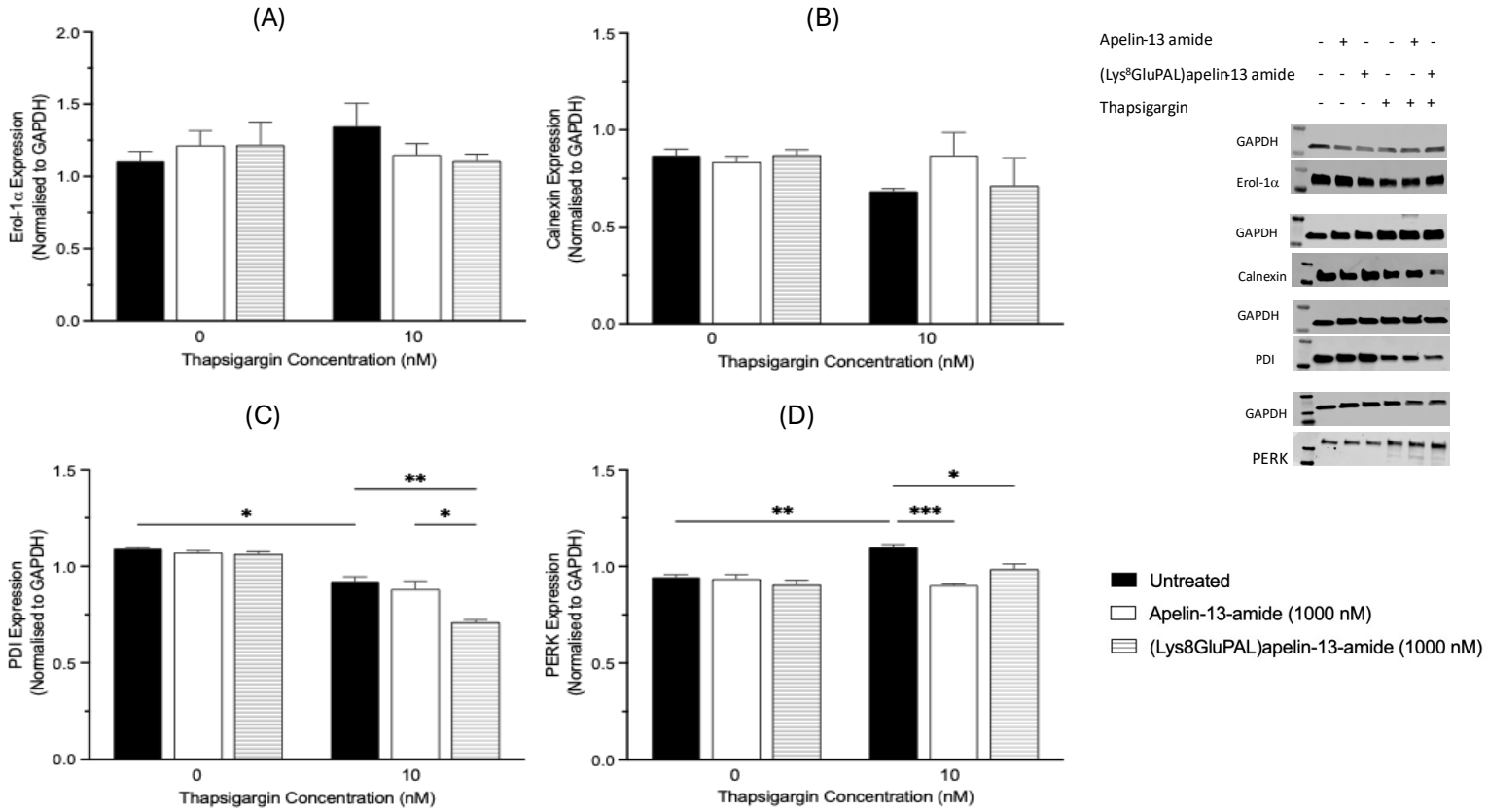

Figure 6.16: Effect apelin-13 amide and (Lys^{8}GluPAL)apelin-13-amide on ER stress responses induced by thapsigargin in SH-SY5Y cells. Western blot analysis was performed to measure the expression of key ER stress-associated proteins in SH-SY5Y cells. (A) is Calnexin, (B) is Erol1a, (C) is PDI and (D) is PERK expression. GAPDH was used as a loading control and the band intensity was measured by image J. Data is expressed as fold change to control (Untreated control) and analysed by one-way ANOVA. Values represents mean ±SEM for n=3 where *p<0.05, **p<0.01, and **p<0.001.

6.2.17: Effect of apelin-13 analogues on thapsigargin-induced autophagy.

The western blot analysis was used to measure autophagy related proteins due to the ER stress induced by 10 nM thapsigargin in SH-SY5Y cells. One-way ANOVA analysis showed that apelin-13 amide (Figure 6.17A, $p>0.05$) and (Lys^8GluPAL)apelin-13-amide (Figure 6.17A, $p>0.05$) increased ATG3 expression non-significantly by 23%, compared to untreated control. There were no changes in ATG5 and ATG7 expression when treated with apelin-13 analogues. The treatments with 10 nM thapsigargin slightly increased ATG3 expression by 6% (Figure 6.17A, $p>0.05$), ATG7 expression by 2% (Figure 6.17B, $p>0.05$) and ATG5 expression by 20% (Figure 6.17C, $p>0.05$), compared to untreated control. compared to the thapsigargin alone, co-treatment of apelin-13 amide and thapsigargin improved the ATG3 expression by 32% (Figure 6.17A, $p>0.05$), ATG7 expression by 14% (Figure 6.17B, $p>0.05$) and ATG5 expression by 6% (Figure 6.17C, $p>0.05$). The ATG3 expression was increased by 21%, (Figure 6.17A, $p>0.05$), ATG7 by 7% (Figure 6.17B, $p>0.05$) and reduced ATG5 expression by 11% (Figure 6.17C, $p>0.05$) when treated concurrently with thapsigargin and (Lys^8GluPAL)apelin-13-amide, compared to thapsigargin alone.

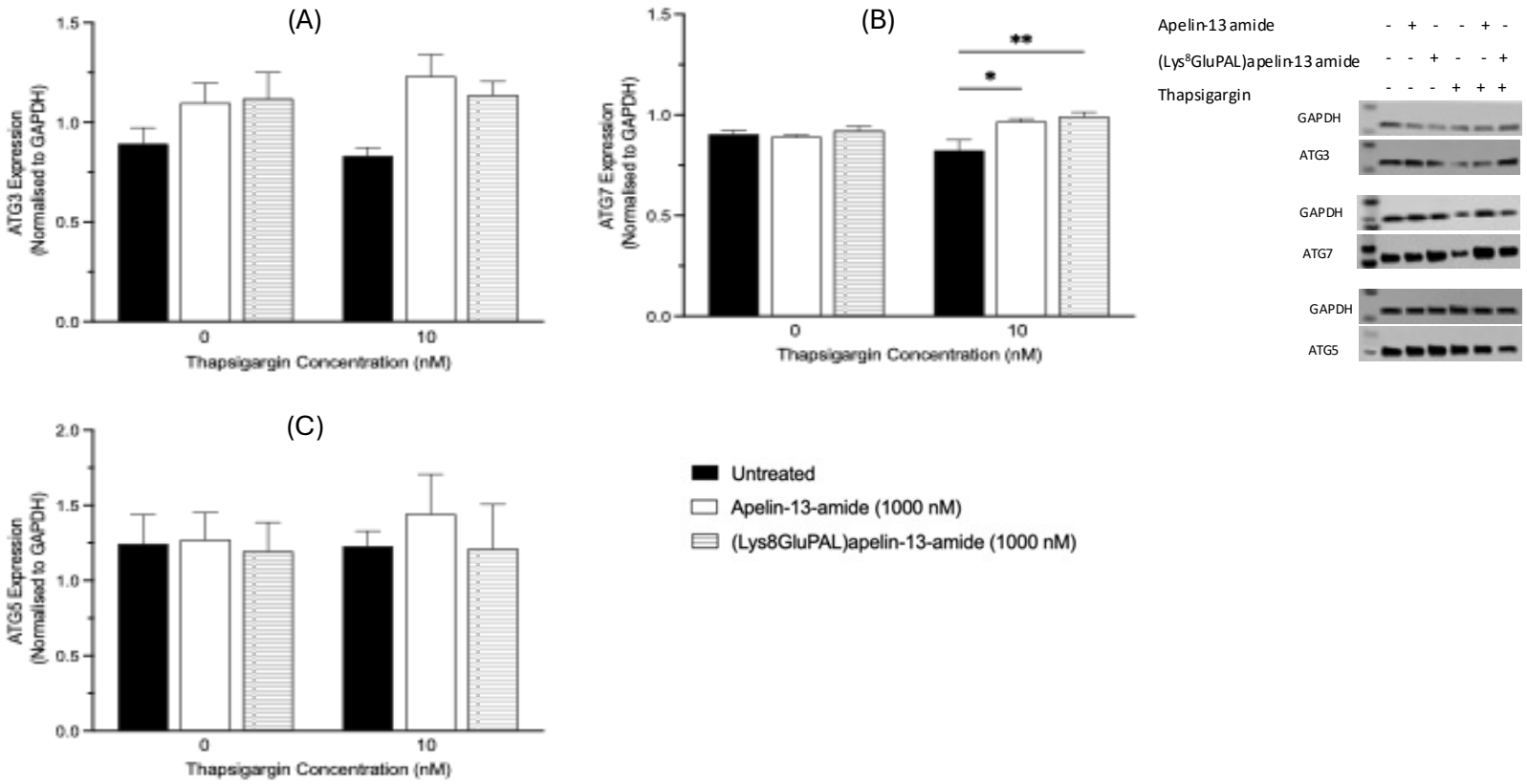

Figure 6.17: Effect of apelin-13 analogues on thapsigargin-induced autophagy. Apelin-13 amide and (Lys^{8}GluPAL)apelin-13-amide rescues autophagy impairment in the neuroblastoma SH-SY5Y cell line upon persistent ER stress induced by 10 nM thapsigargin. After the treatments with thapsigargin alone and along with apelin-13 analogues, the cells were harvested and expression of (A) ATG3, (B) ATG7 and (C) ATG5 was determined by western blotting. GAPDH was used as a loading control and the band intensity was measured by image J. Data is expressed as fold change to control (Untreated control) and analysed by one-way ANOVA. Values represents mean ±SEM for n=3 where *$p<0.05$, **$p<0.01$.

6.2.18: Effect of apelin-13 analogues on cell viability and cell toxicity in Thapsigargin-induced stress after AMPK inhibition by compound C in SH-SY5Y cells.

The AMP-activated protein kinase (AMPK) is the key energy sensor and maintain energy homeostasis in cells. Compound C an AMPK inhibitor was used to analyse the effect of apelin-13 analogues on cell viability and cell toxicity under stress induced by thapsigargin in SH-SY5Y cells in-vitro. AMPK is activated by binding to AMP or ADP and compound C inhibits ATP competition by attaching to the ATP-binding site of the AMPK catalytic α-subunit. This inhibits AMPK activation and phosphorylation. Cell viability was significantly improved by 24% (Figure 6.18A, $p<0.01$) when treated with apelin-13 amide and by 25% (Figure 6.18A, $p<0.001$) for (Lys^8GluPAL)apelin-13-amide, compared to untreated control. The cells viability was significantly reduced by 10 nM thapsigargin by 23% (Figure 6.18A, $p<0.01$), compared to untreated control. However, compared to the thapsigargin alone, when the cells were co-treated with 10 nM thapsigargin and apelin-13 amide the cell viability was improved by 30% (Figure 6.18A, $p<0.01$) and 46% (Figure 6.18A, $p<0.0001$) for (Lys^8GluPAL)apelin-13-amide.

On the other hand, when the cells were pre-treated with compound C, the cell viability had no change when treated with apelin-13 analogues and the cell viability was significantly reduced when treated with 10 nM thapsigargin by 31% (Figure 6.18A, $p<0.0001$), compared to the untreated control. However, when the cells were co-treated with apelin-13 amide and (Lys^8GluPAL)apelin-13-amide alongside with 10 nM thapsigargin there was no change seen (Figure 6.18A, $p>0.05$), compared to thapsigargin alone.

The cell toxicity assay was used to measure the toxicity induced by 10 nM thapsigargin and impact of apelin-13 analogues in the presence or absence of compound C. The results demonstrated that apelin-13 amide and (Lys^8GluPAL)apelin-13-amide reduced the cell toxicity by 11% (Figure 6.18B, $p<0.05$) and 15% (Figure 6.18B, $p<0.01$)

respectively, compared to untreated control. Toxicity was increased significantly (114% Figure 6.18B, p<0.0001) by 10 nM thapsigargin, compared to untreated control. Co-treatment of thapsigargin with apelin-13 amide reduced the toxicity by 52% (Figure 6.18B, p<0.0001) and by 48% for (Lys^{8}GluPAL)apelin-13-amide (Figure 6.18B, p<0.0001), compared to thapsigargin alone. However, in the presence of compound C, no changes to cell toxicity were observed when treated with apelin-13 analogues alone (Figure 6.18B, p>0.05) or co-treated with apelin-13 analogues and 10 nM thapsigargin (Figure 6.18B, p>0.05), compared to the controls. Thapsigargin (10 nM) reduced the cell toxicity by 112% (Figure 6.18B, p<0.0001), compared to untreated control.

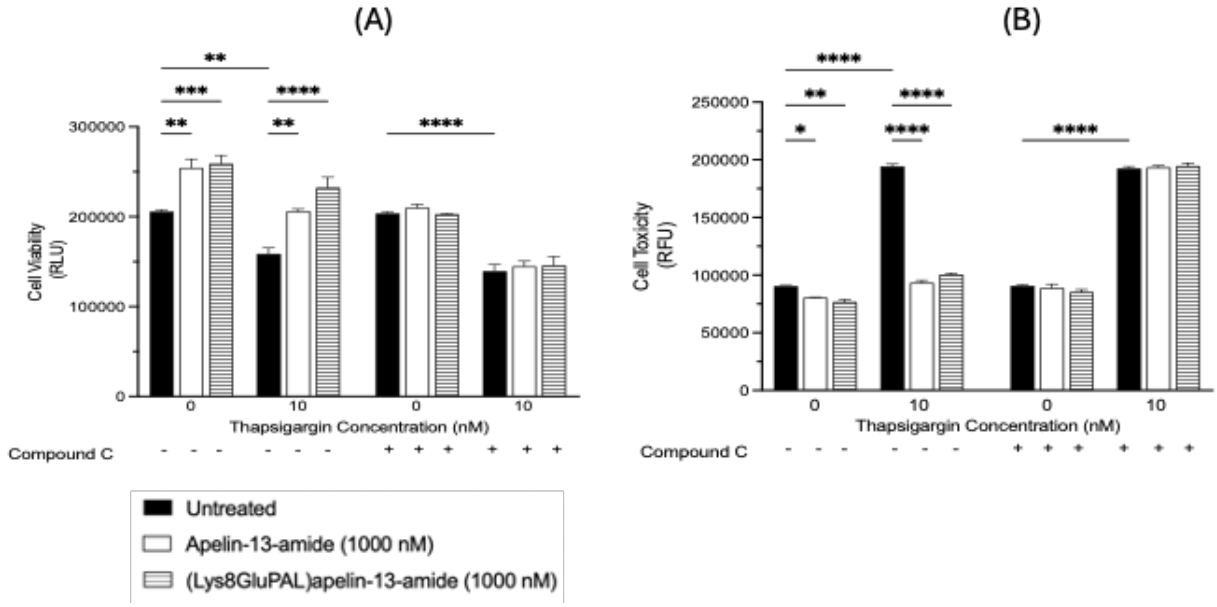

Figure 6.18: Effect of apelin-13 analogues on cell viability and cell toxicity in Thapsigargin-induced stress after AMPK inhibition by compound C in SH-SY5Y cells. Compound C inhibited AMPK pathway and led to reduced cell viability and increased cell toxicity in SH-SY5Y cells in-vitro. The cells were treated with compound C for 30 minutes prior to the aplin-13 analogues and thapsigargin treatments for 6 hours. The CellTiter-Glo viability assay and CytoTox 96® Non-Radioactive Cytotoxicity Assay was used and the viability and cell toxicity. (A) Cell viability assay and (B) Cell toxicity assay. Values represents mean ±SEM for n=3 where *p<0.05, **p<0.01, ***p<0.001, ****p<0.0001.

6.3: Discussion

In this study we have explored the positive effect of the stable apelin analogues on restoring deleterious effects of thapsigargin.

Cell Viability

In this chapter we used thapsigargin as a stress model and results showed that apelin-13 amide and (Lys^{8}GluPAL)apelin-13-amide significantly improved the viability of cells by mitigating the effect of thapsigargin at different timepoints. Prolonged or severe stress triggers apoptosis, thereby reducing cell viability. This study has shown that (Lys^{8}GluPAL)apelin-13-amide was more potent compared to apelin-13 amide due to the peptide's stability and bioavailability. Several studies have shown that apelin involvement in energy metabolism and cell survival. Apelin-13 is known to stimulate the insulin secretion and increase glucose uptake. Study by O'Harte et al (2018) showed that modified analogues of apelin-13 have extended half-life and bioactive. Our research aligns with the previous findings indicating that apelin-13 analogues mitigate the ER stress and oxidative stress by activating signalling pathways such as AMPK, PI3/Akt, MAPK (Parthsarathy et al., 2017).

Cell proliferation and differentiation

The protective effect of apelin-13 against the thapsigargin-induced stress, was evident in cell proliferation and cell differentiation in SH-SY5Y cells. During the S-phase, the thymidine analogue BrdU (bromodeoxyuridine) is integrated into the DNA of cells that are multiplying (Snyder et al., 2021). BrdU incorporation has been significantly reduced in

thapsigargin-treated cells, indicating decreased cell proliferation. ER stress disrupts intracellular calcium levels and triggers the unfolded protein response (UPR), which stops the cell cycle and impairs DNA synthesis. Previous studies have showed that thapsigargin effect the cell proliferation and differentiation by activation of PERK pathway which is the key branches of UPR and plays critical role (Snyder et al., 2021). Apelin-13 have shown to improve the cell proliferation and differentiation by activating AMPK pathway, PI3/Akt pathway and by NRF-2 pathway (Li et al., 2022). Apelin-13 activates AMPK which regulates the energy homeostasis and promotes autophagy, PI3/Akt pathway which activated anti-apoptotic factors like Bcl-2 and inhibits pro-apoptotic factors like BAD and capase-9 to maintain the cell viability and integrity (Zhong et al., 2016).

Studies suggested that oxidative stress lead to the impaired neurite outgrowth (Lankford et al., 1995). Study by Audesirk et al, also showed that intracellular free Ca2+ concentrations, plays a key role in the neurite outgrowth regulations (1990). Studies have shown that thapsigargin can modulates the balance between the ERK1/2 pathways and disrupts the normal cellular mechanism by triggering the UPR. ERK1/2 pathways play a critical function in cell survival, proliferation and differentiation (Zhong et al., 2016). Apelin-13 not only increases the number of neurons extending processes, a critical feature for neuronal communication and function, but also extended their length.

These results are consistent with previous works that describe the function of Apelin-13 in neurogenesis and synaptic plasticity (Zhang et al., 2023). These data indicate that Apelin-13 not only prevents damage to neurons, but it also promotes neuronal recovery and regeneration with a potential treatment for neurodegenerative diseases which are associated by loss of degraded neurons (Zhang et al., 2023). Apelin-13 is known to restore ERK1/2 activity by activating ERK1/2 pathways (Bai et al., 2008). These finding suggests that the apelin-13 can be used to enhance the cell proliferation, differentiation and neurite extension in stress-induced neurodegenerative conditions.

Cell toxicity

Cell toxicity assay plays key role in assessing the toxic effect of stress-inducing agents and the protective effect of the therapeutic against them. This chapter focused on looking at the cell toxicity induced by thapsigargin and how apelin-13 analogues impacted on it. Our results illustrated that thapsigargin induced cell toxicity in SH-SY5Y cells at different time-points and apelin-13 amide and (Lys^{8}GluPAL)apelin-13-amide reduced cell toxicity in co-treatment to the thapsigargin. The Apelin-13 analogues were most effective in reducing cell toxicity at 4 hours post treatment compared to 2 hours and 24 hours.

Studies have suggested that the concurrent rise in free calcium in the cytoplasm is a potent signal that promotes apoptosis in a variety of cell types, in addition to ER stress triggering pathways that can cause cell death (Kim et al., 2008). Previous research has shown that apelin-13 analogues have protective effect against the oxidative stress and ER stress (Than et al., 2014). Studies proved that apelin-13 mitigated cytotoxicity by activating AMPK/GSK-3b/NRF-2 pathway and reducing oxidative stress (Yin et al., 2020).

Mitochondrial and Oxidative stress

Neurodegenerative diseases such as Alzheimer's are mainly triggered by oxidative stress and mitochondrial dysfunction. We utilized thapsigargin to disrupt calcium homeostasis and ER stress and thus affect the mitochondrial membrane potential by in SHY-SY5Y cells. Due to the inhibition of the SERCA, calcium is stopped from being pumped into the ER. The depletion of the calcium from the ER leads to the calcium overload in mitochondria and it reduces the mitochondrial membrane potential (Andersen et al., 2015). Apelin-13 analogues restored mitochondrial membrane potential, indicating its role in in preserving mitochondrial integrity. Previous research has shown that apelin-13 analogues can reduce oxidative stress and protect mitochondria by activating the AMPK

pathway (Guo et al., 2024). Study by Zhang et al, showed that in lung injury models, apelin reduced the oxidative stress and mitochondrial pathway apoptosis (2018).

We used thapsigargin to stress the cell in producing increased ROS and a disturbed redox balance. Apelin-13 significantly reduced ROS levels and improved the GSH/GSSG ratio slightly, demonstrating its antioxidant properties. Studies have suggested that redox balance by apelin-13 analogues is important to generate GSH and reduce oxidative stress (Fernández-Sánchez et al., 2011). This is supported by another study showing the inhibition of ROS production in cardiac cells by apelin-13 analogues (Pisarenko et al., 2015).

Apoptosis

The ability of apelin-13 analogues to prevent apoptosis was evaluated by measuring the caspase 3/7activity and BAX and Bcl-2 protein expression in SH-SY5Y cells. Caspase 3/7 and BAX/Bcl-2 are the key players in the intrinsic pathway of apoptosis, a programmed cell death. Intrinsic apoptotic pathway regulates the process that responds to the ER stress, cellular stress and DNA damage (Al-Qathama et al., 2017). Increased caspase 3/7 activity was observed in thapsigargin treated cells which was restored when treated apelin-13 amide and (Lys^{8}GluPAL)apelin-13-amidesuggesting a key role of our peptides in apoptosis . The BAX/Bcl-2 ratio was increased by thapsigargin treatment indicating apoptosis and reduced by apelin-13 analogues to support the cell survival. Studies showed that increased BAX expression leads to the permeabilization of the mitochondrial membrane and release of cytochrome C and activation of caspase 3/7 (Vince et al., 2018). Studies have shown that PI3K/Akt pathway inhibits apoptosis by preventing the activation of BAX and upregulation of Bcl-2 protein. AMPK activation by apelin leads to the increased anti-apoptotic proteins and inhibiting mTOR pathway to reduce cellular stress and apoptosis (Meng et al., 2017).

ER stress and UPR pathway

The activity calcium dependant chaperons in the ER are disrupted by the depletion of Calcium in the ER due to the inhibition of SERCA pump by thapsigargin (Lindner et al., 2020). Due to the stress induced the cells undergo unfolded protein response a network of pathways including PERK, IRE1α and ATF6 (Panagaki et al., 2017). PERK, ATF6 and IRE1 are the three key sensors by which UPR balances the ER stress and cell survival (Hiramatsu et al., 2015). EIF2α phosphorylation by PERK reduces protein synthesis and increases ATF4 expression, leading to CHOP-mediated apoptosis under stress. Under stress ATF6 translocate to Golgi and activates chaperones. If the stress persists, IRE1 splices XBP1 mRNA to increase protein folding and breakdown and activate pro-apoptotic JNK signalling (Hiramatsu et al., 2015). BiP (GRP78) binds to these sensors normally and releases them during stress to start UPR. However, ERO1α supports oxidative protein folding, it can increase stress and apoptosis by generating ROS. Caspase-12 is an ER-resident caspase, and it is activated in response to ER stress (Hiramatsu et al., 2015).

In our results, thapsigargin treatment led to increased expression of PERK, ATF6, IRE1, BiP, ER oxidoreductase 1α (ERO1α), and caspase-12, while reducing calnexin levels, a key chaperone involved in calcium homeostasis. The co-treatment of thapsigargin with apelin-13 amide and (Lys^{8}GluPAL)apelin-13-amide reversed the effects by reducing the expression of PERK, ATF6, IRE1, BiP, ERO1α, and caspase-12, indicating the mitigating effect of apelin-13 on UPR response. Moreover, apelin-13 analogues restored calnexin levels, which is fundamental for retaining ER proteostasis and calcium homeostasis, thereby reducing the ER stress response. This suggests that apelin-13 analogues modulate the UPR by downregulating pro-apoptotic signals to reduce apoptosis in SH-SY5Y cells.

Autophagy

The transcription factor NRF-2 is the crucial regulator of antioxidant defence mechanisms against oxidative stress. Our results showed increased nuclear NRF-2 expression in cells treated with thapsigargin which is then normalized by apelin-13 analogues, suggesting that apelin-13 enhances the cellular defense against oxidative damage by activating the NRF-2 pathway (Ramyaa et al., 2014). These findings provide insight into how apelin-13 mitigates mitochondrial and oxidative stress, which are central to the pathology of neurodegenerative diseases.

The current study suggested that thapsigargin, an inducer of ER stress, slightly elevated the expression of ATG3, ATG5, and ATG7, important regulators of the autophagy process. The expression of these genes was notably elevated with co-treatment with apelin-13, indicating a possible link between autophagy and apoptotic pathways in the context of ER stress. Apoptosis and autophagy are closely related mechanisms. While apoptosis results in programme cell death, autophagy usually serves as a cell survival strategy, breaking down damaged proteins and organelles (Brunelli et al., 2022). The slight increase in ATG3, ATG5, and ATG7 expression after thapsigargin administration suggests that autophagy may be initially triggered by the cell as a defence mechanism against ER stress (Lindner et al., 2020). However, this autophagic response could not be enough if the stress is extended, as seen in severe ER stress brought on by thapsigargin, and cells might finally experience apoptosis. Research has shown that apelin-13 analogues can stimulate autophagy as a survival mechanism in several cases, such as cardiovascular and neurological illnesses, where ER stress is crucial (Wan et al., 2021). Based on previous studies, cells respond adaptively to ER stress by upregulating autophagy-related proteins, especially in the early stages before apoptosis is initiated (Hetz & Papa, 2018). These results support the idea that increasing autophagy may be a therapeutic approach to reducing ER stress-related disorders, especially in neurodegenerative illnesses where long-term stress causes neuronal death. Apelin-13's double function of increasing

autophagy and decreasing apoptosis creates opportunities for additional research into its neuroprotective properties.

Mechanism action of apelin-13 analogues

The AMP-activated protein kinase (AMPK) pathway is the key pathway involved in maintaining cell survival under stress by maintaining energy balance and regulating cellular mechanism (Kazyken et al., 2019). Apelin-13 analogues are known to promote cell survival by activating AMPK pathway. Previous studies have shown that apelin-13 analogues protect cardiomyocytes and endothelial cells from apoptosis by activating the AMPK pathway (Zeng et al., 2024). Apelin showed a protective effect against the ER stress in previous studies (Peng et al., 2023). Study by Kamińska et al, have shown that apelin plays an important role in cell viability and cell protection against ER and oxidative stress (2024). Studies have used compound C to inhibit the AMPK pathway and compound C is shown to induce cell death by inhibiting proliferation (Liu et al., 2014).

In contrast, to confirm that apelin-13 action is AMPK-dependant in our study, we did cell viability and cell toxicity analysis of SH-SY5Y cells by pre-treating cells with compound C, an AMPK inhibitor. Compound C is only cell permeable biochemical also known as dorsomorphin is widely used in cell-based assays for selective AMPK inhibition (Liu et al., 2014). Pre-incubation with Compound C, affectively blocked AMPK activation and apelin-13 analogues action and showed no reduction in cell toxicity and no improvement in cell viability.

6.4: Conclusion

In summary, our study highlighted the protective role of apelin-13 analogues to mitigate ER stress-induced apoptosis by thapsigargin. The thapsigargin is a stress model used to mimic the pathological condition observed in AD. The result demonstrates that apelin-13 analogues significantly reduce ER stress, apoptosis and improved cell survival. Apelin-13 amide and (Lys^{8}GluPAL)apelin-13-amide treatments demonstrated a significant protective effect against the oxidative stress induced by thapsigargin by activating AMPK pathway and reducing the pro-apoptotic protein expressions. Additionally, apelin-13 analogues have showed increased MAP2 expression, a critical marker of neuronal integrity and neurite outgrowth (shown in table 6). This suggest that apelin-13 analogues not only protect against ER stress but also supports neuronal survival and growth. The results from this study suggest that apelin-13 analogues play a key role in mitigating the chronic stress induced by thapsigargin, making it a promising therapeutic target for various diseases.

Experiments	Assays Used	Thapsigargin Effect	Apelin-13 Effect	Pathway Impact
Cell Viability	MTT, CellTiter-Glo	↓ cell viability	↑ viability under Thapsigargin-induced stress	PI3K/Akt activation for cell survival signalling
Proliferation & Differentiation	BrdU, MAP2, Neurite Outgrowth	↓ cell proliferation and neurite outgrowth	↑ cell proliferation and ↑ neurite outgrowth	PI3K/Akt/mTOR for proliferation, ERK/MAPK for differentiation
Cell Toxicity	LDH, CellTox Green	↑ cell toxicity	↓ toxicity	AMPK activation, NRF-2 and UPR regulation
Mitochondrial & Oxidative Stress	JC-1, ROS-Glo, GSH/GSSG, Hyper-7	↓ MMP, ↑ ROS, disturbed redox balance	↑ MMP, ↓ ROS, normalized redox balance	AMPK/NRF-2 pathway activated, mitochondrial support
Apoptosis	Caspase 3/7, BAX, Bcl-2	↑ apoptosis, ↑ pro-apoptotic and ↓ anti-apoptotic protein expression	↓ caspase activity, ↓ BAX and ↑ Bcl-2 expression	PI3K/Akt inhibits apoptosis, AMPK/MAPK inhibit caspase activation
ER Stress & UPR	ATF6, NRF-2,PERK, BiP, PDI, Calnexin	↑ ER stress markers	↓ ATF6, PERK, BiP, and calnexin	↓ ER stress via AMPK and PI3K/Akt modulation and UPR pathway
Autophagy	ATG3, ATG5, ATG7	↓ autophagy related proteins	↑ expression of autophagy proteins	NRF-2 pathway activation for cellular defence, AMPK inhibits mTOR and promotes autophagy

AMPK Role Confirmation	Compound C, AMPK siRNA	↓ cell viability and ↑ cell toxicity	Loss of protection when AMPK inhibited and AMPK knockdown	AMPK plays a central role in regulating neuroprotection

Table 6: Collective summary effect of apelin-13 and its analogues on SH-SY5Y cells LPS-induced inflammatory stress.

Summarised table shows that apelin-13 and its analogues mitigated ER stress, reduced UPR activation and restored autophagy under thapsigargin-induced stress in SH-SY5Y

Chapter 7

Effect of apelin-13 analogues as a protective agent on cell survival, growth, proliferation and differentiation against the Amyloid beta-42 induced toxicity in SH-SY5Y cells in-vitro.

7.1: Introduction

Neurodegenerative disease is the most common growing problem among groups worldwide. It characterises a broad spectrum of chronic, progressive disorders of gradual loss of neuronal function and structure in the brain. Dementia is an umbrella term used to characterise neurological conditions affecting the memory, thinking ability and behaviour. Currently more than 55 million people have dementia worldwide and every year there is rise of 10 million new cases (Kumar and Ekavali, 2015; World Health Organisation, 2023). The most common form of dementia is AD, accounting for approximately 60-70% of these cases worldwide which is set to increase to 150 million by 2050 (Canevelli et al., 2019; Alzheimer's Disease International, 2020). Despite decades of research, AD remain incurable, and the current therapeutic strategies offer limited symptomatic relief.

Several pathogenic hallmarks are common to neurological disorders, such as oxidative stress, abnormal protein aggregation, and dysregulation of essential processes in cells like autophagy, apoptosis, and UPR (DeTure & Dickson, 2019). The development of neuronal damage in AD is mostly attributed to Amyloid beta (Aβ), especially the $A\beta_{42}$ isoforms, which create extracellular plaques that impair cellular homeostasis and encourage neurodegeneration (Schweig et al., 2017). The balance between the generation of Aβ and clearance is key to maintain the homeostasis and prevent the aggregation of the misfolded protein (Bateman et al., 2006). Aβ peptides are amyloid precursor protein (APP) proteolytic fragments that are produced by the sequential cleavage by β- and γ-secretases and this proteolytic processing is implicated in the pathogenic cascade of AD. (Schweig et al., 2017). $A\beta_{42}$ is the most toxic form, and it aggregates into fibrils and oligomers that impair synaptic plasticity and lead to cell death. These oligomers eventually combine to form fibrils, which deposit as extracellular plaques, a characteristic of AD pathogenesis (Thal et al., 2014). The hippocampus and cortex, two areas of the brain important for memory and cognition, are where these plaques are most frequently detected and the impairment led to the memory loss and cognitive decline and synaptic failure. $A\beta_{42}$ plays critical role in oxidative stress and ER

stress and number of studies uncovered that it is involved in several degenerative processes, including as, oxidative stress, mitochondrial dysfunction, and endoplasmic reticulum (ER) stress (DeTure & Dickson., 2019; Zhang et al., 2023).

Number of interconnected pathways are involved in the $A\beta_{42}$ induced neuronal death with oxidative stress being the earliest pathological events. $A\beta_{42}$ lead to overproduction of reactive oxygen species (ROS) through metal ion interactions, NAPDH oxidase activation and mitochondria dysfunction (Cheignon et al., 2018). The excessive ROS production disrupts mitochondrial electron transport, induce oxidative stress and impair ATP synthesis which leads to the neuronal dysfunction by damaging cellular components like lipids, proteins, and DNA (Zhao & Zhao, 2013). Oxidative stress is intently connected to mitochondrial dysfunction, another important aspect of $A\beta_{42}$-induced toxicity (Zhao & Zhao, 2013). Studies have shown that mitochondrial dysfunction is the main cause for cognitive impairments and synaptic failure (Guo et al., 2017). Mitochondria is particularly vulnerable to ROS damage, which can result in a vicious cycle of oxidative damage and decreased energy generation (Storozhuk et al., 2005). $A\beta_{42}$ disrupts the protein folding capacity in the ER and leads to ER stress, triggering the UPR (Fonseca et al., 2013). The UPR is the defense mechanism against stress to restore the ER homeostasis by stopping the protein synthesis and increasing the production of molecular chaperones. However, under prolonged ER stress, UPR changes from a protective function to a pro-apoptotic response, triggering pathways like intrinsic pathway that result in cell death (Oslowski & Urano, 2011).

Apelin, a peptide hormone originally isolated from bovine stomach, an endogenous ligand for the APJ receptor, has been investigated for its neuroprotective, metabolic, and cardioprotective properties (O'Harte et al., 2017). Apelin-13 is most active subtype, and its role has been investigated on several diseases. Studies showed that apelin-13 protect neurons against oxidative stress, ischemia, inflammation and toxicity (Kawamata et al., 2001).

The aim of this chapter is to investigate the protective effect of apelin-13 amide and (Lys8GluPAL) apelin-13 amide on oxidative stress and ER stress induced by $A\beta_{42}$. We

focused on pathways involved in mitigating the ER stress and oxidative stress by modulating apoptosis in the SH-SY5Y cells.

Objectives:

1. To investigate the protective effect of apelin-13 amide and (Lys^{8}GluPAL)apelin-13 amide against $A\beta_{42}$ on cell survival, differentiation and proliferation in SH-SY5Y cells.
2. To evaluate how apelin-13 analogues protect neuronal cells from oxidative damage and ER stress induced by $A\beta_{42}$ in SH-SY5Y cells
3. To evaluate the effect of apelin-13 analogues on apoptosis induced by $A\beta_{42}$ in SH-SY5Y cells.

7.2: Results

7.2.1: Effect of apelin-13 analogues on cell viability under $A\beta_{42}$-Induced toxicity in SH-SY5Y cells in-vitro.

To evaluate the effects of apelin-13 analogues on cell viability in $A\beta_{42}$ treatment, cells were treated at different timepoints with $A\beta_{42}$ and 1000 nM Apelin-13 amide or (Lys^8GluPAL)apelin-13 amide and viability measured using CyQUANT ™ MTT Cell Viability Assay Kit. The results indicated that compared to untreated control, apelin-13 amide and (Lys^8GluPAL)apelin-13 amide alone at 2 hours increased the cell viability by 13% (Figure 7.1A, $p<0.05$) and 17% (Figure 7.1A, $p<0.01$) respectively. The cell viability was reduced by 3% (Figure 7.1A, $p>0.05$) with Aβ-42, compared to untreated control. Co-treatment of $A\beta_{42}$ with apelin-13 amide restored cell viability by 10% (Figure 7.1A, $p>0.05$) and 20% (Figure 7.1A, $p<0.001$) when treated with (Lys^8GluPAL)apelin-13 amide, compared to Aβ-42.

At 4 hours, the cell viability was significantly improved by 32% with apelin-13 amide (Figure 7.1B, $p<0.0001$) and 37% by (Lys^8GluPAL)apelin-13 amide (Figure 7.1B, $p<0.0001$), however reduced by 23% for $A\beta_{42}$ (Figure 7.1B, $p<0.0001$), compared to untreated control. Compared to $A\beta_{42}$ alone, co-treatment of $A\beta_{42}$ with apelin-13 amide increased cell viability by 44% (Figure 7.1B, $p<0.0001$), and 48% (Figure 7.1B, $p<0.0001$), with (Lys^8GluPAL)apelin-13 amide.

At 24 hours post treatment, no change was observed in cell viability with apelin-13 analogues for 24 hours (Figure 7.1C, $p>0.05$), and significant reduction in cell viability was observed when treated with $A\beta_{42}$ (28%, Figure 7.1C, $p<0.0001$) was observed compared to untreated control. Co-treatments of $A\beta_{42}$ with apelin-13 amide led to significant increase by 42% (Figure 7.1C, $p<0.0001$) and 48% (Figure 7.1C, $p<0.0001$) with (Lys^8GluPAL)apelin-13 amide co-treatment.

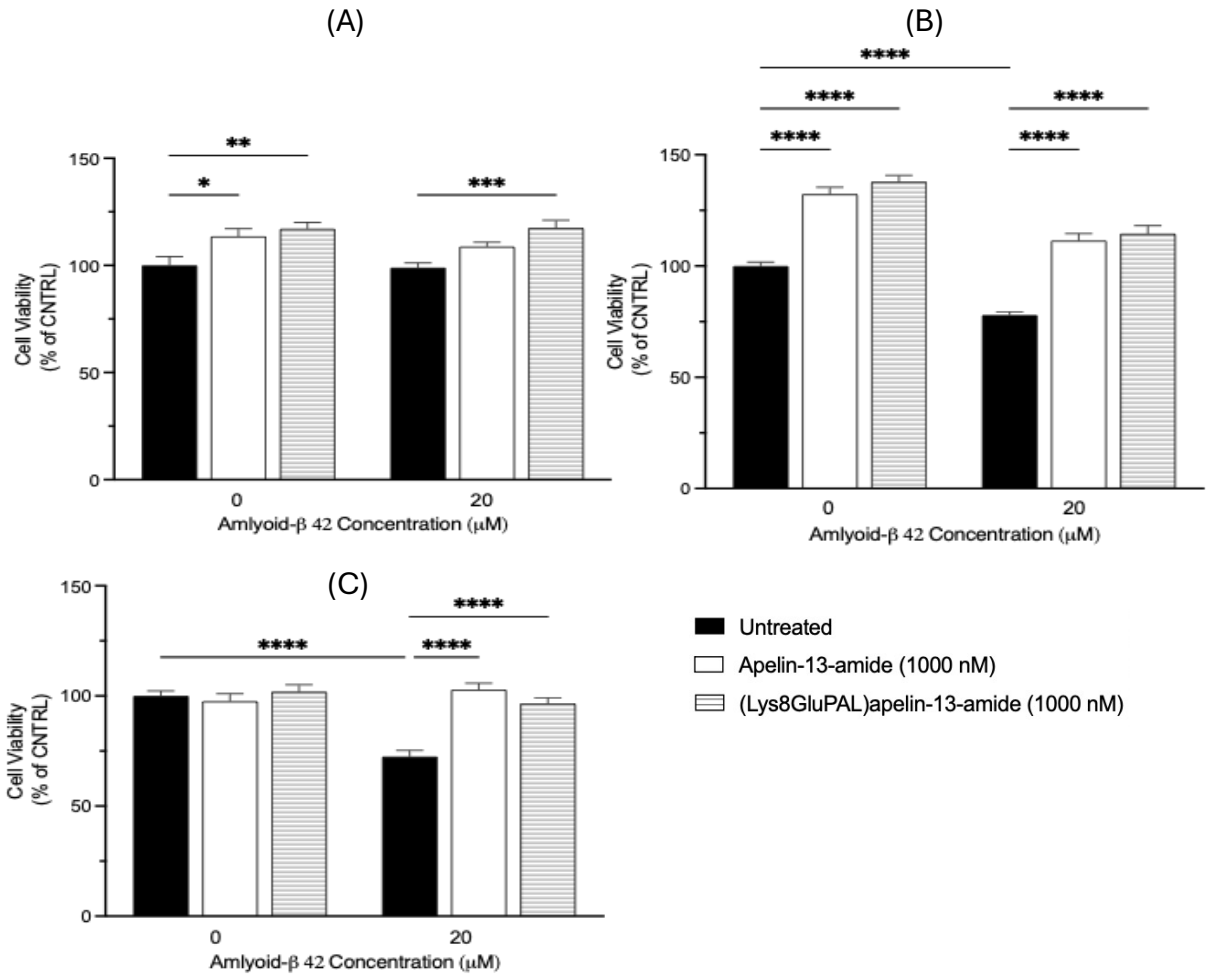

Figure 7.1: Effect of apelin-13 analogues on cell viability under Aβ$_{42}$-Induced toxicity in SH-SY5Y cells in-vitro. Apelin-13 analogues restore cell viability when treated with and without Aβ$_{42}$ in SH-SY5Y cells *in-vitro*. MTT colorimetric assay based on the reduction of MTT to formazan was used to measure cell viability. Cells were treated at different timepoints (A) 2 hours, (B) 4 hour and (C) 24 hours. Data represents mean ±SEM one-way ANOVA, n=3 where *p<0.05, **p<0.01,***p<0.001, and ****p<0.0001 compared to control.

7.2.2: Effect of apelin-13 analogues against dose dependent deterioration of cell viability by $A\beta_{42}$ in SH-SY5Y cells.

The cell viability based on the ATP release from metabolic active cells was measured using the CellTiter-Glo viability kit at 6 hours in SH-SY5Y cells in-vitro. The results showed that the cell viability was significantly improved by apelin-13 amide by 16% (Figure 7.2, $p<0.01$) and by 8% (Figure 7.2, $p>0.05$) with (Lys^8GluPAL)apelin-13 amide, compared to untreated control. $A\beta_{42}$ reduced cell viability by 28% (Figure 7.2, $p<0.0001$), compared to untreated control. Co-treatments of $A\beta_{42}$ with apelin-13 analogues led to 15% (Figure 7.2, $p<0.01$) increase in cell viability, compared to Aβ-42 treatment alone.

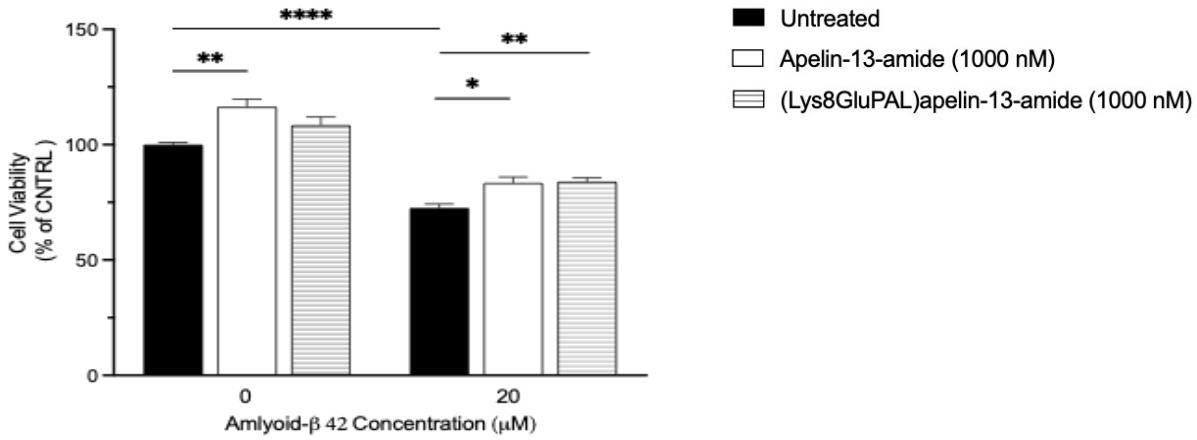

Figure 7.2: Effect of apelin-13 analogues against dose dependent deterioration of cell viability by $A\beta_{42}$ in SH-SY5Y cells. The protecting effect of apelin-13 on cell viability when stress-induced by $A\beta_{42}$ in SH-SY5Y cells *in-vitro* was measure by quantifying ATP present in cells. The cells were treated for 6 hours with and without the apelin-13 amide and (Lys^8GluPAL)apelin-13 amide and the Celltiter-Glo reagent was used to measure the viability. Values represents mean ±SEM for n=3 where *p<0.05, **p<0.01, ****p<0.0001.

7.2.3: Effect of apelin-13 analogues on cell proliferation in SH-SY5Y cells under Aβ-42-induced stress.

The cell proliferation of SH-SY5Y cells in-vitro was measured using the BrdU incorporation assay, where BrdU binds to the newly synthesized DNA. Representative images of BrdU immunofluorescent under Olympus Inverted Microscope at 20X magnification are shown Figure 7.3A. The results showed that compared to untreated control, apelin-13 amide and (Lys^8GluPAL)apelin-13 amide improved cell proliferation by 4% (Figure 7.3B, $p>0.05$) and 14% (Figure 7.3B, $p>0.05$) respectively and $A\beta_{42}$ reduced the cell proliferation by 36% (Figure 7.3B, $p<0.05$). Co-treatment of $A\beta_{42}$ with Apelin-13 amide improved cell proliferation by 37% (Figure 7.3B, $p>0.05$) and (Lys^8GluPAL)apelin-13 amide by 56% (Figure 7.3B, $p>0.05$).

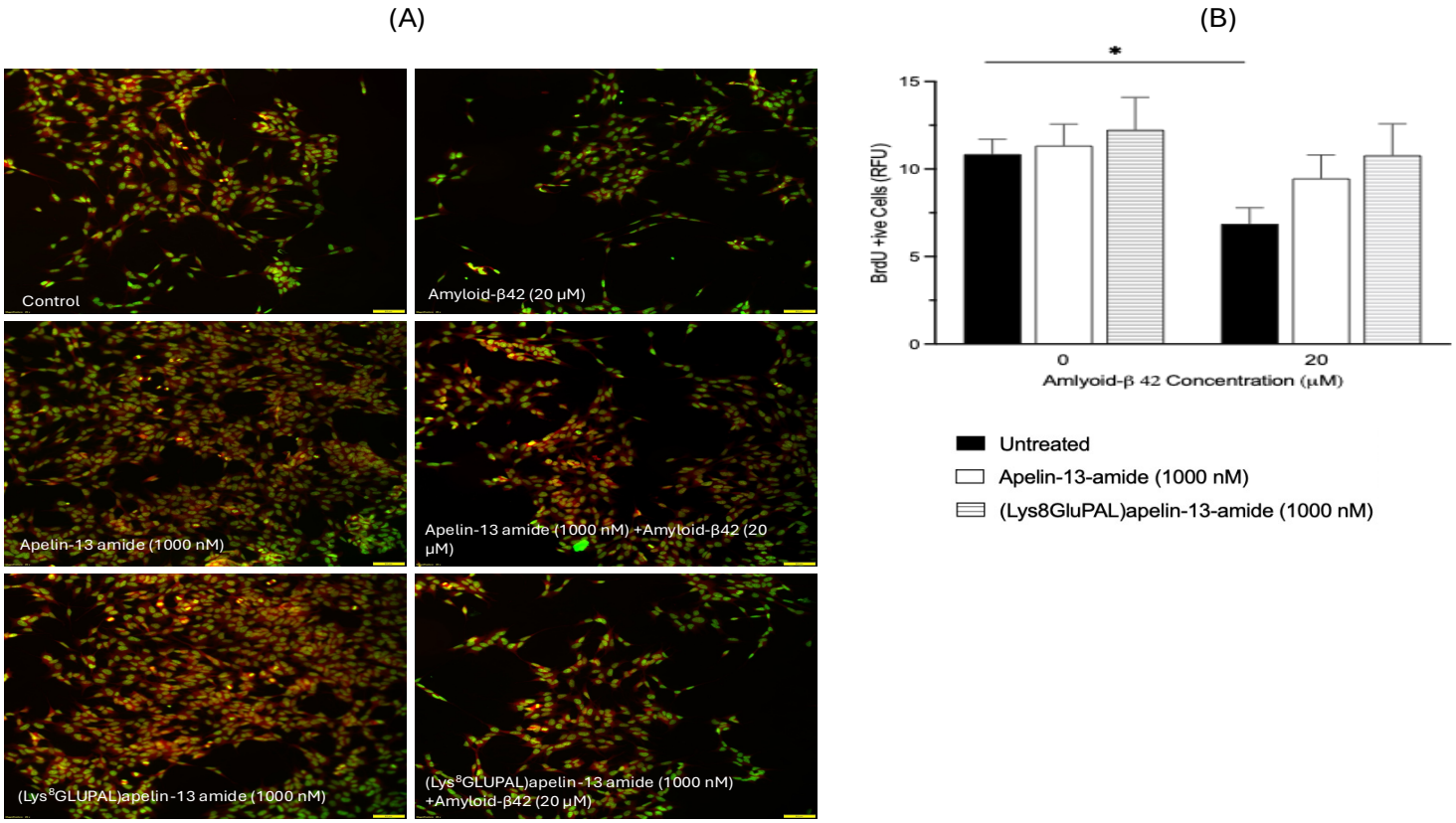

Figure 7.3: Effect of apelin-13 analogues on cell proliferation in SH-SY5Y. (A)Representative images of SH-SY5Y cells labelled with BrdU as pseudo green colour and DAPI as red colour captured at 20X magnification (B) Graph quantification of BrdU positive cells treated with $A\beta_{42}$ and Apelin-13 analogues treatments measured by image J and analysed by GraphPad PRISM. Images were captured using the Olympus inverted microscope and analysed the RFU as a measure of cell proliferation using Image J. Values represent mean ±SEM for n=3 where $^{*}p<0.05$.

7.2.4: Effect of apelin-13 analogues on neurite outgrowth.

The cells were differentiated with retinoic acid for 72 hours and treated with Apelin-13 analogues and $A\beta_{42}$ for 24 hours to look at the neuronal differentiation in SH-SY5Y cells in-vitro. The changes in morphology of the cells were seen under upright light microscope at 20X magnification and represented in Figure 7.4A. Coomassie brilliant blue staining method was used to look at the neurite extensions and were counted manually by observing neurites double the size of the cell body. Compared to untreated control, apelin-13 amide and (Lys^8GluPAL)apelin-13 amide showed non-significant growth in the neurite extensions by 12% (Figure 7.4B, $p>0.05$), and 21% (Figure 7.4B, $p>0.05$), respectively and $A\beta_{42}$ reduced the neurite outgrowth by 50% (Figure 7.4B, $p<0.001$). When the cells were treated with $A\beta_{42}$ and apelin-13 amide the neurite growth improved by 54% (Figure 7.4B, $p<0.01$) and 72% (Figure 7.4B, $p<0.05$) by (Lys^8GluPAL)apelin-13 amide, compared to $A\beta_{42}$ alone.

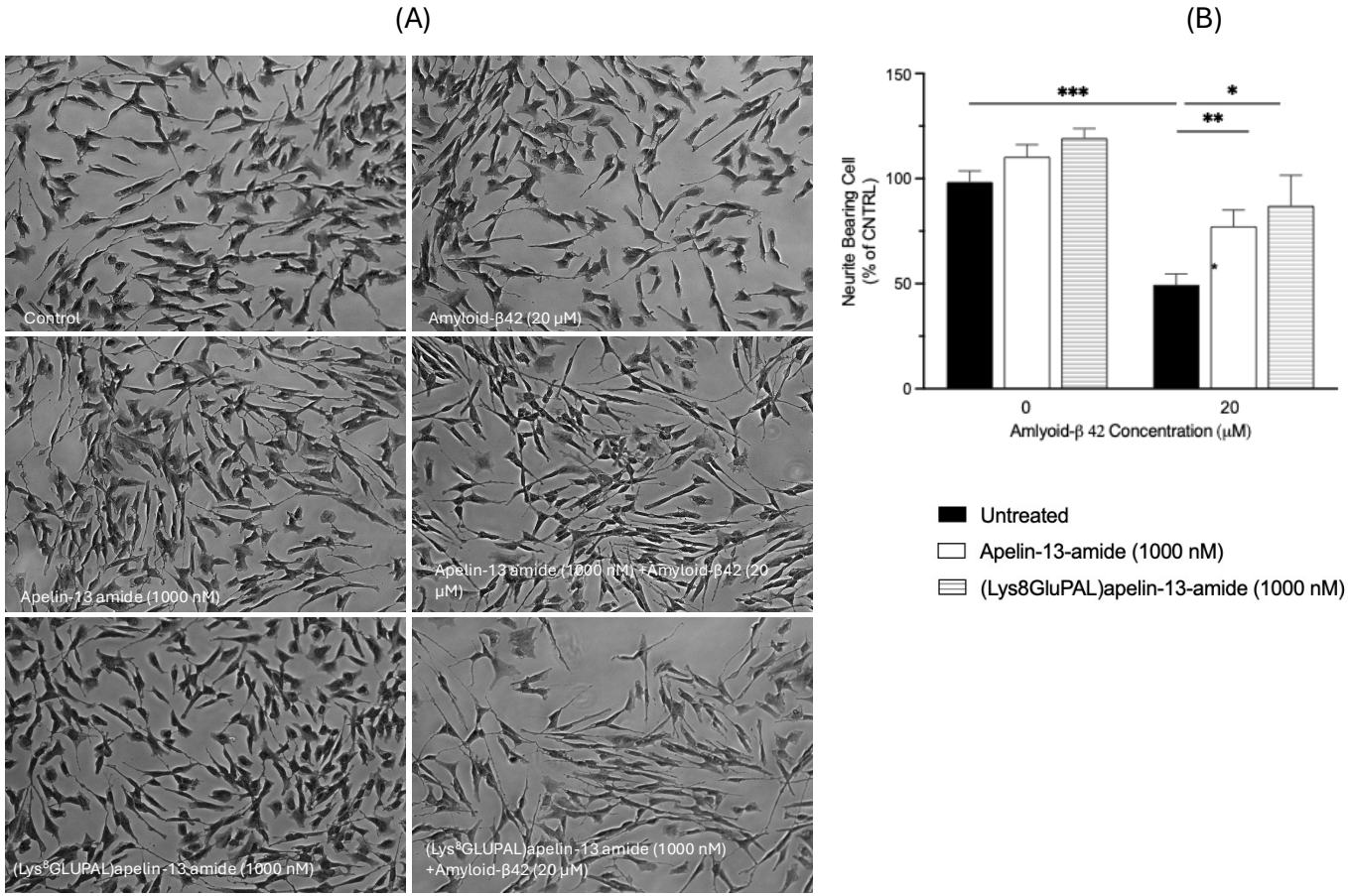

Figure 7.4: Effect of apelin-13 analogues on neurite outgrowth. Improved neurite outgrowth by Apelin-13 against $A\beta_{42}$-induced stress was measured using the Coomassie brilliant blue staining. The cells were treated with RA for 24 hours before treatments, (A) representative images of stained cells and (B) graph of neurite bearing cells analysed by GraphPad PRISM. Values represent mean ±SEM for n=3 where *p<0.05, **p<0.01, and ***p<0.001.

7.2.5: Effect of apelin-13 analogues on neuronal differentiation in SH-SY5Y cells under $A\beta_{42}$-induced stress.

The SH-SY5Y cells were labelled with MAP2 antibody to analyse the impact of apelin-13 analogues on the structural integrity in-vitro. The representative images in Figure 7.5A shows the MAP2 staining by DAB substrate under upright microscope at 20X magnification. The results illustrated that MAP2 expression compared to untreated control was increased by 11% (Figure 7.5B, $p>0.05$) with apelin-13 amide and 29% (Figure 7.5B, $p>0.05$) by (Lys^8GluPAL)apelin-13 amide, when treated with and without $A\beta_{42}$. The MAP2 was significantly reduced by 45% (Figure 7.5B, $p<0.01$) when treated with Aβ-42 alone, compared to untreated control. Co-treatment of $A\beta_{42}$ with apelin-13 amide led to increase by 25% (Figure 7.5B, $p>0.05$) and with (Lys^8GluPAL)apelin-13 amide by 17% (Figure 7.5B, $p>0.05$), compared to $A\beta_{42}$ treatment.

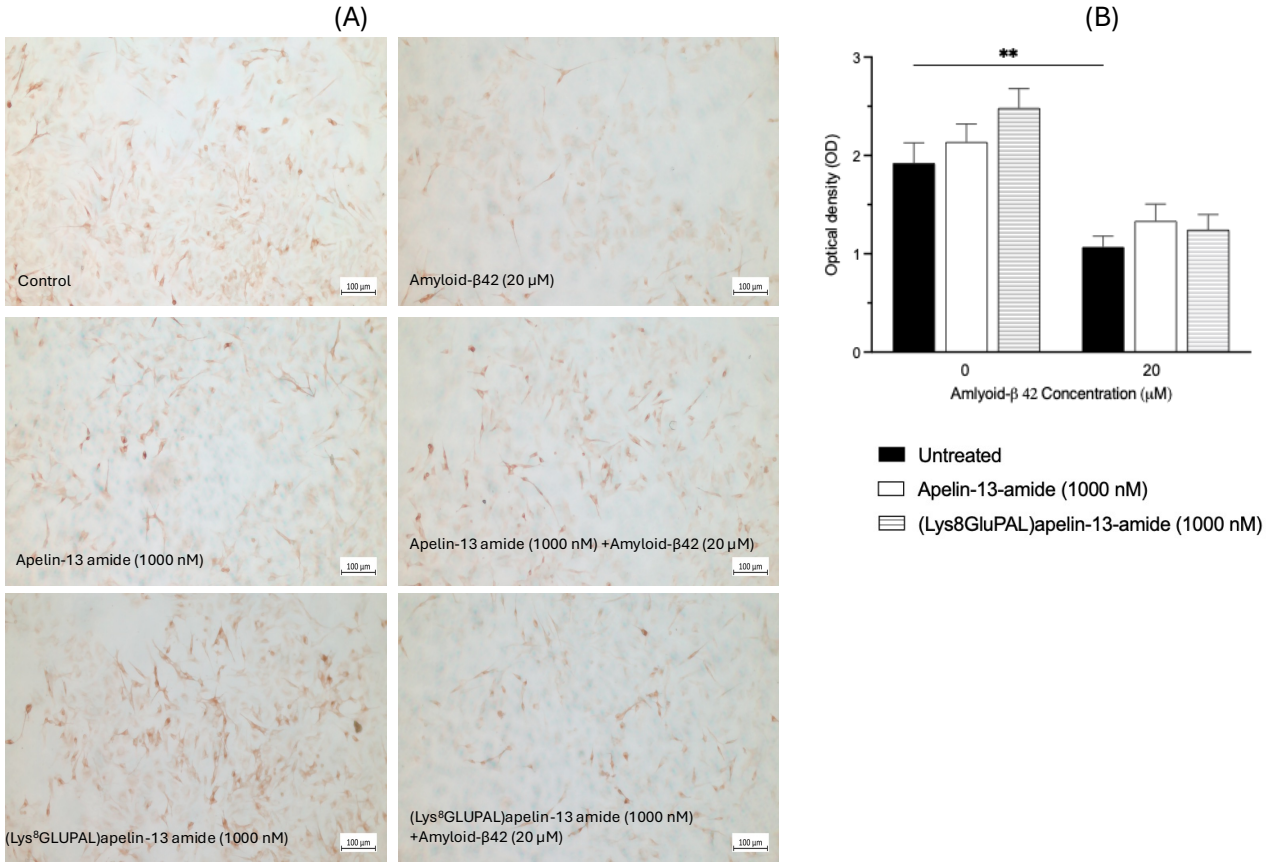

Figure 7.5: Effect of apelin-13 analogues on neuronal differentiation in SH-SY5Y cells under $A\beta_{42}$-induced stress. (A) Representative photographs depicting MAP2 expression induced by apelin-13 analogues against Aβ-42 induced stress in SH-SY5Y cells. (B) graph showing quantification of MAP2 expression under Light microscope. The cells were differentiated with RA prior to apelin-13 and Aβ-42 treatments. Values represent mean ±SEM for n=3 where **p<0.01.

7.2.6: Effect of apelin-13 analogues on cell toxicity induced by $A\beta_{42}$ in SH-SY5Y cells.

LDH assay to measure the release of the Lactate dehydrogenase enzyme from damaged cells as an indicator of cell toxicity. The results showed that at 2 hour the cell toxicity was significantly reduced by 18% (Figure 7.6A, $p<0.001$) with apelin-13 amide and 17% (Figure 7.6A, $p<0.001$) with (Lys^8GluPAL)apelin-13 amide and increased by 25% (Figure 7.6A, $p<0.0001$) with Aβ-42 , compared to untreated control. Both apelin-13 amide (39% reduction, Figure 7.6A, $p<0.0001$) and (Lys^8GluPAL)apelin-13 amide (37% reduction, Figure 7.6A, $p<0.0001$) restored $A\beta_{42}$ induced cell toxicity.

The treatments with apelin-13 amide and (Lys^8GluPAL)apelin-13 amide at 4 hours showed significant reduction in cell toxicity by 30% (Figure 7.6B, $p<0.0001$) and 33% (Figure 7.6B, $p<0.0001$) respectively and increased by 27% (Figure 7.6B, $p<0.0001$) with $A\beta_{42}$ compared to untreated control. The cell toxicity was reduced when cells were co-currently treated with $A\beta_{42}$ and apelin-13 amide by 11% (Figure 7.6B, $p<0.001$) and by 12% (Figure 7.6B, $p<0.0001$) with Aβ-42 and (Lys^8GluPAL)apelin-13 amide, compared to $A\beta_{42}$ treatment alone.

At 24 hours both apelin-13 analogues showed no changes to cell toxicity (Figure 7.6C, $p>0.05$), though it was increased by 16% (Figure 7.6C, $p<0.0001$) with $A\beta_{42}$ treatment. The co-treatment of $A\beta_{42}$ with apelin-13 amide reduced cell toxicity y 10% (Figure 7.6C, $p<0.001$) and with (Lys^8GluPAL)apelin-13 amide by 13% (Figure 7.6C, $p<0.0001$), compared to $A\beta_{42}$ treatment alone.

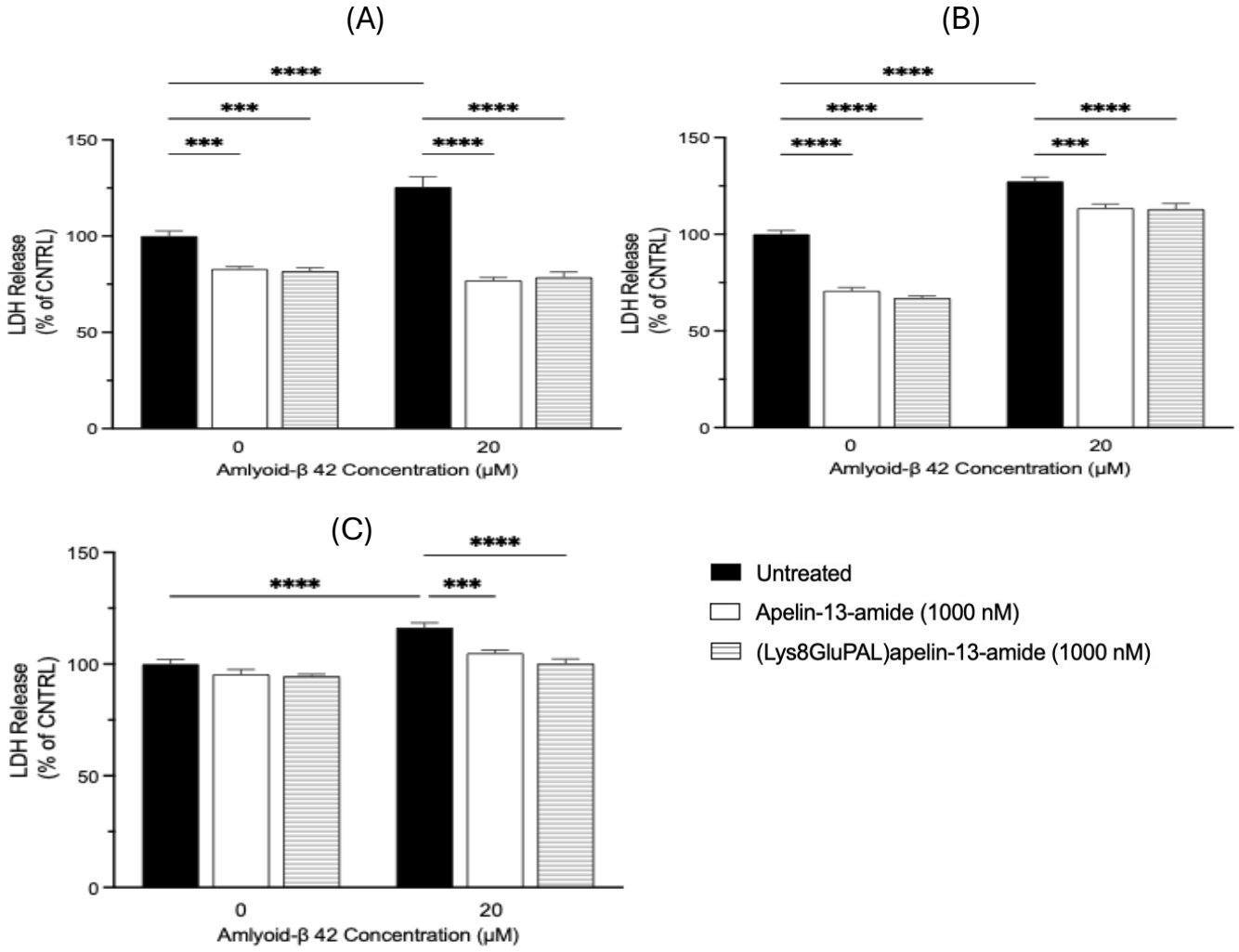

Figure 7.6: Effect of apelin-13 analogues on cell toxicity induced by $A\beta_{42}$ in SH-SY5Y cells. LDH cytotoxicity assay showing the percentage of cell death in SH-SY5Y cells treated with $A\beta_{42}$ and apelin-13 analogues alone and combined for (A) 2 hours, (B) 4 hours and (C) 24 hours. GraphPad PRISM was used analyse the data and values represents mean ±SEM for n=3 where ***p<0.001, and ****p<0.001.

7.2.7: Effect of apelin-13 analogues on cell toxicity measured by DNA damage in SH-SY5Y cells.

The real-time cell toxic effect of $A\beta_{42}$ and role of apelin on toxicity was confirmed using the CellTox Green cytotoxicity assay kit in SH-SY5Y cells in-vitro. The cells were treated with $A\beta_{42}$, apelin-13 amide or (Lys^{8}GluPAL)apelin-13 amide alone and co-currently for 6 hours. The data showed that the cell toxicity was significantly reduced by 20% (Figure 7.7, $p<0.01$) by apelin-13 amide and 22% (Figure 7.7, $p<0.001$) by (Lys^{8}GluPAL)apelin-13 amide at 6 hours, however $A\beta_{42}$ increased the cell toxicity by 30% (Figure 7.7, $p<0.01$) when compared to untreated control. The co-current treatments of $A\beta_{42}$ with apelin-13 amide showed reduction in cell toxicity by 18% (Figure 7.7, $p<0.05$) and by 17% (Figure 7.7, $p>0.05$) for (Lys^{8}GluPAL)apelin-13 amide, compared to $A\beta_{42}$ treatment alone.

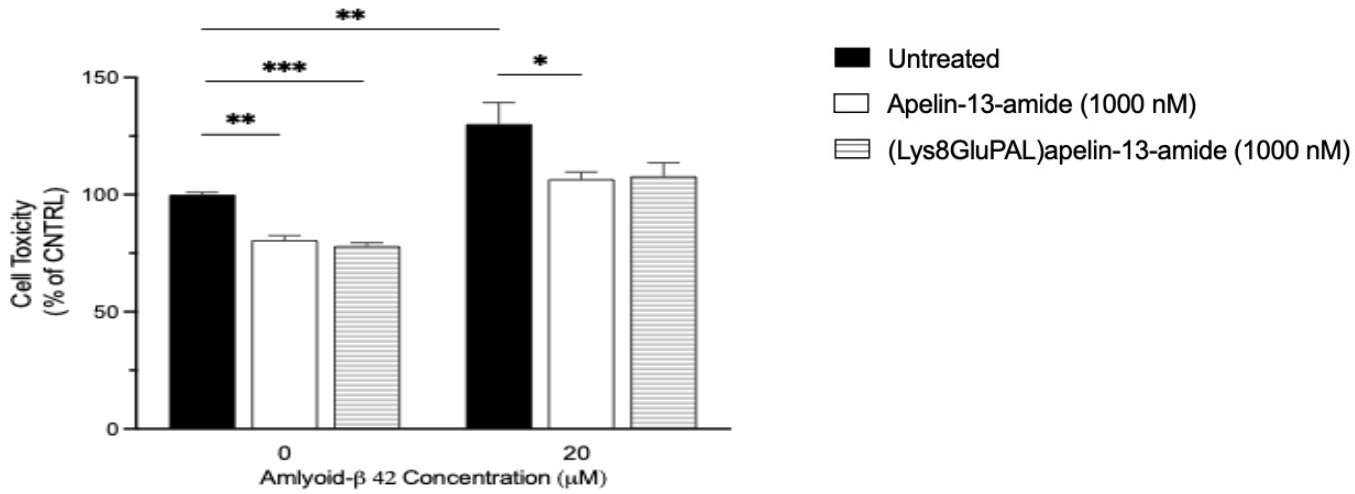

Figure 7.7: Effect of apelin-13 analogues on cell toxicity measured by DNA damage in SH-SY5Y cells. $A\beta_{42}$ induced cell toxicity was mitigated by apelin-13 amide and (Lys^{8}GluPAL)apelin-13 amide in SH-SY5Y cells. The cells were seeded and treated with treatment for 6 hours and cell toxicity was measured by detecting the DNA released from cells into medium. Values represents mean ±SEM for n=3 where *p<0.05, **p<0.01, and ***p<0.001.

7.2.8: Effect of apelin-13 analogues on cellular redox balance in and oxidative stress in SH-SY5Y cells.

The ROS levels and the GSH/GSSG balance was measured in SH-SY5Y cells in-vitro in cells treated with apelin-13 analogues and $A\beta_{42}$. The results indicated that compared to untreated control, the ROS levels had no change when cells were treated alone with apelin-13 amide and (Lys^{8}GluPAL)apelin-13 amide (Figure 7.8A, $p>0.05$), however $A\beta_{42}$ treatment led to a significant rise in ROS by 47% (Figure 7.8A, $p<0.05$). Apelin-13 amide had no significant change when co-currently treated with $A\beta_{42}$ (Figure 7.8A, $p>0.05$) and (Lys^{8}GluPAL)apelin-13 amide reduced the ROS% by 14% (Figure 7.8A, $p>0.05$), compared to $A\beta_{42}$treatment alone.

The GSH/GSSG ratio was reduced non significantly by apelin-13 amide (10%reduction, Figure 7.8B, $p>0.05$) and (Lys^{8}GluPAL)apelin-13 amide (11% reduction, Figure 7.8B, $p>0.05$) treatment alone and $A\beta_{42}$ reduced significantly by 50% (Figure 7.8B, $p<0.01$), compared to untreated control. Compared to $A\beta_{42}$ the GSH/GSSG ratio was increased but not significantly by 10% (Figure 7.8B, $p>0.05$) and 14% (Figure 7.8B, $p>0.05$) for apelin-13 amide and (Lys^{8}GluPAL)apelin-13 amide respectively.

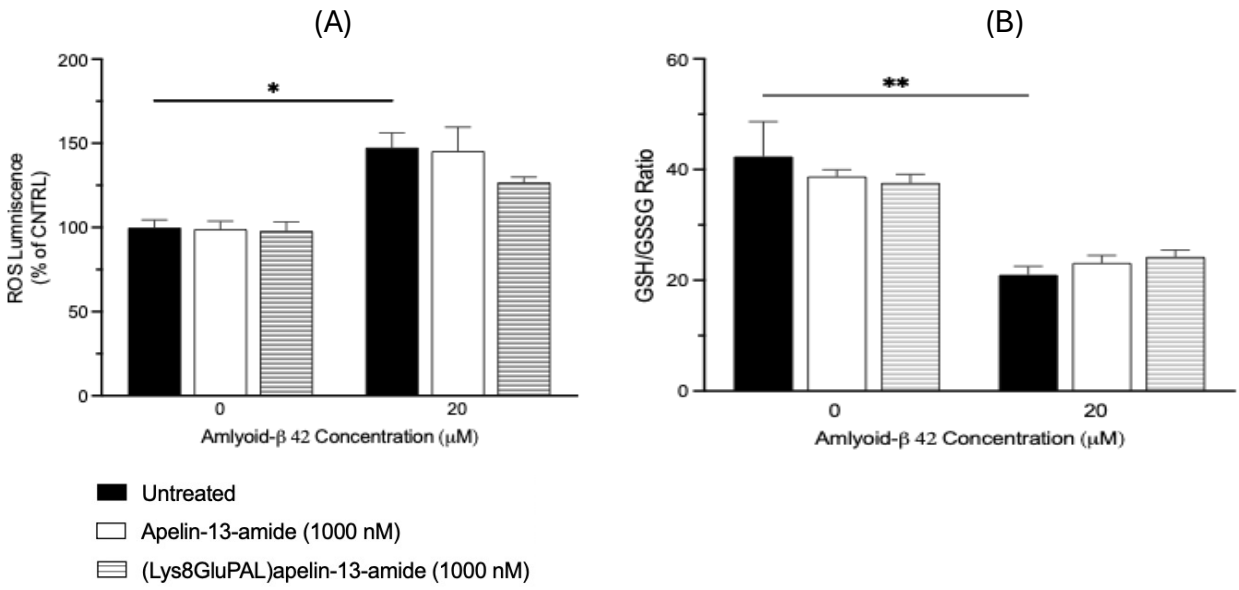

Figure 7.8: Effect of apelin-13 analogues on cellular redox balance in and oxidative stress in SH-SY5Y cells. The ROS and GSH/GSSG ratio were measured in SH-SY5Y cells treated with $A\beta_{42}$ and apelin-13 analogues. The cells were treated for 6 hours (A) ROS% and (B) is the GSH/GSSG ratio graph analysed by One-Way ANOVA. Values represents mean ±SEM for n=3 where *p<0.05, and **p<0.01.

7.2.9: Effect of apelin-13 analogues on mitochondrial membrane potential under Aβ-42-induced stress.

JC-1 dye was used to measure the mitochondrial membrane potential in SH-SY5Y cells in-vitro. The JC-1 is commonly used to study mitochondrial health and when it enters in the mitochondria and forms aggregates in healthy cells emitting red fluorescence. In damaged cells it remains in monomers and emit green light. . The results showed that apelin-13 amide and (Lys^{8}GluPAL)apelin-13 amide both increased the intensity of JC-1 Red/Green ratio by 83% (Figure 7.9B, $p<0.05$) and 60% (Figure 7.9B, $p>0.05$) respectively, indicating improved mitochondrial membrane potential, however $A\beta_{42}$ reduced it by 83% (Figure 7.9B, $p<0.01$), compared to untreated control. Compared to

$A\beta_{42}$ treatment alone, the mitochondrial membrane potential was restored by 305% (Figure 7.9B, $p<0.01$), by apelin-13 amide and by 238% (Figure 7.9B, $p<0.01$), by $A\beta_{42}$ and (Lys^{8}GluPAL)apelin-13 amide.

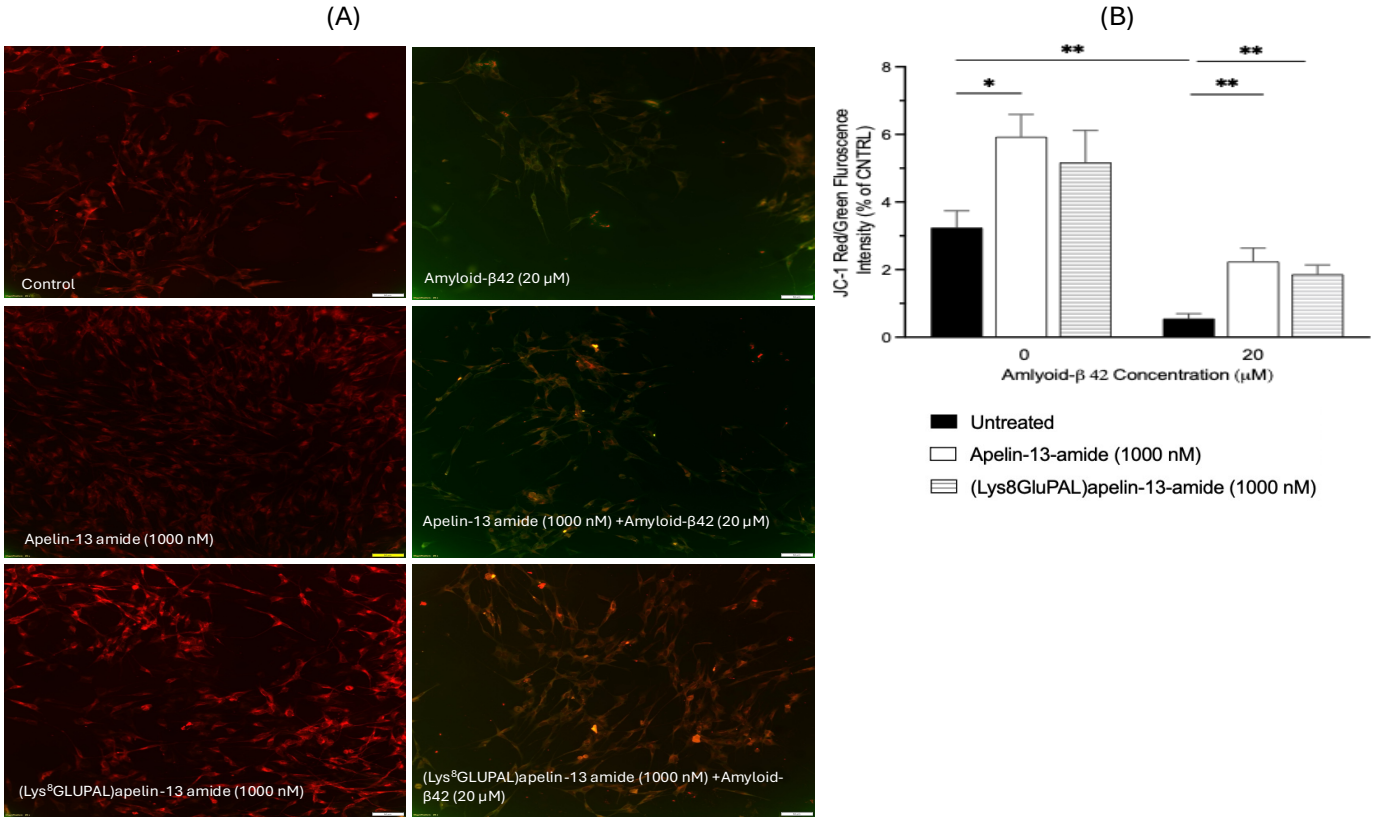

Figure 7.9: Effect of apelin-13 analogues on mitochondrial membrane potential under Aβ42-induced stress. The Mitochondrial membrane potential in SH-SY5Y cells *in-vitro* was measured by JC-1 staining method. The cells were microscope at 20X magnification. (A) representative images of SH-SY5Y cells stained with JC-1 dye and (B) is the graph of the Red/Green florescent ratio. Values represent mean ±SEM for n=3 where *p<0.05, and **p<0.01.

7.2.10: Effect of Apelin-13 analogues on apoptosis under Aβ-42 - induced stress.

The apoptosis induced by $A\beta_{42}$ and the protective role of apelin-13 analogues was measured by caspase3/7-Glo activity kit in SH-SY5Y cells in-vitro. The cells were treated alone and together with $A\beta_{42}$, apelin-13 amide and (Lys^8GluPAL)apelin-13 amide for 24 hours and the results indicated that apelin-13 amide was able to reduce the apoptosis by 24% (Figure 7.10, $p<0.01$) and (Lys^8GluPAL)apelin-13 amide by 30% (Figure 7.10, $p<0.05$) compared to untreated control. However, the caspase 3/7 activity was increased significantly by 1077% (Figure 7.10, $p<0.0001$) when treated with $A\beta_{42}$. Compared to Aβ-42 alone, the caspase 3/7 activity was restored significantly by 54% (Figure 7.10, $p<0.0001$) by apelin-13 amide and by 54% (Figure 7.10, $p<0.0001$) with (Lys^8GluPAL)apelin-13 amide.

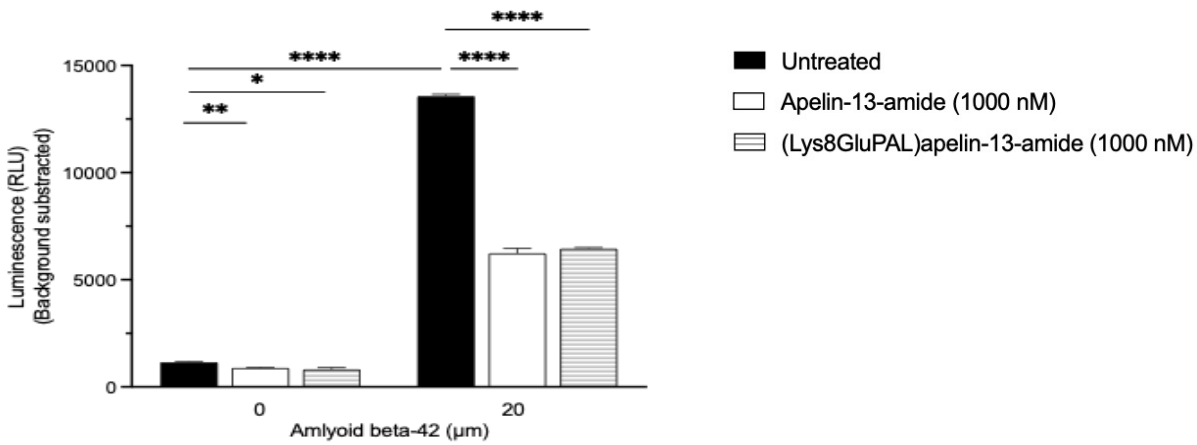

Figure 7.10: Effect of apelin-13 analogues on apoptosis under $A\beta_{42}$-induced stress. SH-SY5Y cells were treated with apelin-13 analogues with and without $A\beta_{42}$ to induce apoptosis for 24 hours. The apoptosis was measured using caspase-Glo 3/7 assay and fold change from control was calculated and analysed by GraphPad PRISM. Values represents mean ±SEM for n=3 where *p<0.05, **p<0.01, and ****p<0.0001.

7.2.11: Effect of apelin-13 analogues on expression of NRF-2 under Aβ-42 -induced stress.

The cells were seeded and treated for 24 prior to the harvesting and GAPDH is used as a loading control. The western blot results for NRF-2 expression no significant change when treated with apelin-13 amide or (Lys^{8}GluPAL)apelin-13 amide (Figure 7.11, $p>0.05$) but increased by 14% (Figure 7.11, $p>0.05$) when treated with $A\beta_{42}$, compared to untreated control. The NRF-2 expression was reduced by 32% (Figure 7.11, $p>0.05$) and 15% (Figure 7.11, $p>0.05$) when the cells were co-currently treated with apelin-13 amide or (Lys^{8}GluPAL)apelin-13 amide with $A\beta_{42}$ respectively, compared to $A\beta_{42}$ treatment alone.

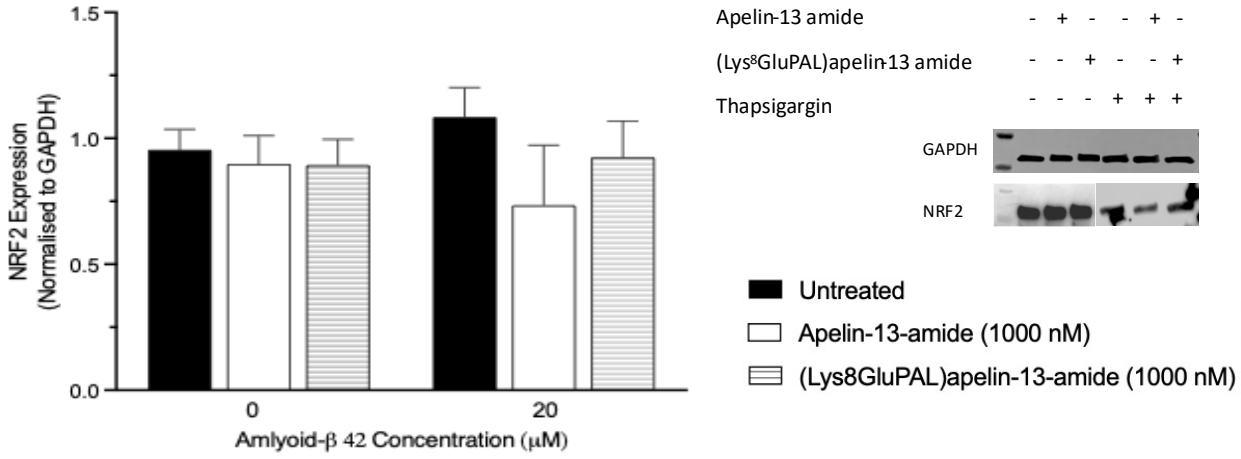

Figure 7.11: Effect of apelin-13 analogues on expression of NRF-2 under $A\beta_{42}$-induced stress. Apelin-13 amide and (Lys^{8}GluPAL)apelin-13 amide mitigated the effect of $A\beta_{42}$ and resolves the UPR in the SH-SY5Y cells in-vitro. After 24 hours seeding the cells were serum starved and treated with the $A\beta_{42}$ with and without the apelin-13 analogues for 24 hours. GAPDH was used as a loading control. Quantitative analysis was performed using densitometry, and data were analysed using One-Way ANOVA. Values are presented as mean ± SEM for n = 3.

7.2.12: Effect of apein-13 analogues apoptotic pathway under $A\beta_{42}$-induced stress in SH-SY5Y cells.

Apelin-13 role on the apoptosis related proteins like BAX and Bcl-2 was analysed using western blot. The cells were treated for 24 hours with apelin-13 amide and (Lys^{8}GluPAL)apelin-13 amide with and without $A\beta_{42}$. The results showed that the expression of pro-apoptotic protein BAX had no significant change when treated with apelin-13 analogues (Figure 7.12A, $p>0.05$) but increased by 85% when treated with $A\beta_{42}$ (Figure 7.12A, $p>0.05$). This increase was mitigated when co-treated with either apelin-13 amide (47% reduction, Figure 7.12A, $p>0.05$) or (Lys^{8}GluPAL)apelin-13 amide (56% reduction, Figure 7.12A, $p<0.05$). The expression of Bcl-2, an anti-apoptotic protein was reduced by 14% (Figure 7.12B, $p>0.05$) when treated with $A\beta_{42}$, but increased by 10% (Figure 7.12B, $p>0.05$) with apelin-13 amide and 17% (Figure 7.12B, $p>0.05$) with (Lys^{8}GluPAL)apelin-13 amide, compared to untreated control. Compared to $A\beta_{42}$ treatment alone, the expression of Bcl2 was increased by 43% (Figure 7.12B, $p>0.05$) and 27% (Figure 7.12B, $p>0.05$) when treated with apelin-13 amide and (Lys^{8}GluPAL)apelin-13 amide respectively. To analyse the balance between the pro-apoptotic and anti-apoptotic proteins BAX/Bcl-2 ratio was quantified. The results indicated that there was no change when treated with (Lys^{8}GluPAL)apelin-13 amide, but the ratio was increased by 21% (Figure 7.12C, $p>0.05$) with apelin-13 amide and 78% (Figure 7.12C, $p>0.05$) with $A\beta_{42}$, compared to untreated control. the co-treatment of $A\beta_{42}$ with apelin-13 amide reduced the ratio by 51% (Figure 7.12C, $p>0.05$) and 62% (Figure 7.12C, $p>0.05$) with (Lys^{8}GluPAL)apelin-13 amide, compared to $A\beta_{42}$ treatment alone.

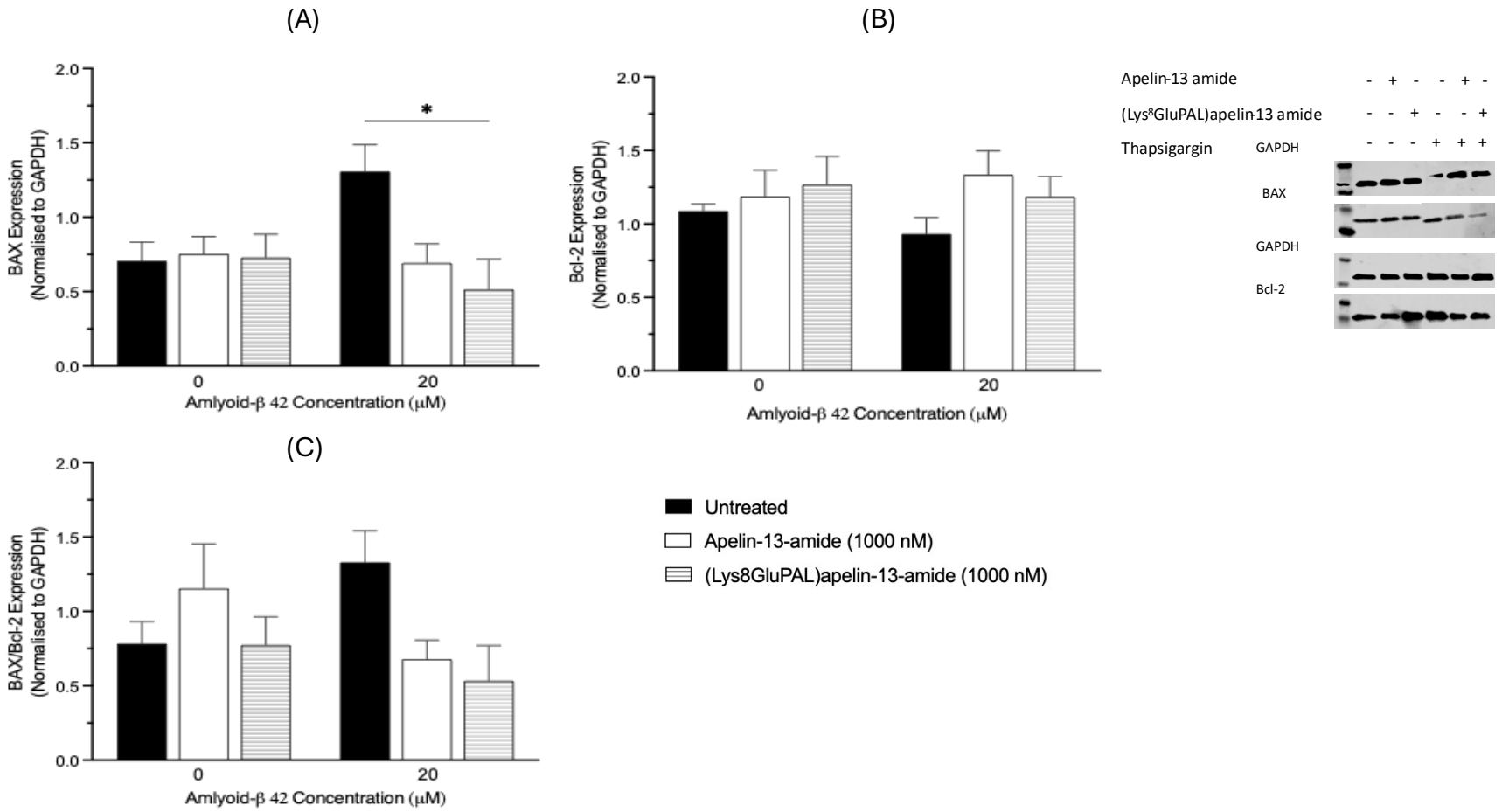

Figure 7.12: Effect of apein-13 analogues apoptotic pathway under Aβ$_{42}$-induced stress in SH-SY5Y cells. Western blot analysis of protein involved in apoptosis when cells exposed to Aβ$_{42}$ and Apelin-13 analogues co-treatments for 24 hours. The relative quantification of Protein (A) BAX, (B) Bcl-2 and (C) BAX/Bcl-2 were normalized by GAPDH. Values represents average ± SEM for n=3.

7.2.13: Effect of apelin-13 analogues on ER stress response under Aβ-42 -induced stress.

To analyse the pathways involved in the ER stress induced by $A\beta_{42}$, we looked at the expression of IRE1α and BiP in SH-SY5Y cells. The results showed that treatments with apelin-13 amide and (Lys^{8}GluPAL)apelin-13 amide led to a decline in the expression of IRE1a by 12% (Figure 7.13A, p>0.05) and 13% (Figure 7.13A, p>0.05) respectively, but apelin-13 analogues had no impact on the expression of BiP (Figure 7.13A, p>0.05), compared to untreated control. However, when treated with $A\beta_{42}$, the IRE1α had no change (Figure 7.13A, p>0.05) and BiP expression increased by 10% (Figure 7.13B, p>0.05), compared to untreated control. When treated with apelin-13 amide and $A\beta_{42}$, the IRE1α and BiP expression was reduced by 20% (Figure 7.13A, p>0.05) and 26% (Figure 7.13B, p>0.05) respectively, compared to $A\beta_{42}$ treatment alone. Compared to $A\beta_{42}$, the co-treatment of $A\beta_{42}$ and (Lys^{8}GluPAL)apelin-13 amide reduced expression by 12% (Figure 7.13A, p>0.05) of IRE1α and 7% (Figure 7.13B, p>0.05) of BiP.

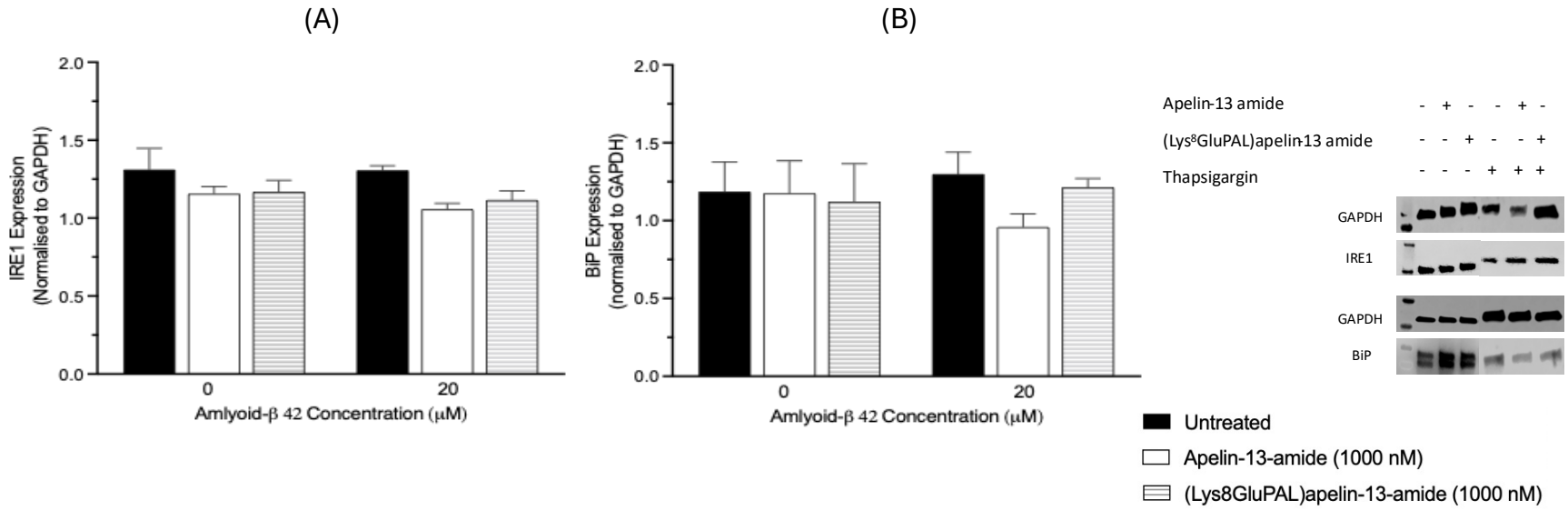

Figure 7.13: Effect of apelin-13 analogues on ER stress response under Aβ$_{42}$-induced stress. Western blot analysis was performed to assess the protein expression of the IRE1a and BiP in SH-SY5Y cells *in-vitro*. The cells were treated with and without the Aβ$_{42}$ to look at the protective effect of apelin-13 amide and (Lys^{8}GluPAL)apelin-13 amide. (A) the graph representation of the IRE1α and (B) graph representation of BiP. GAPDH was used as a loading control and the band intensity was measured by image J. Data was normalised with GAPDH and analysed by one-way ANOVA. Data are presented as mean ±SEM for n=3.

7.2.14: Effect of apelin-13 analogues on ER stress markers under $A\beta_{42}$-induced stress in SH-SY5Y cells.

The protein expression of major quality-control chaperons like Ero1-Lα (ER oxidoreductase 1α), Calnexin, PDI, and PERK proteins were analysed by western blot to evaluate the restorative effect of apelin-13 analogues on the UPR and ER proteostasis . The results showed that apelin-13 amide and (Lys^8GluPAL)apelin-13-amide increased the expression of Calnexin by 37% (Figure 7.14A, $p>0.05$) and 17% (Figure 7.14A, $p>0.05$), however the expression was reduced by 25% (Figure 7.14A, $p>0.05$) $A\beta_{42}$ compared to untreated alone. Co-treatments with apelin-13 amide and $A\beta_{42}$ increased the calnexin expression by 125% (Figure 7.14A, $p>0.05$) and 95% (Figure 7.14A, $p>0.05$) with (Lys^8GluPAL)apelin-13-amide, compared to $A\beta_{42}$ treatment alone.

Apelin-13 analogues did not change the expressions of Ero1-Lα (Figure 7.14B, $p>0.05$) and PDI (Figure 7.14C, $p>0.05$) but increased the expression of PERK by 10% (Figure 7.14D, $p>0.05$). The $A\beta_{42}$ treatment alone led to a decrease by 43% (Figure 7.14B, $p>0.05$) for Ero1-Lα and 19% (Figure 7.14C, $p>0.05$) for PDI but increased the expression of PERK by 40% (Figure 7.14D, $p>0.05$), compared to untreated control. The co-treatment of $A\beta_{42}$ with apelin-13 amide increased expression of Ero1-Lα by 24% (Figure 7.14B, $p>0.05$), however reduced the expression of PDI by 51% (Figure 7.14C, $p<0.05$) and PERK by 6% (Figure 7.14D, $p>0.05$). Compared to $A\beta_{42}$ treatment, co-treatment of $A\beta_{42}$ with (Lys^8GluPAL)apelin-13-amide increased the Ero1-Lα expression by 24% (Figure 7.14B, $p>0.05$) and reduced by 16% (Figure 7.14C, $p>0.05$) of PDI and 12% (Figure 7.14D, $p>0.05$) of PERK.

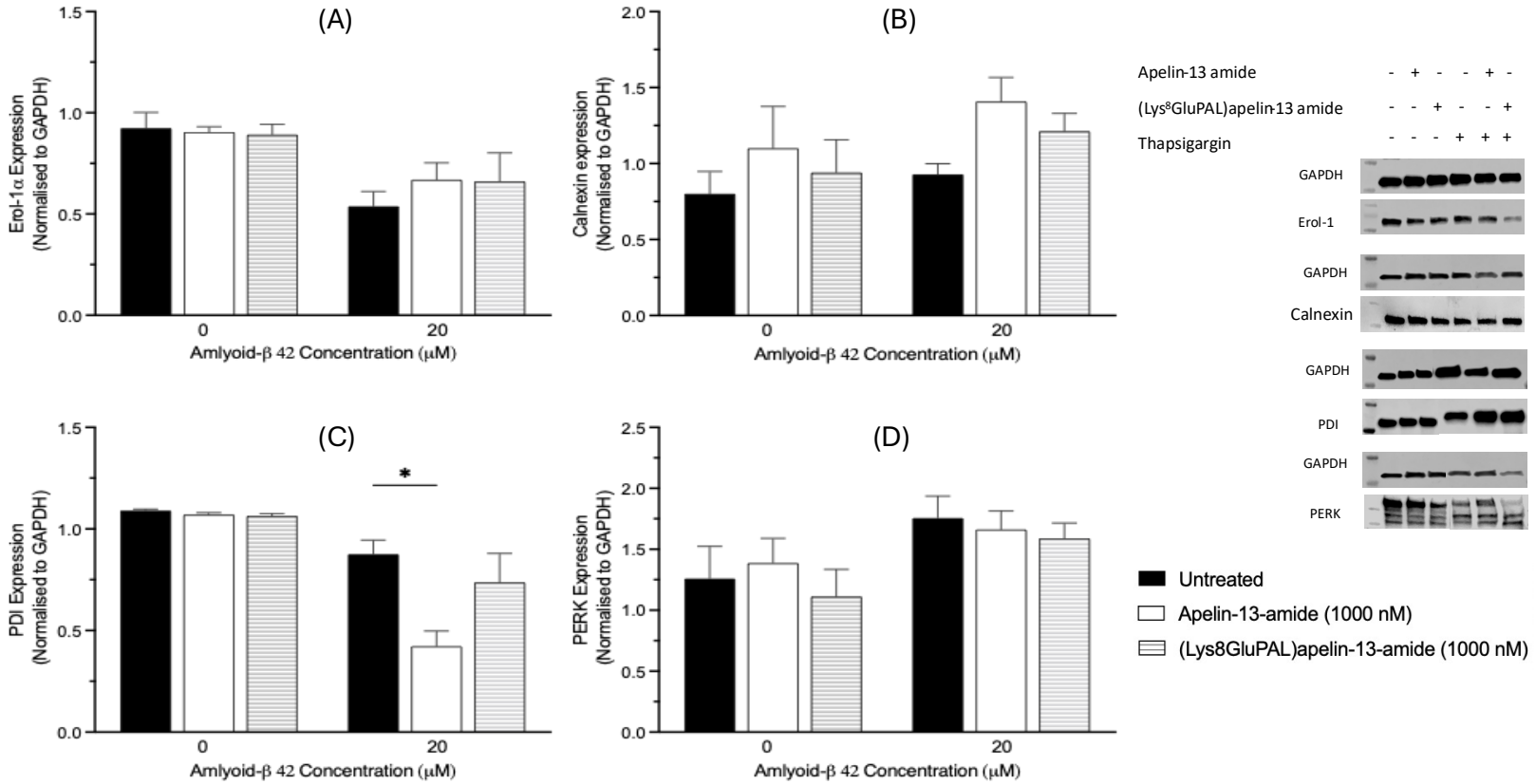

Figure 7.14: Effect of apelin-13 analogues on ER stress markers under Aβ$_{42}$-induced stress in SH-SY5Y cells. Impact of apelin-13 analogues on expression of ER associated protein under stress by Aβ$_{42}$ was measured using western blot, (A) is expression of Calnexin, (B) Ero1-Lα (C) PDI and (D) PERK in SH-SY5Y cells. The cells were treated for 24 hours before harvesting and the results were normalised with GAPDH. Data is expressed as fold change to untreated control and analysed by one-way ANOVA. Values represents mean ±SEM for n=3 where *p<0.05.

7.2.15: Effect of apelin-13 analogues on expression of autophagy-related proteins under $A\beta_{42}$-induced stress.

Autophagy related proteins expression under ER stress induced by $A\beta_{42}$ in SH-SY5Y cells was measured by western blot analysis. One-way ANOVA analysis revealed that apelin-13 amide and (Lys^8GluPAL)apelin-13-amide did not significantly change the expression of ATG3, ATg7 and ATG5 (Figure 7.15A, $p>0.05$). $A\beta_{42}$ slightly reduced ATG3 expression by 10% (Figure 7.15A, $p>0.05$), ATG7 expression by 20% (Figure 7.15B, $p>0.05$) and increased ATG5 expression by 9% (Figure 7.15C, $p>0.05$), compared to untreated control. Compared to the $A\beta_{42}$ alone, co-treatment of apelin-13 amide and $A\beta_{42}$ improved the ATG3 expression by 24% (Figure 7.15A, $p>0.05$), ATG7 expression by 27% (Figure 7.15B, $p>0.05$) and reduced ATG5 expression by 4% (Figure 7.15C, $p>0.05$). The ATG3 expression was increased by 17%, (Figure 7.15A, $p>0.05$), ATG7 by 25% (Figure 7.15B, $p>0.05$) and ATG5 expression reduced by 13% (Figure 7.15C, $p>0.05$) when treated concurrently with $A\beta_{42}$ and (Lys^8GluPAL)apelin-13-amide.

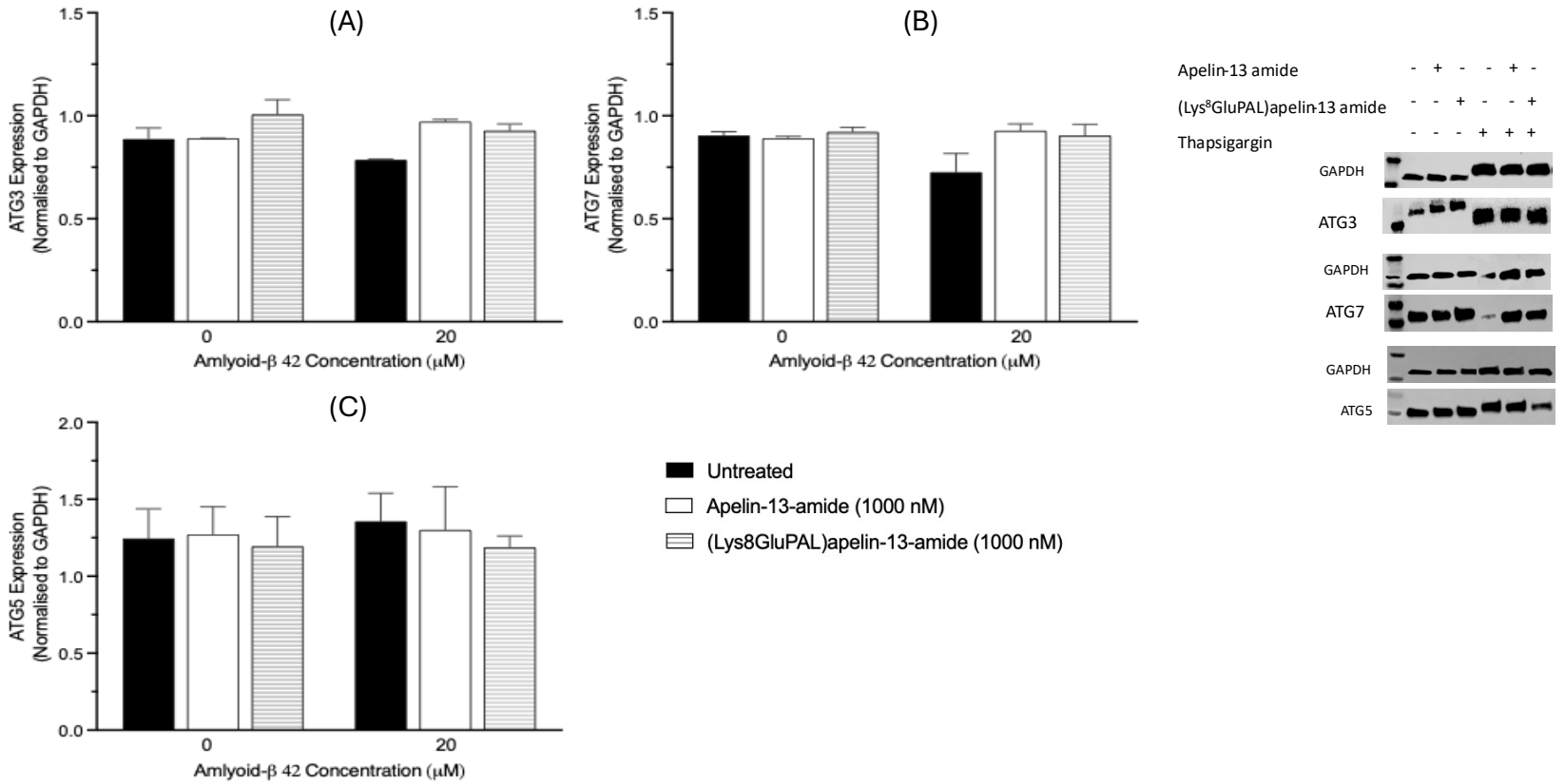

Figure 7.15: Effect of apelin-13 analogues on expression of autophagy-related proteins under Aβ$_{42}$-induced stress. Autophagy related protein expression in SH-SY5Y cells were measured by western blot (A) ATG3, ATG7 and (C) ATG5. The cells were treated with apelin-13 analogue and Aβ$_{42}$ for 24 hours before harvesting. The results were normalized by GAPDH and analysed using One-Way ANOVA. Values represents mean ±SEM for n=3.

7.2.16: Effect apelin-13 on cell viability and toxicity in AMPK regulated pathways through AMPK knockdown and inhibition by compound C.

To examine if AMPK was involved in the survival effect of apelin-13 amide and (Lys^{8}GluPAL)apelin-13 amide on cell apoptosis induced by $A\beta_{42}$, we knocked down AMPKα by SiRNA plasmid specific for AMPK in SH-SY5Y cells. After 24 hours of transfection, we determined cell viability and cell toxicity. In non-transfected cells, cell viability was reduced by 46% with $A\beta_{42}$ treatments (Figure 7.16A, $p<0.0001$). The co-treatment of apelin-13 amide restored the cell viability by (97% increase, Figure 7.16A, $p<0.0001$) and (Lys^{8}GluPAL)apelin-13 amide by (79% increase, Figure 7.16A, $p<0.0001$), compared to untreated control. Cells with AMPK knockdown showed that apelin-13 analogues were not able to restore cell viability but further reduced by 47% with co-treatments of $A\beta_{42}$, compared to non-transfected co-treatments.

The cell toxicity was shown in Figure 7.16B, where apelin-13 amide and (Lys^{8}GluPAL)apelin-13 amide's protective effect was attenuated. The cell toxicity was increased by 21% (Figure 7.16B, $p<0.0001$) for $A\beta_{42}$ treatment compared to untreated control and reduced significantly by co-treatment of $A\beta_{42}$ with apelin-13 analogues (22%, Figure 7.16B, $p<0.0001$). However, when the AMPK was knockdown, apelin-13 analogues had no significant impact on the cell toxicity induced by $A\beta_{42}$ (Figure 7.16B, $p>0.05$). The results indicate that apelin-13 works by AMPK signalling pathway.

To further investigate the effect of AMPK, we used compound C an AMPK inhibitor and used cell viability and cell toxicity assay. The SH-SY5Y cells were seeded for 24 hours following an incubation with compound c for 30 minutes and then treated with $A\beta_{42}$, apelin-13 amide and (Lys^{8}GluPAL)apelin-13 amide. The results showed that cell viability was enhanced when treated with apelin-13 amide by 23% (Figure 7.16C, $p<0.05$) and 25% (Figure 7.16C, $p<0.01$) by (Lys^{8}GluPAL)apelin-13 amide, compared to untreated control, However, the cell viability was reduced by 14% (Figure 7.16C, $p>0.05$) with $A\beta_{42}$. The co-treatment of $A\beta_{42}$ with apelin-13 amide resulted in significant improvement in cell

viability by 30% (Figure 7.16C, $p<0.01$) and for (Lys^8GluPAL)apelin-13 amide by 33% (Figure 7.16C, $p<0.01$), compared to $A\beta_{42}$ treatment alone. However, compound C treated cells showed that apelin-13 amide and (Lys^8GluPAL)apelin-13 amide had no significant change in viability (Figure 7.16C, $p>0.05$), and $A\beta_{42}$ significantly reduced cell viability by 25% (Figure 7.16C, $p<0.01$), compared to untreated control. The co-treatments of apelin-13 analogues with $A\beta_{42}$ did not make any significant change compared to $A\beta_{42}$ treatment alone (Figure 7.16C, $p>0.05$).

The cell toxicity was reduced by 11% (Figure 7.16D, $p>0.05$) with apelin-13 amide and 15% (Figure 7.16D, $p<0.05$) with (Lys^8GluPAL)apelin-13 amide, but $A\beta_{42}$ led to 90% (Figure 7.16D, $p<0.0001$) increase, compared to untreated control. Compared to and $A\beta_{42}$ alone, cell toxicity was significantly reduced by 48% (Figure 7.16D, $p<0.0001$) with co-treatment of apelin-13 amide with $A\beta_{42}$, and by 44% (Figure 7.16D, $p<0.0001$) with co-treatment of (Lys^8GluPAL)apelin-13 amide with $A\beta_{42}$.

Conversely, when cells were incubated with compound C prior to the apelin-13 analogue treatments, the cell toxicity had no impact (Figure 7.16D, $p>0.05$) and increased by 90% (Figure 7.16D, $p<0.0001$) when treated with and $A\beta_{42}$, compared to untreated control. The co-treatment had no significant effect of apelin-13 analogues on the cell toxicity induced by $A\beta_{42}$ (Figure 7.16D, $p>0.05$), compared to $A\beta_{42}$ treatment alone.

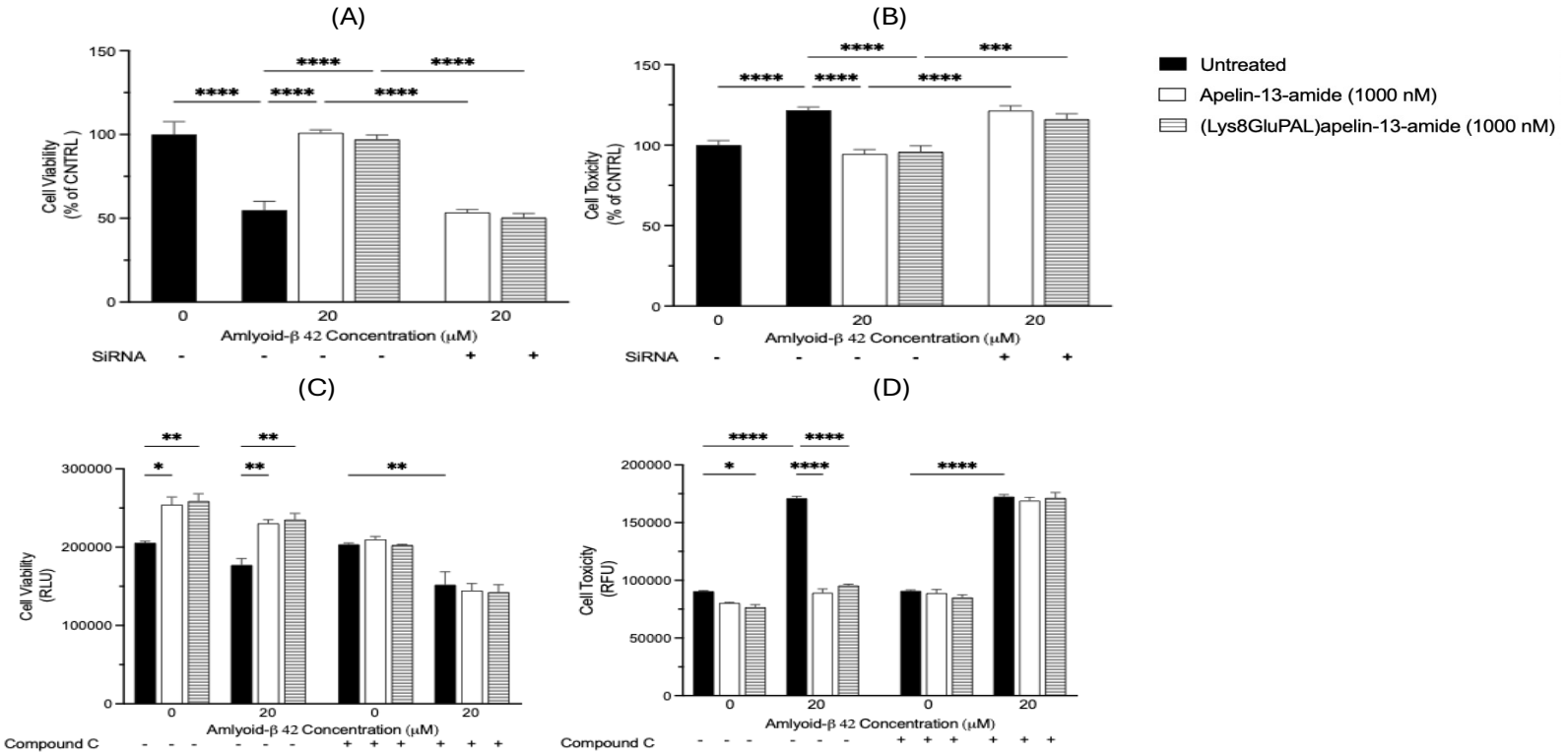

Figure 7.16: Effect apelin-13 on cell viability and toxicity in AMPK regulated pathways through AMPK knockdown and inhibition by compound C. To look at the impact of apelin-13 analogue's protective effect via AMPK pathway, AMPK knockdown by SiRNA ad AMPK inhibitor compound C was used to measure cell viability and cell toxicity. (A) Cell viability after AMPK knockdown by SiRNA (B) cell toxicity after AMPK knockdown by SiRNA (C) cell viability when cells treated with and without compound c and (D) cell toxicity when cells treated with and without compound c in SH-SY5Y cells. Values represents mean ±SEM for n=3 where *p<0.05, **p<0.01, ***p<0.001and ****p<0.0001.

7.3: Discussion

In this chapter we looked at the impact of apelin-13 amide and (Lys8GluPAL)apelin-13-amide on the cell survival, growth and the protective effect under stress induced by amyloid beta-42 in SH-SY5Y cells. Apelin-13 is known to have a protective effect against the cellular stress, and we have used apelin-13 amide and (Lys^{8}GluPAL)apelin-13-amide due to its longer half-life and bioavailability. Aβ_{42} is known to have the adverse effect on the neuronal health, and it is a common hallmark of the AD.

Cell Viability

The Aβ_{42} showed a decline in cell viability via several interconnected mechanisms like oxidative stress, inflammation, mitochondrial dysfunction and apoptosis (Fukui et al., 2017). Aβ_{42} is prone to aggregation due to its hydrophobic nature, and it forms neurotoxic soluble oligomers and insoluble fibrils (Song et al., 2022). Previous studies have suggested that amyloid beta accumulation is the leading cause to AD and both intra cellular and extra cellular peptide cause cytotoxicity (Haque et al., 2022). Decrease in cell viability due to the Aβ_{42} accumulation in SH-SY5Y cells has been reported previously (Song et al., 2022).

Results shows that apelin-13 analogues restored cell viability under Aβ_{42}-induced stress. Apelin-13 is used in previous studies to look at the effect on the cell survival, cell growth in obesity, diabetes, metabolic bone disease, and cardiovascular diseases (Wen et al., 2023). A study showed that apelin-13 had a protective effect against the destructive effect of Aβ and apelin-13 suppressed both autophagy and apoptosis (Aminyavari et al., 2019). Apelin-13 works as an anti-inflammatory agent and suppresses oxidative reaction induced by ROS, apoptosis and inflammatory response (Yan et al., 2020).

Cell proliferation and differentiation

In this chapter we focused on the impact of apelin-13 analogues on the cell proliferation and differentiation under stress induced by $A\beta_{42}$. $A\beta_{42}$ exerts its toxic effect by engaging pathways like JNK, MAPK, UPR, caspase activation and ERK1/2 leading to apoptosis and impaired proliferation and differentiation (Saha et al., 2020). The results indicated that apelin-13 analogues have the capacity to improve the cell proliferation and differentiation under $A\beta_{42}$ induced cytotoxicity in SH-SY5Y cells. Previous studies have stated that $A\beta_{42}$ induces stress by pathways like ROS, ER stress, and mitochondrial dysfunction (Butterfield & Boyd-Kimball, 2018). Our results align with the previous studies showing that apelin-13 promotes pro-apoptotic and anti-apoptotic signalling pathways, such as PI3K/Akt, NRF-2 and AMPK, via its interaction with APJ receptor. These pathways play an essential role for cell survival and proliferation under stress conditions (Duan et al., 2019). The activation of the PI3K/Akt signalling pathway, which encourages cell survival and blocks apoptotic processes, is one of the methods by which apelin-13 mediates its neuroprotective benefits (Jiang et al., 2018).

MAP2 is a marker for mature neurons, the MAP2 assay is used to look at the neuronal differentiation of SH-SY5Y cells (Soltani et al., 2005). MAP2 expression was markedly decreased by $A\beta_{42}$, demonstrating compromised differentiation and possibly a loss of neuronal identity. This finding is in line with research showing that tau hyperphosphorylation and disruption of neurotrophic signalling pathways like BDNF/TrkB are two mechanisms by which $A\beta_{42}$ disrupts cytoskeletal integrity and hinders differentiation (Gao et al., 2022). Equally, MAP2 expression was restored after apelin-13 analogues treatments, proposing that it can promote neuronal differentiation. The restoration effect of the apelin-13 analogues attributed to its role in modulating the NRF-2 pathway, which leads to the antioxidant defense and mitigate the effect of oxidative stress on the neuronal differentiation (Fibbi et al., 2023).

To further look at the protective impact of apelin-13 analogues on neurite length and branching we used in-vitro neurite outgrowth assay, as critical indicator of neuronal health and functionality. Our results showed that the neuronal length was significantly

reduced when the cells were treated with $A\beta_{42}$ which can be due to the disruption of cytoskeletal dynamics and inhibition of Rho GTPase signalling, which is aa key regulator of the neurite outgrowth (Petratos et al., 2007). The treatment of $A\beta_{42}$ with apelin-13 analogues led to the restored neurite outgrowth suggesting apelin-13's protective effect against the stress induced by $A\beta_{42}$. Study by Zhang et al, illustrated that the $A\beta_{42}$ aggregated led to the impaired neurite outgrowth in SH-SY5Y cells (2022). Studies have shown that apelin-13 promotes cell proliferation and differentiation by activation of PI3/Akt pathway, ERK1/2, AMPK, and NRF-2 pathways (Zhong et al., 2016) (Li et al., 2022). These findings suggest that apelin-13 analogues can be used to restore the cell proliferation, differentiating and neurite lengths, under stress-induced by $A\beta_{42}$.

Cell toxicity

To measure the cell toxicity- induced by $A\beta_{42}$, we used two different cell toxicity assays, one is based on the LDH release in the medium and for three different timepoints, and the other was based on the detecting damaged DNA in SH-SY5Y cells. Our results from both assays illustrated that there was significant release of LDH and damaged DNA in the cells treated with the $A\beta_{42}$, compared to the untreated cells indicating the stress induced by the $A\beta_{42}$. The cell co-currently treated with $A\beta_{42}$ and apelin-13 analogues indicated that apelin-13 mitigate the cell toxicity induced by $A\beta_{42}$.This aligns with the previous findings indicating that $A\beta_{42}$ leads to cell toxicity via oxidative stress, activation of apoptotic pathways and caspase-3 and capase-9. The time-dependent analysis showed the consistency of apelin-13 analogues and sustained protective effect at different timepoints. In addition, SH-SY5Y exposed to $A\beta_{42}$ induced toxicity can modify cell cycle progression by activating MAPK-ERK1/2 (Song et al., 2022). Recent research on the ischemic models shows that apelin-13 has the capability to enhance the neurogenesis and protect against the oxidative stress and upregulate the expression of antioxidant enzymes (Duan et al., 2019).

Mitochondrial and oxidative stress

Mitochondrial dysfunction and oxidative stress are the key factors in the progression of AD and $A\beta_{42}$ is shown to aggravate the stress (Wang et al., 2014). Intracellular accumulation in the cells, including mitochondria leads to the cellular dysfunction (Reddy & Beal, 2008). To investigate the role of apelin-13 analogues on the oxidative stress and mitochondrial dysfunction induced by $A\beta_{42}$, we used JC-1 assay to measure mitochondrial potential, ROS (Reactive oxygen species), GSH/GSSG assay as an indicator of redox balance and NRF-2 protein expression as a marker for antioxidant response by western blot. Our results illustrated that apelin-13 amide and (Lys^{8}GluPAL)apelin-13-amide has protective effect against the stress induced by $A\beta_{42}$ in SH-SY5Y cells.

Our results showed that cells treated with $A\beta_{42}$ had significant reduction in the red/green fluorescence ratio, reflecting compromised mitochondrial integrity and possible apoptotic activation. $A\beta_{42}$-induced mitochondrial depolarization is a hallmark of mitochondrial dysfunction and attributed to calcium dysregulation, increased ROS generation, and impairment of the electron transport chain (Han et al., 2017; Chen & Yan, 2007). However, apelin-13 analogues restored the red/green fluorescence ratio, showing the maintenance of mitochondrial membrane potential and protection of mitochondrial health. Research have shown that apelin-13 possibly protect through activation of pathways such as AMPK and PI3K/Akt, which are known to maintain mitochondrial bioenergetics and protect against stress-induced damage (Yang et al., 2016).

The ROS assay showed that there was significantly increase in ROS levels by the $A\beta_{42}$ treatment indicating the oxidative burden caused by $A\beta_{42}$. However, when the cells were treated with apelin-13 analogues there was no significant change was seen in ROS levels, which can be due to the excessive ROS production under $A\beta_{42}$ induced stress and this overwhelms the cells or the concentration of apelin-13 analogues (Simpson & Oliver, 2020). Although the studies have shown the protective effect of apelin-13 analogues at higher concentrations (2μg, 5μg and 10μg) on ROS production and mitigate the oxidative stress (Oruç et al., 2025). Similarly, GSH/GSSG ratio, an

indicator of redox balance was significantly reduced by the $A\beta_{42}$ treatment indicating the oxidative stress (Zitka et al., 2012), whereas the treatment with apelin-13 analogues did not significantly protect the cells against the oxidative stress, suggesting its limited effect and impact on the intrinsic antioxidant mechanism under severe oxidative stress. Previous, studies have shown that apelin-13 have protective effect against the oxidative stress and improves the GSH/GSSG ratio (Li et al., 2024).

Apoptosis

Apoptosis is the key factor in progression of AD and $A\beta_{42}$ is the well-known apoptotic pathway induced in the neuronal cells (Yao et al., 2005). In this chapter we focused on the role of apelin-13 analogues on apoptosis induced by $A\beta_{42}$, and we used caspase 3/7 assay as a marker for caspase activation and BAX/Bcl-2 expression by western blot to analyse balance between pro-apoptotic and anti-apoptotic signals. The results showed that apelin-13 mitigated the $A\beta_{42}$-induced apoptosis which could be due to modulation of key signalling pathways like JNK, p38 MAPK and AMPK (Yao et al., 2005). The increased caspase 3/7 activity by $A\beta_{42}$ indicates the activation of the intrinsic apoptotic pathway and trigger of mitochondrial dysfunction, release of cytochrome c and ROS production (Li et al., 2022). However, the co-treatment of $A\beta_{42}$ with apelin-13 analogues led to the significant decline in caspase activity indicating the protective role against the apoptotic signalling by activating AMPK and PI3K/Akt pathways known to inhibit the caspase activation to preserve the cell survival (Xing et al., 2011).

To further analyse the impact of apelin-13 we looked at the expression of BAX and Bcl-2 and it showed that the $A\beta_{42}$ treatments led to the increased BAX/Bcl-2 ratio indicating activation of the apoptosis pathway (Paradis et al., 1996). The co-treatment of the apelin-13 amide and (Lys^{8}GluPAL)apelin-13-amide led to the reduced ratio of BAX/Bcl-2 due to the protective effect, suggesting the shift toward the cell survival. Studies have showed that apelin-13 analogues activate the Akt, which phosphorylates and inhibits pro-apoptotic proteins like BAX and increases the production of anti-apoptotic proteins like Bcl-2 (Cheng et al., 2021).

ER stress and UPR pathway

ER stress is an important physiological process including cell survival and homeostasis that are triggered in pathological situations like stress produced by $A\beta_{42}$ (Yang et al., 2020). The accumulatio of misfolded proteins in ER triggers the UPR, a protective mechanism mediated by ATF6, IRE1 and PERK to cope with the protein misfolding's and restore proteostasis (Yang et al., 2020). Prolonged UPR activated under sustained stress, disrupts the protein homeostasis and leads to apoptosis, caspase-12 activation and ER stress (Yang et al., 2020). In AD, persistent ER stress exacerbates neuroinflammation, synaptic dysfunction and tau hyperphosphorylation accelerating neurodegeneration (Hiramatsu et al., 2015). We looked at the impact of the apelin-13 analogues on the key ER stress markers and UPR pathways via western blot analysis. The results revealed that PERK was significantly activated when treated $A\beta_{42}$ and it aligns with the previous study stating that the $A\beta_{42}$ disrupted in the protein folding by AMPK and leading to the phosphorylation of eIF2 α in response to ER stress (Teske et al., 2011).

$A\beta_{42}$ did not change the levels of IRE1α, but expression was reduced when co-treated with apelin-13. This indicates that apelin-13 suppresses UPR, maybe by improving proteostasis or lowering upstream stresses. Apelin-13 reduced ATF6 and BiP levels, which were stable with $A\beta_{42}$ treatments, suggesting that apelin-13 plays a part in reducing misfolded protein load and ER stress signaling. Improved ER oxidative capacity was indicated by the reduction of ERO1α, an enzyme essential for oxidative protein folding, with $A\beta_{42}$ and its restoration with apelin-13 (Zito et al., 2010). The reduction of PDI, another protein-folding enzyme, with $A\beta_{42}$ and apelin-13, on the other hand, may indicate a compensatory adjustment in the regulation of redox enzymes. Glycoprotein folding chaperone calnexin expression increased slightly with $A\beta_{42}$ and more prominently with apelin-13 analogues, suggesting an increased protein folding capacity. Recent study illustrated that apelin-13 treatment inhibits the IRE1α and JNK activation, indicating apelin modulates JNK-regulated cell death pathways and IRE1α-associated ER stress (Chen et al., 2011). By activating the PI3K/Akt pathway, apelin-13 reduces ER stress-induced apoptosis in endothelial cells, signifying a possible therapeutic use of apelin-13 for ER stress-related disorders (Chen et al., 2011). Recent

studies have shown that apelin-13 mitigate the pro-apoptotic signalling pathways triggered by $A\beta_{42}$ and reduce the expression of ER stress markers like ATF6, IRE1 and BiP (Xu et al., 2018). Apelin-13's capacity to alter important pathways implicated in $A\beta_{42}$-induced neurotoxicity has made it an intriguing therapeutic option in the setting of AD.

Autophagy

Autophagy is an important process in the neurodegenerative diseases process to maintain the cellular homeostasis by degrading the damaged organelles and misfolded proteins (Guo et al., 2017). To determine the impact of apelin-13 analogues we looked at the autophagy related proteins ATG3, ATG5 and ATG7 and the results indicated that $A\beta_{42}$ treatments significantly reduced the expression of ATG3 and ATG7, key enzymes involved in the autophagosome elongation and formation. The reduction in the expression suggest that $A\beta_{42}$ treatment disrupts the autophagy by inhibiting pathways like AMPK/mTOR (Wang & Jia, 2023). The expression of the ATG5 had no significant change that can be due to the sensitivity of the protein towards the oxidative stress. The co-treatment of $A\beta_{42}$ with apelin-13 amide led to the non-significant rise in ATG3 and ATG7, suggesting that apelin-13 analogues are involved in the restoration of autophagic function by reactivating the early stages of autophagosome formation. Apelin-13 promotes the autophagy by AMPK pathway, a key pathway for the restoration and it inhibits the mTOR signalling pathway (Wang & Jia, 2023). Conversely, ATG5 expression was reduced with apelin-13 co-treatment with $A\beta_{42}$, and this reduction may reveal a shift in the regulation of autophagosome maturation. Studies showed that the decreased ATG5 expression with apelin-13 might represent a feedback mechanism to optimize autophagic efficiency or to prevent overactivation of autophagy, which can be detrimental in certain contexts (JIAO et al., 2013).

The NRF-2 expression analysis showed that $A\beta_{42}$treatment led to the increased expression of NRF-2 due to the oxidative stress and co-treatment with apelin-13 analogues mitigated the stress by activating the NRF-2 pathway. Studies have shown that NRF-2 activation by apelin-13 led to protective effect against the oxidative stress

(Duan et al., 2019). Studies showed that NRF-2, a transcription factor that controls the production of antioxidant genes like heme oxygenase-1 (HO-1) and NAD(P)H quinone dehydrogenase 1 (NQO1), has been demonstrated to be activated by apelin-13 (Lu et al., 2024). Apelin-13 improves the cellular antioxidant response by encouraging the activation of NRF-2, which lowers ROS levels and stops oxidative damage (Lu et al., 2024). Apelin-13 exerts its protective effect by modulation the oxidative stress and ER stress and by activating AMPK and UPR pathways (Kim et al., 2020).

Mechanism action of apelin-13 analogues

AMPK is a cellular energy sensor important for cell growth, proliferation, survival and metabolic regulation, that can regulate glycolysis and fatty acid production to provide energy under hypoxic, ischemic and nutritional deficiency conditions (Liu et al., 2014). To maintain fundamental resources and energy for cells during metabolic crises, active AMPK suppresses biosynthetic enzymes such as mTOR and acetyl CoA carboxylase, which are necessary for protein and lipid synthesis, respectively (Foretz et al., 1998). The apelin-13 analogues showed to regulate AMPK pathway and to confirm that we have used compound C, an AMPK inhibitor and SiRNA transfections to knockdown of AMPK (Kong et al., 2021).

The results confirmed that apelin-13 analogues work via AMPK activation as the cell viability and cell toxicity for both compound C treated cells and transfected cells with siRNA showed that when the AMPK was inhibited there was no changes seen in the cell viability with apelin-13 analogues compared to the ones without the AMPK inhibition. Study by Kong et al, showed that AMPK inhibition by compound C markedly decreased the apelin-13 analogues improved mitochondrial potential (2021). Study showed that apelin-13 analogues can modulates PI3K/Akt and ERK1/2 pathways involved in cell survival and inhibit apoptotic signalling (Yang et al., 2014).Previous study showed that apelin-13 analogues induced glucose uptake and Akt phosphorylation were significantly reduced in the presence of compound C, suggesting that AMPK is certainly involved in mediating the effects of apelin-13 analogues (Yue et al., 2010).

7.4: Conclusion

To conclude, the apelin-13 amide and (Lys^{8}GluPAL)apelin-13-amide had protective effect against Aβ_{42}-induced stress in SH-SY5Y cells. Aβ_{42} is known to disrupts the cellular mechanism by inducing ER stress, oxidative stress, mitochondrial dysfunction, cell toxicity and affecting the proliferation and cell survival. Apelin-13 analogues have demonstrated the ability to mitigate the negative impact of the Aβ_{42} and restore the cellular homeostasis. Apelin-13 revealed a multifaceted mode of action that addressed both stress resolution and cellular recovery through modulation of important signalling pathways, such as AMPK activation and NRF-2-mediated antioxidant responses (shown in table 7). This study supports the therapeutic potential of apelin-13 analogues in reducing the cellular damage by various stressors and its potential to treat AD.

Experiments	Assays Used	$A\beta_{42}$ Effect	Apelin-13 Effect	Pathway Impact
Cell Viability	MTT, CellTiter-Glo	↓ cell viability	↑ viability under $A\beta_{42}$-induced stress	PI3K/Akt activation for cell survival signalling
Proliferation & Differentiation	BrdU, MAP2, Neurite Outgrowth	↓ cell proliferation and neurite outgrowth	↑ cell proliferation and ↑ neurite outgrowth	PI3K/Akt/mTOR for proliferation, ERK/MAPK for differentiation
Cell Toxicity	LDH, CellTox Green	↑cell toxicity	↓ toxicity	AMPK activation, NRF-2-linked antioxidant response and UPR regulation
Mitochondrial & Oxidative Stress	JC-1, ROS-Glo, GSH/GSSG, Hyper-7	↓ MMP, ↑ ROS, disturbed redox balance	↑ MMP, ↓ ROS, normalized redox balance	AMPK/NRF-2 pathway activated, mitochondrial support
Apoptosis	Caspase 3/7, BAX, Bcl-2	↑ apoptosis, ↑ pro-apoptotic and ↓ anti-apoptotic protein expression	↓ caspase activity, ↓ BAX and ↑ Bcl-2 expression	PI3K/Akt inhibits apoptosis, AMPK/MAPK inhibit caspase activation
ER Stress & UPR	ATF6, NRF-2, PERK, BiP, PDI, Calnexin	↑ ER stress markers	↓ ATF6, PERK, BiP, and calnexin	Reduced ER stress via AMPK and PI3K/Akt modulation and UPR pathway
Autophagy	ATG3, ATG5, ATG7	↓ autophagy related proteins	↑ expression of autophagy proteins	AMPK inhibits mTOR and promotes autophagy
AMPK Role Confirmation	Compound C, AMPK siRNA	↓ cell viability and ↑ cell toxicity	Loss of protection when AMPK inhibited and AMPK knockdown	AMPK plays a central role in regulating neuroprotection

Table 7: Amyloid-beta 42 chapter summarised as a table.

Summarised table illustrates that apelin-13 and its analogues reversed the toxicity effect of $A\beta_{42}$ and improved cell viability, antioxidant response, restoring autophagy and mitigating apoptosis in SH-SY5Y cells.

Chapter 8

General Discussion

Alzheimer's is progressive neurodegenerative disorder characterised by synaptic dysfunction, memory loss, cognitive decline and neuronal death (Evans, 1989). The two main hallmark of disease are accumulation of Aβ and tau tangles. These two leads to oxidative stress by ROS generation, impaired mitochondrial membrane potential, neuronal damage and mitochondrial dysfunction (Sadigh-Eteghad et al., 2014). Additionally, ER stress caused by AD causes the UPR, which promotes apoptosis via caspase activation and deregulation of pro-survival pathways (Javaid et al., 2024). Prolonged stress leads to autophagic dysfunction and neuroinflammation, which leads to extensive neurodegeneration (Qu et al., 2022).

Apelin is an endogenous ligand of APJ and there are number of active forms of apelin including, apelin-13, apelin-17, apelin-19, and apelin-36, though apelin-13 is most potent (Falcão-Pires, Ladeiras-Lopes and Leite-Moreira, 2010). Apelin and its receptor are expressed in several tissues for instance lung, brain, and kidney. Apelin function depends on the interaction of G-protein-coupled to APJ receptor (Reaux et al., 2001). Number of studies have showed the protective effect of Apelin-13 and its analogues in various diseases (Habata et al., 1999).

This study highlights the novel and significant effect of apelin-13 amide and its synthetic analogue (Lys^{8}GluPAL)apelin-13 amide on neuroprotection in AD. We used SH-SY5Y cells and treated them with various stressors to create an AD like environment and then treated with the peptide analogues. Apelin-13 amide is the modified bioactive peptide apelin-13. The amidation at the c-terminal of the peptide enhanced its stability, bioactivity and receptor binding affinity. However, (Lys^{8}GluPAL)apelin-13 amide is further enhanced analogues of apelin-13 amide, featuring a palmitoylated glutamic acid substitution at position 8. This modification increased the half-life to 24 hours . Our results have showed the neuroprotective effect of this analogues throughout research and indicating its potential as a therapeutic peptide for AD.

8.1. Cell Viability

The finding suggests that across all stress conditions, the cell viability of SH-SY5Y cells was improved. The cells treated with the stressors, Palmitate, H2O2, LPS, Thapsigargin and $A\beta_{42}$, led to reduced cell viability due to its nature of inducing oxidative stress, inflammation, ER stress, apoptosis and mitochondrial dysfunction. Apelin-13 amide and (Lys^8GluPAL)apelin-13 amide reversed the viability decline by activating the APJ receptor, which is responsible for activating cell survival pathways like PI3K/AKT and AMPK.

To further understand the activation of AMPK by apelin-13 analogues and role in mediating the protective effect of the analogues, we used the AMPK inhibitor. The results illustrated that inhibiting AMPK reduced the protecting effect of apelin-13 amide and (Lys^8GluPAL)apelin-13 amide, confirming that AMPK activation is a key mediator of its neuroprotection. By restoring the viability of cell under stress, highlights its potential to maintain neuronal survival in AD and its therapeutic potential.

8.2. Cell proliferation and differentiation

Apelin-13 analogues did not only restore the cell viability of the SH-SY5Y cells but also promoted cell proliferation and differentiation under stress induced by different stressors. BrdU, a proliferation marker was used to study the effect of apelin-13 amide and (Lys^8GluPAL)apelin-13 amide on cell proliferation and the results indicated that significant improvement in the cell proliferation after the treatment with the apelin-13 analogues compared to the stressors alone.

Moreover, neurite outgrowth a marker for neurite differentiation and MAP2 a marker for differentiation, neuronal health and synaptic plasticity was also enhanced when cells treated with apelin-13 analogues, indicating its effect on the neuronal regeneration and synaptic plasticity. Studies have showed that apelin-13 analogues

promote cell proliferation by PI3K/Akt signalling pathway or MAPK pathway (Hu et al., 2021).

8.3. Cell toxicity

Apelin-13 protect against oxidative stress, inflammation, apoptosis and by modulating key pathways like NRF-2, PI3K/AKT, ATF6 and MAPK. The treatment with stressor led to increased cell toxicity and apelin-13 analogues significantly mitigated the toxicity across all stress condition at different timepoints. The LDH release indicative of cell membrane damage and cell death were significantly reduced by the Apelin-13 amide and (Lys^{8}GluPAL)apelin-13 amide. Apelin-13's antioxidative and anti-inflammatory properties promoted the protective effect. apelin-13 analogues enhanced the antioxidant defence against the oxidative stress and led to the downregulation of ROS production and inhibition of inflammatory mediators. Apelin-13 analogues activated the NRF-2 pathways which then enhanced the expression of antioxidant response elements and leads to the production of antioxidant enzymes (Li et al., 2024).

The AMPK inhibition by compound C, showed that apelin-13 analogues were unable to mitigate the toxic effect of the stressor as apelin-13 is known to effect via AMPK. AMPK is a key energy sensor, and it is responsible for cellular homeostasis. Studies have shown that apelin-13 activates the AMPK which leads to the increased ATP production, mitochondrial function and glucose uptake. Apelin-13 activates the AMPK and leads to the inhibition of mTOR pathways and promotes autophagy related protein expression (Wang & Jia, 2023).

8.4. Mitochondrial and oxidative stress

In AD the major contributors of neuronal cell death are the oxidative stress and mitochondrial dysfunction. The stressors used in this research significantly depolarised the mitochondrial membrane potential, reduced ATP production and

increased ROS production in SH-SY5Y cells (Han et al., 2017). However, when the cells were treated with apelin-13 amide and (Lys^{8}GluPAL)apelin-13 amide, the mitochondrial membrane potential was significantly improved and reduced the mitochondrial ROS and normalised the redox state (Guo et al., 2024). The results indicate protective role of apelin-13 analogues on the energy homeostasis and mitochondrial integrity. Studies have showed that apelin-13 analogues inhibited apoptosis and oxidative stress and elevated mitochondrial membrane potential in high glucose induced stress (Huo et al., 2024).

To analyse the impact of apelin-13 analogues on oxidative stress induced by various stressors used in this study we used JC-1 assay, ROS and GSH/GSSG assays. The results revealed that when the stress was induced the ROS production was increased as the redox balance was disturbed. The treatments with apelin-13 analogues led to a reduced levels of ROS and balance in GSH/GSSG ratio. The mitochondrial membrane potential was improved by apelin-13 analogues suggesting as a potent regulator of mitochondrial function and oxidative balance. Apelin-13 activates the PI3K/AKT pathway and upregulates the antioxidant enzymes to mitigate the oxidative stress (Yang et al., 2016). The results of this study also showed that upregulated expression of NRF, a key regulator of antioxidant defence led to increased expression of SOD and catalase and mitigate the oxidative stress (Ma, 2013).

8.5. Apoptosis

In our study, apoptosis was the key factor, and all the stressors used activated the intrinsic apoptotic pathway in SH-SY5Y cells. It was evidenced by the increased caspase 3/7 activity and elevated BAX/Bcl2 ratio. Apelin-13 is known to modulate the pathways like p38, MAPK, JNK and AMPK and involved in mitigating the apoptosis (Yao et al., 2005). The studies have shown that apelin-13 analogues significantly mitigated the pro-apoptotic effects by modulating key pathways like AMPK and PI3K/AKT pathway (Duan et al., 2019). The PI3K/AKT pathway activation leads to the

upregulation of anti-apoptotic proteins like Bcl-2 and inhibited pro-apoptotic protein BAX. Also, studies have shown that apelin-13 analogues prevented the cytochrome C release, a crucial step in intrinsic apoptotic cascade and stabilised mitochondrial function (Xu et al., 2017). The results across all the stressors conformed that caspase 3/7 activity was significantly reduced by apelin-13 analogues, confirming its anti-apoptotic effects and suggests its therapeutic potential in neurodegenerative diseases.

8.6. ER tress and UPR pathway

In AD, the ER stress and UPR plays a key role and are critical contributor to the neurodegeneration (Yang et al., 2020). Number of studies reported the ER stress and UPR activation in the brain of AD models. ER stress is caused by the accumulation of misfolded proteins in the ER, and it activates the UPR (Tsai & Weissman, 2010). Aβ buildup in the brain, is a specific characteristic of AD, it triggers neuronal dysfunction and cognitive loss. Aβ mainly alters the cellular redox state and abnormally raises the calcium, which then lead to ER stress, mitochondrial malfunction, and consequently neuronal damage. Three main ER membrane sensors that trigger the UPR under stress are ATF6, PERK and IRE1. These sensors are inactivated under normal conditions by bonding to the ER chaperone BiP/GRP78. However, these sensors are activated when BiP dissociates to bind misfolded proteins during ER stress (Silvestro et al., 2023).

Our results indicated after the stressor treatment there was an increase of ER stress markers PERK, IRE1 and ATF6, indicating UPR activation. However, apelin-13 amide and (Lys^{8}GluPAL)apelin-13 amide treatment normalised the expression of these markers suggesting role in mitigating ER stress. Apelin-13 showed to modulate the PERK-eIF2α pathway and reduce the translation to lower the ER's protein folding load (Silvestro et al., 2023).

8.7. Autophagy

Autophagy is the natural process that occurs in cells essential for maintaining homeostasis by recycling, degrading damaged organelles, misfolded proteins and debris (Lindner et al., 2020). In AD, the accumulation of Aβ-42, leads to the autophagy dysfunctions and causes neuronal damage (Wang & Jia, 2023). In our study we used H_2O_2, thapsigargin and $A\beta_{42}$ to induce stress and disrupt the autophagy and the expression of autophagy related protein ATG3, ATG5 and ATG7 was declined compared to the normal conditions. ATG3 is involved in the lipidation of LC3 and ATG5 and ATG7 are key for autophagosome elongation and membrane dynamics (Li et al., 2020). Under stress conditions, the downregulation of these proteins indicate the blockade of autophagic flux and accumulation of cellular stress and debris (Li et al., 2020).

When the cells were treated with apelin-13 analogues, the autophagy was improved and there was increased expression of the autophagy related proteins were seen. Apelin-13 is known to activate the AMPK pathway a key regulator of energy homeostasis and autophagy (Duan et al., 2019). Studies have showed that activation of AMPK inhibits mTOR and promote autophagosome (Wang & Jia, 2023). Apelin-13 amide provides a promising approach to treating the proteostasis imbalance in Alzheimer's disease by promoting effective autophagy, which decreases the toxic buildup of amyloid-beta and other aggregates.

8.9. Conclusion

This thesis explored the neuroprotective effect of stable novel peptide apelin-13 and its analogues in mitigating neurodegeneration in AD. We used **five different stress model** (PA, H2O2, LPS, Thapsigargin and $A\beta_{42}$) *in-vitro* to mimic the AD like pathology. All these stressors contribute to cellular dysfunction through distinctive but interconnected pathways, involving **ER stress, oxidative stress, mitochondrial impairment, apoptosis and inflammation.**

Apelin-13 analogues treatments showed a significant improvement in cell viability, proliferation and differentiation by mitigating oxidative stress, modulating inflammation and apoptosis, maintaining mitochondrial membrane potential and regulating UPR (shown in table 8). These results focus on apelin-13 analogues as a promising therapeutic agent for neuroprotection, especially in AD. Given the novelty of this work, future studies should further focus on the **molecular mechanisms underlying apelin-13 analogues protective effects and assess its potential clinical applications.** This study delivers a foundation for advancing our understanding of apelin-13 analogues as a neuroprotective agent and encourages further exploration into its therapeutic potential for neurodegenerative disorders.

8.10. Limitations

It is important to recognise a few limitations even if this work offers insightful information about apelin-13's neuroprotective potential against various stressors. First, this research was carried out in-vitro using SH-SY5Y cells often used to study neurodegenerative diseases, which do not accurately mimic the complicated cellular environment of the human brain. Due to the **lack of the interactions with other cell types** like astrocytes and microglia, how apelin-13 may affect neuroinflammation and synaptic function in a more physiologically relevant situation is limited.

Secondly, although five different stressors were used in this study, but the **combination of the stressors were not explored** which more accurately represents

the disease nature. The absence of in-vivo model is another limitation, as the in-vitro model prevent the assessment of the long-term effectiveness and bioavailability.

8.11. Future directions

- To validate the protective effect of the apelin-13 analogues we will involve in-vivo models of AD like mouse models (PS19, APP23 and PD-APP) .
- The in-vivo models will be involved to look at blood brain barrier permeability of apelin-13 analogues, it's bioavailability, toxicology studies and chronic effectiveness.
- The future research will also focus on combination of stressors in disease model to create more accurate pathology and to explore how apelin-13 analogues respond to the combined stressors.
- After pre-clinical validation of this compound, we would like to take this into clinical trials.

Assays	Effect of stressors (Palmitate, H_2O_2, LPS, Thapsigargin, $A\beta_{42}$)	Apelin-13 analogue effects
Cell Viability (MTT, CellTiter-Glo)	↓ Viability across all stressors	↑ Cell viability across all models (especially Aβ42 and H2O2)
Cell Toxicity (LDH, CellTox Green)	↑ LDH, ↑ DNA damage	↓ LDH and CellTox Green signals, indicating protection
Oxidative Stress (ROS, GSH/GSSG)	↑ ROS, ↓ GSH/GSSG, redox imbalance	↓ ROS, ↑ GSH/GSSG, restored redox balance
Cell Proliferation & Differentiation (BrdU, MAP2)	↓ BrdU and MAP2, impaired neurogenesis	↑ BrdU, ↑ MAP2, promotion of neuronal proliferation and structure
Mitochondrial Function (JC-1)	↓ JC-1 ratio, mitochondrial depolarisation	↑ JC-1 ratio, ↑ mitochondrial integrity
Apoptosis (Caspase 3/7, BAX/Bcl-2)	↑ Caspase activity, ↑ BAX/Bcl-2 ratio, intrinsic pathway activation	↓ Caspase, ↑ Bcl-2, ↓ BAX/Bcl-2 ratio, anti-apoptotic effects
ER Stress (ATF6, PERK, BiP, IRE1)	↑ ATF6, ↑ PERK, ↑ BiP, ↑ IRE1 (thapsigargin & $A\beta_{42}$)	↓ ATF6, ↓ PERK, ↓ BiP,
Autophagy Markers (ATG3/5/7)	↓ ATG3/5/7, disrupted autophagic flux	↑ ATG3/5/7, restored autophagy balance
Pathways Impacted	Activation of apoptotic, oxidative, ER stress, and inflammatory pathways	AMPK and PI3K/Akt activation, NRF-2 upregulation, mTOR regulation

Table 8: General overview of apelin-13 and its analogues protective effect on SH-SY5Y cells under different stress conditions.

The table summarised the combined finding of the multiple assays assessing cell viability, proliferation, toxicity, apoptosis, autophagy and ER stress. Apelin-13 and its analogues has improved the cell viability, mitigated UPR activation and reduced apoptosis in SH-SY5Y cells.

Chapter 9

Reference

Aguayo-Ortiz, R. and Espinoza-Fonseca, L.M. (2020) ‘Linking biochemical and structural states of Serca: Achievements, challenges, and new opportunities’, *International Journal of Molecular Sciences*, 21(11), p. 4146. doi:10.3390/ijms21114146.

Al-Qathama, A., Gibbons, S. and Prieto, J.M. (2017) ‘Differential modulation of BAX/BCL-2 ratio and onset of caspase-3/7 activation induced by derivatives of justicidin B in human melanoma cells A375’, *Oncotarget*, 8(56), pp. 95999–96012. doi:10.18632/oncotarget.21625.

Aliev, G., Obrenovich, M., Reddy, V., Shenk, J., Moreira, P., Nunomura, A., Zhu, X., Smith, M. and Perry, G. (2008). Antioxidant Therapy in Alzheimers Disease: Theory and Practice. Mini-Reviews in Medicinal Chemistry, 8(13), pp.1395-1406.

A*lzheimer’s disease facts and figures* (2024) *Alzheimer’s & dementia : the journal of the Alzheimer’s Association*. Available at: https://pubmed.ncbi.nlm.nih.gov/38689398/ (Accessed: 03 December 2024).

Aminyavari, S. *et al.* (2019) ‘Protective role of apelin-13 on amyloid B25–35-induced memory deficit; involvement of autophagy and apoptosis process’, *Progress in Neuro-Psychopharmacology and Biological Psychiatry*, 89, pp. 322–334. doi:10.1016/j.pnpbp.2018.10.005.

Andersen, T. *et al.* (2015) ‘Thapsigargin—from Thapsia L. to Mipsagargin’, *Molecules*, 20(4), pp. 6113–6127. doi:10.3390/molecules20046113.

Andrés, C.M. *et al.* (2022) ‘Chemistry of hydrogen peroxide formation and elimination in mammalian cells, and its role in various pathologies’, *Stresses*, 2(3), pp. 256–274. doi:10.3390/stresses2030019.

Ansari, M.A. and Scheff, S.W. (2010) ‘Oxidative stress in the progression of Alzheimer disease in the frontal cortex’, *Journal of Neuropathology & Experimental Neurology*, 69(2), pp. 155–167. doi:10.1097/nen.0b013e3181cb5af4.

Armstrong, J.S. *et al.* (2002) ‘Role of glutathione depletion and reactive oxygen species generation in apoptotic signaling in a human B lymphoma cell line’, *Cell Death & Differentiation*, 9(3), pp. 252–263. doi:10.1038/sj.cdd.4400959.

Armstrong, R. (2019) ‘Risk factors for alzheimer’s disease’, *Folia Neuropathologica*, 57(2), pp. 87–105. doi:10.5114/fn.2019.85929.

Arnold, S., Arvanitakis, Z., Macauley-Rambach, S., Koenig, A., Wang, H., Ahima, R., Craft, S., Gandy, S., Buettner, C., Stoeckel, L., Holtzman, D. and Nathan, D. (2018). Brain insulin resistance in type 2 diabetes and Alzheimer disease: concepts and conundrums. *Nature Reviews Neurology*, 14(3), pp.168-181.

Askari, S. *et al.* (2022) ‘Behavioral and molecular effects of Thapsigargin-induced brain er- stress: Encompassing inflammation, MAPK, and insulin signaling pathway’, *Life*, 12(9), p. 1374. doi:10.3390/life12091374.

Azargoonjahromi, A. (2024) ‘The duality of amyloid-β: Its role in normal and alzheimer’s disease states’, *Molecular Brain*, 17(1). doi:10.1186/s13041-024-01118-1.

Azzam, S.M. *et al.* (2023) ‘Lipopolysaccharide induced neuroprotective effects of bacterial protease against alzheimer’s disease in male wistar albino rats’, *International Journal of Biological Macromolecules*, 230, p. 123260. doi:10.1016/j.ijbiomac.2023.123260.

Bai, B. *et al.* (2008) ‘Apelin-13 induces ERK1/2 but not p38 MAPK activation through coupling of the human apelin receptor to the G_{I2} pathway’, *Acta Biochimica et Biophysica Sinica*, 40(4), pp. 311–318. doi:10.1111/j.1745-7270.2008.00403.x.

Balaban, R.S., Nemoto, S. and Finkel, T. (2005) ‘Mitochondria, oxidants, and aging’, *Cell*, 120(4), pp. 483–495. doi:10.1016/j.cell.2005.02.001.

Baldwin, A.C. *et al.* (2012) ‘A role for aberrant protein palmitoylation in FFA-induced ER stress and β-cell death’, *American Journal of Physiology-Endocrinology and Metabolism*, 302(11). doi:10.1152/ajpendo.00519.2011.

Banovic, S., Zunic, L. and Sinanovic, O. (2018) ‘Communication difficulties as a result of dementia’, *Materia Socio Medica*, 30(2), p. 221. doi:10.5455/msm.2018.30.221-224.

Barnes, J. *et al.* (2018) ‘Disease course varies according to age and symptom length in alzheimer’s disease’, *Journal of Alzheimer’s Disease*, 64(2), pp. 631–642. doi:10.3233/jad-170841.

Bateman, R.J. *et al.* (2006) ‘Human amyloid-β synthesis and clearance rates as measured in cerebrospinal fluid in vivo’, *Nature Medicine*, 12(7), pp. 856–861. doi:10.1038/nm1438.

Batista, C.R. *et al.* (2019) ‘Lipopolysaccharide-induced neuroinflammation as a bridge to understand neurodegeneration’, *International Journal of Molecular Sciences*, 20(9), p. 2293. doi:10.3390/ijms20092293.

Bertani, B. and Ruiz, N. (2018) ‘Function and biogenesis of lipopolysaccharides’, *EcoSal Plus*, 8(1). doi:10.1128/ecosalplus.esp-0001-2018.

Bhuiyan, N.Z. *et al.* (2023) ‘Prevention of alzheimer’s disease through diet: An exploratory review’, *Metabolism Open*, 20, p. 100257. doi:10.1016/j.metop.2023.100257.

Bi, C., Bi, S. and Li, B. (2019) ‘Processing of mutant β-amyloid precursor protein and the CLINICOPATHOLOGICAL features of familial alzheimer’s disease’, *Aging and disease*, 10(2), p. 383. doi:10.14336/ad.2018.0425.

Bird, T.D. (2018) *Alzheimer disease overview*, *GeneReviews® [Internet].* Available at: https://www.ncbi.nlm.nih.gov/books/NBK1161/ (Accessed: 03 December 2024).

Birks, J.S. (2006) ‘Cholinesterase inhibitors for alzheimer’s disease’, *Cochrane Database of Systematic Reviews*, 2016(3). doi:10.1002/14651858.cd005593.

Bondi, M.W., Edmonds, E.C. and Salmon, D.P. (2017) ‘Alzheimer’s disease: Past, present, and future’, *Journal of the International Neuropsychological Society*, 23(9–10), pp. 818–831. doi:10.1017/s135561771700100x.

Brini, M. *et al.* (2014) 'Neuronal calcium signaling: Function and dysfunction', *Cellular and Molecular Life Sciences*, 71(15), pp. 2787–2814. doi:10.1007/s00018-013-1550-7.

Brown, G.C. (2019) 'The endotoxin hypothesis of neurodegeneration', *Journal of Neuroinflammation*, 16(1). doi:10.1186/s12974-019-1564-7.

Brunelli, F. *et al.* (2022) 'PINK1 protects against Staurosporine-induced apoptosis by interacting with Beclin1 and impairing its pro-apoptotic cleavage', *Cells*, 11(4), p. 678. doi:10.3390/cells11040678.

Bufill, E., Ribosa-Nogué, R. and Blesa, R. (2020) 'The therapeutic potential of epigenetic modifications in alzheimer's disease', *Alzheimer's Disease: Drug Discovery*, pp. 151–164. doi:10.36255/exonpublications.alzheimersdisease.2020.ch9.

Butterfield, D.A. and Boyd-Kimball, D. (2018) 'Oxidative stress, amyloid-β peptide, and altered key molecular pathways in the pathogenesis and progression of alzheimer's disease', *Journal of Alzheimer's Disease*, 62(3), pp. 1345–1367. doi:10.3233/jad-170543.

Canevelli, M. *et al.* (2019) 'Estimating dementia cases amongst migrants living in Europe', *European Journal of Neurology*, 26(9), pp. 1191–1199. doi:10.1111/ene.13964.

Cdc.gov. 2021. *What is Alzheimer's Disease?* | *CDC*. [online] Available at: <https://www.cdc.gov/aging/aginginfo/alzheimers.htm> [Accessed 22 June 2021].

Che, J. *et al.* (2024) 'Blood-brain barrier disruption: A culprit of cognitive decline?', *Fluids and Barriers of the CNS*, 21(1). doi:10.1186/s12987-024-00563-3.

Cheignon, C. *et al.* (2018) 'Oxidative stress and the amyloid beta peptide in alzheimer's disease', *Redox Biology*, 14, pp. 450–464. doi:10.1016/j.redox.2017.10.014.

Chen, G. *et al.* (2017) 'Amyloid beta: Structure, biology and structure-based therapeutic development', *Acta Pharmacologica Sinica*, 38(9), pp. 1205–1235. doi:10.1038/aps.2017.28.

Chen, H. *et al.* (2011) ‘Apelin alleviates diabetes-associated endoplasmic reticulum stress in the pancreas of akita mice’, *Peptides*, 32(8), pp. 1634–1639. doi:10.1016/j.peptides.2011.06.025.

Chen, J.X. and Yan, S.D. (2007) ‘Amyloid-β-induced mitochondrial dysfunction’, *Journal of Alzheimer’s Disease*, 12(2), pp. 177–184. doi:10.3233/jad-2007-12208.

Chen, L. *et al.* (2009) ‘Hydrogen peroxide-induced neuronal apoptosis is associated with inhibition of protein phosphatase 2A and 5, leading to activation of MAPK pathway’, *The International Journal of Biochemistry & Cell Biology*, 41(6), pp. 1284–1295. doi:10.1016/j.biocel.2008.10.029.

Chen, P. *et al.* (2020) ‘Apelin-13 protects dopaminergic neurons against rotenone—induced neurotoxicity through the AMPK/mTOR/ULK-1 mediated autophagy activation’, *International Journal of Molecular Sciences*, 21(21), p. 8376. doi:10.3390/ijms21218376.

Chen, X., Du, Y. and Chen, L. (2019). Neuropeptides Exert Neuroprotective Effects in Alzheimer's Disease. Frontiers in Molecular Neuroscience, 11, p.493.

Chen, Y. (2014) ‘Apelin-13 decreases lipid storage in hypertrophic adipocytes in vitro through the upregulation of AQP7 expression by the PI3K signaling pathway’, *Medical Science Monitor*, 20, pp. 1345–1352. doi:10.12659/msm.890124.

Cheng, B.-H. *et al.* (2021) ‘Apelin-13 inhibits apoptosis and excessive autophagy in cerebral ischemia/reperfusion injury’, *Neural Regeneration Research*, 16(6), p. 1044. doi:10.4103/1673-5374.300725.

Cheng, B., Chen, J., Bai, B. and Xin, Q. (2012). Neuroprotection of apelin and it signaling pathway. *Peptides*, 37(1), pp.171-173.

Ciesielska, A., Matyjek, M. and Kwiatkowska, K. (2020) ‘TLR4 and CD14 trafficking and its influence on LPS-induced pro-inflammatory signaling’, *Cellular and Molecular Life Sciences*, 78(4), pp. 1233–1261. doi:10.1007/s00018-020-03656-y.

Cummings, J. (2023) ‘Anti-amyloid monoclonal antibodies are transformative treatments that redefine alzheimer’s disease therapeutics’, *Drugs*, 83(7), pp. 569–576. doi:10.1007/s40265-023-01858-9.

Dai, R.Y. *et al.* (2013) ‘Implication of transcriptional repression in compound C-induced apoptosis in cancer cells’, *Cell Death & Disease*, 4(10). doi:10.1038/cddis.2013.419.

de Dios, C. *et al.* (2019) ‘Oxidative inactivation of amyloid beta-degrading proteases by cholesterol-enhanced mitochondrial stress’, *Redox Biology*, 26, p. 101283. doi:10.1016/j.redox.2019.101283.

de la Monte, S.M. (2012) ‘Contributions of brain insulin resistance and deficiency in amyloid-related neurodegeneration in ALZHEIMER’S disease’, *Drugs*, 72(1), pp. 49–66. doi:10.2165/11597760-000000000-00000.

Dementia in the UK: preparing the NHS for new treatments. (2018). The Lancet, 391(10127), p.1237.

Deng, S. *et al.* (2022) ‘PI3K/akt signaling tips the balance of cytoskeletal forces for cancer progression’, *Cancers*, 14(7), p. 1652. doi:10.3390/cancers14071652.

DeTure, M.A. and Dickson, D.W. (2019) ‘The neuropathological diagnosis of alzheimer’s disease’, *Molecular Neurodegeneration*, 14(1). doi:10.1186/s13024-019-0333-5.

Duan, J. *et al.* (2019) ‘Neuroprotective effect of Apelin 13 on ischemic stroke by activating AMPK/GSK-3B/Nrf2 signaling’, *Journal of Neuroinflammation*, 16(1). doi:10.1186/s12974-019-1406-7.

Durazzo, T.C., Mattsson, N. and Weiner, M.W. (2014) ‘Smoking and increased alzheimer’s disease risk: A review of potential mechanisms’, *Alzheimer’s & Dementia*, 10(3S). doi:10.1016/j.jalz.2014.04.009.

Elmore, S. (2007) ‘Apoptosis: A review of Programmed Cell Death’, *Toxicologic Pathology*, 35(4), pp. 495–516. doi:10.1080/01926230701320337.

Erridge, C., Bennett-Guerrero, E. and Poxton, I.R. (2002) ‘Structure and function of lipopolysaccharides’, *Microbes and Infection*, 4(8), pp. 837–851. doi:10.1016/s1286-4579(02)01604-0.

Esteves, A.R. *et al.* (2023) ‘LPS-induced mitochondrial dysfunction regulates innate immunity activation and α-synuclein oligomerization in parkinson’s disease’, *Redox Biology*, 63, p. 102714. doi:10.1016/j.redox.2023.102714.

Evans, D. (1989). Prevalence of Alzheimer's Disease in a Community Population of Older Persons. *JAMA*, 262(18), p.2551.

Facts for the media about dementia (2024) *Alzheimer’s Society*. Available at: https://www.alzheimers.org.uk/about-us/news-and-media/facts-media (Accessed: 03 December 2024).

Falcão-Pires, I., Ladeiras-Lopes, R. and Leite-Moreira, A. (2010). The apelinergic system: a promising therapeutic target. *Expert Opinion on Therapeutic Targets*, 14(6), pp.633-645.

Fan, X.-F. *et al.* (2015) ‘The apelin-APJ axis is an endogenous counterinjury mechanism in experimental acute lung injury’, *Chest*, 147(4), pp. 969–978. doi:10.1378/chest.14-1426.

Fang, Y.-Z., Yang, S. and Wu, G. (2002) ‘Free radicals, antioxidants, and Nutrition’, *Nutrition*, 18(10), pp. 872–879. doi:10.1016/s0899-9007(02)00916-4.

Fang, Y., Yang, S. and Wu, G. (2002). Free radicals, antioxidants, and nutrition. *Nutrition*, 18(10), pp.872-879.

Farr, S., Price, T., Banks, W., Ercal, N. and Morley, J., 2012. Effect of Alpha-Lipoic Acid on Memory, Oxidation, and Lifespan in SAMP8 Mice. *Journal of Alzheimer's Disease*, 32(2), pp.447-455.

Fernández-Sánchez, A. *et al.* (2011) ‘Inflammation, oxidative stress, and Obesity’, *International Journal of Molecular Sciences*, 12(5), pp. 3117–3132. doi:10.3390/ijms12053117.

Fibbi, B. *et al.* (2023) ‘The Yin and Yang effect of the APELINERGIC system in oxidative stress’, *International Journal of Molecular Sciences*, 24(5), p. 4745. doi:10.3390/ijms24054745.

Findeis, M.A. (2007) ‘The role of amyloid β peptide 42 in alzheimer’s disease’, *Pharmacology & Therapeutics*, 116(2), pp. 266–286. doi:10.1016/j.pharmthera.2007.06.006.

Folch, J., Petrov, D., Ettcheto, M., Abad, S., Sánchez-López, E., García, M., Olloquequi, J., Beas-Zarate, C., Auladell, C. and Camins, A. (2016). Current Research Therapeutic Strategies for Alzheimer’s Disease Treatment. Neural Plasticity, 2016, pp.1-15.

Folstein, M.F., Folstein, S.E. and McHugh, P.R. (1975) “‘mini-mental state’”, *Journal of Psychiatric Research*, 12(3), pp. 189–198. doi:10.1016/0022-3956(75)90026-6.

Fonseca, A.C. *et al.* (2013) ‘Activation of the endoplasmic reticulum stress response by the amyloid-beta 1–40 peptide in brain endothelial cells’, *Biochimica et Biophysica Acta (BBA) - Molecular Basis of Disease*, 1832(12), pp. 2191–2203. doi:10.1016/j.bbadis.2013.08.007.

Foretz, M. *et al.* (1998) ‘AMP-activated protein kinase inhibits the glucose-activated expression of fatty acid synthase gene in rat hepatocytes’, *Journal of Biological Chemistry*, 273(24), pp. 14767–14771. doi:10.1074/jbc.273.24.14767.

Forman, H., Zhang, H. and Rinna, A. (2009). Glutathione: Overview of its protective roles, measurement, and biosynthesis. Molecular Aspects of Medicine, 30(1-2), pp.1-12.

Gao, C. *et al.* (2023) ‘Microglia in neurodegenerative diseases: Mechanism and potential therapeutic targets’, *Signal Transduction and Targeted Therapy*, 8(1). doi:10.1038/s41392-023-01588-0.

Gao, L. *et al.* (2022) ‘Brain-derived neurotrophic factor in alzheimer’s disease and its pharmaceutical potential’, *Translational Neurodegeneration*, 11(1). doi:10.1186/s40035-022-00279-0.

García-Cruz, V.M. and Arias, C. (2024) ‘Palmitic acid induces posttranslational modifications of tau protein in alzheimer’s disease–related epitopes and increases intraneuronal Tau Levels’, *Molecular Neurobiology* [Preprint]. doi:10.1007/s12035-023-03886-8.

Ge, M. *et al.* (2022) ‘Role of calcium homeostasis in alzheimer’s disease’, *Neuropsychiatric Disease and Treatment*, Volume 18, pp. 487–498. doi:10.2147/ndt.s350939.

Georgiev, K. *et al.* (2024) ‘Predicting incident dementia in community-dwelling older adults using primary and secondary care data from Electronic Health Records’, *Brain Communications*, 7(1). doi:10.1093/braincomms/fcae469.

Glass, C.K. *et al.* (2010) ‘Mechanisms underlying inflammation in neurodegeneration’, *Cell*, 140(6), pp. 918–934. doi:10.1016/j.cell.2010.02.016.

Gonzalez-Ortiz, F. *et al.* (2023) ‘Plasma phospho-tau in alzheimer’s disease: Towards diagnostic and therapeutic trial applications’, *Molecular Neurodegeneration*, 18(1). doi:10.1186/s13024-023-00605-8.

Gugliandolo, A., Bramanti, P. and Mazzon, E. (2017). Role of Vitamin E in the Treatment of Alzheimer’s Disease: Evidence from Animal Models. International Journal of Molecular Sciences, 18(12), p.2504.

Guo, F. *et al.* (2017) ‘Autophagy in neurodegenerative diseases: Pathogenesis and therapy’, *Brain Pathology*, 28(1), pp. 3–13. doi:10.1111/bpa.12545.

Guo, L., Tian, J. and Du, H. (2017) ‘Mitochondrial dysfunction and synaptic transmission failure in alzheimer’s disease’, *Journal of Alzheimer’s Disease*, 57(4), pp. 1071–1086. doi:10.3233/jad-160702.

Guo, Q. *et al.* (2024) ‘Apelin regulates mitochondrial dynamics by inhibiting MST1-JNK-DRP1 signaling pathway to reduce neuronal apoptosis after spinal cord injury’, *Neurochemistry International*, 180, p. 105885. doi:10.1016/j.neuint.2024.105885.

Habata, Y. *et al.* (1999) ‘Apelin, the natural ligand of the orphan receptor APJ, is abundantly secreted in the colostrum’, *Biochimica et Biophysica Acta (BBA) - Molecular Cell Research*, 1452(1), pp. 25–35. doi:10.1016/s0167-4889(99)00114-7.

Habib, A., Sawmiller, D. and Tan, J. (2016) ‘Restoring soluble amyloid precursor protein α functions as a potential treatment for alzheimer’s disease’, *Journal of Neuroscience Research*, 95(4), pp. 973–991. doi:10.1002/jnr.23823.

Halliwell, B., Clement, M.V. and Long, L.H. (2000) ‘Hydrogen peroxide in the human body’, *FEBS Letters*, 486(1), pp. 10–13. doi:10.1016/s0014-5793(00)02197-9.

Hamman, B.D., Hendershot, L.M. and Johnson, A.E. (1998) ‘BIP maintains the permeability barrier of the ER membrane by sealing the lumenal end of the translocon pore before and early in translocation’, *Cell*, 92(6), pp. 747–758. doi:10.1016/s0092-8674(00)81403-8.

Hampel, H. *et al.* (2021) ‘The amyloid-β pathway in alzheimer’s disease’, *Molecular Psychiatry*, 26(10), pp. 5481–5503. doi:10.1038/s41380-021-01249-0.

Han, X.-J. *et al.* (2017) ‘Amyloid β-42 induces neuronal apoptosis by targeting mitochondria’, *Molecular Medicine Reports*, 16(4), pp. 4521–4528. doi:10.3892/mmr.2017.7203.

Hashimoto, S. *et al.* (2018) ‘Endoplasmic Reticulum stress responses in mouse models of alzheimer’s disease: Overexpression paradigm versus Knockin Paradigm’, *Journal of Biological Chemistry*, 293(9), pp. 3118–3125. doi:10.1074/jbc.m117.811315.

Hauck, A.K. and Bernlohr, D.A. (2016) ‘Oxidative stress and lipotoxicity’, *Journal of Lipid Research*, 57(11), pp. 1976–1986. doi:10.1194/jlr.r066597.

He, Q. *et al.* (2020) ‘Apelin-36 protects against lipopolysaccharide-induced acute lung injury by inhibiting the ASK1/MAPK signaling pathway’, *Molecular Medicine Reports*, 23(1), pp. 1–1. doi:10.3892/mmr.2020.11644.

Head, E. *et al.* (2015) ‘Aging in down syndrome and the development of alzheimer’s disease neuropathology’, *Current Alzheimer Research*, 13(1), pp. 18–29. doi:10.2174/1567205012666151020114607.

Hetz, C. and Papa, F.R. (2018) ‘The unfolded protein response and Cell Fate Control’, *Molecular Cell*, 69(2), pp. 169–181. doi:10.1016/j.molcel.2017.06.017.

Hippius, H., & Neundörfer, G. (2003). The discovery of Alzheimer's disease. *Dialogues in clinical neuroscience*, *5*(1), 101–108.

Hiramatsu, N. *et al.* (2015) ‘Multiple mechanisms of unfolded protein response–induced cell death’, *The American Journal of Pathology*, 185(7), pp. 1800–1808. doi:10.1016/j.ajpath.2015.03.009.

Holmquist, L., Stuchbury, G., Berbaum, K., Muscat, S., Young, S., Hager, K., Engel, J. and Münch, G., 2007. Lipoic acid as a novel treatment for Alzheimer's disease and related dementias. *Pharmacology & Therapeutics*, 113(1), pp.154-164.

Hölscher, C. and Li, L., 2010. New roles for insulin-like hormones in neuronal signalling and protection: New hopes for novel treatments of Alzheimer’s disease?. *Neurobiology of Aging*, 31(9), pp.1495-1502.

Hooper, C., Killick, R. and Lovestone, S. (2007). The GSK3 hypothesis of Alzheimer’s disease. *Journal of Neurochemistry*, 104(6), pp.1433-1439.

Hsiao, Y.-H. *et al.* (2014) ‘Palmitic acid-induced neuron cell cycle G2/m arrest and endoplasmic reticular stress through protein palmitoylation in SH-SY5Y Human Neuroblastoma Cells’, *International Journal of Molecular Sciences*, 15(11), pp. 20876–20899. doi:10.3390/ijms151120876.

Hu, G. *et al.* (2021) ‘The role of Apelin/Apelin receptor in energy metabolism and water homeostasis: A comprehensive narrative review’, *Frontiers in Physiology*, 12. doi:10.3389/fphys.2021.632886.

Hu, S. *et al.* (2022) ‘Apelin-13 reduces lipopolysaccharide-induced neuroinflammation and cognitive impairment via promoting glucocorticoid receptor

expression and nuclear translocation', *Neuroscience Letters*, 788, p. 136850. doi:10.1016/j.neulet.2022.136850.

Huang, C. *et al.* (2016) 'Apelin-13 protects neurovascular unit against ischemic injuries through the effects of vascular endothelial growth factor', *Neuropeptides*, 60, pp. 67–74. doi:10.1016/j.npep.2016.08.006.

Huang, S. *et al.* (2024) 'Single-molecule-level quantification based on atomic force microscopy data reveals the interaction between Melittin and lipopolysaccharide in gram-negative bacteria', *International Journal of Molecular Sciences*, 25(19), p. 10508. doi:10.3390/ijms251910508.

Huang, Z. *et al.* (2025) 'Effects and mechanisms of Apelin in treating central nervous system diseases', *Neuroscience*, 566, pp. 177–189. doi:10.1016/j.neuroscience.2024.12.025.

Huo, Z., Gu, J. and He, T. (2024) 'Apelin-13 reduces high glucose-induced mitochondrial dysfunction in cochlear hair cells by inhibiting endoplasmic reticulum stress', *Experimental and Therapeutic Medicine*, 27(5). doi:10.3892/etm.2024.12515.

HYND, M. (2004). Glutamate-mediated excitotoxicity and neurodegeneration in Alzheimer?s disease. *Neurochemistry International*, 45(5), pp.583-595.

Ishida, J. *et al.* (2004) 'Regulatory roles for APJ, a seven-transmembrane receptor related to angiotensin-type 1 receptor in blood pressure in vivo', *Journal of Biological Chemistry*, 279(25), pp. 26274–26279. doi:10.1074/jbc.m404149200.

Janyou, A. *et al.* (2015) 'Suppression effects of O-demethyldemethoxycurcumin on thapsigargin triggered on endoplasmic reticulum stress in SK-n-SH cells', *NeuroToxicology*, 50, pp. 92–100. doi:10.1016/j.neuro.2015.08.005.

Jaskulska, A., Janecka, A.E. and Gach-Janczak, K. (2020) 'Thapsigargin—from traditional medicine to anticancer drug', *International Journal of Molecular Sciences*, 22(1), p. 4. doi:10.3390/ijms22010004.

Javaid, M., Arain, F. and Javaid, M.D. (2024) ‘Oxidative stress in Neurodegenerative Diseases’, *Fundamental Principles of Oxidative Stress in Metabolism and Reproduction*, pp. 167–183. doi:10.1016/b978-0-443-18807-7.00011-9.

Jeong, K. *et al.* (2014a) ‘Apelin is transcriptionally regulated by ER stress-induced ATF4 expression via a p38 MAPK-dependent pathway’, *Apoptosis*, 19(9), pp. 1399–1410. doi:10.1007/s10495-014-1013-0.

Jiang, Y. *et al.* (2018) ‘Apelin-13 attenuates er stress-associated apoptosis induced by MPP+ in SH-SY5Y cells’, *International Journal of Molecular Medicine* [Preprint]. doi:10.3892/ijmm.2018.3719.

JIAO, H. *et al.* (2013) ‘Mechanism underlying the inhibitory effect of apelin-13 on glucose deprivation-induced autophagy in rat cardiomyocytes’, *Experimental and Therapeutic Medicine*, 5(3), pp. 797–802. doi:10.3892/etm.2013.902.

Jo, D., Yoon, G. and Song, J. (2021) ‘Role of exendin-4 in brain insulin resistance, mitochondrial function, and neurite outgrowth in neurons under palmitic acid-induced oxidative stress’, *Antioxidants*, 10(1), p. 78. doi:10.3390/antiox10010078.

Kametani, F. and Hasegawa, M. (2018). Reconsideration of Amyloid Hypothesis and Tau Hypothesis in Alzheimer's Disease. Frontiers in Neuroscience, 12, p.25.

Kamińska, K. *et al.* (2024) ‘Neuroprotective effect of Apelin-13 and other Apelin forms—a review’, *Pharmacological Reports*, 76(3), pp. 439–451. doi:10.1007/s43440-024-00587-4.

Kar, F. *et al.* (2022) ‘Probiotics ameliorates LPS induced neuroinflammation injury on AB 1–42, app, γ-β secretase and BDNF levels in maternal gut microbiota and fetal neurodevelopment processes’, *Metabolic Brain Disease*, 37(5), pp. 1387–1399. doi:10.1007/s11011-022-00964-z.

Karaskov, E. *et al.* (2006) ‘Chronic palmitate but not oleate exposure induces endoplasmic reticulum stress, which may contribute to INS-1 pancreatic β-cell apoptosis’, *Endocrinology*, 147(7), pp. 3398–3407. doi:10.1210/en.2005-1494.

Kawamata, Y. *et al.* (2001) ‘Molecular properties of apelin: Tissue distribution and receptor binding’, *Biochimica et Biophysica Acta (BBA) - Molecular Cell Research*, 1538(2–3), pp. 162–171. doi:10.1016/s0167-4889(00)00143-9.

Kazyken, D. *et al.* (2019) ‘AMPK directly activates mtorc2 to promote cell survival during acute energetic stress’, *Science Signaling*, 12(585). doi:10.1126/scisignal.aav3249.

Kien, C.L. *et al.* (2014) ‘Dietary intake of palmitate and oleate has broad impact on systemic and tissue lipid profiles in humans’, *The American Journal of Clinical Nutrition*, 99(3), pp. 436–445. doi:10.3945/ajcn.113.070557.

Kim, H. soo *et al.* (2021) ‘Gram-negative bacteria and their lipopolysaccharides in alzheimer’s disease: Pathologic roles and therapeutic implications’, *Translational Neurodegeneration*, 10(1). doi:10.1186/s40035-021-00273-y.

Kim, I., Xu, W. and Reed, J.C. (2008) ‘Cell death and endoplasmic reticulum stress: Disease relevance and therapeutic opportunities’, *Nature Reviews Drug Discovery*, 7(12), pp. 1013–1030. doi:10.1038/nrd2755.

Kim, Sujin *et al.* (2020) ‘Apelin-13 inhibits methylglyoxal-induced unfolded protein responses and endothelial dysfunction via regulating AMPK pathway’, *International Journal of Molecular Sciences*, 21(11), p. 4069. doi:10.3390/ijms21114069.

Kleinz, M. and Davenport, A. (2005). Emerging roles of apelin in biology and medicine. *Pharmacology & Therapeutics*, 107(2), pp.198-211.

Kleizen, B. and Braakman, I. (2004) ‘Protein folding and quality control in the endoplasmic reticulum’, *Current Opinion in Cell Biology*, 16(5), p. 597. doi:10.1016/j.ceb.2004.08.003.

Kong, X. *et al.* (2021) ‘Apelin-13-mediated AMPK ameliorates endothelial barrier dysfunction in acute lung injury mice via improvement of mitochondrial function and autophagy’, *International Immunopharmacology*, 101, p. 108230. doi:10.1016/j.intimp.2021.108230.

Konno, T. *et al.* (2021) ‘Intracellular sources of ROS/H2O2 in health and neurodegeneration: Spotlight on Endoplasmic Reticulum’, *Cells*, 10(2), p. 233. doi:10.3390/cells10020233.

Kovacs, G., 2018. Concepts and classification of neurodegenerative diseases. *Handbook of Clinical Neurology*, pp.301-307.

Kratzer, E. *et al.* (2012) ‘Oxidative stress contributes to lung injury and barrier dysfunction via microtubule destabilization’, *American Journal of Respiratory Cell and Molecular Biology*, 47(5), pp. 688–697. doi:10.1165/rcmb.2012-0161oc.

Kremer, A. (2011). GSK3 and Alzheimer’s disease: facts and fiction…. Frontiers in Molecular Neuroscience, 4.

Kulasiri, D., Aberathne, I. and Samarasinghe, S. (2023) ‘Detection of alzheimer’s disease onset using MRI and PET neuroimaging: Longitudinal Data Analysis and machine learning’, *Neural Regeneration Research*, 18(10), p. 2134. doi:10.4103/1673-5374.367840.

Kumar, A. *et al.* (2025) ‘Alzheimer Disease’, in *StatPearls*. Treasure Island (FL): StatPearls. Available at: https://www.ncbi.nlm.nih.gov/books/NBK499922/.

Kutzing, M.K., Luo, V. and Firestein, B.L. (2011) ‘Protection from glutamate-induced excitotoxicity by memantine’, *Annals of Biomedical Engineering*, 40(5), pp. 1170–1181. doi:10.1007/s10439-011-0494-z.

Kuzmich, N. *et al.* (2017) ‘TLR4 signaling pathway modulators as potential therapeutics in inflammation and sepsis’, *Vaccines*, 5(4), p. 34. doi:10.3390/vaccines5040034.

Lankford, K.L. *et al.* (1995) ‘Blocking ca2+ mobilization with thapsigargin reduces neurite initiation in cultured adult rat DRG neurons’, *Developmental Brain Research*, 84(2), pp. 151–163. doi:10.1016/0165-3806(94)00159-w.

Lanoiselée, H.-M. *et al.* (2017) ‘App, PSEN1, and PSEN2 mutations in early-onset alzheimer disease: A genetic screening study of familial and sporadic cases’, *PLOS Medicine*, 14(3). doi:10.1371/journal.pmed.1002270.

Lansdall, C. (2014). An effective treatment for Alzheimer's disease must consider both amyloid and tau. Bioscience Horizons, 7(0), p.2.

Lee, C.Y. and Landreth, G.E. (2010) 'The role of microglia in amyloid clearance from the AD brain', *Journal of Neural Transmission*, 117(8), pp. 949–960. doi:10.1007/s00702-010-0433-4.

Lee, H., Seo, H., Cha, H., Yang, Y., Kwon, S. and Yang, S. (2018). Diabetes and Alzheimer's Disease: Mechanisms and Nutritional Aspects. *Clinical Nutrition Research*, 7(4), p.229.

Lennicke, C. *et al.* (2015) 'Hydrogen peroxide – production, fate and role in redox signaling of Tumor Cells', *Cell Communication and Signaling*, 13(1). doi:10.1186/s12964-015-0118-6.

Li, J. *et al.* (2022) 'The beneficial roles of Apelin-13/APJ system in cerebral ischemia: Pathogenesis and therapeutic strategies', *Frontiers in Pharmacology*, 13. doi:10.3389/fphar.2022.903151.

Li, N. *et al.* (2004) 'NRF2 is a key transcription factor that regulates antioxidant defense in macrophages and epithelial cells: Protecting against the proinflammatory and oxidizing effects of diesel exhaust chemicals', *The Journal of Immunology*, 173(5), pp. 3467–3481. doi:10.4049/jimmunol.173.5.3467.

Li, R.-L. *et al.* (2022) 'Regulation of mitochondrial dysfunction induced cell apoptosis is a potential therapeutic strategy for herbal medicine to treat neurodegenerative diseases', *Frontiers in Pharmacology*, 13. doi:10.3389/fphar.2022.937289.

Li, X. *et al.* (2024) 'Protective effect of apelin-13 in lens epithelial cells via inhibiting oxidative stress-induced apoptosis', *BMC Ophthalmology*, 24(1). doi:10.1186/s12886-024-03746-6.

Li, X., He, S. and Ma, B. (2020) 'Autophagy and autophagy-related proteins in cancer', *Molecular Cancer*, 19(1). doi:10.1186/s12943-020-1138-4.

Li, Z. *et al.* (2020) 'Intermedin protects thapsigargin-induced endoplasmic reticulum stress in cardiomyocytes by modulating protein kinase A and sarco/endoplasmic

reticulum ca2+-atpase', *Molecular Medicine Reports*, 23(2). doi:10.3892/mmr.2020.11746.

Lin, M.T. and Beal, M.F. (2006) 'Mitochondrial dysfunction and oxidative stress in Neurodegenerative Diseases', *Nature*, 443(7113), pp. 787–795. doi:10.1038/nature05292.

Lindner, P. *et al.* (2020) 'Cell death induced by the ER stressor thapsigargin involves death receptor 5, a non-autophagic function of MAP1LC3B, and distinct contributions from unfolded protein response components', *Cell Communication and Signaling*, 18(1). doi:10.1186/s12964-019-0499-z.

Liu, C.-C. *et al.* (2013) 'Apolipoprotein E and alzheimer disease: Risk, mechanisms and therapy', *Nature Reviews Neurology*, 9(2), pp. 106–118. doi:10.1038/nrneurol.2012.263.

Liu, M. *et al.* (2023) 'Apelin-13 facilitates mitochondria homeostasis via mitophagy to prevent against airway oxidative injury in asthma', *Molecular Immunology*, 153, pp. 1–9. doi:10.1016/j.molimm.2022.11.012.

Liu, X. *et al.* (2014) 'The AMPK inhibitor compound C is a potent AMPK-independent Antiglioma agent', *Molecular Cancer Therapeutics*, 13(3), pp. 596–605. doi:10.1158/1535-7163.mct-13-0579.

Liu, Y. *et al.* (2019) 'Apelin-13 attenuates early brain injury following subarachnoid hemorrhage via suppressing neuronal apoptosis through the GLP-1R/PI3K/Akt signaling', *Biochemical and Biophysical Research Communications*, 513(1), pp. 105–111. doi:10.1016/j.bbrc.2019.03.151.

Long, H.-Z. *et al.* (2021) 'PI3K/AKT signal pathway: A target of natural products in the prevention and treatment of alzheimer's disease and parkinson's disease', *Frontiers in Pharmacology*, 12. doi:10.3389/fphar.2021.648636.

Lopez-Suarez, L. *et al.* (2022) 'The SH-sy5y human neuroblastoma cell line, a relevant in vitro cell model for investigating neurotoxicology in human: Focus on

organic pollutants', *NeuroToxicology*, 92, pp. 131–155. doi:10.1016/j.neuro.2022.07.008.

Lu, H., Chen, M. and Zhu, C. (2024) 'Intranasal administration of Apelin-13 ameliorates cognitive deficit in streptozotocin-induced alzheimer's disease model via enhancement of NRF2-HO1 PATHWAYS', *Brain Sciences*, 14(5), p. 488. doi:10.3390/brainsci14050488.

Lu, Q. *et al.* (2013) 'Apelin-13 regulates proliferation, migration and survival of retinal Müller cells under hypoxia', *Diabetes Research and Clinical Practice*, 99(2), pp. 158–167. doi:10.1016/j.diabres.2012.09.045.

Luo, H. *et al.* (2019) 'Apelin-13 suppresses neuroinflammation against cognitive deficit in a streptozotocin-induced rat model of alzheimer's disease through activation of BDNF-TrkB signaling pathway', *Frontiers in Pharmacology*, 10. doi:10.3389/fphar.2019.00395.

Luo, H., Xiang, Y., Qu, X., Liu, H., Liu, C., Li, G., Han, L. and Qin, X. (2019). Apelin-13 Suppresses Neuroinflammation Against Cognitive Deficit in a Streptozotocin-Induced Rat Model of Alzheimer's Disease Through Activation of BDNF-TrkB Signaling Pathway. *Frontiers in Pharmacology*, 10.

Lv, S.-Y., Chen, W.-D. and Wang, Y.-D. (2020) 'The apelin/APJ system in psychosis and neuropathy', *Frontiers in Pharmacology*, 11. doi:10.3389/fphar.2020.00320.

Ma, Q. (2013) 'Role of NRF2 in oxidative stress and toxicity', *Annual Review of Pharmacology and Toxicology*, 53(1), pp. 401–426. doi:10.1146/annurev-pharmtox-011112-140320.

MacLeod, R. *et al.* (2015) 'The role and therapeutic targeting of α-, β- and γ-secretase in alzheimer's disease', *Future Science OA*, 1(3). doi:10.4155/fso.15.9.

Maitra, U. *et al.* (2009) 'Irak-1 contributes to lipopolysaccharide-induced reactive oxygen species generation in macrophages by inducing NOx-1 transcription and RAC1 activation and suppressing the expression of antioxidative enzymes', *Journal of Biological Chemistry*, 284(51), pp. 35403–35411. doi:10.1074/jbc.m109.059501.

Maldonado, E. *et al.* (2023) ‘Aging hallmarks and the role of oxidative stress’, *Antioxidants*, 12(3), p. 651. doi:10.3390/antiox12030651.

Malhotra, J.D. and Kaufman, R.J. (2007) ‘The endoplasmic reticulum and the unfolded protein response’, *Seminars in Cell & Developmental Biology*, 18(6), pp. 716–731. doi:10.1016/j.semcdb.2007.09.003.

Manjarrés, I.M. *et al.* (2010) ‘The Sarco/endoplasmic reticulum ca2+ atpase (SERCA) is the third element in capacitative calcium entry’, *Cell Calcium*, 47(5), pp. 412–418. doi:10.1016/j.ceca.2010.03.001.

Martín, D., Salinas, M., López-Valdaliso, R., Serrano, E., Recuero, M. and Cuadrado, A. (2001). Effect of the Alzheimer amyloid fragment Aβ(25-35) on Akt/PKB kinase and survival of PC12 cells. Journal of Neurochemistry, 78(5), pp.1000-1008.

Masoumi, J. *et al.* (2018) ‘Apelin, a promising target for alzheimer disease prevention and treatment’, *Neuropeptides*, 70, pp. 76–86. doi:10.1016/j.npep.2018.05.008.

Maurer, K., Volk, S. and Gerbaldo, H. (1997) ‘Auguste D and alzheimer’s disease’, *The Lancet*, 349(9064), pp. 1546–1549. doi:10.1016/s0140-6736(96)10203-8.

McGleenon, Dynan and Passmore (1999) ‘Acetylcholinesterase inhibitors in alzheimer’s disease’, *British Journal of Clinical Pharmacology*, 48(4), pp. 471–480. doi:10.1046/j.1365-2125.1999.00026.x.

Meng, Y. *et al.* (2017) ‘Role of the PI3K/akt signalling pathway in apoptotic cell death in the cerebral cortex of streptozotocin-induced diabetic rats’, *Experimental and Therapeutic Medicine*, 13(5), pp. 2417–2422. doi:10.3892/etm.2017.4259.

Mietelska-Porowska, A. *et al.* (2014) ‘Tau protein modifications and interactions: their role in function and dysfunction’, *International Journal of Molecular Sciences*, 15(3), pp. 4671–4713. doi:10.3390/ijms15034671.

Milton, N.G. (2004) ‘Role of hydrogen peroxide in the aetiology of Alzheimer??S Disease’, *Drugs & Aging*, 21(2), pp. 81–100. doi:10.2165/00002512-200421020-00002.

Min, S., Park, J., Luo, L., Kwon, Y., Lee, H., Jung Shim, H., Kim, I., Lee, J. and Shin, H. (2015). Assessment of C-phycocyanin effect on astrocytes-mediated neuroprotection against oxidative brain injury using 2D and 3D astrocyte tissue model. *Scientific Reports*, 5(1).

Misrani, A., Tabassum, S. and Yang, L. (2021) ‘Mitochondrial dysfunction and oxidative stress in alzheimer’s disease’, *Frontiers in Aging Neuroscience*, 13. doi:10.3389/fnagi.2021.617588.

Mlyczyńska, E. *et al.* (2021) ‘Anti-apoptotic effect of Apelin in human placenta: Studies on bewo cells and villous explants from third-Trimester human pregnancy’, *International Journal of Molecular Sciences*, 22(5), p. 2760. doi:10.3390/ijms22052760.

Mohandas, E., Rajmohan, V. and Raghunath, B. (2009). Neurobiology ofAlzheimer′s disease. Indian Journal of Psychiatry, 51(1), p.55.

Moon, D.-O. (2023) ‘Calcium’s role in orchestrating cancer apoptosis: Mitochondrial-centric perspective’, *International Journal of Molecular Sciences*, 24(10), p. 8982. doi:10.3390/ijms24108982.

Morishima, N. *et al.* (2002) ‘An endoplasmic reticulum stress-specific caspase cascade in apoptosis’, *Journal of Biological Chemistry*, 277(37), pp. 34287–34294. doi:10.1074/jbc.m204973200.

Morris, J. and Burns, J., 2012. Insulin: An Emerging Treatment for Alzheimer’s Disease Dementia?. *Current Neurology and Neuroscience Reports*, 12(5), pp.520-527.

Moya-Alvarado, G., Gershoni-Emek, N., Perlson, E. and Bronfman, F. (2015). Neurodegeneration and Alzheimer's disease (AD). What Can Proteomics Tell Us About the Alzheimer's Brain?. *Molecular & Cellular Proteomics*, 15(2), pp.409-425.

Munford, R.S. (2008) ‘Sensing Gram-negative bacterial lipopolysaccharides: A human disease determinant?’, *Infection and Immunity*, 76(2), pp. 454–465. doi:10.1128/iai.00939-07.

Na, K., Oh, B.-C. and Jung, Y. (2023) ‘Multifaceted role of CD14 in innate immunity and tissue homeostasis’, *Cytokine & Growth Factor Reviews*, 74, pp. 100–107. doi:10.1016/j.cytogfr.2023.08.008.

Naumenko, V.S. and Ponimaskin, E. (2018) ‘Palmitoylation as a functional regulator of neurotransmitter receptors’, *Neural Plasticity*, 2018, pp. 1–18. doi:10.1155/2018/5701348.

Ng, Y.-W. and Say, Y.-H. (2018) ‘Palmitic acid induces neurotoxicity and gliatoxicity in SH-Sy5y Human Neuroblastoma and T98G human glioblastoma cells’, *PeerJ*, 6. doi:10.7717/peerj.4696.

Ngo, V. and Duennwald, M.L. (2022) ‘Nrf2 and oxidative stress: A general overview of mechanisms and implications in human disease’, *Antioxidants*, 11(12), p. 2345. doi:10.3390/antiox11122345.

Nguyen, Thuy Trang *et al.* (2020) ‘Type 3 diabetes and its role implications in alzheimer’s disease’, *International Journal of Molecular Sciences*, 21(9), p. 3165. doi:10.3390/ijms21093165.

NIH (2023) *Alzheimer’s disease genetics fact sheet* | *National Institute on Aging*, *National Institute on Aging*. Available at: https://www.nia.nih.gov/health/alzheimers-causes-and-risk-factors/alzheimers-disease-genetics-fact-sheet (Accessed: 22 November 2024).

NIH (2023) *Understanding different types of dementia* | *National Institute on Aging*. Available at: https://www.nia.nih.gov/health/alzheimers-and-dementia/understanding-different-types-dementia (Accessed: 17 January 2025).

O’Brien, M.A. and Kirby, R. (2008) ‘Apoptosis: A review of Pro-apoptotic and anti-apoptotic pathways and dysregulation in disease’, *Journal of Veterinary Emergency and Critical Care*, 18(6), pp. 572–585. doi:10.1111/j.1476-4431.2008.00363.x.

O'Carroll, A., Lolait, S., Harris, L. and Pope, G. (2013). The apelin receptor APJ: journey from an orphan to a multifaceted regulator of homeostasis. *Journal of Endocrinology*, 219(1), pp.R13-R35.

O'Donnell, L.A. *et al.* (2007) 'Apelin, an endogenous neuronal peptide, protects hippocampal neurons against excitotoxic injury', *Journal of Neurochemistry*, 102(6), pp. 1905–1917. doi:10.1111/j.1471-4159.2007.04645.x.

O'Harte, F.P. *et al.* (2018) 'Long-term treatment with acylated analogues of apelin-13 amide ameliorates diabetes and improves lipid profile of high-fat fed mice', *PLOS ONE*, 13(8). doi:10.1371/journal.pone.0202350.

O'Harte, F.P.M. *et al.* (2017) 'Acylated Apelin-13 amide analogues exhibit enzyme resistance and prolonged insulin releasing, glucose lowering and anorexic properties', *Biochemical Pharmacology*, 146, pp. 165–173. doi:10.1016/j.bcp.2017.10.002.

Oruç, K.Y. *et al.* (2025) 'Protective effect of apelin-13 on D-glutamic acid-induced excitotoxicity in SH-Sy5y Cell Line: An in-vitro study', *Neuropeptides*, 109, p. 102483. doi:10.1016/j.npep.2024.102483.

Oslowski, C.M. and Urano, F. (2011) 'Measuring er stress and the unfolded protein response using mammalian tissue culture system', *Methods in Enzymology*, pp. 71–92. doi:10.1016/b978-0-12-385114-7.00004-0.

Ozcan, L. and Tabas, I. (2012) 'Role of endoplasmic reticulum stress in metabolic disease and other disorders', *Annual Review of Medicine*, 63(1), pp. 317–328. doi:10.1146/annurev-med-043010-144749.

Pahlavani, H.A. (2023) 'Exercise therapy to prevent and treat alzheimer's disease', *Frontiers in Aging Neuroscience*, 15. doi:10.3389/fnagi.2023.1243869.

Pak, V.V. *et al.* (2020) 'Ultrasensitive genetically encoded indicator for hydrogen peroxide identifies roles for the oxidant in cell migration and mitochondrial function', *Cell Metabolism*, 31(3). doi:10.1016/j.cmet.2020.02.003.

Pallepati, P. and Averill-Bates, D.A. (2011) 'Activation of ER stress and apoptosis by hydrogen peroxide in Hela cells: Protective role of mild heat preconditioning at

40°C', *Biochimica et Biophysica Acta (BBA) - Molecular Cell Research*, 1813(12), pp. 1987–1999. doi:10.1016/j.bbamcr.2011.07.021.

Panagaki, T., Michael, M. and Hölscher, C. (2017) 'Liraglutide restores chronic ER stress, autophagy impairments and apoptotic signalling in SH-SY5Y cells', *Scientific Reports*, 7(1). doi:10.1038/s41598-017-16488-x.

Panov, A. *et al.* (2014) 'Fatty acids in energy metabolism of the Central Nervous System', *BioMed Research International*, 2014, pp. 1–22. doi:10.1155/2014/472459.

Paradis, E. *et al.* (1996) 'Amyloid β peptide of alzheimer's disease downregulates bcl-2 and upregulates Bax expression in human neurons', *The Journal of Neuroscience*, 16(23), pp. 7533–7539. doi:10.1523/jneurosci.16-23-07533.1996.

Parthsarathy, V. *et al.* (2017) 'Beneficial long-term antidiabetic actions of n- and c-terminally modified analogues of Apelin-13 in diet-induced obese diabetic mice', *Diabetes, Obesity and Metabolism*, 20(2), pp. 319–327. doi:10.1111/dom.13068.

Patil, S. and Chan, C. (2005) 'Palmitic and stearic fatty acids induce alzheimer-like hyperphosphorylation of tau in primary rat cortical neurons', *Neuroscience Letters*, 384(3), pp. 288–293. doi:10.1016/j.neulet.2005.05.003.

Peng, Y. *et al.* (2023) '*The protective effect of apelin-13 against cardiac hypertrophy through activating the PI3K-akt-mtor signaling pathway*', *Iranian journal of basic medical sciences*, 26(2).doi :10.22038/IJBMS.2022.65160.14356.

Perl, D.P. (2010) 'Neuropathology of Alzheimer's disease', Mount Sinai Journal of Medicine: A Journal of Translational and Personalized Medicine, 77(1), pp. 32–42. doi:10.1002/msj.20157.

Petratos, S. *et al.* (2007) 'The β-amyloid protein of alzheimer's disease increases neuronal CRMP-2 phosphorylation by a rho-GTP mechanism', *Brain*, 131(1), pp. 90–108. doi:10.1093/brain/awm260.

Pisarenko, O. *et al.* (2015) 'Structural apelin analogues: Mitochondrial ros inhibition and cardiometabolic protection in myocardial ischaemia reperfusion injury', *British Journal of Pharmacology*, 172(12), pp. 2933–2945. doi:10.1111/bph.13038.

Pistollato, F. *et al.* (2018) 'Nutritional patterns associated with the maintenance of neurocognitive functions and the risk of dementia and alzheimer's disease: A Focus on Human Studies', *Pharmacological Research*, 131, pp. 32–43. doi:10.1016/j.phrs.2018.03.012.

Popov, S.V. *et al.* (2023) 'Apelin is a prototype of novel drugs for the treatment of acute myocardial infarction and adverse myocardial remodeling', *Pharmaceutics*, 15(3), p. 1029. doi:10.3390/pharmaceutics15031029.

Pouresmaeili-Babaki, E. *et al.* (2018) 'Protective effect of neuropeptide apelin-13 on 6-hydroxydopamine-induced neurotoxicity in SH-SY5Y dopaminergic cells: Involvement of its antioxidant and antiapoptotic properties', *Rejuvenation Research*, 21(2), pp. 162–167. doi:10.1089/rej.2017.1951.

Prevalence and incidence (2024) *Dementia Statistics Hub*. Available at: https://dementiastatistics.org/about-dementia/prevalence-and-incidence/ (Accessed: 21 November 2024).

Qu, K. *et al.* (2022) 'Mitochondrial dysfunction in vascular endothelial cells and its role in atherosclerosis', *Frontiers in Physiology*, 13. doi:10.3389/fphys.2022.1084604.

Rahman, M., Rahman, M., Rahman, M., Rasheduzzaman, M., Mamun-Or-Rashid, A., Uddin, M., Rahman, M., Hwang, H., Pang, M. and Rhim, H., 2020. Modulatory Effects of Autophagy on APP Processing as a Potential Treatment Target for Alzheimer's Disease. *Biomedicines*, 9(1), p.5.

Ramyaa, P., krishnaswamy, R. and Padma, V.V. (2014) 'Quercetin modulates OTA-induced oxidative stress and redox signalling in HEPG2 cells — up regulation of NRF2 expression and down regulation of NF-KB and COX-2', *Biochimica et Biophysica Acta (BBA) - General Subjects*, 1840(1), pp. 681–692. doi:10.1016/j.bbagen.2013.10.024.

Read, C. *et al.* (2019) 'International Union of Basic and Clinical Pharmacology. CVII. structure and pharmacology of the Apelin receptor with a recommendation that elabela/toddler is a second endogenous peptide ligand', *Pharmacological Reviews*, 71(4), pp. 467–502. doi:10.1124/pr.119.017533.

Reddy, P.H. and Beal, M.F. (2008) 'Amyloid beta, mitochondrial dysfunction and synaptic damage: Implications for cognitive decline in aging and alzheimer's disease', *Trends in Molecular Medicine*, 14(2), pp. 45–53. doi:10.1016/j.molmed.2007.12.002.

Reinhardt, H.C. *et al.* (2007) 'P53-deficient cells rely on ATM- and ATR-mediated checkpoint signaling through the p38mapk/MK2 pathway for survival after DNA damage', *Cancer Cell*, 11(2), pp. 175–189. doi:10.1016/j.ccr.2006.11.024.

Ribarič, S. (2018). Peptides as Potential Therapeutics for Alzheimer's Disease. *Molecules*, 23(2), p.283.

Roy, A. *et al.* (2017) 'Tobacco and cardiovascular disease: A summary of evidence', *Disease Control Priorities, Third Edition (Volume 5): Cardiovascular, Respiratory, and Related Disorders*, pp. 57–77. doi:10.1596/978-1-4648-0518-9_ch4.

Sadigh-Eteghad, S. *et al.* (2014) 'Amyloid-beta: A crucial factor in alzheimer's disease', *Medical Principles and Practice*, 24(1), pp. 1–10. doi:10.1159/000369101.

Saha, P., Guha, S. and Biswas, S.C. (2020) 'P38k and JNK pathways are induced by amyloid-β in astrocyte: Implication of MAPK pathways in astrogliosis in alzheimer's disease', *Molecular and Cellular Neuroscience*, 108, p. 103551. doi:10.1016/j.mcn.2020.103551.

Saputra, F., Kishida, M. and Hu, S.-Y. (2024) 'Oxidative stress induced by hydrogen peroxide disrupts zebrafish visual development by altering apoptosis, antioxidant and estrogen related genes', *Scientific Reports*, 14(1). doi:10.1038/s41598-024-64933-5.

Savova, M.S. *et al.* (2023) 'Targeting PI3K/akt signaling pathway in obesity', *Biomedicine & Pharmacotherapy*, 159, p. 114244. doi:10.1016/j.biopha.2023.114244.

Scarmeas, N. and Stern, Y. (2003) ‘Cognitive Reserve and lifestyle’, *Journal of Clinical and Experimental Neuropsychology*, 25(5), pp. 625–633. doi:10.1076/jcen.25.5.625.14576.

Schieber, M. and Chandel, N.S. (2014) ‘Ros function in redox signaling and oxidative stress’, *Current Biology*, 24(10). doi:10.1016/j.cub.2014.03.034.

Schulz, R. and Sherwood, P.R. (2008) ‘Physical and mental health effects of family caregiving’, *AJN, American Journal of Nursing*, 108(9), pp. 23–27. doi:10.1097/01.naj.0000336406.45248.4c.

Schweig, J.E. *et al.* (2017) ‘Alzheimer’s disease pathological lesions activate the spleen tyrosine kinase’, *Acta Neuropathologica Communications*, 5(1). doi:10.1186/s40478-017-0472-2.

Sędzikowska, A. and Szablewski, L. (2021) ‘Insulin and insulin resistance in alzheimer’s disease’, *International Journal of Molecular Sciences*, 22(18), p. 9987. doi:10.3390/ijms22189987.

Sehgal, P. *et al.* (2017) ‘Inhibition of the sarco/endoplasmic reticulum (ER) ca2+-atpase by thapsigargin analogs induces cell death via er ca2+ depletion and the unfolded protein response’, *Journal of Biological Chemistry*, 292(48), pp. 19656–19673. doi:10.1074/jbc.m117.796920.

Selkoe, D.J. and Hardy, J. (2016) ‘The amyloid hypothesis of alzheimer’s disease at 25 Years’, *EMBO Molecular Medicine*, 8(6), pp. 595–608. doi:10.15252/emmm.201606210.

Senturk, E. and Manfredi, J.J. (2012) ‘P53 and cell cycle effects after DNA damage’, *Methods in Molecular Biology*, pp. 49–61. doi:10.1007/978-1-62703-236-0_4.

Sgourakis, N.G. *et al.* (2007) ‘The alzheimer’s peptides AB40 and 42 adopt distinct conformations in water: A combined MD / NMR study’, *Journal of Molecular Biology*, 368(5), pp. 1448–1457. doi:10.1016/j.jmb.2007.02.093.

Shao, Z.-Q. *et al.* (2021) ‘Apelin-13 inhibits apoptosis and excessive autophagy in cerebral ischemia/reperfusion injury’, *Neural Regeneration Research*, 16(6), p. 1044. doi:10.4103/1673-5374.300725.

Shipley, M.M., Mangold, C.A. and Szpara, M.L. (2016) ‘Differentiation of the SH-sy5y human neuroblastoma cell line’, *Journal of Visualized Experiments* [Preprint], (108). doi:10.3791/53193.

Silva, M., Loures, C., Alves, L., de Souza, L., Borges, K. and Carvalho, M., 2019. Alzheimer’s disease: risk factors and potentially protective measures. *Journal of Biomedical Science*, 26(1).

Silva, M.V. *et al.* (2019) ‘Alzheimer’s disease: Risk factors and potentially protective measures’, *Journal of Biomedical Science*, 26(1). doi:10.1186/s12929-019-0524-y.

Silvestro, S., Raffaele, I. and Mazzon, E. (2023) ‘Modulating stress proteins in response to therapeutic interventions for parkinson’s disease’, *International Journal of Molecular Sciences*, 24(22), p. 16233. doi:10.3390/ijms242216233.

Simpson, D.S. and Oliver, P.L. (2020) ‘Ros generation in microglia: Understanding oxidative stress and inflammation in neurodegenerative disease’, *Antioxidants*, 9(8), p. 743. doi:10.3390/antiox9080743.

Śliwińska-Mossoń, M. and Milnerowicz, H. (2017) ‘The impact of smoking on the development of diabetes and its complications’, *Diabetes and Vascular Disease Research*, 14(4), pp. 265–276. doi:10.1177/1479164117701876.

Snyder, J.T. *et al.* (2021) ‘Endoplasmic Reticulum stress induced proliferation remains intact in aging mouse β-cells’, *Frontiers in Endocrinology*, 12. doi:10.3389/fendo.2021.734079.

Soares, J.-B. *et al.* (2010) ‘The role of lipopolysaccharide/toll-like receptor 4 signaling in Chronic liver diseases’, *Hepatology International*, 4(4), pp. 659–672. doi:10.1007/s12072-010-9219-x.

Soltani, M.H. *et al.* (2005) ‘Microtubule-associated protein 2, a marker of neuronal differentiation, induces mitotic defects, inhibits growth of melanoma cells, and

predicts metastatic potential of cutaneous melanoma', *The American Journal of Pathology*, 166(6), pp. 1841–1850. doi:10.1016/s0002-9440(10)62493-5.

Song, Z. *et al.* (2022) 'Baicalin attenuated AB1-42-induced apoptosis in SH-SY5Y cells by inhibiting the Ras-Erk Signaling Pathway', *BioMed Research International*, 2022, pp. 1–11. doi:10.1155/2022/9491755.

Srivareerat, M. *et al.* (2011) 'Chronic nicotine restores normal AB levels and prevents short-term memory and E-LTP impairment in AB rat model of alzheimer's disease', *Neurobiology of Aging*, 32(5), pp. 834–844. doi:10.1016/j.neurobiolaging.2009.04.015.

Storozhuk, M.V. *et al.* (2005) 'Possible role of mitochondria in posttetanic potentiation of GABAergic synaptic transmission in rat neocortical cell cultures', *Synapse*, 58(1), pp. 45–52. doi:10.1002/syn.20186.

Sulatskaya, A.I. *et al.* (2017) 'Thioflavin t fluoresces as excimer in highly concentrated aqueous solutions and as monomer being incorporated in amyloid fibrils', *Scientific Reports*, 7(1). doi:10.1038/s41598-017-02237-7.

Sun, P. *et al.* (2014) 'Neuroprotective effects of geniposide in SH-SY5Y cells and primary hippocampal neurons exposed to a*β*42', *BioMed Research International*, 2014, pp. 1–11. doi:10.1155/2014/284314.

Swerdlow, R.H. (2018) 'Mitochondria and mitochondrial cascades in alzheimer's disease', *Journal of Alzheimer's Disease*, 62(3), pp. 1403–1416. doi:10.3233/jad-170585.

Takadera, T., Yoshikawa, R. and Ohyashiki, T. (2006) 'Thapsigargin-induced apoptosis was prevented by glycogen synthase kinase-3 inhibitors in PC12 cells', *Neuroscience Letters*, 408(2), pp. 124–128. doi:10.1016/j.neulet.2006.08.066.

Takeo, T., Miyake, M. and Mizuno, H. (2024) 'Neuroprotective effects of PROBUCOL against rotenone-induced toxicity *via* suppression of reactive oxygen species production in SH-Sy5y Cells', *Biological and Pharmaceutical Bulletin*, 47(6), pp. 1154–1162. doi:10.1248/bpb.b24-00099.

Tan, B.L. and Norhaizan, M.E. (2019) ‘Effect of high-fat diets on oxidative stress, cellular inflammatory response and cognitive function’, *Nutrients*, 11(11), p. 2579. doi:10.3390/nu11112579.

Tangestani Fard, M. and Stough, C. (2019). A Review and Hypothesized Model of the Mechanisms That Underpin the Relationship Between Inflammation and Cognition in the Elderly. *Frontiers in Aging Neuroscience*, 11.

Tapiola, T. *et al.* (2009) ‘Cerebrospinal fluid β-amyloid 42 and tau proteins as biomarkers of alzheimer-type pathologic changes in the brain’, *Archives of Neurology*, 66(3). doi:10.1001/archneurol.2008.596.

TCW, J. and Goate, A.M. (2016) ‘Genetics of β-amyloid precursor protein in alzheimer’s disease’, *Cold Spring Harbor Perspectives in Medicine*, 7(6). doi:10.1101/cshperspect.a024539.

Teske, B.F. *et al.* (2011) ‘The eif2 kinase perk and the integrated stress response facilitate activation of ATF6 during endoplasmic reticulum stress’, *Molecular Biology of the Cell*, 22(22), pp. 4390–4405. doi:10.1091/mbc.e11-06-0510.

Thal, D.R. *et al.* (2014) ‘Neuropathology and biochemistry of AB and its aggregates in alzheimer’s disease’, *Acta Neuropathologica*, 129(2), pp. 167–182. doi:10.1007/s00401-014-1375-y.

Than A. *et al.* (2014) ‘Apelin attenuates oxidative stress in human adipocytes’, *Journal of Biological Chemistry*, 289(6), pp. 3763–3774. doi:10.1074/jbc.m113.526210.

The Lancet (2018) ‘Dementia in the UK: Preparing the NHS for new treatments’, *The Lancet*, 391(10127), p. 1237. doi:10.1016/s0140-6736(18)30709-8.

Thinakaran, G. (1999) ‘The role of presenilins in alzheimer’s disease’, *Journal of Clinical Investigation*, 104(10), pp. 1321–1327. doi:10.1172/jci8728.

TOCHIGI, M. *et al.* (2013) ‘Hydrogen peroxide induces cell death in human trail-resistant melanoma through intracellular superoxide generation’, *International Journal of Oncology*, 42(3), pp. 863–872. doi:10.3892/ijo.2013.1769.

Tönnies, E. and Trushina, E. (2017) ‘Oxidative stress, synaptic dysfunction, and alzheimer’s disease’, *Journal of Alzheimer’s Disease*, 57(4), pp. 1105–1121. doi:10.3233/jad-161088.

Tönnies, E. and Trushina, E. (2017) ‘Oxidative stress, synaptic dysfunction, and alzheimer’s disease’, *Journal of Alzheimer’s Disease*, 57(4), pp. 1105–1121. doi:10.3233/jad-161088.

Tsai, Y.C. and Weissman, A.M. (2010) ‘The unfolded protein response, degradation from the endoplasmic reticulum, and cancer’, *Genes & Cancer*, 1(7), pp. 764–778. doi:10.1177/1947601910383011.

Ullrich, C. and Humpel, C. (2009) ‘The pro-apoptotic substance thapsigargin selectively stimulates re-growth of brain capillaries’, *Current Neurovascular Research*, 6(3), pp. 171–180. doi:10.2174/156720209788970063.

Van Cauwenberghe, C., Van Broeckhoven, C. and Sleegers, K. (2016) ‘The genetic landscape of alzheimer disease: Clinical implications and perspectives’, *Genetics in Medicine*, 18(5), pp. 421–430. doi:10.1038/gim.2015.117.

Vesga-Jiménez, D.J. *et al.* (2022) ‘Fatty acids: An insight into the pathogenesis of Neurodegenerative Diseases and therapeutic potential’, *International Journal of Molecular Sciences*, 23(5), p. 2577. doi:10.3390/ijms23052577.

Vince, J.E. *et al.* (2018) ‘The mitochondrial apoptotic effectors BAX/bak activate caspase-3 and -7 to trigger NLRP3 inflammasome and caspase-8 driven il-1β activation’, *Cell Reports*, 25(9). doi:10.1016/j.celrep.2018.10.103.

Vogels, T., Murgoci, A.-N. and Hromádka, T. (2019) ‘Intersection of pathological tau and microglia at the Synapse’, *Acta Neuropathologica Communications*, 7(1). doi:10.1186/s40478-019-0754-y.

Walsh, D.M. and Teplow, D.B. (2012) ‘Alzheimer’s disease and the amyloid β-protein’, *Progress in Molecular Biology and Translational Science*, pp. 101–124. doi:10.1016/b978-0-12-385883-2.00012-6.

Wan, T. *et al.* (2021) ‘Research progress on mechanism of neuroprotective roles of apelin-13 in prevention and treatment of alzheimer’s disease’, *Neurochemical Research*, 47(2), pp. 205–217. doi:10.1007/s11064-021-03448-1.

Wang, L. *et al.* (2020) ‘Current understanding of metal ions in the pathogenesis of alzheimer’s disease’, *Translational Neurodegeneration*, 9(1). doi:10.1186/s40035-020-00189-z.

Wang, W. *et al.* (2020) ‘Mitochondria dysfunction in the pathogenesis of alzheimer’s disease: Recent advances’, *Molecular Neurodegeneration*, 15(1). doi:10.1186/s13024-020-00376-6.

Wang, X. and Jia, J. (2023) ‘Magnolol improves alzheimer’s disease-like pathologies and cognitive decline by promoting autophagy through activation of the AMPK/mTOR/Ulk1 Pathway’, *Biomedicine & Pharmacotherapy*, 161, p. 114473. doi:10.1016/j.biopha.2023.114473.

Wang, X. *et al.* (2014) ‘Oxidative stress and mitochondrial dysfunction in alzheimer’s disease’, *Biochimica et Biophysica Acta (BBA) - Molecular Basis of Disease*, 1842(8), pp. 1240–1247. doi:10.1016/j.bbadis.2013.10.015.

Wei, Y. *et al.* (2006) ‘Saturated fatty acids induce endoplasmic reticulum stress and apoptosis independently of ceramide in liver cells’, *American Journal of Physiology-Endocrinology and Metabolism*, 291(2). doi:10.1152/ajpendo.00644.2005.

Wen, R. *et al.* (2023) ‘Beneficial effects of apelin-13 on metabolic diseases and exercise’, *Frontiers in Endocrinology*, 14. doi:10.3389/fendo.2023.1285788.

What are the costs of dementia diagnosis and care in the UK? (2024) *Alzheimer’s Society*. Available at: https://www.alzheimers.org.uk/about-us/policy-and-influencing/dementia-scale-impact-numbers#:~:text=The%20average%20per%20person%20costs%20associated%20with,driven%20by%20increasing%20need%20of%20complex%20care. (Accessed: 21 January 2025).

Who.int. 2021. *Dementia*. [online] Available at: <https://www.who.int/news-room/fact-sheets/detail/dementia> [Accessed March 2021].

Wilson, C. and González-Billault, C. (2015) ‘Regulation of cytoskeletal dynamics by redox signaling and oxidative stress: Implications for neuronal development and trafficking’, *Frontiers in Cellular Neuroscience*, 9. doi:10.3389/fncel.2015.00381.

Wong , W. (2020) ‘Economic burden of alzheimer disease and managed care considerations’, *The American Journal of Managed Care*, 26(Suppl 8). doi:10.37765/ajmc.2020.88482.

Wu, L. *et al.* (2019) ‘thapsigargin induces apoptosis in adrenocortical carcinoma by activating endoplasmic reticulum stress and the JNK signaling pathway: An in vitro and in vivo study ’, *Drug Design, Development and Therapy*, Volume 13, pp. 2787–2798. doi:10.2147/dddt.s209947.

Wysocka, M.B., Pietraszek-Gremplewicz, K. and Nowak, D. (2018) ‘The role of Apelin in cardiovascular diseases, obesity and cancer’, *Frontiers in Physiology*, 9. doi:10.3389/fphys.2018.00557.

Xia, F. *et al.* (2020) ‘Apelin-13 protects the lungs from ischemia-reperfusion injury by attenuating inflammatory and oxidative stress’, *Human & Experimental Toxicology*, 40(4), pp. 685–694. doi:10.1177/0960327120961436.

Xin, X., Gong, T. and Hong, Y. (2022) ‘Hydrogen peroxide initiates oxidative stress and proteomic alterations in meningothelial cells’, *Scientific Reports*, 12(1). doi:10.1038/s41598-022-18548-3.

Xing, G. *et al.* (2011) ‘Neuroprotective effects of puerarin against beta-amyloid-induced neurotoxicity in PC12 cells via a PI3K-dependent signaling pathway’, *Brain Research Bulletin*, 85(3–4), pp. 212–218. doi:10.1016/j.brainresbull.2011.03.024.

Xu, W. *et al.* (2017) ‘Apelin protects against myocardial ischemic injury by inhibiting dynamin-related protein 1’, *Oncotarget*, 8(59), pp. 100034–100044. doi:10.18632/oncotarget.21777.

Xu, W. *et al.* (2019) ‘Apelin-13/APJ system attenuates early brain injury via suppression of endoplasmic reticulum stress-associated TXNIP/NLRP3 inflammasome activation and oxidative stress in a ampk-dependent manner after

subarachnoid hemorrhage in rats', *Journal of Neuroinflammation*, 16(1). doi:10.1186/s12974-019-1620-3.

Yamamoto, N. *et al.* (2021) 'Protein kinases A and C regulate amyloid-β degradation by modulating protein levels of neprilysin and insulin-degrading enzyme in astrocytes', *Neuroscience Research*, 166, pp. 62–72. doi:10.1016/j.neures.2020.05.008.

Yan, J. *et al.* (2020) 'Apelin/APJ system: An emerging therapeutic target for respiratory diseases', *Cellular and Molecular Life Sciences*, 77(15), pp. 2919–2930. doi:10.1007/s00018-020-03461-7.

Yan, X. *et al.* (2020) 'The regulatory role of Apelin on the appetite and growth of common carp (Cyprinus carpio L.)', *Animals*, 10(11), p. 2163. doi:10.3390/ani10112163.

Yang, H. *et al.* (2023) 'Hydrogen peroxide and iron ions can modulate lipid peroxidation, apoptosis, and the cell cycle, but do not have a significant effect on DNA double-strand break', *Biochemical and Biophysical Research Communications*, 651, pp. 121–126. doi:10.1016/j.bbrc.2023.02.023.

Yang, Jian *et al.* (2016) 'Imaging hydrogen peroxide in alzheimer's disease via Cascade Signal Amplification', *Scientific Reports*, 6(1). doi:10.1038/srep35613.

Yang, Y. *et al.* (2014) 'Apelin-13 protects the brain against ischemia/reperfusion injury through activating PI3K/Akt and ERK1/2 signaling pathways', *Neuroscience Letters*, 568, pp. 44–49. doi:10.1016/j.neulet.2014.03.037.

Yang, Y. *et al.* (2016) 'Apelin-13 protects against apoptosis by activating AMP-activated protein kinase pathway in ischemia stroke', *Peptides*, 75, pp. 96–100. doi:10.1016/j.peptides.2015.11.002.

Yang, Y. *et al.* (2020) 'Endoplasmic Reticulum stress and focused drug discovery in cardiovascular disease', *Clinica Chimica Acta*, 504, pp. 125–137. doi:10.1016/j.cca.2020.01.031.

Yao, M., Nguyen, T.-V.V. and Pike, C.J. (2005) ‘B-amyloid-induced neuronal apoptosis involves c-jun N-terminal kinase-dependent downregulation of Bcl-W’, *The Journal of Neuroscience*, 25(5), pp. 1149–1158. doi:10.1523/jneurosci.4736-04.2005.

Yates, S., Zafar, A., Hubbard, P., Nagy, S., Durant, S., Bicknell, R., Wilcock, G., Christie, S., Esiri, M., Smith, A. and Nagy, Z. (2013). Dysfunction of the mTOR pathway is a risk factor for Alzheimer’s disease. Acta Neuropathologica Communications, 1(1), p.3.

Yiannopoulou, K. and Papageorgiou, S., 2012. Current and future treatments for Alzheimer’s disease. *Therapeutic Advances in Neurological Disorders*, 6(1), pp.19-33.

Yin, H. *et al.* (2020) ‘Apelin protects auditory cells from cisplatin-induced toxicity in vitro by inhibiting ROS and apoptosis’, *Neuroscience Letters*, 728, p. 134948. doi:10.1016/j.neulet.2020.134948.

Yoshida, I. *et al.* (2006) ‘Depletion of intracellular ca2+ store itself may be a major factor in thapsigargin-induced ER stress and apoptosis in PC12 cells’, *Neurochemistry International*, 48(8), pp. 696–702. doi:10.1016/j.neuint.2005.12.012.

Yuan, Q. *et al.* (2013) ‘Palmitic acid increases apoptosis of neural stem cells via activating c-jun N-terminal kinase’, *Stem Cell Research*, 10(2), pp. 257–266. doi:10.1016/j.scr.2012.11.008.

Yuan, Y. *et al.* (2022) ‘Apelin-13 attenuates lipopolysaccharide-induced inflammatory responses and acute lung injury by regulating PFKFB3-driven glycolysis induced by Nox4-dependent Ros’, *Journal of Inflammation Research*, Volume 15, pp. 2121–2139. doi:10.2147/jir.s348850.

Yue, P. *et al.* (2010) ‘Apelin is necessary for the maintenance of insulin sensitivity’, *American Journal of Physiology-Endocrinology and Metabolism*, 298(1). doi:10.1152/ajpendo.00385.2009.

Zeng, G.-G. *et al.* (2024) ‘Apelin-13: A protective role in vascular diseases’, *Current Problems in Cardiology*, 49(1), p. 102088. doi:10.1016/j.cpcardiol.2023.102088.

Zhan, X., Stamova, B. and Sharp, F.R. (2018) ‘Lipopolysaccharide associates with amyloid plaques, neurons and oligodendrocytes in alzheimer’s disease brain: A Review’, *Frontiers in Aging Neuroscience*, 10. doi:10.3389/fnagi.2018.00042.

Zhang, Hailin *et al.* (2018) ‘Apelin-13 administration protects against LPS-induced acute lung injury by inhibiting NF-KB pathway and NLRP3 inflammasome activation’, *Cellular Physiology and Biochemistry*, 49(5), pp. 1918–1932. doi:10.1159/000493653.

Zhang, Jifa *et al.* (2024) ‘Recent advances in alzheimer’s disease: Mechanisms, clinical trials and New Drug Development Strategies’, *Signal Transduction and Targeted Therapy*, 9(1). doi:10.1038/s41392-024-01911-3.

Zhang, R. *et al.* (2022) ‘Apelin-13 prevents the effects of oxygen–glucose deprivation/reperfusion on bend.3 cells by inhibiting AKT–mtor signaling’, *Experimental Biology and Medicine*, 248(2), pp. 146–156. doi:10.1177/15353702221139186.

Zhang, T. *et al.* (2022) ‘Different extracellular β-amyloid (1-42) aggregates differentially impair neural cell adhesion and neurite outgrowth through differential induction of Scaffold Palladin’, *Biomolecules*, 12(12), p. 1808. doi:10.3390/biom12121808.

Zhang, X. *et al.* (2011) ‘Up-regulation of Apelin in brain tissue of patients with epilepsy and an epileptic rat model’, *Peptides*, 32(9), pp. 1793–1799. doi:10.1016/j.peptides.2011.08.006.

Zhang, X. *et al.* (2014) ‘Endoplasmic Reticulum stress induced by tunicamycin and Thapsigargin protects against transient ischemic brain injury’, *Autophagy*, 10(10), pp. 1801–1813. doi:10.4161/auto.32136.

Zhang, X. *et al.* (2016) 'Apelin-13 protects against myocardial infarction-induced myocardial fibrosis', *Molecular Medicine Reports*, 13(6), pp. 5262–5268. doi:10.3892/mmr.2016.5163.

Zhang, X.-X. *et al.* (2021) 'The epidemiology of alzheimer's disease modifiable risk factors and prevention', *The Journal of Prevention of Alzheimer's Disease*, pp. 1–9. doi:10.14283/jpad.2021.15.

Zhang, Y. *et al.* (2023) 'Amyloid β-based therapy for alzheimer's disease: Challenges, successes and future', *Signal Transduction and Targeted Therapy*, 8(1). doi:10.1038/s41392-023-01484-7.

Zhang, Y. *et al.* (2023) 'Neuroprotective roles of apelin-13 in neurological diseases', *Neurochemical Research*, 48(6), pp. 1648–1662. doi:10.1007/s11064-023-03869-0.

Zhang, Z. *et al.* (2023) 'The impact of oxidative stress-induced mitochondrial dysfunction on diabetic microvascular complications', *Frontiers in Endocrinology*, 14. doi:10.3389/fendo.2023.1112363.

Zhao, X. *et al.* (2019) 'Artemisinin attenuated hydrogen peroxide (h2o2)-induced oxidative injury in SH-SY5Y and hippocampal neurons via the activation of AMPK pathway', *International Journal of Molecular Sciences*, 20(11), p. 2680. doi:10.3390/ijms20112680.

Zhao, Y. and Zhao, B. (2013) 'Oxidative stress and the pathogenesis of alzheimer's disease', *Oxidative Medicine and Cellular Longevity*, 2013, pp. 1–10. doi:10.1155/2013/316523.

Zheng, X.-D., Huang, Y. and Li, H. (2021) 'Regulatory role of apelin-13-mediated PI3K/akt signaling pathway in the glucose and lipid metabolism of mouse with gestational diabetes mellitus', *Immunobiology*, 226(5), p. 152135. doi:10.1016/j.imbio.2021.152135.

Zhong, W., Chebolu, S. and Darmani, N.A. (2016) 'Thapsigargin-induced activation of ca2+-camkii-ERK in brainstem contributes to substance P release and induction

of emesis in the least shrew', *Neuropharmacology*, 103, pp. 195–210. doi:10.1016/j.neuropharm.2015.11.023.

Zhou, J. *et al.* (2019) 'Imbalance of microglial TLR4/trem2 in LPS-treated app/PS1 transgenic mice: A potential link between alzheimer's disease and systemic inflammation', *Neurochemical Research*, 44(5), pp. 1138–1151. doi:10.1007/s11064-019-02748-x.

Zhu, J. *et al.* (2019) 'Apelin-13 protects dopaminergic neurons in MPTP-induced parkinson's disease model mice through inhibiting endoplasmic reticulum stress and promoting autophagy', *Brain Research*, 1715, pp. 203–212. doi:10.1016/j.brainres.2019.03.027.

Zhu, X., Raina, A., Lee, H., Casadesus, G., Smith, M. and Perry, G. (2004). Oxidative stress signalling in Alzheimer's disease. *Brain Research*, 1000(1-2), pp.32-39.

Zito, E. *et al.* (2010) 'Oxidative protein folding by an endoplasmic reticulum-localized peroxiredoxin', *Molecular Cell*, 40(5), pp. 787–797. doi:10.1016/j.molcel.2010.11.010.

Zou, K. *et al.* (2022) 'Presenilin deficiency increases susceptibility to oxidative damage in fibroblasts', *Frontiers in Aging Neuroscience*, 14. doi:10.3389/fnagi.2022.902525.

Zou, Y. *et al.* (2016) 'Apelin-13 protects PC12 cells from corticosterone-induced apoptosis through PI3K and erks activation', *Neurochemical Research*, 41(7), pp. 1635–1644. doi:10.1007/s11064-016-1878-0.

Zündorf, G. and Reiser, G. (2011) 'Calcium dysregulation and homeostasis of neural calcium in the molecular mechanisms of neurodegenerative diseases provide multiple targets for neuroprotection', *Antioxidants & Redox Signaling*, 14(7), pp. 1275–1288. doi:10.1089/ars.2010.3359.